AD-A034 593 DAVID W TAYLOR NAVAL SHIP RESEARCH AND DEVELOPMENT CE--ETC F/G 13/10
ROTATING ARM EXPERIMENTS FOR SWATH 6A MANEUVERING PREDICTIONS,(U)
JUL 76 J A FEIN, R T WATERS

UNCLASSIFIED SPD-698-01 NL

1 OF 4
AD
A034593

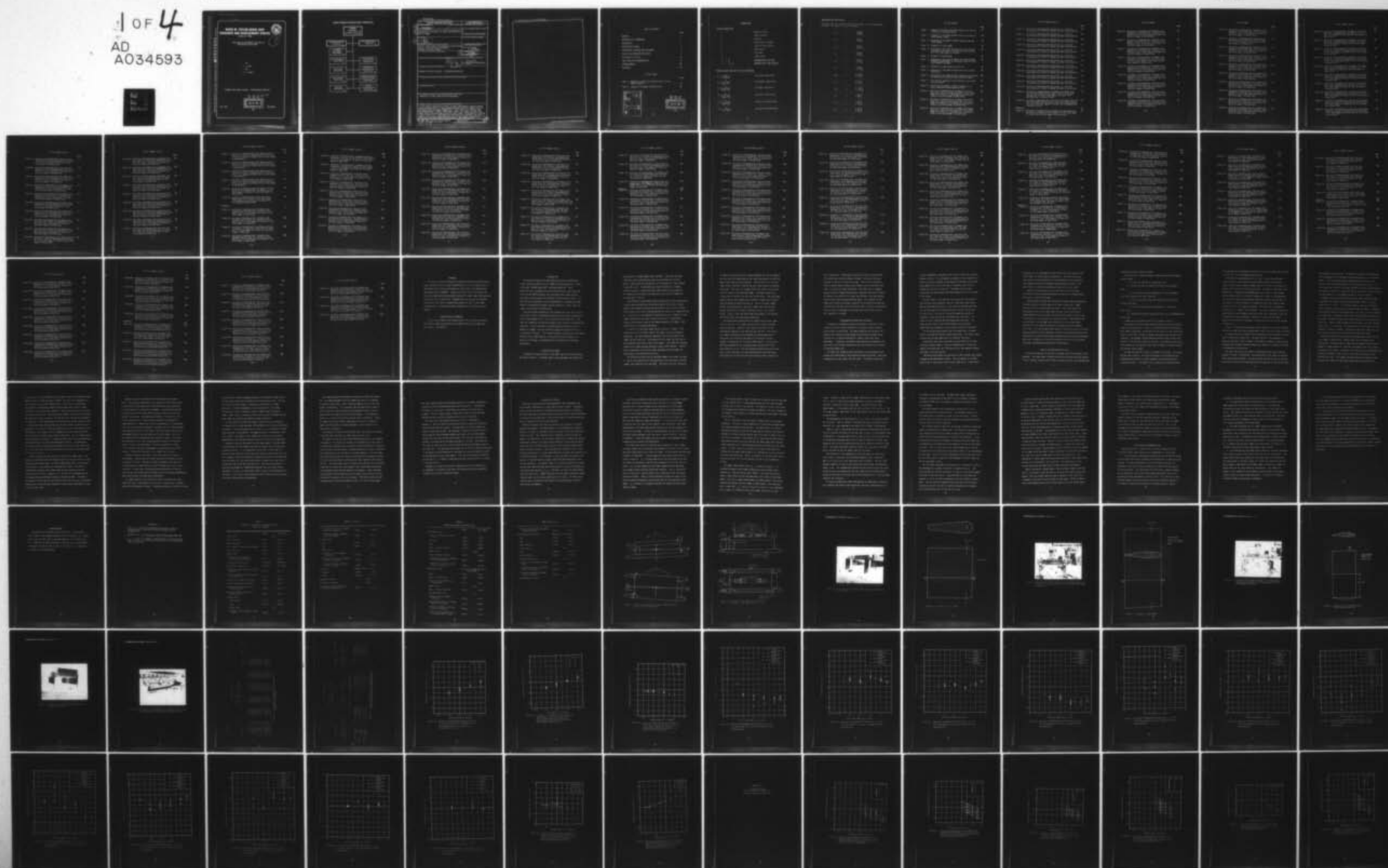

ROTATING ARM EXPERIMENTS FOR SWATH 6A MANEUVERING PREDICTIONS

ADA034593 SPD-698-01

DAVID W. TAYLOR NAVAL SHIP RESEARCH AND DEVELOPMENT CENTER

Bethesda, Md. 20084

11

B.S.

ROTATING ARM EXPERIMENTS FOR SWATH 6A MANEUVERING PREDICTIONS

by

J. A. Fein

and

R. T. Waters

July 1976

SPD-698-01

MAJOR DTNSRDC ORGANIZATIONAL COMPONENTS

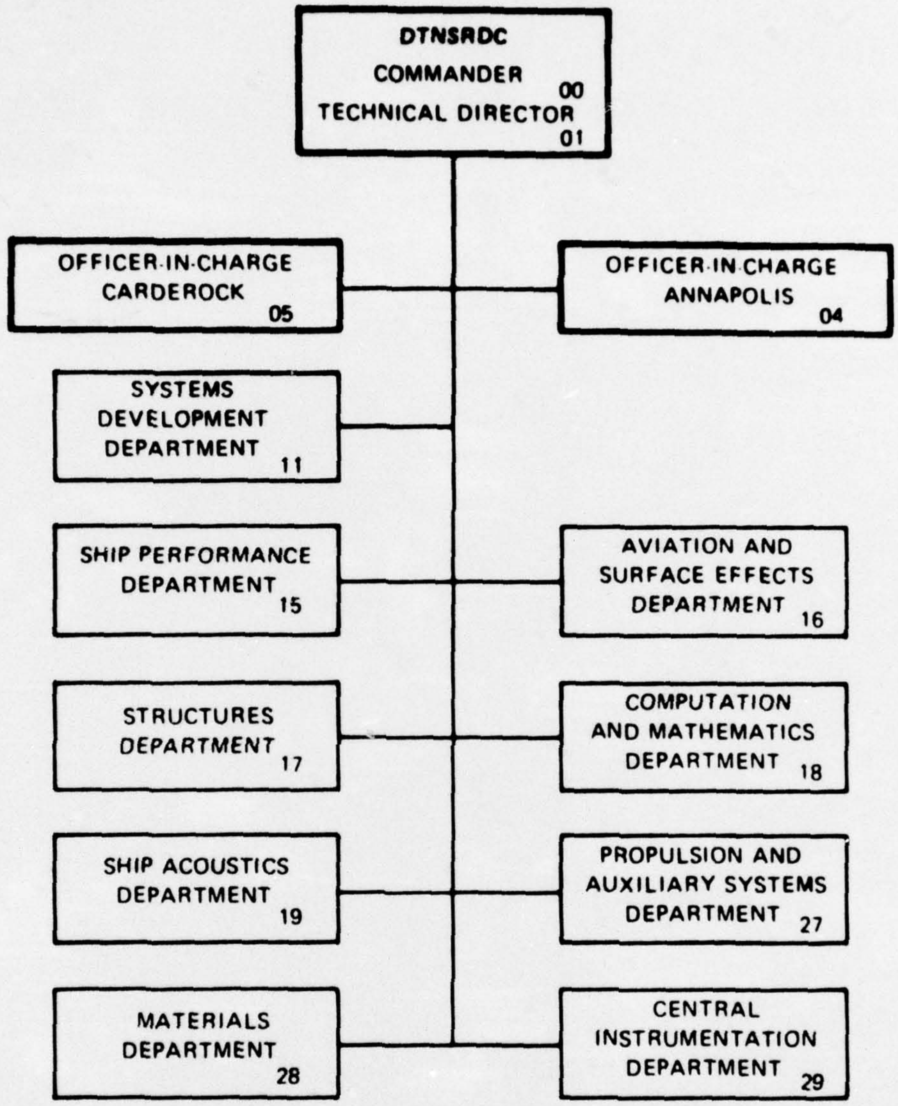

UNCLASSIFIED

SECURITY CLASSIFICATION OF THIS PAGE (When Data Entered)

REPORT DOCUMENTATION PAGE		READ INSTRUCTIONS BEFORE COMPLETING FORM
1. REPORT NUMBER (14) SPD-698-01	2. GOVT ACCESSION NO.	3. RECIPIENT'S CATALOG NUMBER
4. TITLE (and Subtitle) (6) Rotating Arm Experiments for SWATH 6A Maneuvering Predictions.		5. TYPE OF REPORT & PERIOD COVERED
		6. PERFORMING ORG. REPORT NUMBER
7. AUTHOR(s) (10) J. A. Fein, R. T. Waters		8. CONTRACT OR GRANT NUMBER(s)
9. PERFORMING ORGANIZATION NAME AND ADDRESS David W. Taylor Naval Ship Research and Development Center, Ship Performance Department Bethesda, Maryland 20084		10. PROGRAM ELEMENT, PROJECT, TASK AREA & WORK UNIT NUMBERS Work Unit Number 1-1102-003-46
11. CONTROLLING OFFICE NAME AND ADDRESS		12. REPORT DATE (11) July 1976
		13. NUMBER OF PAGES 295
14. MONITORING AGENCY NAME & ADDRESS (if different from Controlling Office) (12) 294p.		15. SECURITY CLASS. (of this report) UNCLASSIFIED
		15a. DECLASSIFICATION/DOWNGRADING SCHEDULE

16. DISTRIBUTION STATEMENT (of this Report)

APPROVED FOR PUBLIC RELEASE: DISTRIBUTION UNLIMITED

17. DISTRIBUTION STATEMENT (of the abstract entered in Block 20, if different from Report)

18. SUPPLEMENTARY NOTES

19. KEY WORDS (Continue on reverse side if necessary and identify by block number)

Maneuvering; SWATH; Rotating Arm Experiments

20. ABSTRACT (Continue on reverse side if necessary and identify by block number)

This report contains the results of model experiments on the horizontal plane characteristics of a Small Waterplane Area Twin Hull (SWATH) ship in the Rotating Arm Facility of the David W. Taylor Naval Ship Research and Development Center. Speed, drift angle, draft, roll angle, yaw rate, and rudder deflection angle were varied for three rudder configurations including a novel forward foil. Nondimensional derivatives are reported along with a comparison of rudder effectiveness for each of the rudder configurations. The results provide a data base for simulation of craft turning.

DD FORM 1473, 1 JAN 73 EDITION OF 1 NOV 65 IS OBSOLETE

S/N 0102-014-6601

389 694

UNCLASSIFIED

SECURITY CLASSIFICATION OF THIS PAGE (When Data Entered)

TABLE OF CONTENTS

LIST OF TABLES

NOMENCLATURE

Physical Quantities

ρ	density of water
L	length (overall)
U	velocity
g	gravitational constant
R	radius of rotating arm
β	drift angle
ϕ	roll angle
δ_r	rudder angle
$r' = \frac{L}{R}$	nondimensional vaw rate
$v' = -\sin \beta$	nondimensional sway velocity

Nondimensional Body Axis Forces and Moments

$K' = \frac{K}{(\rho/2) L^3 U^2}$	roll moment coefficient
$M' = \frac{M}{(\rho/2) L^3 U^2}$	pitch moment coefficient
$N' = \frac{N}{(\rho/2) L^3 U^2}$	yaw moment coefficient
$X' = \frac{X}{(\rho/2) L^2 U^2}$	axial force coefficient
$Y' = \frac{Y}{(\rho/2) L^2 U^2}$	lateral force coefficient
$Z' = \frac{Z}{/2 \ L^2 U^2}$	vertical force coefficient

Nondimensional Derivatives

(The zero subscript indicates derivative is taken at zero velocity, rate, or angle. All angles in terms of radians)

$$N_r' = \left(\frac{\partial N'}{\partial r'}\right)_o$$

$$Y_r' = \left(\frac{\partial Y'}{\partial r'}\right)_o$$

$$K_r' = \left(\frac{\partial K'}{\partial r'}\right)_o$$

$$N_v' = \left(\frac{\partial N'}{\partial v'}\right)_o$$

$$Y_v' = \left(\frac{\partial Y'}{\partial v'}\right)_o$$

$$K_v' = \left(\frac{\partial K'}{\partial v'}\right)_o$$

$$N_{\delta_r}' = \left(\frac{\partial N'}{\partial \delta_r'}\right)_o$$

$$Y_{\delta_r}' = \left(\frac{\partial Y'}{\partial \delta_r'}\right)_o$$

$$K_{\delta_r}' = \left(\frac{\partial K'}{\partial \delta_r'}\right)_o$$

$$N_\phi' = \left(\frac{\partial N'}{\partial \phi'}\right)_o$$

$$Y_\phi' = \left(\frac{\partial Y'}{\partial \phi'}\right)_o$$

$$K_\phi' = \left(\frac{\partial K'}{\partial \phi'}\right)_o$$

LIST OF FIGURES

LIST OF FIGURES (Cont'd)

LIST OF FIGURES

LIST OF FIGURES

LIST OF FIGURES (Cont'd)

LIST OF FIGURES (Cont'd)

LIST OF FIGURES (Cont'd)

LIST OF FIGURES (Cont'd)

LIST OF FIGURES (Cont'd)

LIST OF FIGURES (Cont'd)

LIST OF FIGURES (Cont'd)

LIST OF FIGURES (Cont'd)

LIST OF FIGURES (Cont'd)

LIST OF FIGURES (Cont'd)

LIST OF FIGURES (Cont'd)

LIST OF FIGURES (Cont'd)

LIST OF FIGURES (Cont'd)

LIST OF FIGURES (Cont'd)

LIST OF FIGURES (Cont'd)

LIST OF FIGURES (Cont'd)

LIST OF FIGURES (Cont'd)

LIST OF FIGURES (Cont'd)

Page

LIST OF FIGURES (Cont'd)

ABSTRACT

This report contains the results of model experiments on the horizontal plane characteristics of a Small Waterplane Area Twin Hull (SWATH) ship in the Rotating Arm Facility of the David W. Taylor Naval Ship Research and Development Center (DTNSRDC). Speed, drift angle, draft, roll angle, yaw rate, and rudder deflection angle were varied for three rudder configurations including a novel forward foil. Nondimensional derivatives are reported along with a comparison of rudder effectiveness for each of the rudder configurations. The results provide a data base for simulation of craft turning.

ADMINISTRATIVE INFORMATION

This work was funded by the Advanced Naval Vehicle Concept Evaluation Task (ANVCE) under the direction of the SWATH Project Office under Work Unit Number 1-1102-003-46.

INTRODUCTION

An extensive rotating arm experimental program was conducted on a Small Waterplane Area Twin Hull (SWATH) ship represented by a 1/22.5 scale model (DTNSRDC Mode 5337), designated SWATH 6A. These experiments were conducted to evaluate the horizontal plane characteristics of the SWATH 6A design and to evaluate three rudder designs including a novel forward foil proposed for use on SWATH vessels. The data from this experiment will be incorporated in a mathematical model that will be employed to predict turning capability, rudder size, and rudder system design for SWATH ships.

Experiments were conducted at five nondimensional yaw rates, varying from 0.093 to 0.441 on the Rotating Arm Facility at speeds corresponding to full scale speeds of 5, 7, 10, 15, 20, 22.5, 25 and 28 knots. The craft was completely captive with respect to the towing rig throughout the experiment. Forces and moments were measured and recorded in all six degrees of freedom, with the coordinate system and positive directions as indicated in Figure 1. This report includes a description of the model and each of the rudder designs, a discussion of test procedures, an analysis of the data, an interpretation of the results and pertinent conclusions.

DESCRIPTION OF MODEL

The geometric characteristics of the model and the full-scale design are given in Table 1. The model used in this experiment was fitted with

two propellers (DTNSRDC Numbers 4416 and 4417). These were the same propellers used to evaluate the propulsive characteristics of the design. Model power was provided by a 5.4 horsepower D.C. motor housed in each demi-hull. The two demi-hulls were connected by a plywood bridging structure, to which the block gage assemblies were attached. The forward and aft control fins were set to zero angle of attack and are described in Table 1.

Three different rudder designs were evaluated during these experiments: a strut rudder attached near the trailing edge of each strut; a spade rudder placed between the strut and the propeller on each hull; and the fixed forward turning foil attached beneath the inboard hull forward of the CG. A comparison of the geometric characteristics and a schematic of the rudder placement can be found in Table 2 and Figure 2, respectively. Figure 3 shows photos of two of the rudders mounted on the model. Each rudder design was evaluated separately.

A schematic of the strut rudder design is shown in Figure 4. The hinge axis was at the leading edge of the rudder, which was therefore unbalanced. The chord length was defined by the trailing edge of the rudder and the hinge axis. The planform of this rudder was the same as the planform of the strut in way of the rudder. This rudder was representative of the rudder designs previously used on SWATH designs. Figure 5 shows a photograph of the strut rudder deflected while the model was being towed in the Rotating Arm Facility.

The profile and plane view of the spade rudders can be seen in Figure 6. Due to time constraints at the beginning of the experiment, existing rudders were modified to fit the model. The chord length was limited by

the need to provide sufficient clearance between the trailing edge of the strut and the leading edge of the rudder and between the trailing edge of the rudder and the propeller. The availability of existing rudder models, therefore, defined the exact chord length and section shape used. The hinge axis (rudder stock) was placed at the quarter chord to provide a semi-balanced rudder. The spade rudders were surface piercing and did not have ventilation fences. Both the spade rudders and the strut rudders were limited to a deflection angle of about 40 degrees by model construction. During the spade rudder section of the experiments, the strut rudders were fixed at zero degrees deflection to provide a continuous strut of the correct length. Figure 7 shows the SWATH model being towed in the Rotating Arm Facility with the spade rudders deflected.

The fixed forward turning foil was tested with two sizes, both shown in Figure 8. This rudder design did not rotate as did the other two designs. Instead, it was stored inside the hull and activated by dropping it into the flow past the hull. This particular rudder configuration was designed to provide added control force while not increasing the power of the hydraulic actuator systems in the design of a full-scale SWATH vessel. It also had to meet the constraint of not projecting below the baseline of the vessel when not in use. Only the starboard forward turning foil was used, as only starboard turns were executed during the experiment. The turning foil in the port hull would normally remain stored for a

turn to starboard. A NACA 63_2-15 Section was chosen to maximize the lift coefficient for small angles of attack. The aspect ratio was arbitrarily chosen at 2.0 for this study. The foil was arbitrarily set at 5 degree angle of attack with respect to the centerline of the model to provide the proper side force. The rudder used a cambered section to give increased force without increasing the angle of attack. To determine the effect of foil area, two different sizes were tested, both with the same chord but different spans. The placement of the rudder was limited by structural supports for the mounting bracket and the ability of the foil to fit inside the strut in the full-scale design. Figure 9 shows a photograph of the large span fixed forward turning foil attached to the model.

EXPERIMENTAL EQUIPMENT AND PROCEDURES

The model was completely captive with respect to the tow rig (see Figure 10) and was rigidly attached to a structural channel through spacer blocks at five points. Two gage assemblies were bolted to the channel, each containing three modular force balances oriented along the body axis to measure longitudinal, lateral, and normal force components. In addition, one modular force balance was mounted on the port side of the bridging structure at the LCG to measure roll force at a prescribed moment arm.

The three gage assemblies were connected to struts mounted on the surface ship towing beam of the rotating arm towing carriage. Each strut connection had a yaw, pitch, and roll pivot. In addition, each strut

could be independently adjusted in the vertical direction to effect changes in draft. This arrangement provided all force components at each of the struts attached to the channel and allowed pitching and yawing moments to be calculated about a reference point half-way between the two struts at the LCG. The moment arm for these calculations was the distance from the reference point to the center of the struts.

The roll angle of the model was set by adjusting the height of the strut which was attached to the roll force block gage at the edge of the bridging structure. This strut was adjusted each time the roll angle was set to transmit body axis vertical force only. For each run at a non zero roll angle the gages were zeroed at standstill, canceling out the roll moment due to buoyancy. Yaw angle was set by rotating the entire apparatus from above. The model was set at zero pitch angle throughout the experiments. Rudder angle was changed by a servo-actuator mounted on the model.

The force measurement outputs were integrated over a standard time of 6 seconds and multiple samples were taken. All forces, angle settings and carriage speed were also stored on stripchart.

Centripetal tares were calculated using the model mass and the carriage rotational speed. Tares were removed and all forces and moments calculated about the reference point by the computer program described in the next section.

The design displacement was maintained at 250 kilograms (551 pounds) throughout the experimental program. This corresponds to a design draft of 36.11 centimeters (14.22 inches) model scale. A deep draft

condition of 41.2 centerimeters (16.22 inches) was also tested for the strut rudder and spade rudder configurations. The draft was set by screw jacks and measured optically at the beginning of each condition, then checked periodically throughout the experimental program. The water level was carefully monitored and kept to the proper level.

Standstill measurements in air on the inertia gear at various roll and trim angles provided the actual CG position of the model which were used in correcting the data.

The experimental program for the strut and spade rudder configurations included variations of drift angle, roll angle, speed, draft, rudder deflection angle, propeller RPM, and radius. The fixed forward foil configuration phase of the experiments did not include variation of rudder deflection angle or draft, but did include variation of foil size. The forward foil was tested only at the design draft. The propeller RPM was adjusted to provide model self-propulsion in the straight ahead condition for each speed and varied to investigate propulsion effects on the data. All the variables were chosen to represent a range of realistic operating conditions and to develop a data base for maneuvering predictions. Combinations of variables were often examined and check points were obtained. Radius was limited by the size of the Rotating Arm Facility and the need to prevent interference and reflection from the beach.

ANALYSIS AND PRESENTATION OF DATA

The raw test data was in the form of voltages read off the modular force balances. The signals were filtered and sent to stripcharts and the computer. A set of computer programs was utlized to convert the data into nondimensional

coefficients and to correct for tares.

The on-carriage Interdata computer program performed the following analysis tasks.

1. Convert the voltages to engineering units

2. Correct the data for model CG location and centripedal tares

3. Calculate the resultant hydrodynamic forces and moments about the reference point (full scale CG)

4. Print the raw data, along with the statistical measures of data consistency

5. Print the resultant forces and moments in English and metric units

6. Nondimensionalize the results and print out the nondimensional quantitites.

A sample two page computer print out is shown in Figure 11.

The program and printout were flexible enough to allow the identification of bad data points. Errors in carriage speed and angle settings were readily identified. The analysis of only part of a data record was often of use on the carriage to salvage good data without repeating the condition. The computer and the operating system on the arm were very helpful in the efficient conduct of the test. Over 1000 good data points were obtained in less than 150 total hours of testing including rigging and frequent model changes.

The data was taken for a matrix of speeds, drift angles, roll angles and yaw rates (radius). The coupling between all the quantities was determined experimentally so that subsequent simulation would have an empirical basis. The ranges of the variables were determined from

the expected operating envelope of the ship in a turn including the low speed range for the mine countermeasures application.

The nondimensionalized data for N', Y' and K' was plotted for each speed and rudder configuration in three series: against yaw rate for a family of drift angles, against rudder angle for a family of yaw rates and against roll angle for a family of yaw rates. This data is contained in the appendices. In addition the nondimensional axial force, X', was plotted against rudder angle for a family of speeds and is shown in the appendices. The coupling of rudder angle and drift angle was found to be quite small as can be seen in Figure 12 where it is plotted for the strut rudder at deep draft for a full scale speed of 25 knots. This effect was not generally plotted but is included in the simulation. In Figure 13 the drift angle/roll angle effect on yawing moment can be seen to be small; therefore, it was not plotted for the other conditions. Similarly in Figure 14 the rudder angle/roll angle effect is negligible and this coupling also was not plotted for other cases.

Figures 15 through 28 are summary figures showing the relationship between the various rudder types and are described in the Discussion of Results section.

As stated earlier the objective of this experiment was to obtain simulation data for manevuering predictions. The data compiled in the appendices is being incorporated in such a program. The program is based on a table look-up technique that includes nonlinear effects but linearity in the data is of help in implementing the math model.

The linear derivatives are useful in understanding the results and are plotted in Figures 15 through 26. The derivatives are the slopes of straight lines drawn through the data. The sway velocity derivatives (Y'_v, N'_v, and K'_v) were obtained from curves constructed from the intercepts of the yaw rate plots

extrapolated to zero yaw rate. It should be pointed out that zero yaw rate corresponds to the straight-line testing technique (i.e. infinite radii). Since this experiment was conducted without straight line testing, the results depend heavily on the extrapolation process. As can be seen the linearity of the data permitted a reliable extrapolation, thus making it possible to obtain the turning information without straight line experiments at a considerable savings in time and expense.

Appendix A contains the data for the strut rudder at design draft. Figures 29 to 48 present the yaw rate/drift angle effects at various speeds for N', Y' and K'. In all these curves, linearity of the data within the drift angle and yaw rate range of the experiment is apparent. The zero drift angle data extrapolates to a zero value of force or moment as it should for a symmetrical model with counter rotating propellers of equal RPM. The other extrapolation curves are parallel to the zero drift angle case. There is some nonlinearity at the largest yaw rate (smallest radius) for K' in Figure 43. This yaw rate of 0.45 corresponds to a turn diameter of five ship lengths. It should be noted that rudder angle and roll angle were held at zero for the data in the above figures.

Figures 49 through 65 give the yaw rate/rudder angle effects for the strut rudder at design draft. Rudder angles up to 40 degrees were investigated. Yaw moment due to rudder usually peaked between 30 and 40 degrees of rudder deflection. With the curve being linear out to about 20 degrees at all speeds. The effect of yaw rate on the yaw moment and side force due to rudder is small; that is, the lines are parallel at the different yaw rates. This enables the determination of moments at zero yaw rate from a parallel curve drawn through the origin of the plot.

Figure 63 shows that at 20 knots the roll moment curves exhibit some nonlinear effects, especially when yaw rate is 0.305. This yaw rate corresponds to a turn diameter of seven ship lengths which is tight for that speed range. Some scatter in the data was noted at large rudder angles which is understandable as the flow was very dramatic in these conditions and some venting might have been occuring. The direction the rudder was driven did not affect the steady force data in any way. For the most part the data was repeatable and consistent. Drift angle and roll angle were zero for this series of runs.

Figures 66 through 82 show that the roll angle effect on the forces and moments was quite small as might be expected by the wall-sided nature of the SWATH design. Roll angles up to six degrees were investigated and for the most part some consistent trends could be identified. The roll moment curves show a great deal of scatter. It should be noted that by the test technique employed here the curves show the hydrodynamic effects. The hydrostatic and inertia (buoyancy) effects were removed by zeroing the gages before the run. The rudder angle and drift angle were held at zero for the data shown in this set of curves.

Figures 83 shows the axial force as it varied with rudder angle. The model was propelled at the self propulsion point so the axial force is close to zero at zero rudder angle. At large rudder angles there is an increase in drag that is very apparent as a negative axial force. The effect is approximately quadratic with rudder angle but the simulation uses the actual data rather than a quadratic fit. The force is nondimensionalized by speed squared and different speeds are plotted together. The effect of changes in drift angle and roll angle on the axial force was inconsistent and was small, especially when compared to the pronounced dependence of the force on rudder angle.

Appendix B contains the data for the strut rudder at the deep draft. Less data was obtained for this condition as the linear nature of the results at the design draft justified making some assumptions as to the behavior of the forces and moments. Figures 84 through 100 give the yaw rate drift angle effects and show linearity and minimal scatter in all cases. The rudder angle effects in Figures 101 to 112 are well behaved with a linear response extending to 20 degrees of rudder deflection. Rudder stall is not as prononunced as in the design draft, and the yaw moment continues to increase out to 35 degrees though some tapering off occurs in the slope. The large rudder angles at this displacement could not be obtained by driving the rudder servo, thus the rudder had to be deflected at zero speed and clamped. This gives some indication of the large torque required to deflect this type of rudder in a full scale application. The roll variations in Figures 113 to 119 show a very small hydrodynamic contribution due to rolling the ship. Figure 120 gives the X' vs δ_r effects for this case.

Appendix C contains the data for the spade rudder at the design displacement. The yaw rate drift angle variations with speed are given in Figures 121 to 134. The data is linear and repeats well except for the high speed roll moment data of Figure 134 where some scatter occurs. Figure 123, in particular, indicates how data obtained at various yaw rates can be used to determine the values at zero yaw through extrapolation, making the straight line experiments unnecessary.

The rudder angle yaw rate effects are given in Figures 135 to 152. Figure 135 shows a high degree of uncertainty in slope due to a possible bad point at 20 degrees of rudder. In general the data at 5 knots full-scale

speed was often unusable presumably because of low-Reynolds Number effects and that might be true for this data as will be discussed later. The rest of the data at higher speeds is linear out to 20 degrees of rudder deflection. The stall phenomenan is very pronounced for this rudder configuration, with no increase in force or moment beyond 30 degrees rudder. Some scatter is apparent in the results beyond 30 degrees and the model rudder was probably ventilating in these conditions.

The roll effects for the strut rudder at design draft are contained in Figures 153 to 161 and show very little effect of roll angle on the forces and moments. Figure 162 gives the axial force, X', as a function of rudder angle and shows a large effect. The added drag due to the addition of the strut rudder to the model at zero rudder angle could not be accurately determined by this experiment and will have to be analytically determined.

Appendix D contains the results for the spade rudder at the deep draft. The yaw rate drift angle effects are shown in Figures 163 to 174 and show no unusual effects. It is interesting to note that in Figure 165, for example, the extrapolation to zero yaw rate might be aided by the fact that for a symmetric model the condition of negative drift angle at positive yaw rate corresponds to a positive drift angle at a negative yaw rate (that is on the left side of the zero yaw rate axis). Thus the extrapolation to zero yaw rate becomes an interpolation and the cross over point is well specified. This fact is particularly useful if there are nonlinearities in the data. In this case, since the data was quite linear near zero yaw rate, the curves could be easily extrapolated.

The rudder angle/yaw rate effects are given in Figures 175 through 183. The rudder-dependent force and moment are linear out to beyond 20 degrees in most cases. Stall in the yaw moment occurs at 35 or 40 degrees of deflection. It is apparent that the deeper draft tends to postpone the stall angle and from the photographs it seems that the deeper draft also leads to less ventilation effect. The propeller is deeper as is the hull which partly explains this circumstance. Figure 183 summarizes the roll moment rudder angle variation at different speeds and illustrates that speed dependence is very marked for all these forces and moments.

Roll effects in Figures 184 to 189 are small but generally consistent. Figure 190 shows the effect of rudder angle on axial force.

The effects of the full size fixed forward turning foil are contained in Appendix E. The fixed foil produces an incremental force that acts in all conditions so the data for yaw rate at zero drift angle will not extrapolate to zero force and moment. Nonlinear effects will tend to complicate the extrapolation since the model is no longer symmetric. The yaw moment variations with yaw rate for various drift angles are contained in Figures 191 to 196 and show linearity with yaw rate with a definite effect due to the foil. The side force curves in Figures 197 to 202 are less consistent. Figure 197 at 5 knots full scale speed is very inconsistent perhaps due to the boundary layer flow not being fully turbulent. Figure 199 shows nonlinearity with drift angle as the foil seems to be losing lift at the positive drift angles as yaw rate increases. The higher speeds are more consistent and it should be pointed out that it is only at high speeds

that such a device might prove necessary because at low speed, differential propulsion gives the SWATH design good turning properties. Figure 202 at 28 knots full scale also is inconsistent as conflicting results are in evidence. The roll moment curves, Figures 203 to 208 also show nonlinear effects and can be directly related to the side force anomalies.

The short span fixed forward turning foil data is presented in Appendix F. Data was taken at only two yaw rates but seems more consistent than the large span foil results. Yaw rate effects at various speeds are given in Figures 209 to 228. The increment in moment due to this size foil can be seen from the difference between zero moment and the extrapolated value at zero yaw rate for zero drift angle. This quantity can be seen to be small in Figures 209 to 214 where yaw moment is plotted. One reason for this might be that the foil is mostly within the separated boundary layer on the lower hull. The apparently small moment due to the foil might be inaccurate if the trend of the nonlinearity at the higher yaw rate were tending to drive the extrapolation close to zero moment. This can be determined by comparing the results at $r' = 0.092$ for conditions with and without the foil as is done in the next section.

Generally, the data for the total program was quite well behaved and, as presented, it provides a vast matrix for determining turning conditions through the use of the simulation program.

DISCUSSION OF RESULTS

There was a great amount of data generated in this experiment, too much to permit consideration of each piece of data in detail. Estimated turning circles and stability characteristics must await the simulation. The linear derivatives obtained from the results do lead to some observations on the turning characteristics of the various rudder configurations and the effect of speed on the directional stability.

Before considering the linear derivatives, the linearity of the data deserves some comment. The SWATH design is not hydrodynamically complex because it consists of cylindrical hulls with more or less wall-sided flat plates as struts. The propellers are in relatively clean flow when the rudder is not deflected. The flat plate struts give a weather-vane type of directional stability that makes turning difficult so yaw rates and drift angles are low. All these factors lead to linear and well behaved hydrodynamic forces and moments. Only the addition of something like a fixed forward turning foil or a large rudder deflection disturbs the predictability of the flow patterns. This linearity is very convenient for modeling the dynamics of the SWATH and has greatly simplified the development of the turning simulation. For example, there is no coupling between drift angle and yaw rate, which has been taken into account in previous math models as the second order terms N_{vr} or Y_{vr}. Similarly, all the roll angle related terms are nearly zero. Rudder angle yaw rate and rudder angle/drift angle coupling terms are also nearly negligible in all cases. All these facts indicate that a relatively simple theory could be developed to predict these forces and moments.

A nonlinear consideration that cannot be neglected is related to speed. The SWATH, unlike most traditional ships, operates in a Froude Number range that has a strong influence on the flow patterns at high speeds causing the directional stability and maneuvering to be speed dependent. At a full scale speed of 20 knots the level of the flow across the strut rudder corresponds to the zero speed waterline, while at 25 knots the flow past the rudder has dipped considerably. If the pitch fins were used to maintain zero trim angle as was assumed in this experiment, the rudder effectiveness at 25 knots would be much lower than at 20 knots because of the flow on the rudder. In fact all the derivatives (except the roll terms) are highly speed dependent, much like the air cushion vehicles. The data in Reference 1 shows this effect and also presents good agreement between rotating arm and straight line experiments.

The linear derivatives for the four basic conditions of strut rudder and spade rudder each at two drafts are presented in Figures 15 to 26, where they are plotted against full scale ship speed. The derivatives are described in detail in Reference 2. The yaw moment-yaw rate damping derivative N_r' is shown in Figure 15. N_r' is always negative and the more negative the term the better the directional stability and consequently the larger the turn circle. N_r' was most negative at the higher speeds with the deep draft strut rudder showing the most directional stability. The Y_r' derivative given in Figure 16 is usually positive for conventional ships and always positive for SWATH. There is little difference between the values at the various rudder configurations and the term does not vary appreciably with speed. K_r' in Figure 17 is negative and does not change much with either speed or rudder.

The coupling term N_v' given in Figure 18 is negative which is the usual case for surface ships. A more negative value for this term indicates that the turn circle will be smaller. This implies a smaller turn circle for the deep draft conditions as might be expected. The term increases by 50% between 15 and 20 knots so it does show how the Froude Number influences the derivatives.

The Y_v' directional stability term in Figure 19 has a large speed dependence. The term is always negative as it should be but becomes much less negative between 15 and 20 knots. This means there is a loss of directional stability at the 20 knot speed which indicates that the turn diameter at 20 knots could be smaller than at 15 knots at least as far as this term is concerned. The behavior of Y_v' shows that 20 knots may be a speed where the ship turns well and that the spade rudder which has the lowest magnitude of Y_v' should produce good turn performance at the higher speeds. The turn circle is a function of all these terms as well as a function of the rudder effectiveness, so a confirmation of this conclusion must await the simulation. The K_v' in Figure 20 is positive which implies that the ship will roll out of the turn, if roll is not counteracted by fins.

The rudder effectiveness term, N_{δ_r}', is given in Figure 21. As expected the deeper draft rudders produce more turning moment (more negative N_{δ_r}') than the design draft rudders. The design draft spade rudder is more effective than the deep draft strut rudder at the higher speeds. The loss in rudder effectiveness at higher speeds is due to the changing flow pattern over the rudder at those speeds. The side force due to rudder term, Y_{δ_r}', given in Figure 22 is positive, as it should be, and is larger for the design draft strut rudder, especially at lower

speeds. The term is small for all rudder configurations at the higher speeds. The K_{δ_r}' term in Figure 23 is always negative as expected, and tends to decrease in magnitude slightly with speed. The effectiveness of the spade rudder is illustrated by the fact that at 25 knots full scale, N_{δ_r}' for the spade rudder at deep draft is four times greater than for the strut rudder at design draft.

The hydrodynamic roll derivatives N_ϕ', Y_ϕ', and K_ϕ' are given in Figures 24, 25 and 26. There is scatter in the terms and they are generally small, especially K_ϕ', when compared to the static roll stiffness of the design.

These Y_v' and N_v' derivatives may be compared with nondimensional results from the straight-line tests of SSP model over a range of Froude numbers given in Reference 3. The magnitude of the N_v' term is very close to that for the SSP at design displacement while the Y_v' term for SWATH 6A is smaller (less negative) than for SSP at design draft and almost identical to SSP for light draft. The lower directional stability implies that, everything else being equal, the SWATH 6A may turn better than the SSP design.

The collection of low speed data in this experiment was hampered by difficulties in assuring a fully turbulent boundary layer on the model. Results at 5 knots full scale speed were often misleading. The full scale Reynolds number at 5 knots is post-transition but the model scale Reynolds Number is not. The nondimensionalized derivatives below 15 knots full scale should not vary with speed until near zero speed thus the 10 knot values should be sufficient to describe the turning characteristics in the low speed range for the simulation.

It should be noted that rudder effectiveness as summarized in Figure 21 only indicates the slope at zero deflection, the stall characteristics of

the rudder are also important. The deep draft rudder experiments indicated a postponement of the stall of 5 to 10 degrees (compared with design draft) which can produce a significant increase in the turning moment.

The effectiveness of the fixed forward turning foil will be determined from the simulation results. The nonlinear results will be incorporated in the table of values for the math model. The foil at both sizes did produce a positive increment in yaw moment which will decrease the turn circle of the ship.

The relative effect of the foils can be seen in Figure 27 where yaw moment is plotted against rudder angle. The fixed foil experiments were conducted with the strut rudder and design draft configuration so rudder data for that configuration is used for the comparison. It can be seen that the fixed foil produces a larger positive yaw moment than is produced by full deflection of the rudder for this particular radius condition. This is a good sign of foil effectiveness but it must be considered for this radius only as the radius effects on foil performance are nonlinear. The full size foil apparently could turn the ship alone at this radius which is equal to a turn diameter of 20 ship lengths as the net yaw moment is zero.

The side force generated by the turning foil is opposite in sign to that generated by a rudder as the foil is forward of the CG. This effect should also help the turning as it gives a force directed toward the center of the turn circle. Figure 28 shows the side force and compares it to the side force generated by the strut rudder at design draft. The full size foil generates more than twice the side force produced by the half size foil as might be expected due to boundary layer effects being equal for the two foil sizes.

The fixed forward turning foil thus shows promise for application to the SWATH design if draft limitation problems can be overcome by deploying it only in deep water. The foil design evaluated here with its camber and 5 degree angle of attack was generally designed to give maximum lift when deployed. Such a foil would be useful in generating an angle of attack on the ship and, in that way, improve the initial phases of the turn even if performance degenerates at the high yaw rates as indicated by the data. By deploying the foil only on the inboard hull, the drag on the foil also helps the turning performance while it does not add drag to the cruising configuration of the ship. The cambered foil may be prone to vortex shedding and other phenomena that lead to nonlinearities at the smaller radii. These coupled effects might also be due to center of pressure shifts as the model is towed at higher yaw rates. The foil could be placed more forward on the final ship design to improve its effectiveness. A simpler foil plan form might also be employed. The assumption that the forward foil was not coupled to the rudder forces was made in these experiments since the foil was below the lower hulls and the rudders were all above the lower hulls. The combination of spade rudder and fixed forward turning foil which holds great promise will be evaluated in the simulation. The simulation will also consider drag flaps and other means of improving turning performance.

Overall the results indicate that if the directional stability of this SWATH is low enough so that the ship can assume a drift angle of about two degrees, the strut rudder should be able to generate a turn circle with a diameter of less than 10 ship lengths at high speed. The use of deeper draft, fixed forward turning foil, or other device could give a high speed

turn diameter on the other of the desired seven ship lengths. The strut rudder does not show promise for producing the required turn unless greatly increased in size, which might be impractical for a ship design. Elimination of the strut rudder from consideration however, should await the simulation results.

The intent of this program of experiments was to provide a data base extensive enough to allow for predicting maneuvers regardless of the rudder finally chosen for the SWATH design, and to determine the rudder size required to meet the design criteria for turning. Thus, it was intended that the mathematical model to be based on the data include the full range of experimentally determined nonlinearities and cross couplings without restricting it to narrow curve-fit standards reflected in two or three term Taylor series.

CONCLUSIONS AND RECOMMENTATIONS

Though the analysis of SWATH turning is heavily dependent on the simulation results some conclusions and recommendations can be made.

1. The rotating arm experimental technique can be utilized to provide all the static derivatives involved with the prediction of maneuvering performance. This was accomplished in this case without straight line experiments, thus saving time and expense, by extrapolating the results to infinite radius. The rotating arm with the current computer programs can be operated as an efficient and accurate experimental facility for evaluating turning performance of surface craft. This technique is more straight-forward than the horizontal planar-motion-mechanism approach as it does not require the elimination of frequency effects, though

acceleration dependent derivatives must be obtained analytically.

2. The experimental data from the rotating arm experiments for the SWATH design are linear except at large yaw rates. This eases the extrapolation process and allows for the elimination of some matrix data points. The linearity implies that a theoretical formulation for the forces and moments due to roll, drift and yaw rate could be devised. The forces are very nonlinearly dependent on speed as the flow patterns along the hull change considerably with Froude Number.

3. The SWATH 6A designs for all rudder configurations and drafts evaluated in this experiment are statically stable in yaw with the linear derivatives always possessing the sign expected from conventional displacement-type ship work. The SWATH has less nondimensional stiffness to drift (Y_v') than was found for the SSP at design draft. The yaw rate damping N_r' is greatest for the strut rudder at the deep draft. The term Y_v' is smallest in magnitude for the spade rudder at design draft.

4. The nondimensionalized rudder effectiveness for the SWATH decreased with increasing speed as the level of the flow over the rudders fell. The rudder effectiveness was greatest for the spade rudder at the deep draft. The spade rudder at the design draft was slightly more effective than the strut rudder at deep draft at the higher speeds, and the strut rudder at design draft was the least effective configuration. The rudders all tended to stall between 30 and 40 degrees though the deep draft rudders usually stalled at higher rudder deflections. There was no evidence of a discrete rudder force hysteresis phenomenon.

5. A fixed forward turning foil that was deployed from the inboard hull with camber and angle of attack was evaluated in this experiment. It was found to be effective in providing yaw moment and side force to improve the turning performance of the design.

6. The results lead to the provisional conclusions that the strut rudder configuration will be insufficient to turn the SWATH adequately within reasonable rudder size and rudder torque limitations. The spade rudder design does hold promise of producing turn diameters of less than 10 ship lengths with a rudder of the size evaluated in this experiment. The spade rudder can be balanced to minimize rudder actuator requirements. The fixed turning foil employed in conjunction with the spade rudder could reduce the turn diameter of the SWATH 6A to around seven ship lengths. This turn diameter would be equivalent to five ship lengths for a destroyer since the destroyer of the same displacement is longer than a SWATH. Refined conclusions of turn performance will be available when the simulation is operational.

ACKNOWLEDGMENTS

The authors wish to express special thanks to J. Brooks Peters for his work on the computer programs for this experiment, to L. Murray and R. Carr for their help in the experiment and to E. Robinson and R. S. Schechter for their assistance in the data analysis and plotting. The support and advice of M. D. Ochi, D. Cieslowski, G. R. Lamb and R. Stevens is also appreciated.

REFERENCES

1. Fein, J.A., "Horizontal Plane Static and Dynamic Stability Characteristics of the JEFF (B) AALC," SPD Report 467-10, November 1975

2. Comstock, J.P., Ed. Principles of Naval Architecture, SNAME 1967

3. Fein, J.A. and J.P. Feldman, "Controllability of the Stable Semi Submerged Ship" 3rd International Ship Control Systems Symposium, Bath, England 1972

TABLE 1

GEOMETRIC AND PHYSICAL CHARACTERISTICS OF THE SWATH 6A DESIGN

	Model	Full Scale
Linear ratio	22.5	
Length (overall)	3.25 m	73.15 m
Submerged length	3.25 m	73.15 m
Strut length (including Strut Rudder)	2.33 m	52.5 m
Strut thickness	0.098 m	2.21 m
Maximum beam	1.22 m	27.43 m
Transverse strut separation, (centerline to centerline)	1.02 m	22.86 m
Displacement, design draft	0.246 MTFW	2900 MTSW
Displacement, deep draft	0.257 MTFW	3015 MTSW
Vertical distance, baseline to design waterline	0.361 m	8.13 m
Vertical distance, baseline to deep draft waterline	0.412 m	9.27 m
Wetted surface area, design draft	5.624 m^2	2847 m^2
Wetted surface area, deep draft	6.10 m^2	3088 m^2
Longitudinal distance, nose to reference point	1.562 m	35.14 m
Vertical distance, baseline to reference point	0.461 m	10.36 m
Canards, each:		
Chord length	0.116 m	2.61 m
Span	0.129 m	2.903 m
Aspect ratio	1.11	
Distance, trailing edge to hinge axis	0.087 m	1.958 m

TABLE 1 continued

Longitudinal distance, reference point to hinge axis	0.819 m	18.428 m
Transverse distance, reference point to midspan	0.345 m	7.76 m
Aft flap, each:		
Chord	0.20 m	4.50 m
Span	0.222 m	5.00 m
Aspect ratio	1.11	
Distance, trailining edge to hinge axis	0.149 m	3.35 m
Longitudinal distance, reference point to hinge axis	1.187 m	26.71 m
Transverse distance, reference point to midspan	0.306 m	6.885 m
Propellers:	Numbers 4416 - 4417	
Diameter	0.194 m	4.36 m
Pitch	0.222 m	5.00 m
Expanded area ratio	0.634	
Direction of rotation	Inward	
Vertical distance, centerline of propeller to waterline	0.25 m	5.80 m

TABLE 2

COMPARISON OF RUDDER CHARACTERISTICS

	Model		Full Scale
Strut Rudder, each:			
Chord, trailing edge to hinge axis	0.254 m		5.72 m
Thickness	0.076 m		1.71 m
Span	0.325 m		7.32 m
Span, to design waterline	0.133 m		2.99 m
Aspect ratio		0.525	
Area, to design waterline	0.043 m^2		21.96 m^2
Longitudinal distance, reference point to hinge axis	0.881 m		19.92 m
Transverse distance, reference point to hinge axis	0.508 m		11.42 m
Spade Rudder, each:	Maximum Thickness 30% Aft of Leading Edge		
Chord	0.241 m		5.42 m
Span, at leading edge	0.481 m		10.82 m
Span to design waterline, at leading edge	0.171 m		3.85 m
Aspect ratio		0.743	
Area, to design waterline	0.043 m^2		21.90 m^2
Thickness/Chord ratio		0.15	
Distance, trailing edge to hinge axis	0.183 m		4.12 m
Longitudinal distance, reference point to hinge axis	1.351 m		30.40 m
Transverse distance, reference point to hinge axis	0.508 m		11.43 m
Distance, trailing edge of strut to leading edge of rudder	0.156 m		11.43 m

TABLE 2 continued

Distance, trailing edge of rudder to propeller disk	0.146 m	3.29 m
Fixed Forward Turning Foil:	NACA 63_2 - 615 Section	
Chord	0.155 m	3.49 m
Span	0.310 m	6.98 m
Span, Half-Size	0.158 m	3.56 m
Aspect ratio	2.00	
Area,	0.048 m^2	24.34 m^2
Area, Half-Size	0.024 m^2	12.42 m^2
Thickness/Chord ratio	0.15	
Distance, trailing edge to hinge axis	0.114 m	2.565 m
Longitudinal distance, reference point to hinge axis	0.819 m	18.42 m
Transverse distance, reference point to hinge axis	0.518 m	11.43 m
Fixed angle of attack	5°	

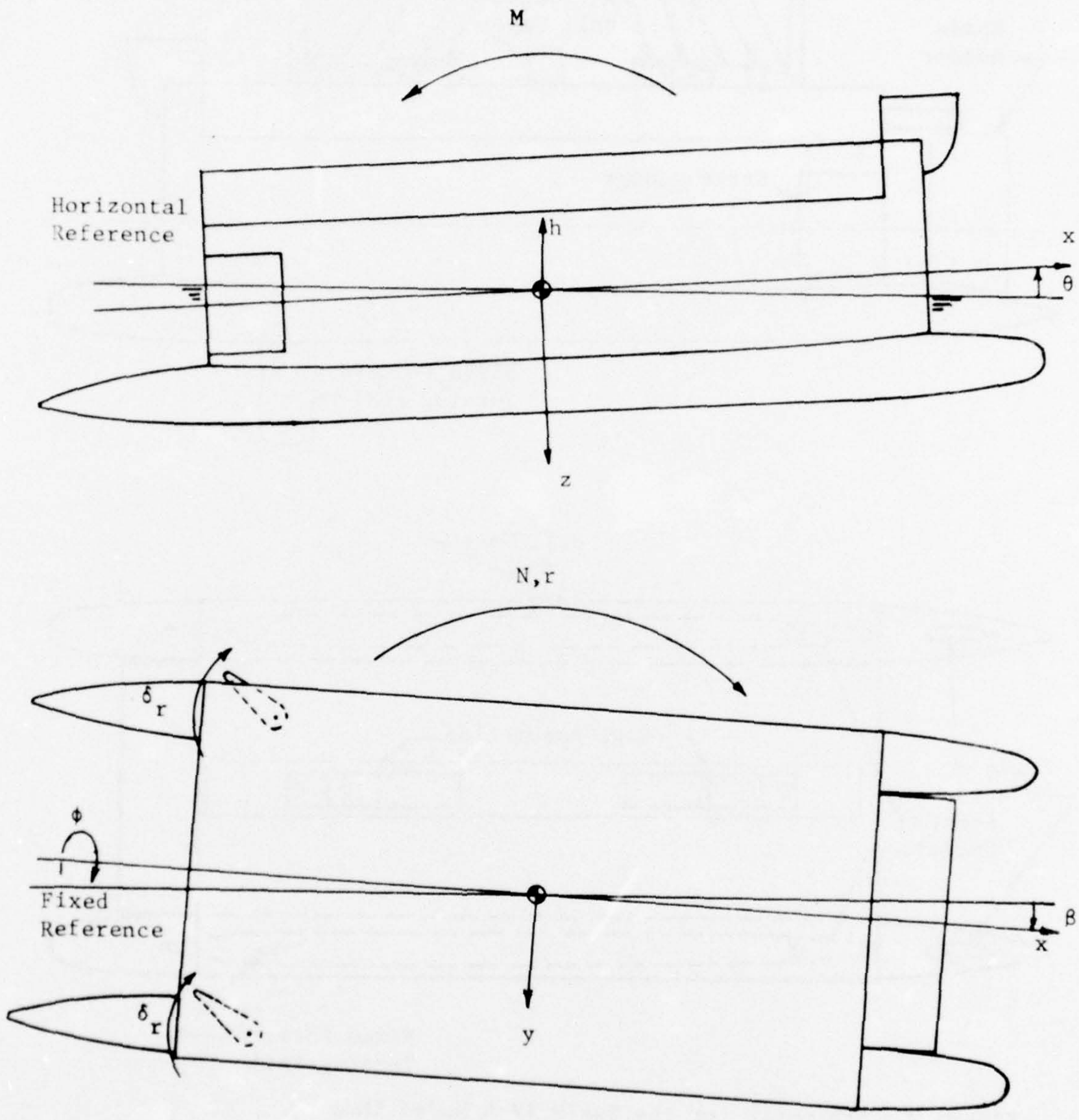

Figure 1 - Schematic Indicating Coordinate Systems and Positive Directions of Measured Values

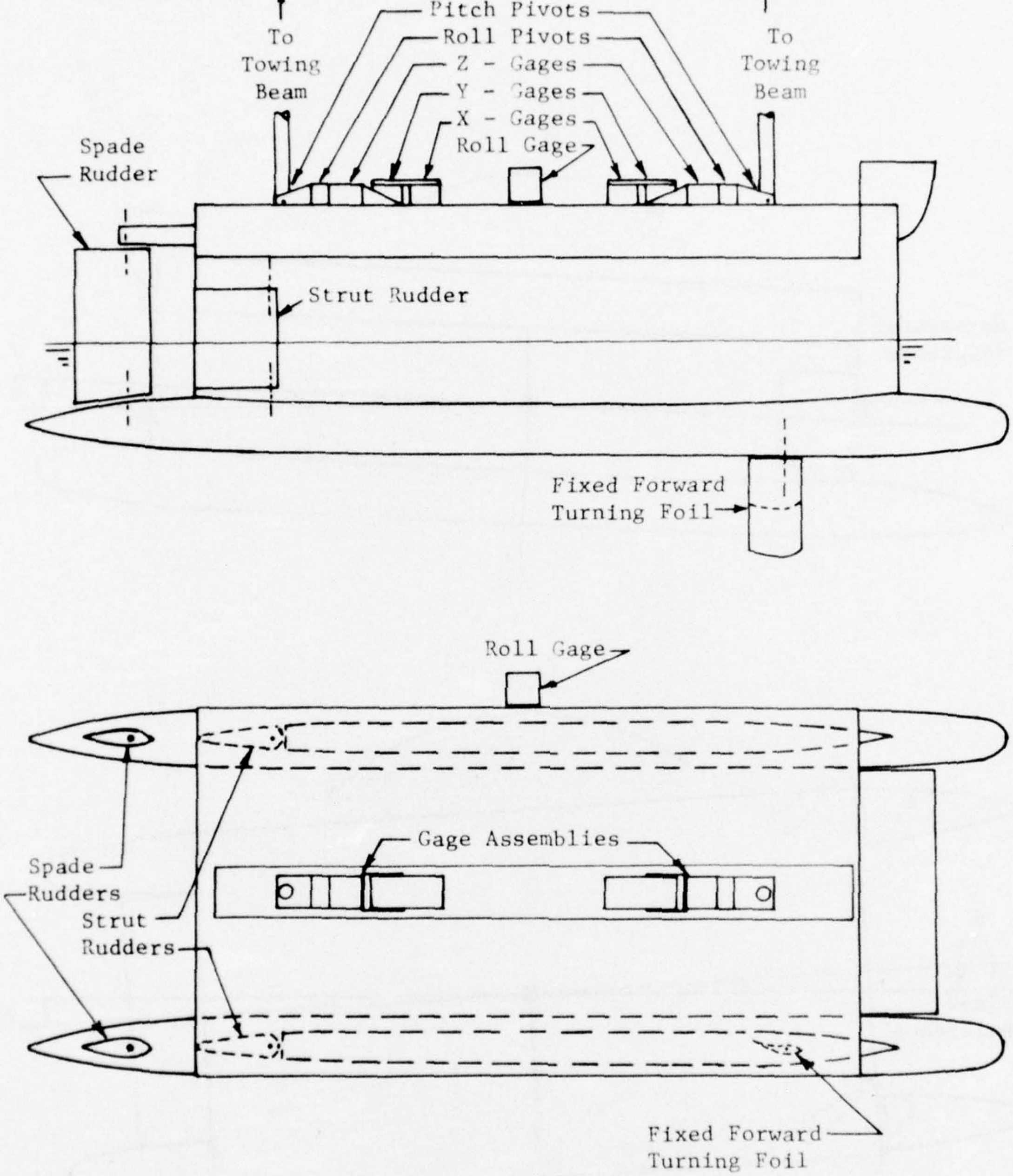

Figure 2 - Schematic for the SWATH IV-A Model Showing Locations of the Three Rudders Tested

PHOTOGRAPH LAY-UP SHEET NDW-NSRDC - 10700/2

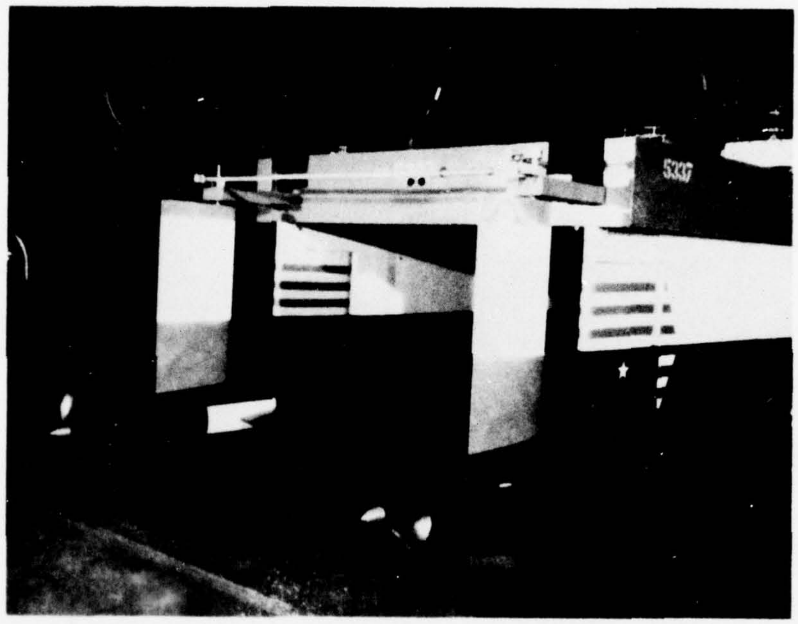

Figure 3 - Photograph of the SWATH 6A Model Showing the Spade and Strut Rudders

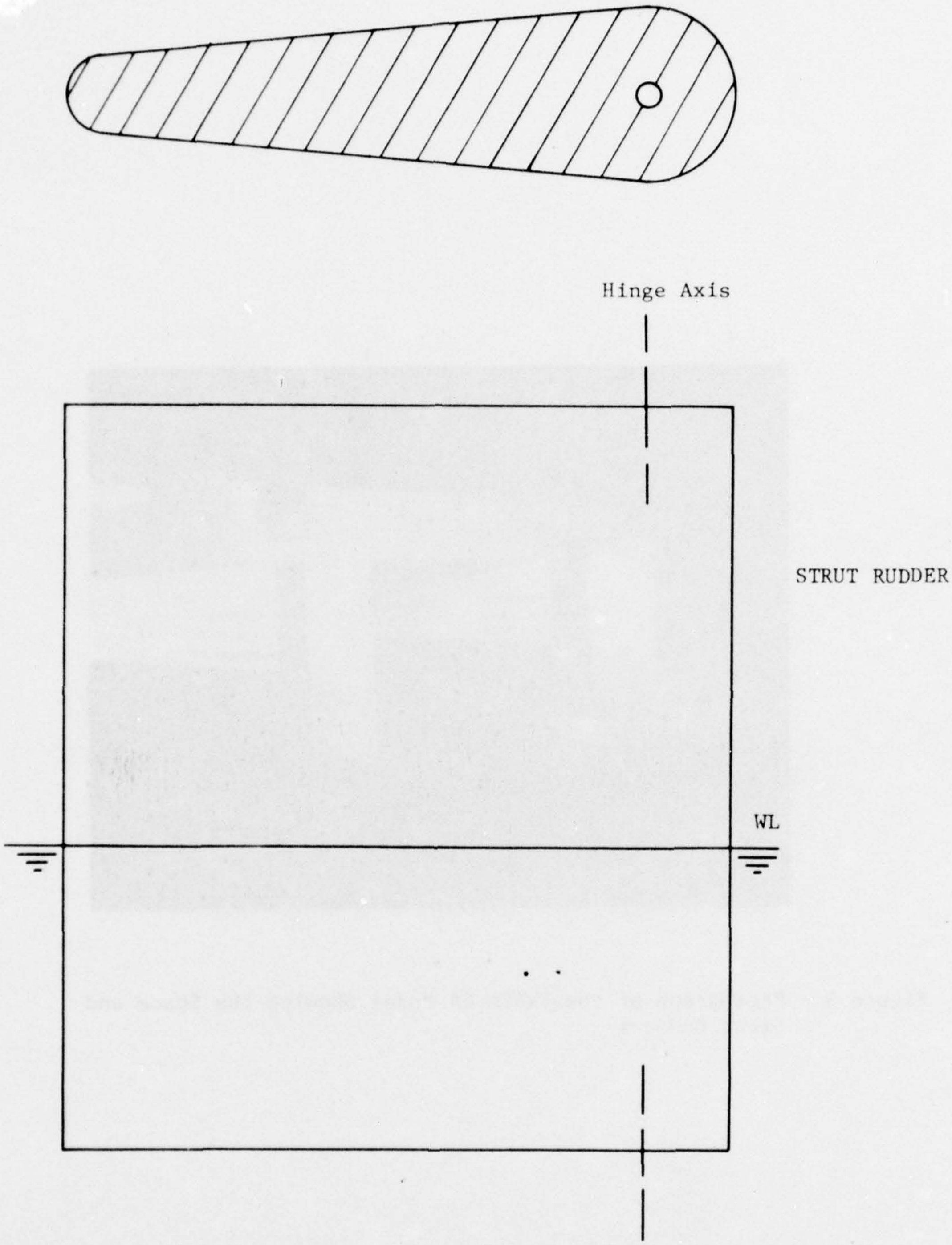

Figure 4 - Schematic of Strut Rudder

PHOTOGRAPH LAY-UP SHEET NDW-NSRDC - 10700/2

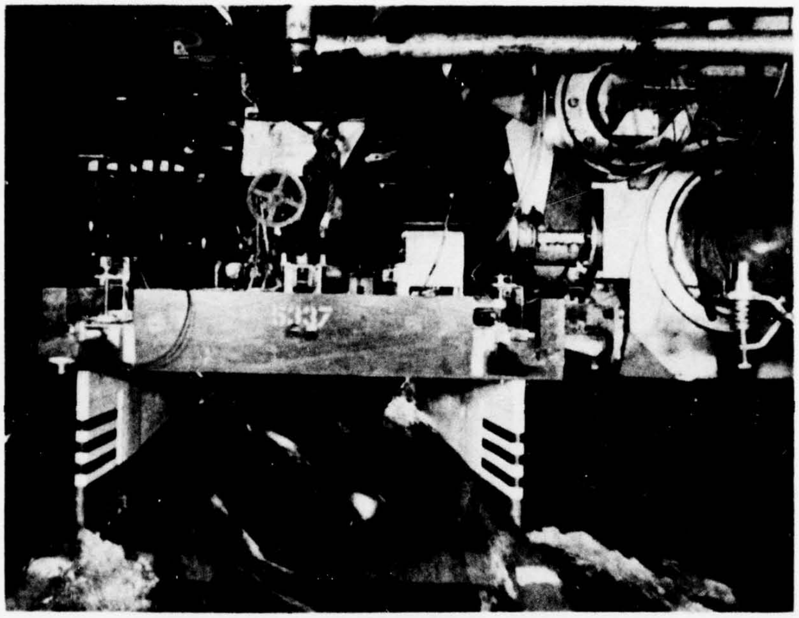

Figure 5 - Photograph of SWATH 6A Model with Strut Rudders Undergoing Experimeriments on the Rotating Arm at a Full Scale Speed of 20 Knots

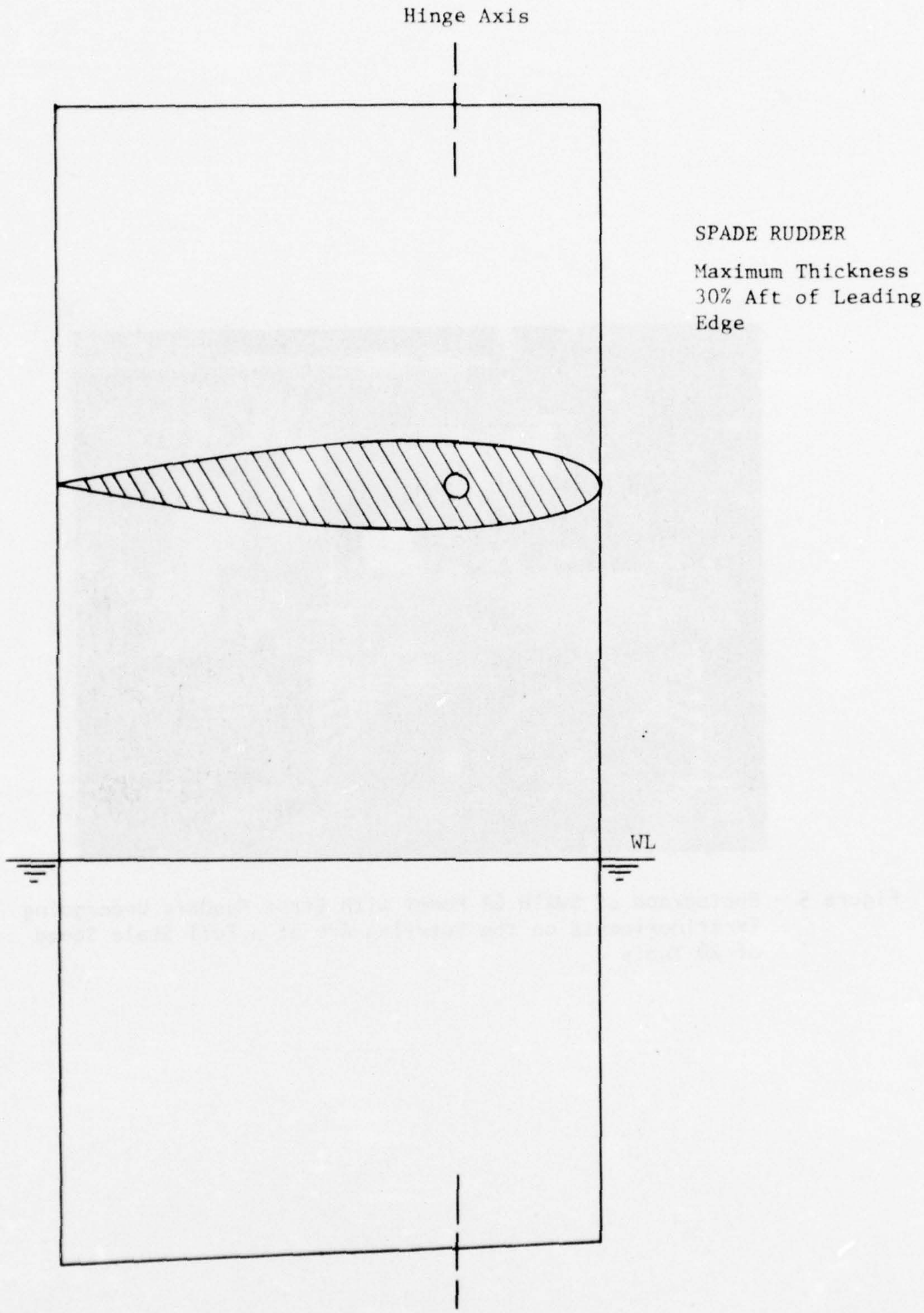

Figure 6 - Schematic of Spade Rudder

PHOTOGRAPH LAY-UP SHEET NDW-NSRDC - 10700/2

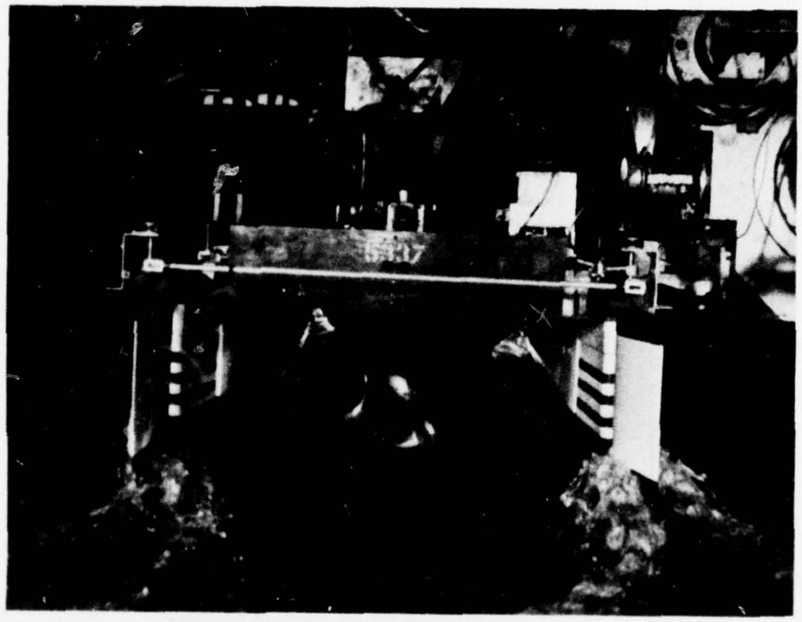

Figure 7 - Photograph of the SWATH 6A Model with Spade Rudders Undergoing Experiments on the Rotating Arm at a Full Scale Speed of 20 Knots

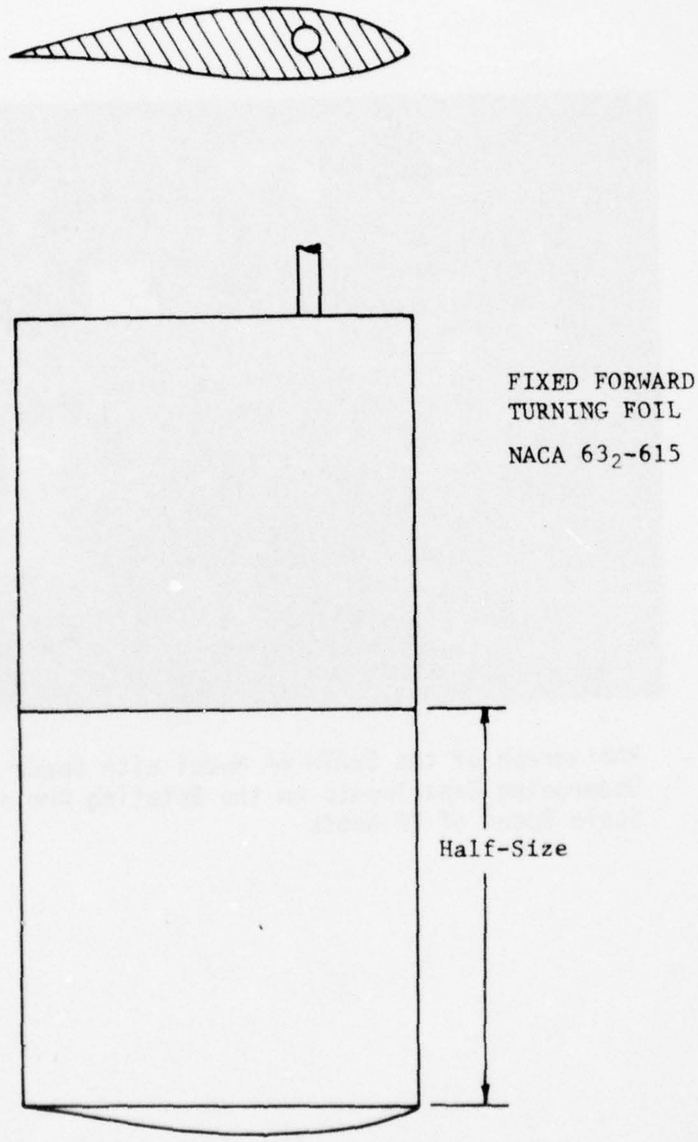

Figure 8 - Schematic of Full and Half-Sized Fixed Forward Turning Foil

PHOTOGRAPH LAY-UP SHEET NDW-NSRDC - 10700/2

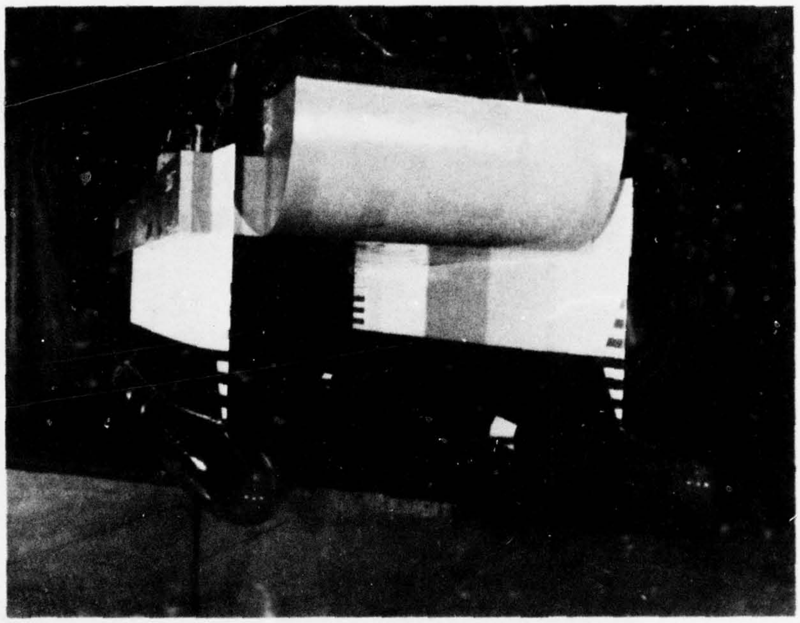

Figure 9 - Photograph of the SWATH 6A Model with Fixed Forward Turning Foil

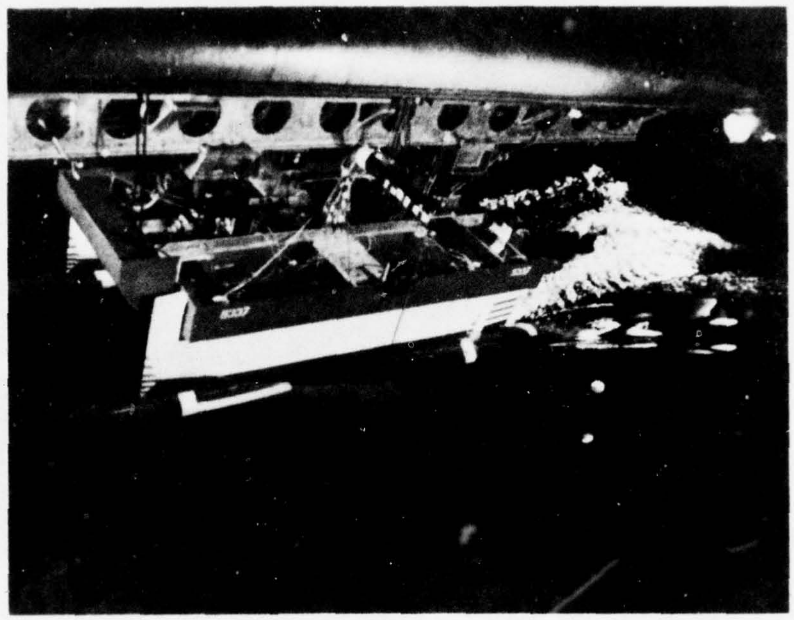

Figure 10 - Photograph of the SWATH 6A Model Undergoing Experiments on the Rotating Arm Showing the Bridging Structure

ROTATING ARM S W A T H V I T U R N I N G T E S T 12 MAY 1976

DESIGN DRAFT
FULL FIXED FWD. RUDDER

TURNING RADIUS : 34.93 FT

MEAS SPEED = 4.19 KNOTS
NOMN SPEED = 4.22 KNOTS

RUN NO 1000

TIME: 0.000 - 5.500
RECORDS: 1 - 5

	CHAN		CALIB	GAIN	MEAN	STDDEV	ROOTOO
1	ROTSPEED	DPS	4.000E 00	1.000E 00	1.159E 01	1.767E-01	2.499E-01
2	ROLL	DEG	4.000E 00	2.000E 00	2.795E 00	8.023E-03	1.135E-02
3	DRIFT	DEG	4.000E 00	4.000E 00	4.385E-02	3.717E-04	5.257E-04
4	XFORCE 1	LBS	2.500E 02	1.000E 01	-5.023E 00	1.949E 00	2.757E 00
5	XFORCE 2	LBS	2.500E 02	1.000E 01	8.152E 00	3.084E 00	4.362E 00
6	YFORCE 1	LBS	1.250E 02	5.000E 00	-2.486E 01	2.072E 00	2.931E 00
7	YFORCE 2	LBS	1.250E 02	5.000E 00	5.631E 01	2.456E 00	3.473E 00
8	ZFORCE 1	LBS	2.500E 02	1.000E 01	2.324E 00	5.019E 00	7.098E 00
9	ZFORCE 2	LBS	2.500E 02	1.000E 01	-1.844E 01	4.719E 00	6.674E 00
10	ZFORCE R	LBS	-2.500E 02	1.000E 01	3.822E 01	1.805E 00	2.553E 00
11	RUDER PT	DEG	4.000E 01	4.000E 00	4.139E-01	3.533E-03	4.997E-03
12	RUDER SB	DEG	4.000E 01	4.000E 00	1.000E 02	1.348E-01	1.907E-01
13	RUDRTORO	INLB	0.000E 00	1.000E 00	0.000E 00	0.000E 00	0.000E 00
14	PT PROP	RPM	1.000E 02	5.000E-01	5.273E 02	7.288E 01	1.031E 02
15	SB PROP	RPM	1.000E 02	5.000E-01	6.576E 02	4.991E 01	7.058E 01
16	H2O LEVL	IN	0.000E 00	1.000E 00	0.000E 00	0.000E 00	0.000E 00

Figure 11 - First Page of Computer Printout Showing List of Data for Each Channel

```
ROTATING ARM              S W A T H   V I   T U R N I N G   T E S T                12 MAY 1976

                                     DESIGN DRAFT
                                 FULL FIXED FWD. RUDDER

                             TURNING RADIUS :  34.93 FT

                                MEAS SPEED =    4.19 KNOTS
                                NOMN SPEED =    4.22 KNOTS

   RUN NO 1000                                                          TIME:        0.000 -    5.500
                                                                        RECORDS:       1   -      5

   ROLL ANGLE :   2.80 DEG          MODEL SPEED :  7.064 FPS            DRIFT ANGLE :   0.04 DEG

 YAW RATE [R'] :  0.3054            RUDDER ANGLE :   0.41 DEG           SWAY VELOCITY : -0.005 FPS

                             CENTRIPEDAL FORCE :  2.735544E 01 LBS
                                                  1.240821E 01 NWT

C.F. COMP. (LBS):      CX =  2.093442E-02         CY =  2.732288E 01        CZ =  1.334033E 00
           [NWT]            [ 9.495690E-03]          [ 1.239345E 01]           [ 6.051070E-01]

FORCES     (LBS):      FX =  3.149568E 00         FY =  5.876675E 01        FZ =  2.076237E 01
           [NWT]            [ 1.428619E 00]          [ 2.665614E 01]           [ 9.417652E 00]
        (NON-DIM)           ( 5.757790E-04)          ( 1.074327E-02)           ( 3.795613E-03)

MOMENTS  (IN-LB):    ROLL = -1.007991E 03      PITCH = -6.558203E 02      YAW = -2.394493E 03
          [NWT-M]           [-1.161331E 01]          [-7.555868E 00]           [-2.758754E 01]
        (NON-DIM)           (-1.439633E-03)          (-9.366553E-04)           (-3.419862E-03)
```

Figure 11a - Second Page of Computer Printout Showing List of Forces and Moments About Reference Point

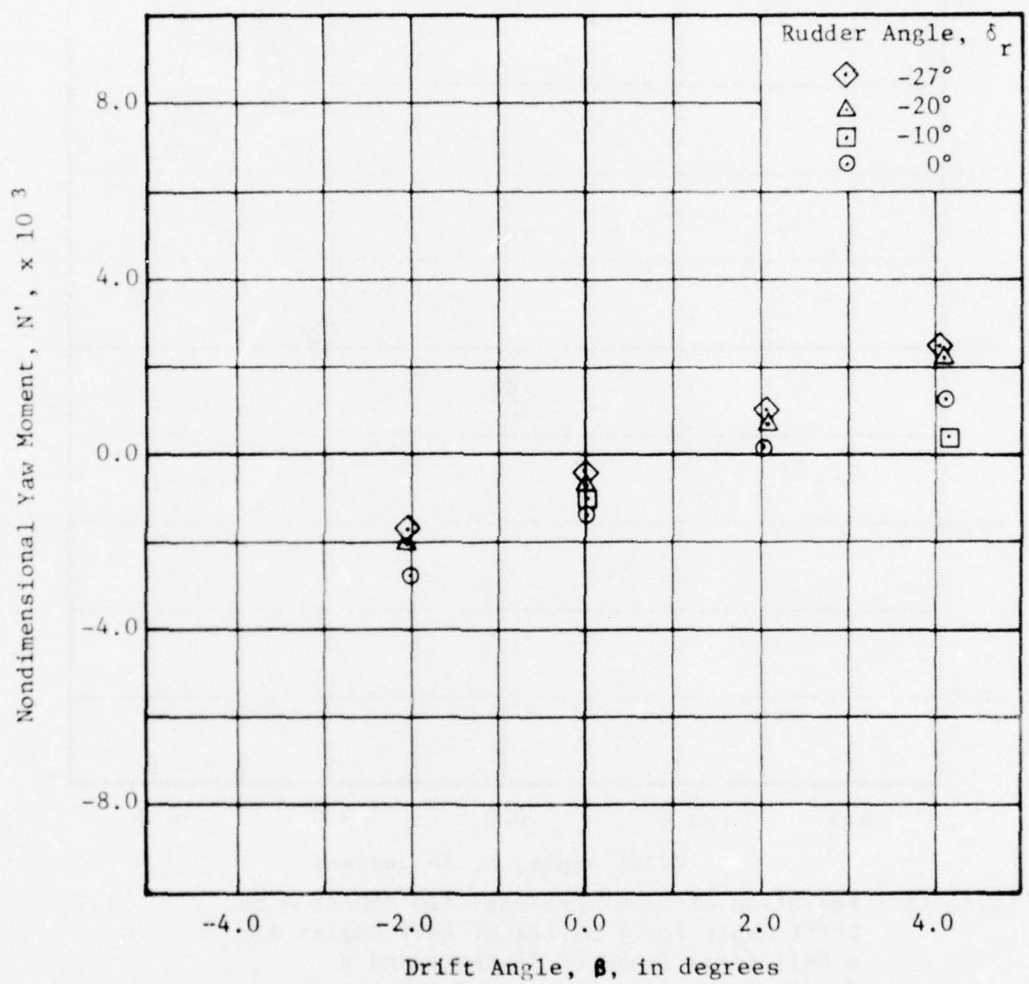

Figure 12 - Variation of Nondimensional Yaw Moment with Drift Angle for a Series of Rudder Angles at a Full Scale Speed of 25 Knots and a Nondimensional Yaw Rate of 0.093 for the Strut Rudder at Deep Draft

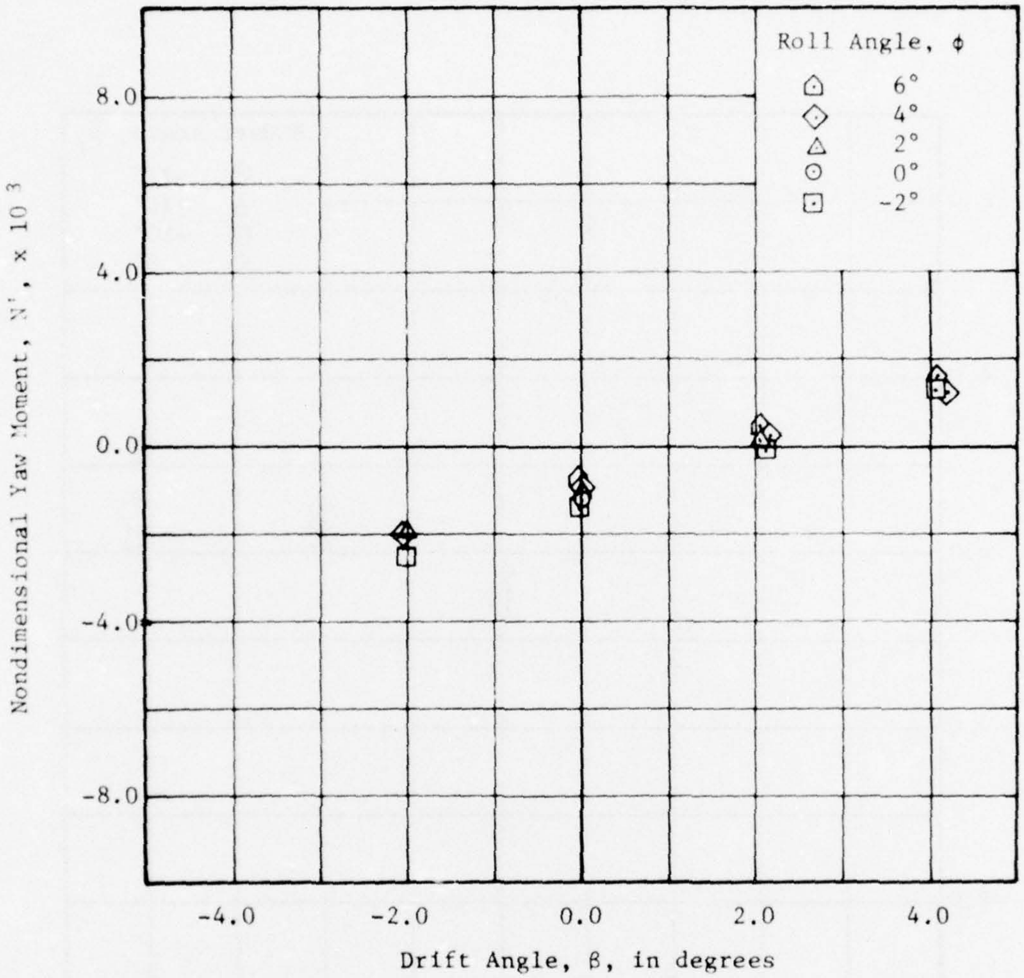

Figure 13 - Variation of Nondimensional Yaw Moment with Drift Angle for a Series of Roll Angles at a Full Scale Speed of 25 Knots and a Nondimensional Yaw Rate of 0.093 for the Strut Rudder at Design Draft

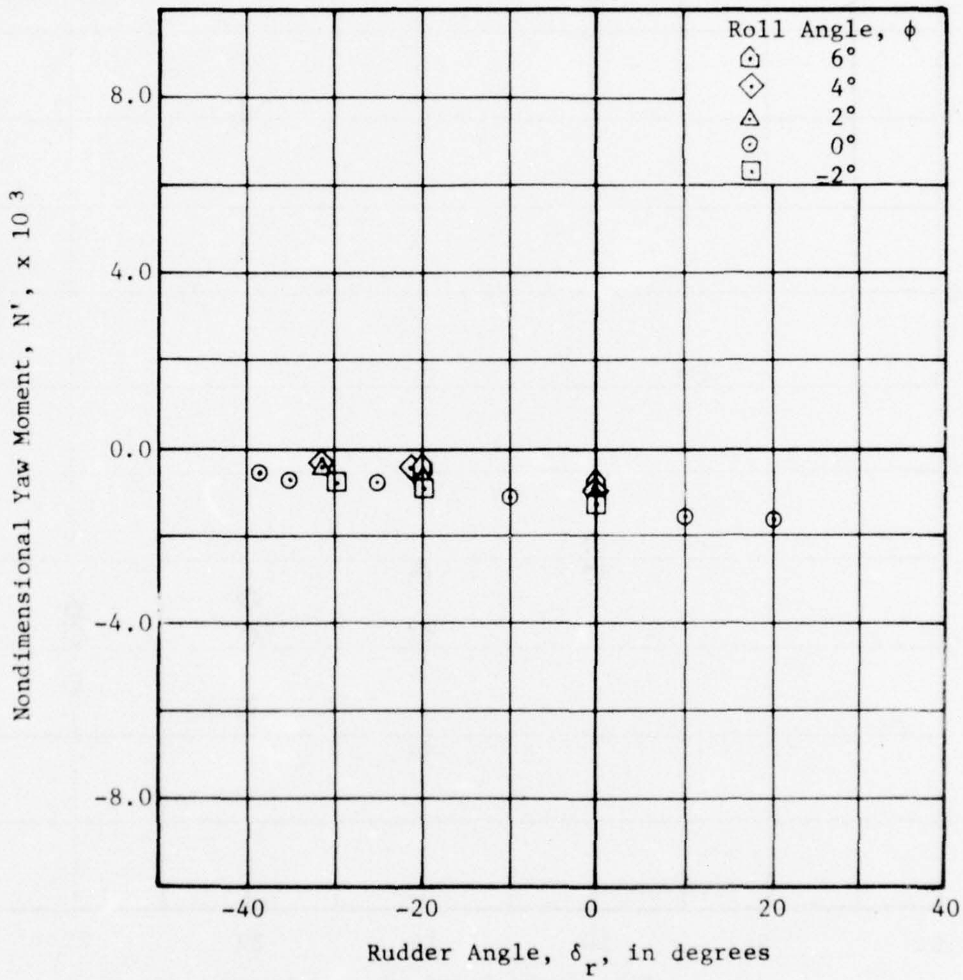

Figure 14 - Variation of Nondimensional Yaw Moment with Rudder Angle for a Series of Roll Angles at a Full Scale Speed of 25 Knots and a Nondimensional Yaw Rate of 0.093 for the Strut Rudder at Design Draft

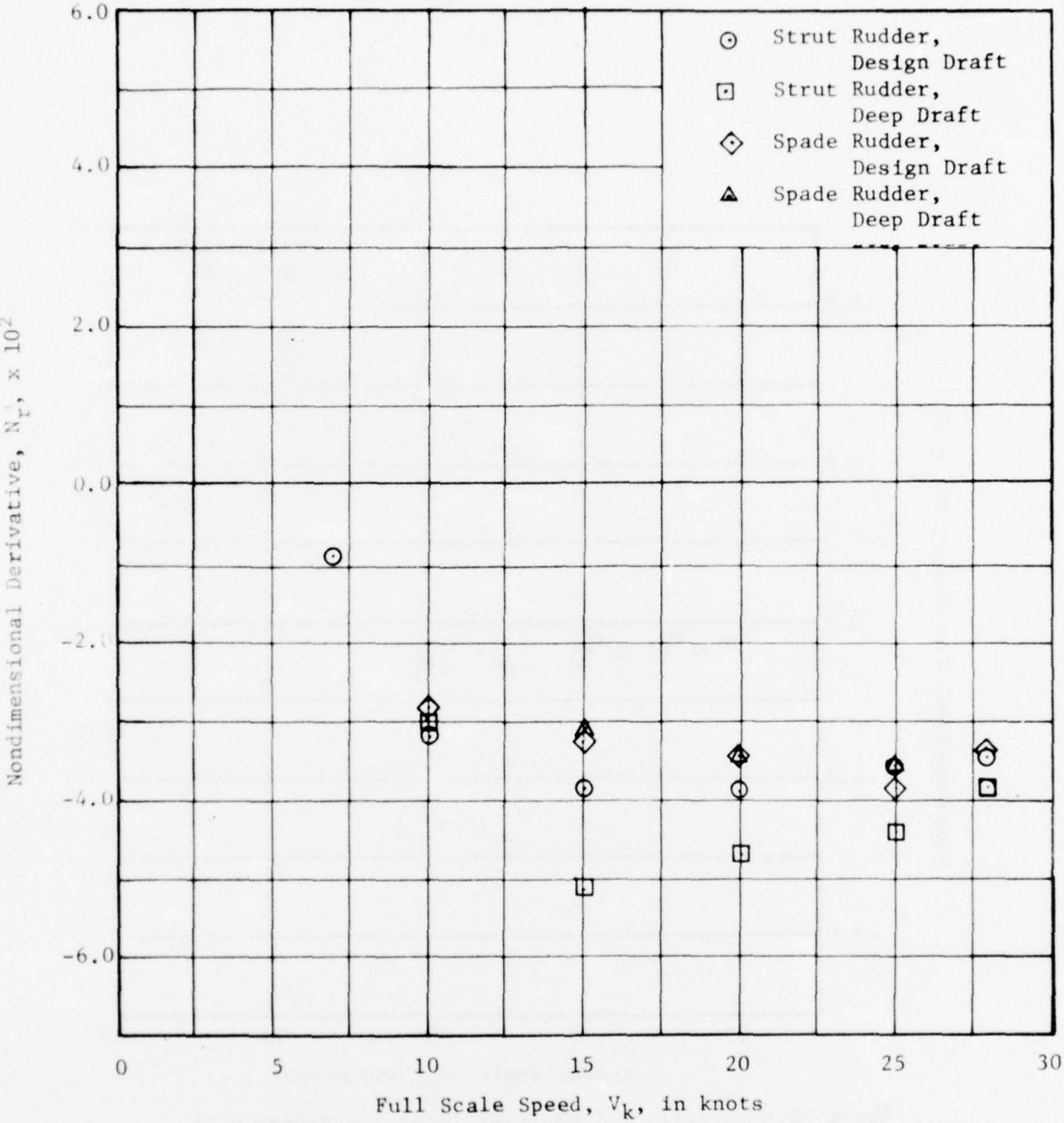

Figure 15 - Variation of Nondimensional Derivative, N_r', with Full Scale Speed for a Series of Rudder and Draft Configurations

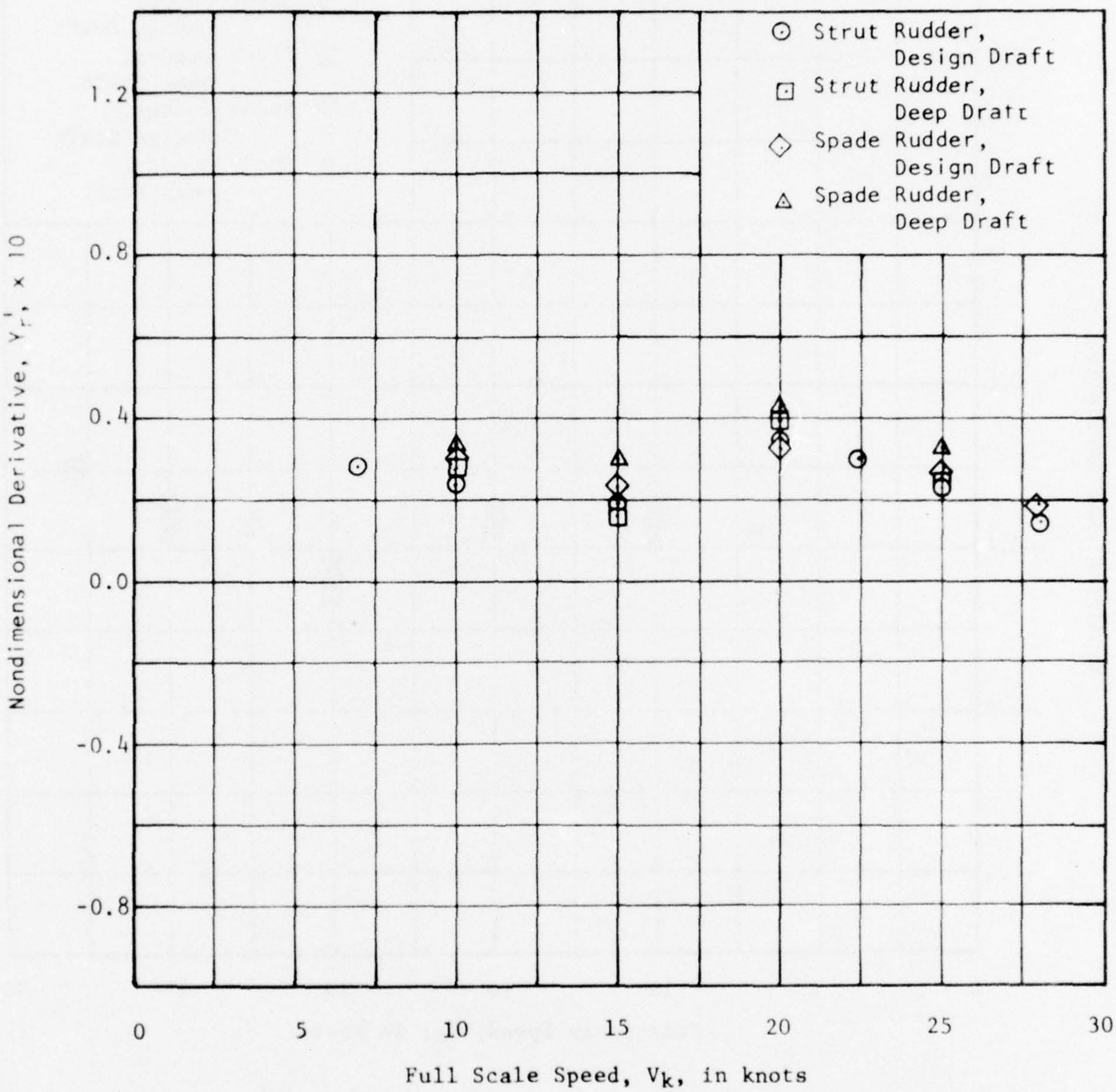

Figure 16 - Variation of Nondimensional Derivative, Y_r', with Full Scale Speed for a Series of Rudder and Draft Configurations

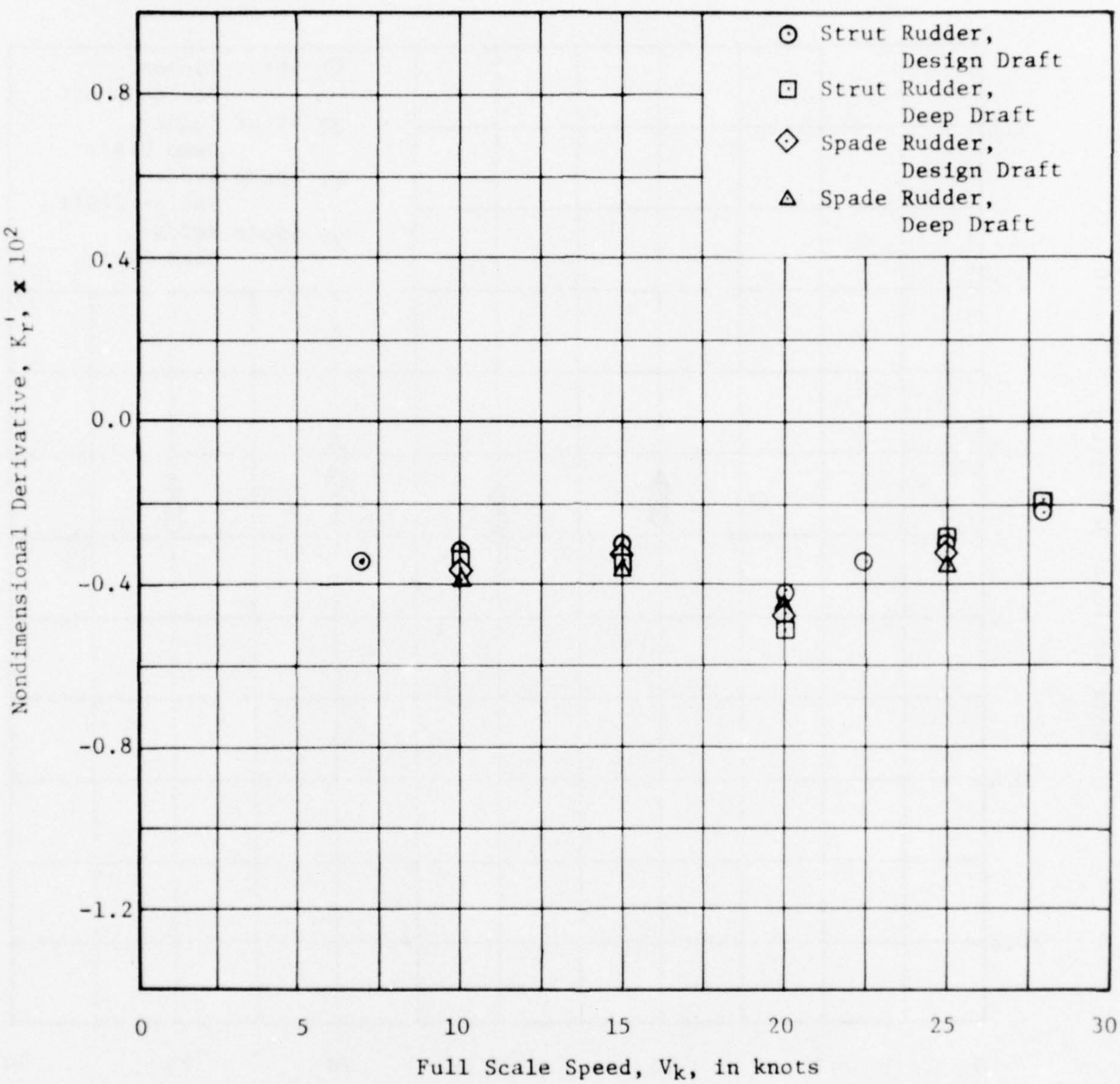

Figure 17 - Variation of Nondimensional Derivative, K_r', with Full Scale Speed for a Series of Rudder and Draft Configurations

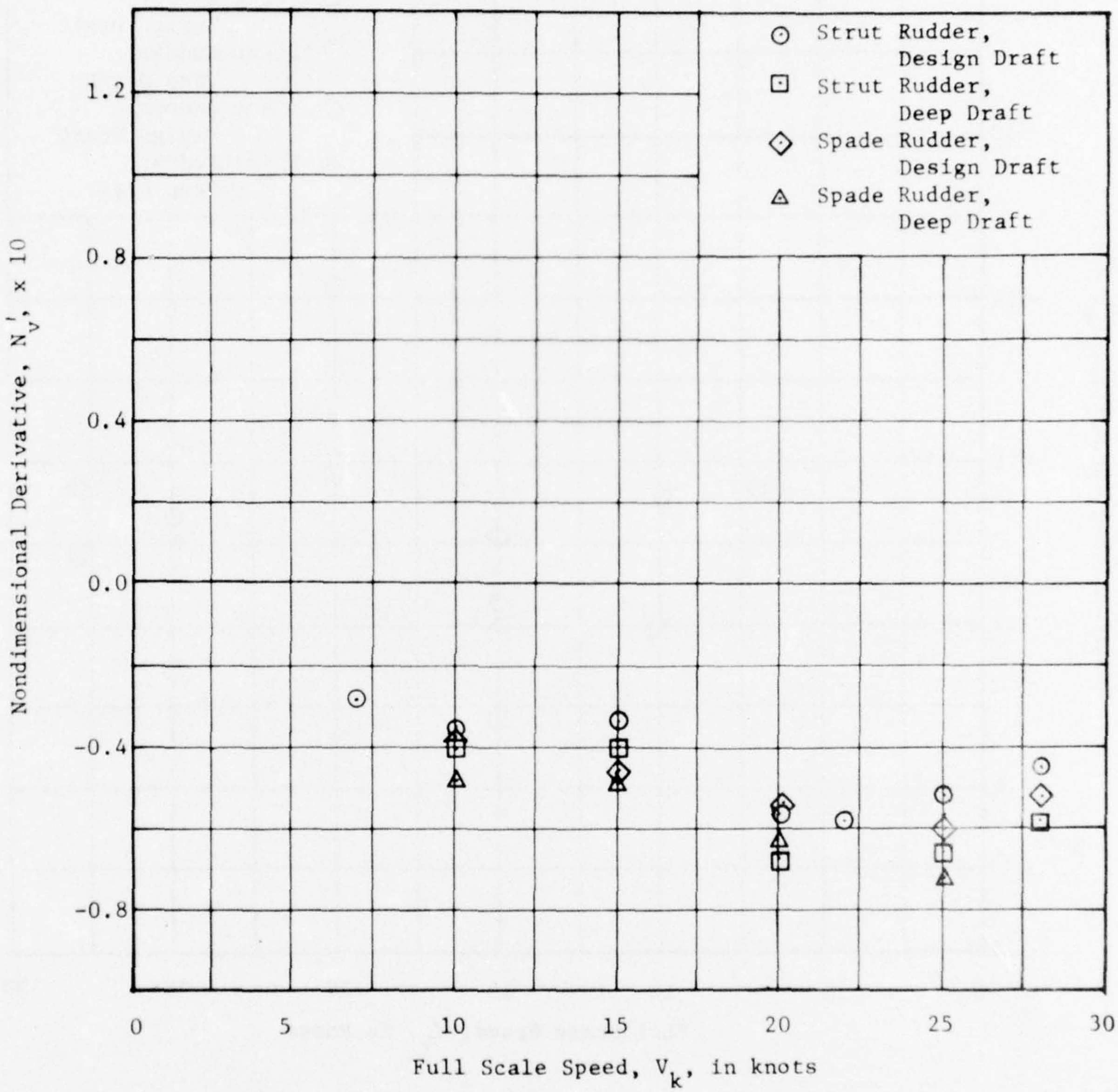

Figure 18 - Variation of Nondimensional Derivative, N_v', with Full Scale Speed for a Series of Rudder and Draft Configurations

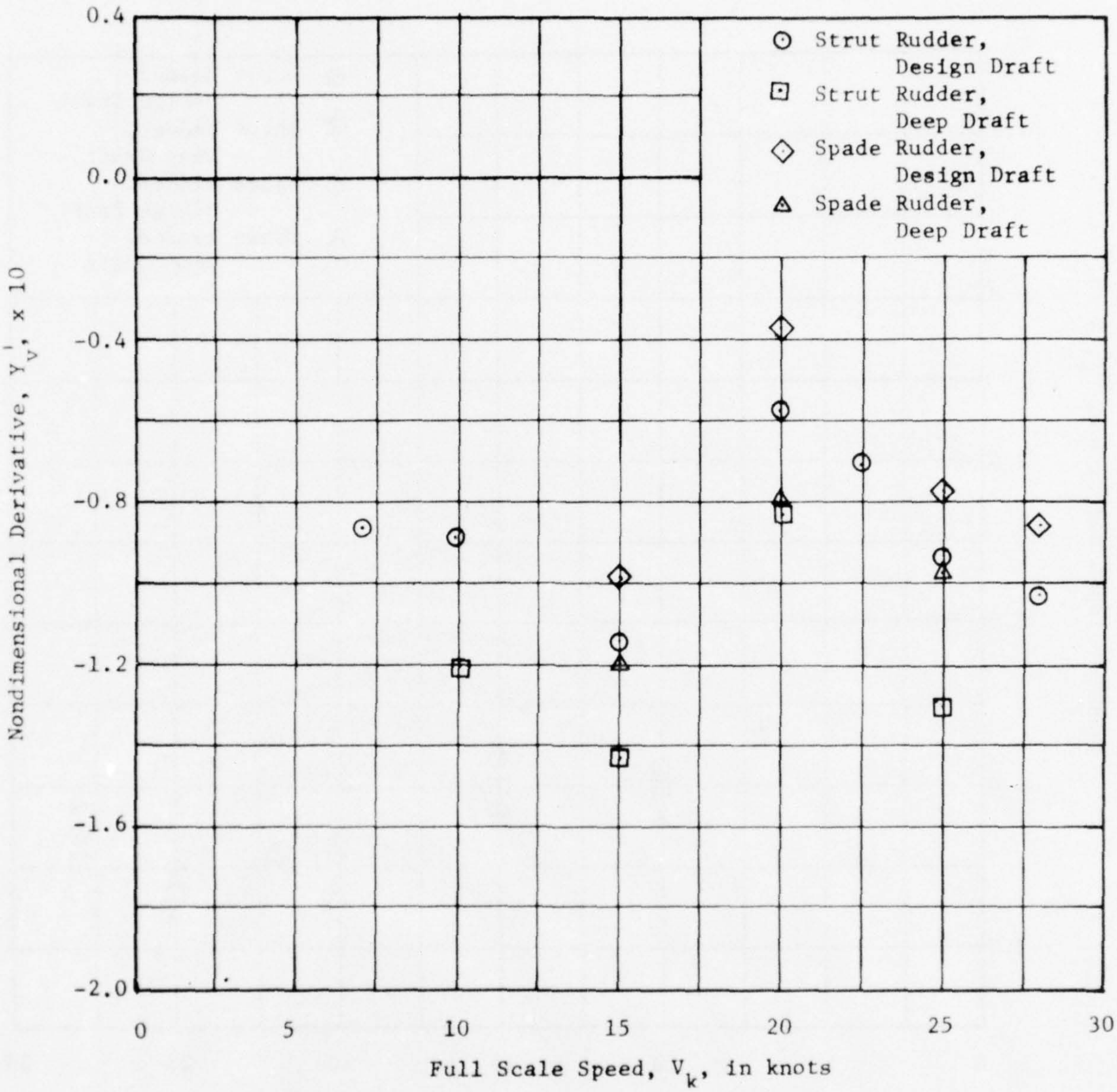

Figure 19 - Variation of Nondimensional Derivative, Y_v', with Full Scale Speed for a Series of Rudder and Draft Configurations

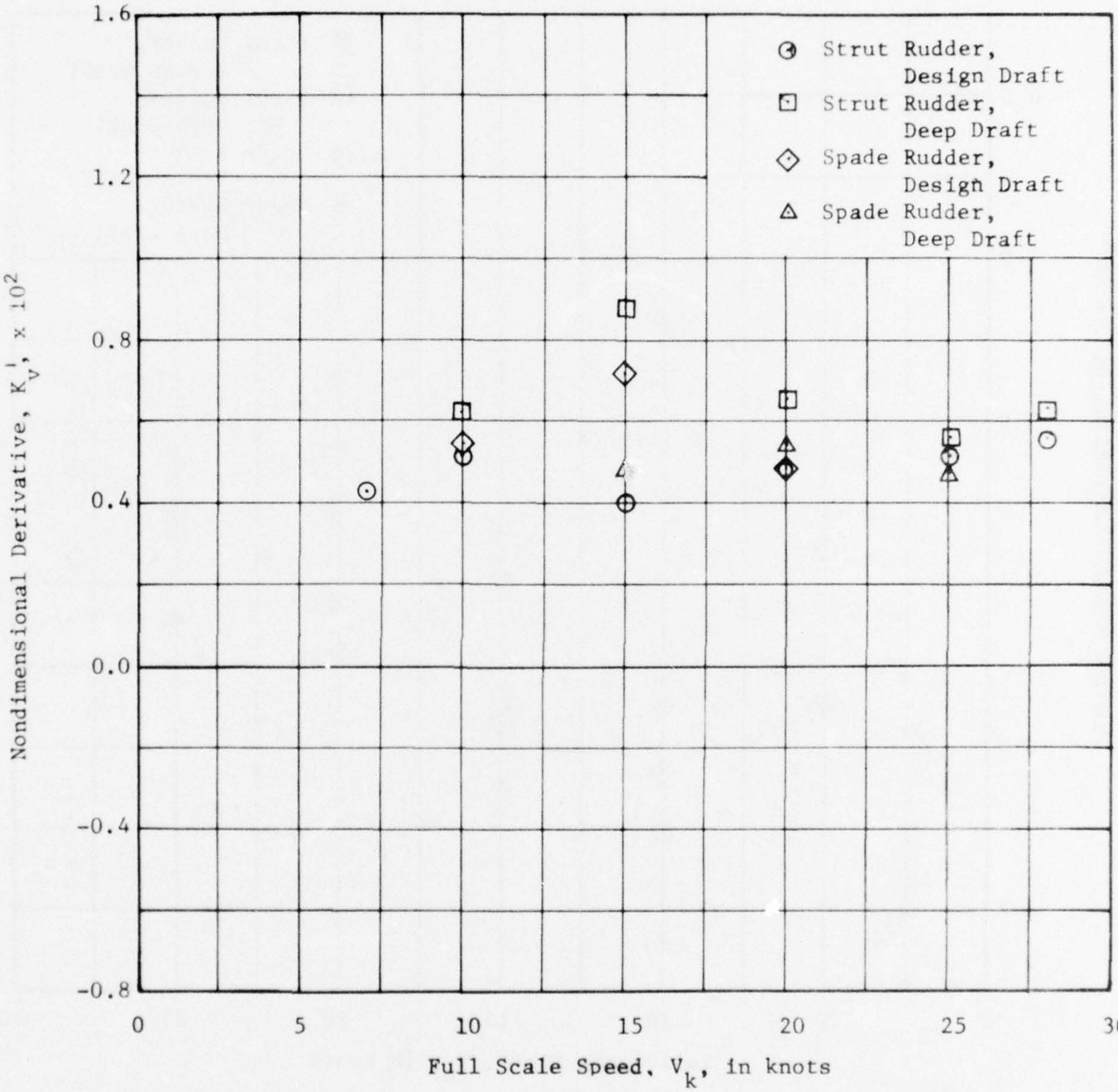

Figure 20 - Variation of Nondimensional Derivative, K_v', with Full Scale Speed for a Series fo Rudder and Draft Configurations

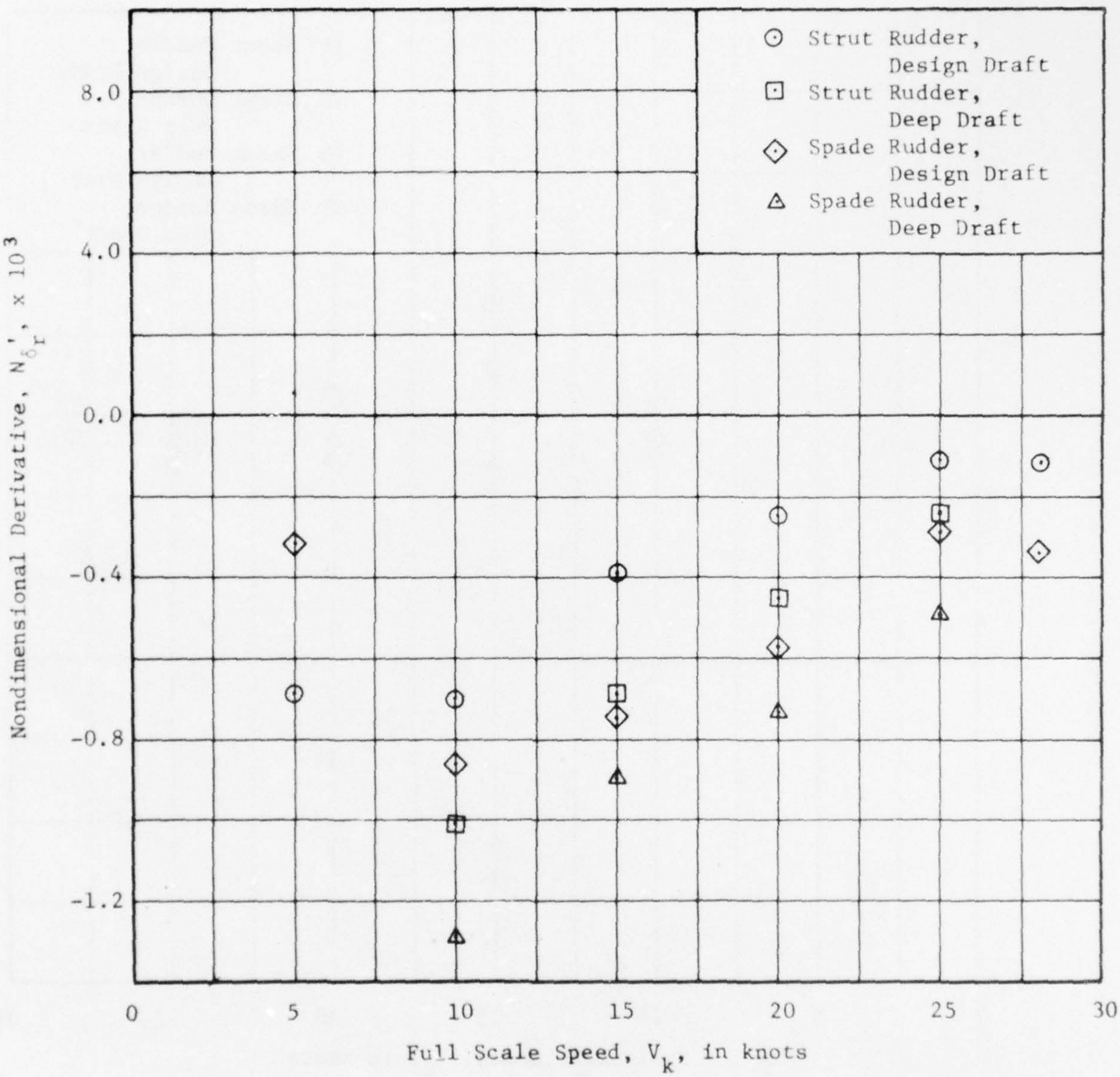

Figure 21 - Variation of Nondimensional Derivative, $N\delta_r'$, with Full Scale Speed for a Series of Rudder and Draft Configurations

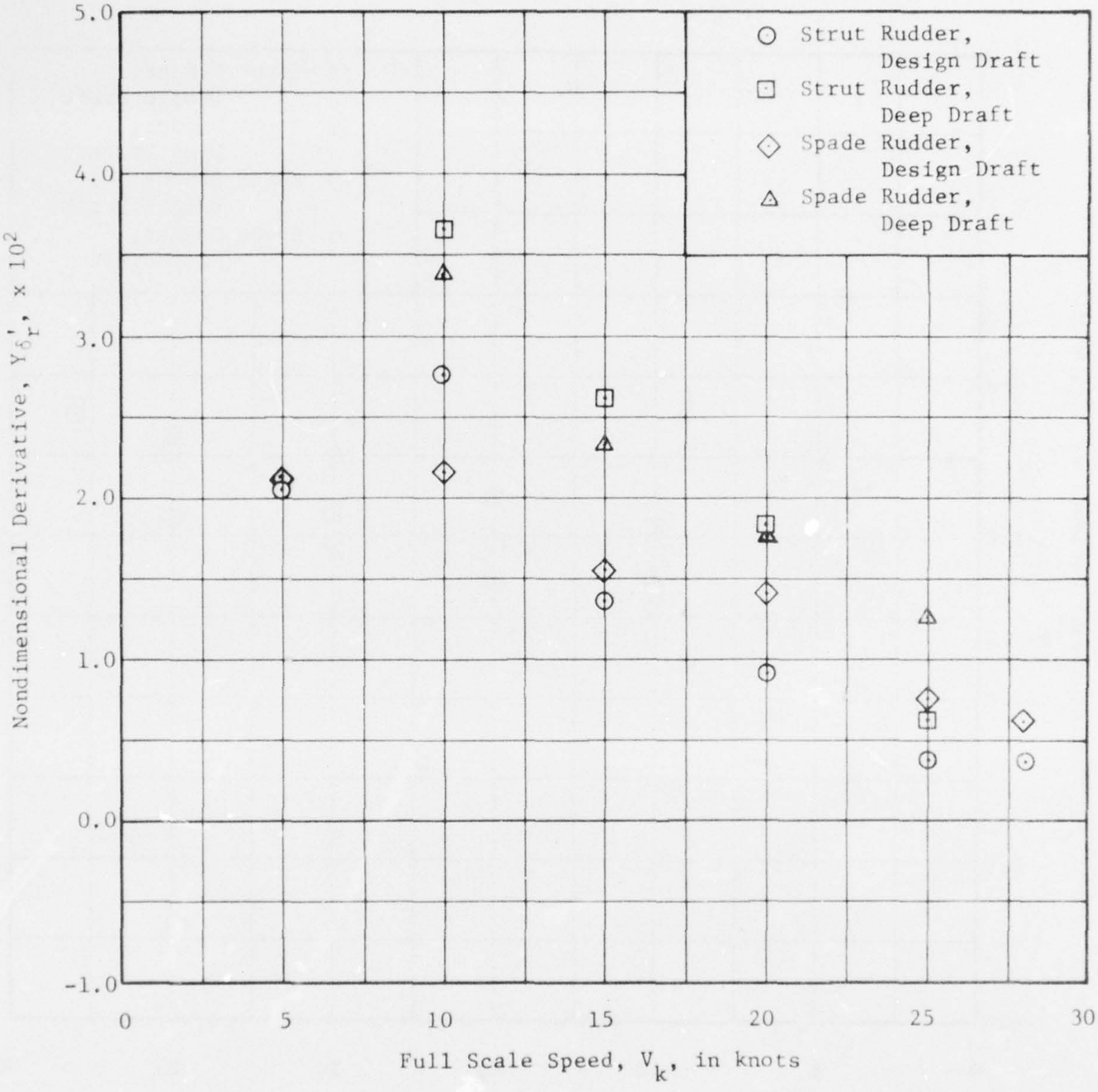

Figure 22 - Variation of Nondimensional Derivative, Y_{δ_r}', with Full Scale Speed for a Series of Rudder and Draft Configurations

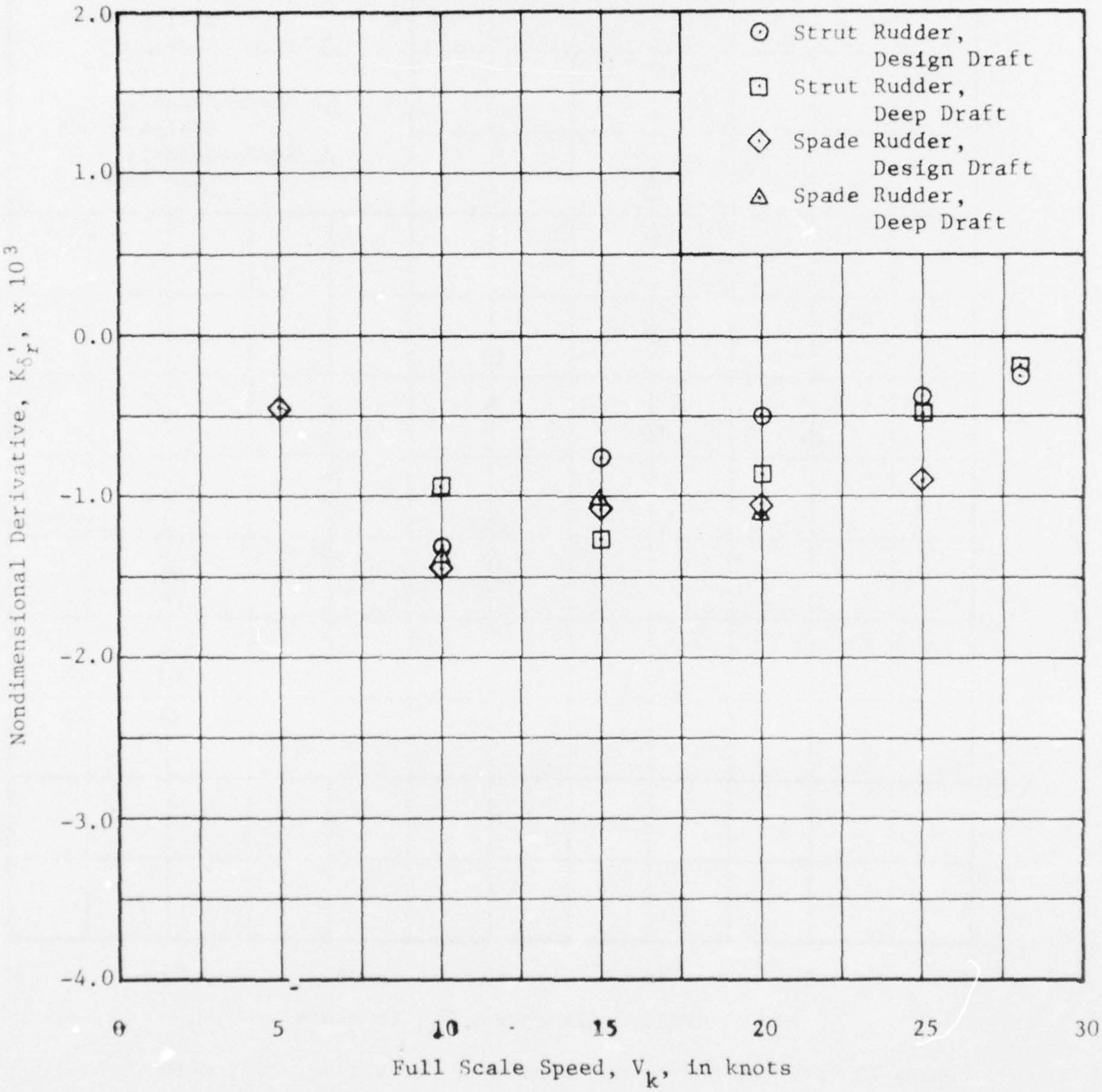

Figure 23 - Variation of Nondimensional Derivative, K_{δ_r}', with Full Scale Speed for a Series of Rudder and Draft Configurations

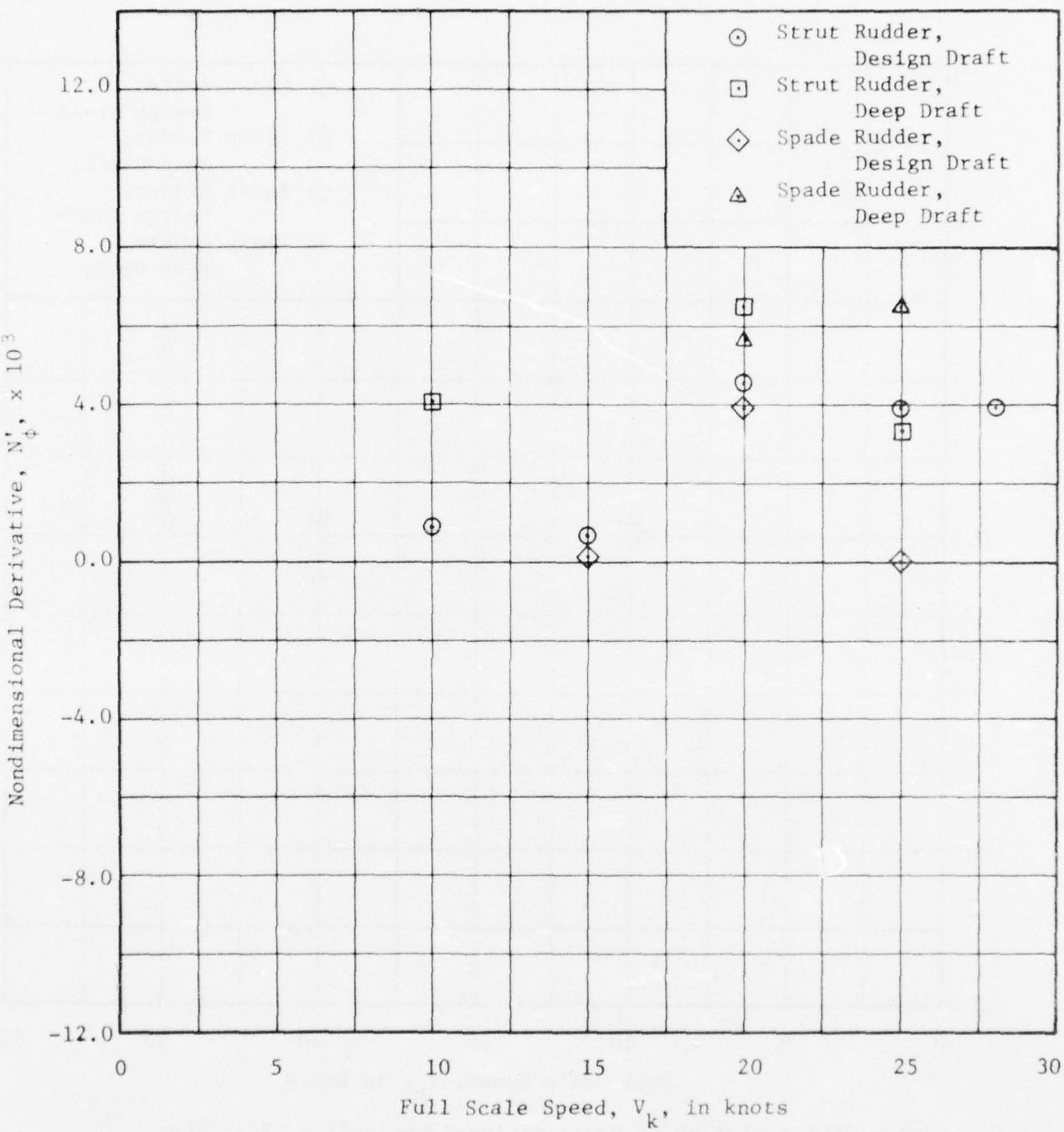

Figure 24 - Variation of Nondimensional Derivative, N'_ϕ, with Full Scale Speed for a Series of Rudder and Draft Configurations

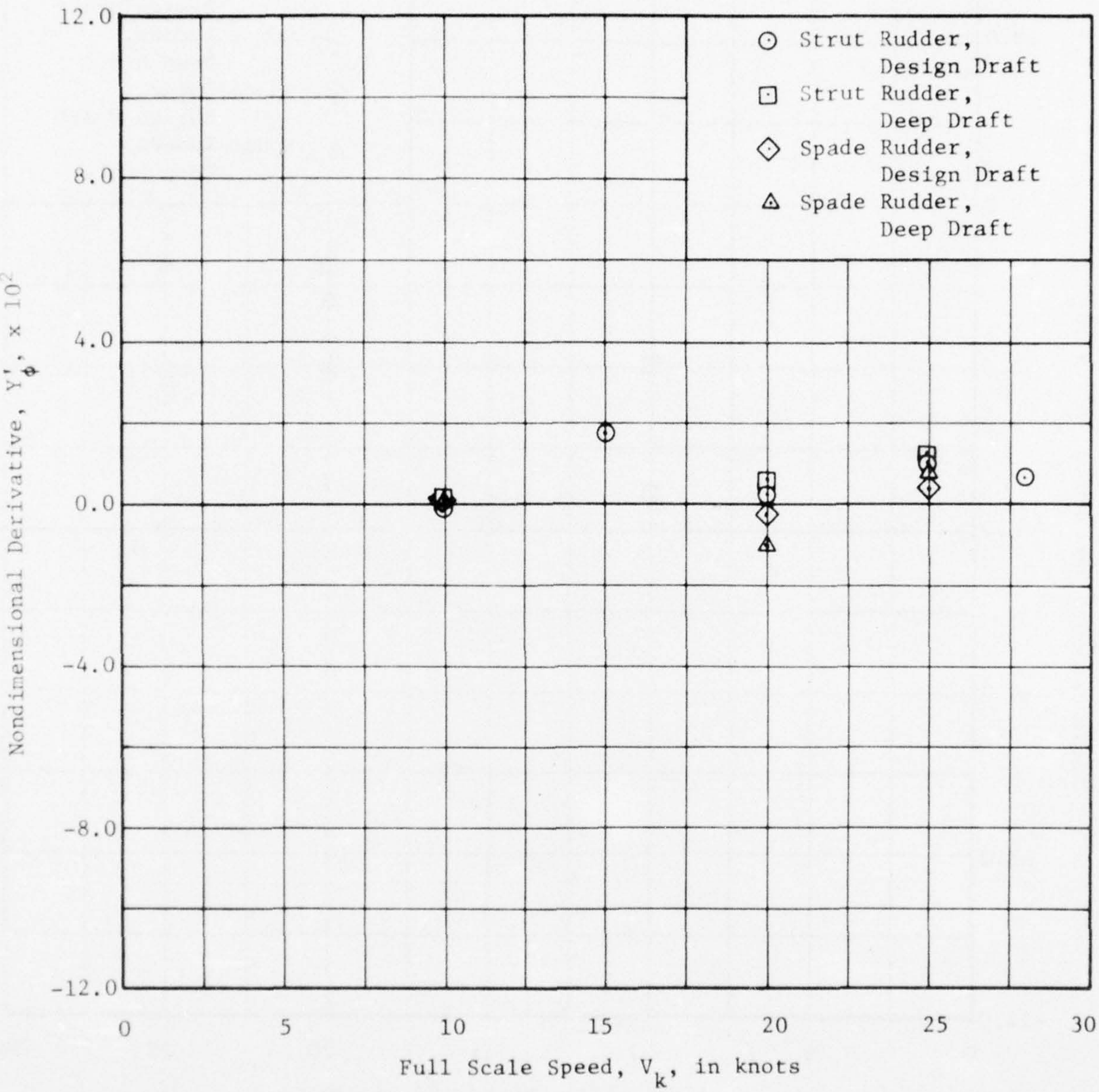

Figure 25 - Variation of Nondimensional Derivative, Y'_ϕ, with Full Scale Speed for a Series of Rudder and Draft Configurations

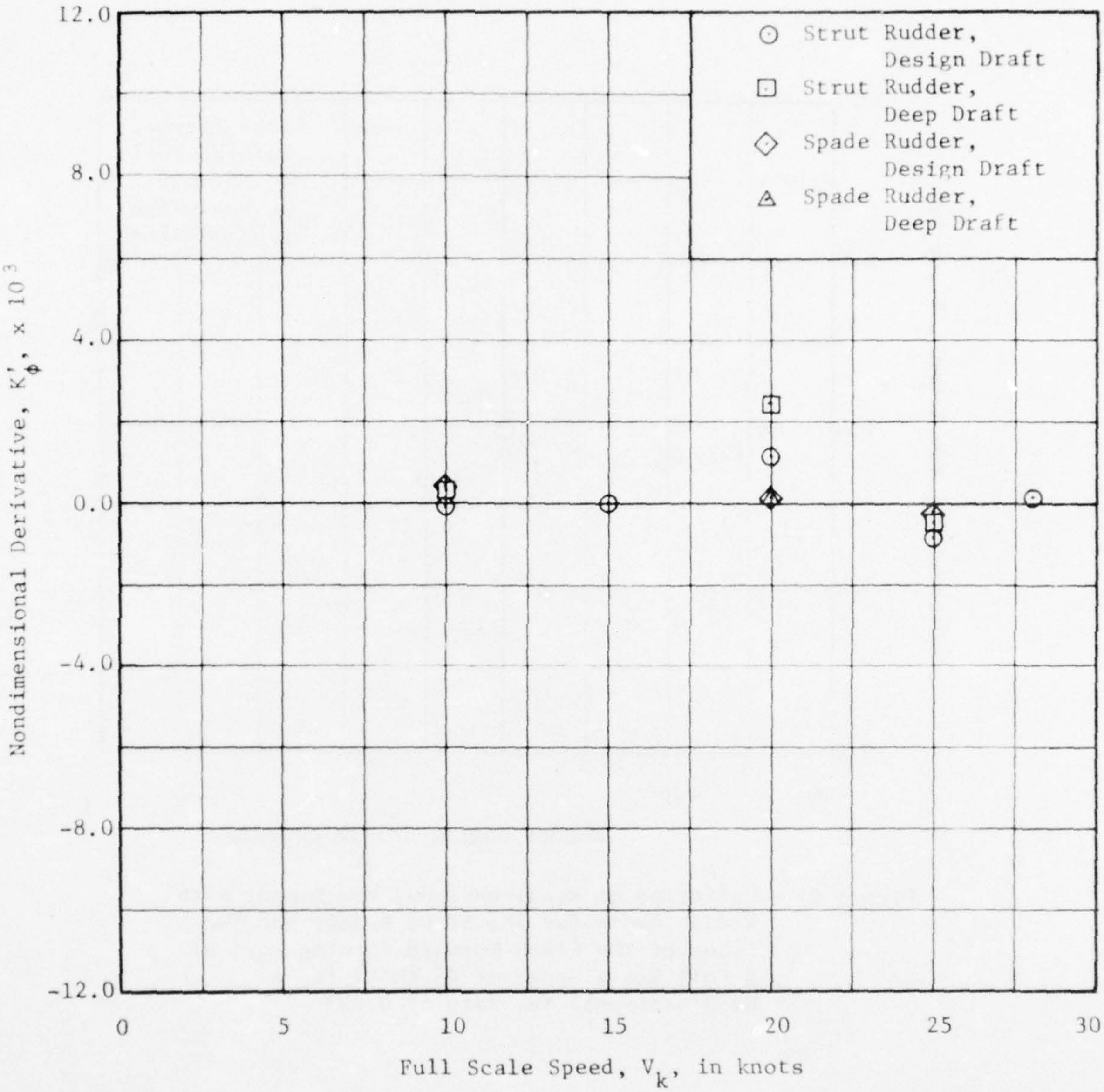

Figure 26 - Variation of Nondimensional Derivative, K'_ϕ, with Full Scale Speed for a Series of Rudder and Draft Configurations

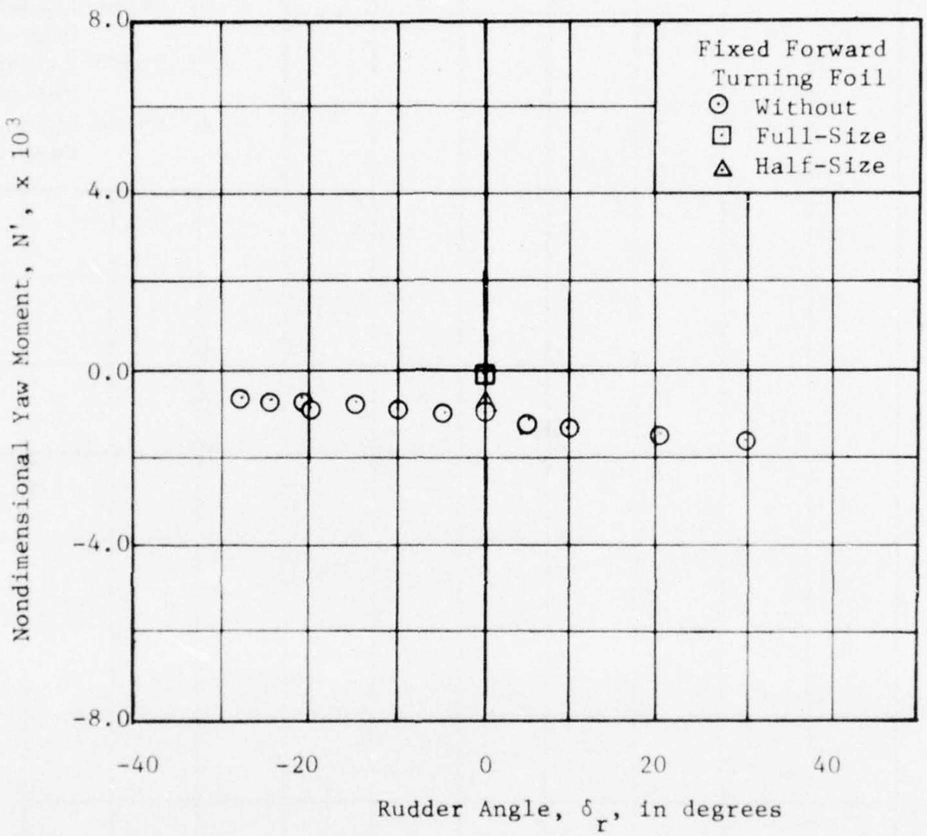

Figure 27 - Variation of Nondimensional Yaw Moment with Rudder Angle for the Strut Rudder and Two Sizes of the Fixed Forward Turning Foil at a Full Scale Speed of 25 Knots for a Nondimensional Yaw Rate of 0.093

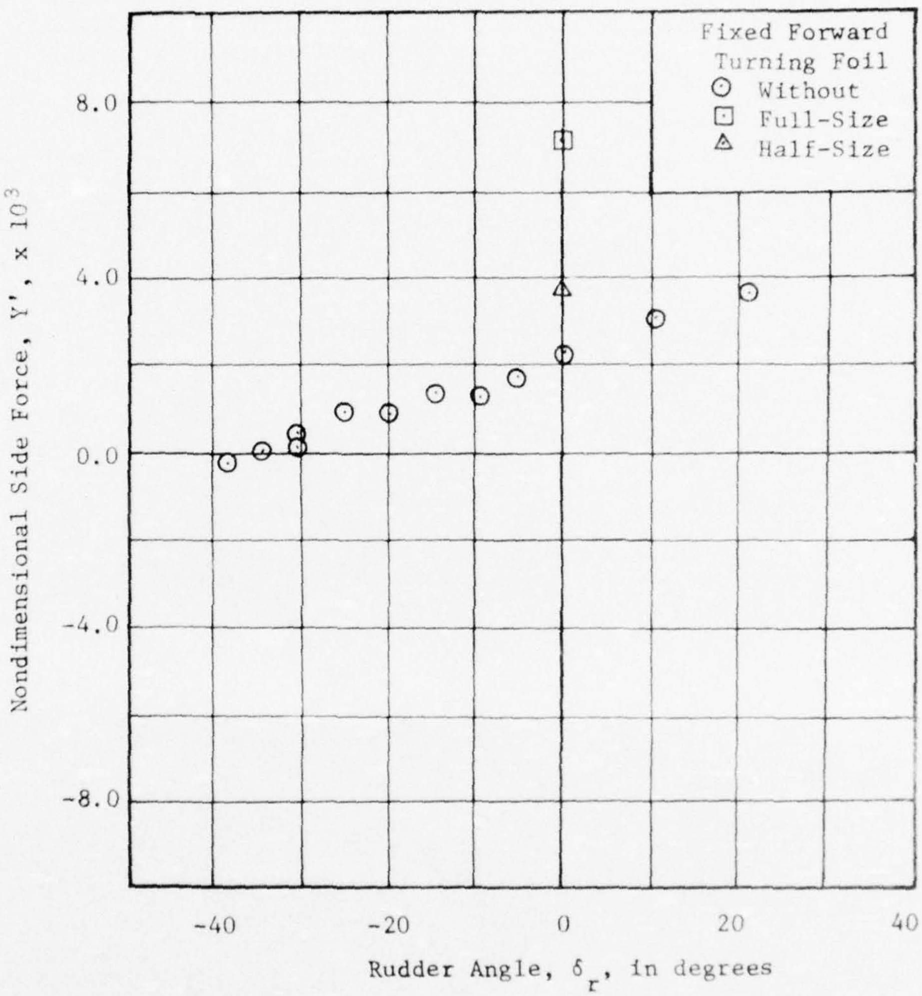

Figure 28 - Variation of Nondimensional Side Force with Rudder Angle for the Strut Rudder and Two Sizes of the Fixed Forward Turning Foil at a Full Scale Speed of 25 Knots for a Nondimensional Yaw Rate of 0.093

Appendix A

(Figures 29 to 83)
Nondimensional Data Curves for
the Strut Rudder at Design Draft

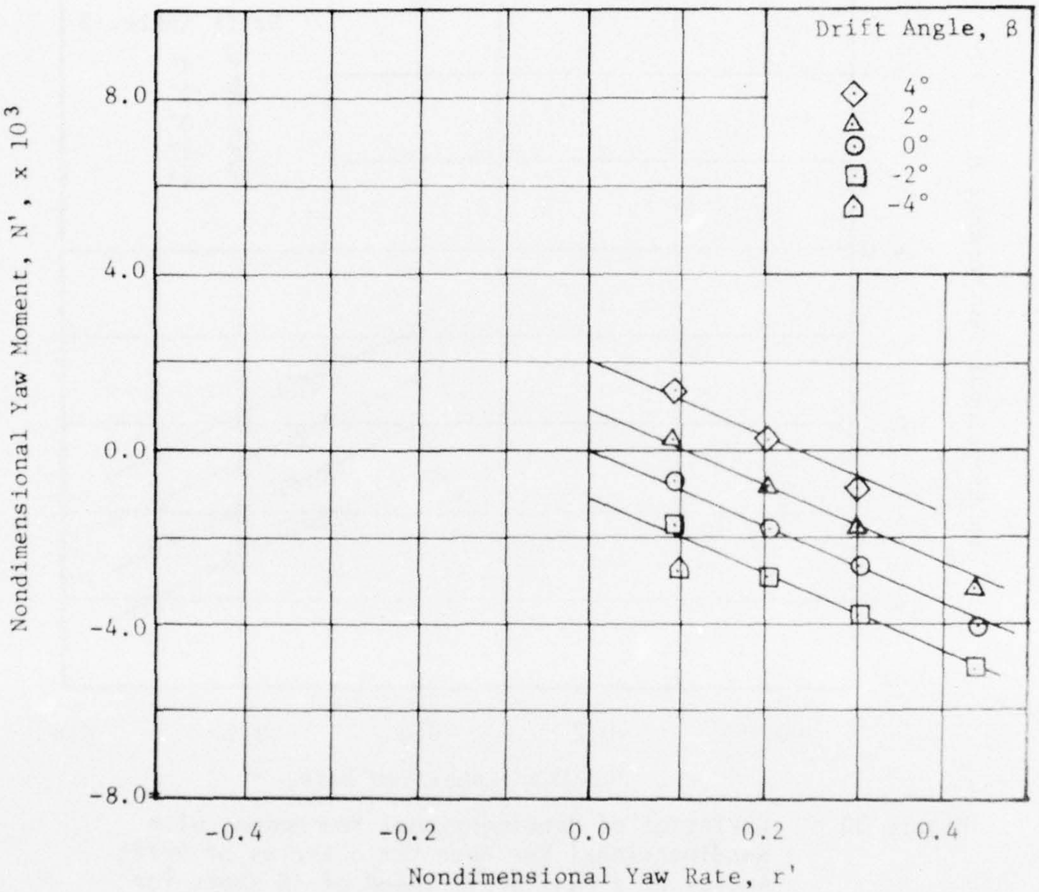

Figure 29 - Variation of Nondimensional Yaw Moment with Nondimensional Yaw Rate for a Series of Drift Angles at a Full Scale Speed of 7 Knots for the Strut Rudder at Design Draft

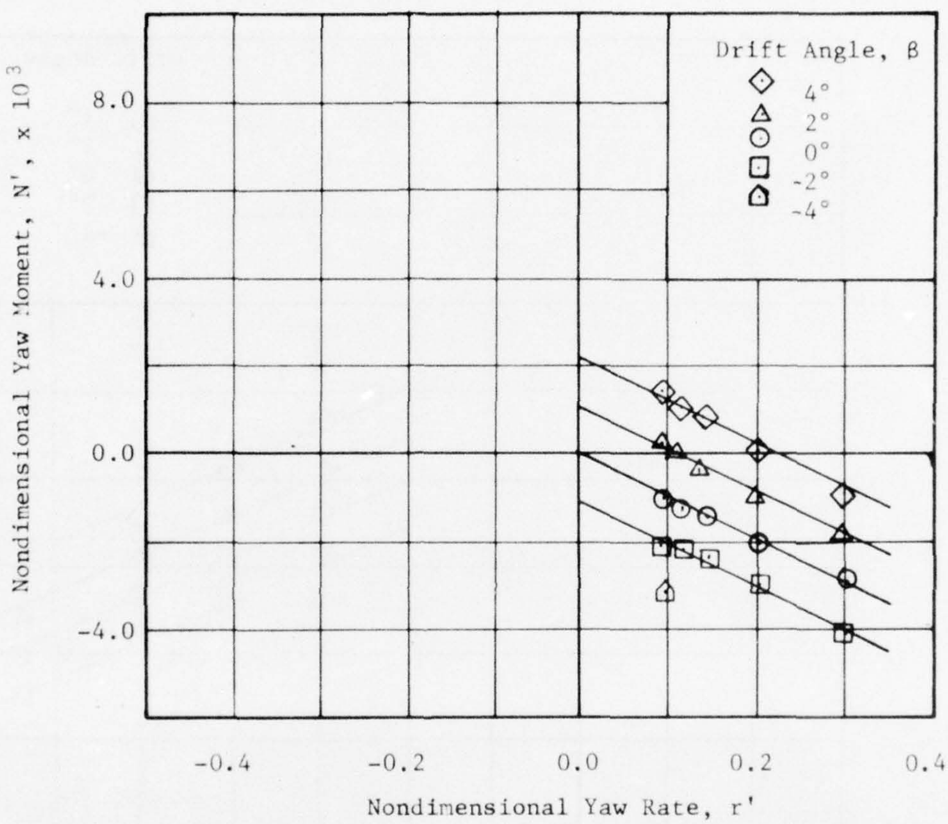

Figure 30 - Variation of Nondimensional Yaw Moment with Nondimensional Yaw Rate for a Series of Drift Angles at a Full Scale Speed of 10 Knots for the Strut Rudder at Design Draft

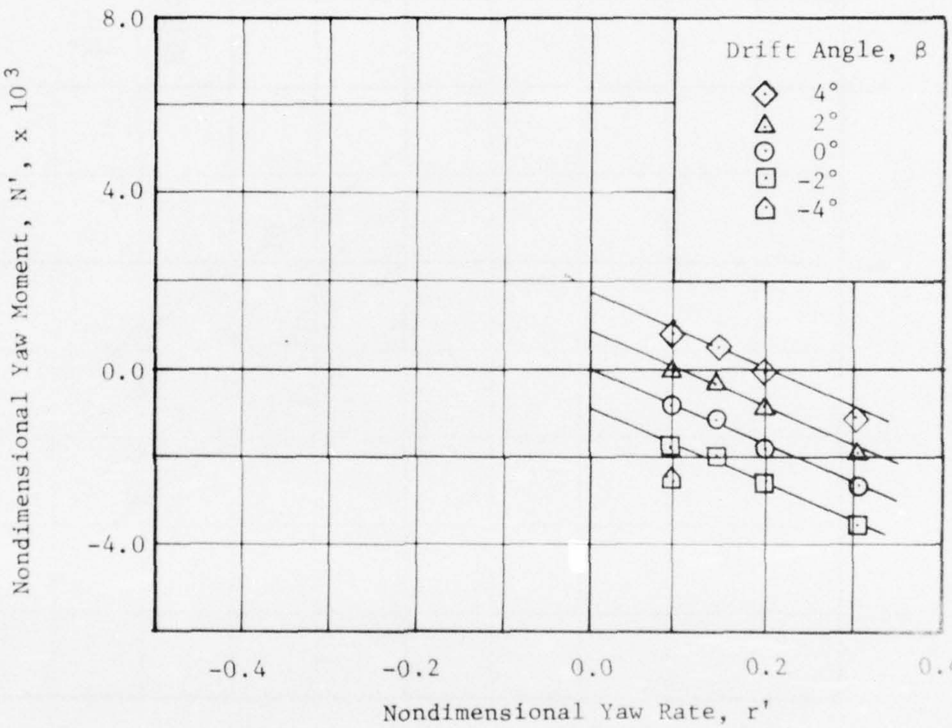

Figure 31 - Variation of Nondimensional Yaw Moment with Nondimensional Yaw Rate for a Series of Drift Angles at a Full Scale Speed of 15 Knots for the Strut Rudder at Design Draft

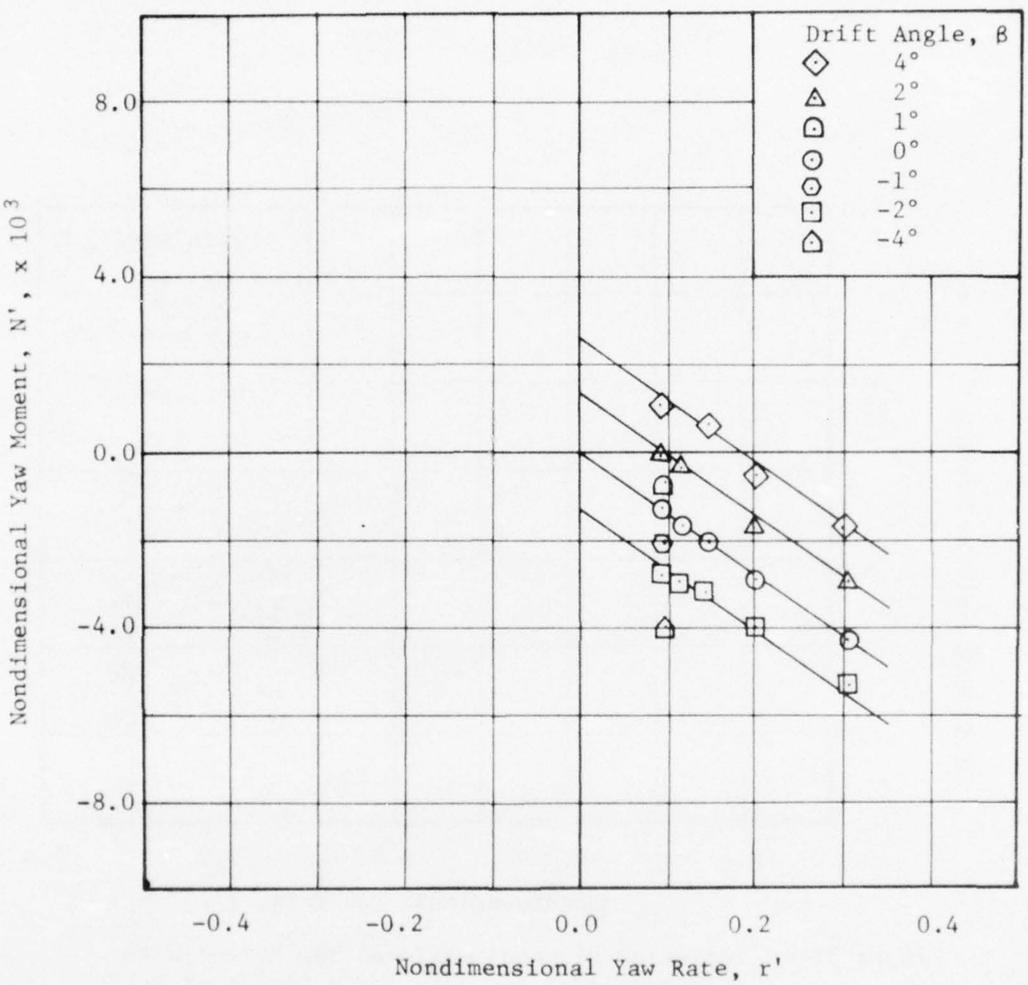

Figure 32 - Variation of Nondimensional Yaw Moment with Nondimensional Yaw Rate for a Series of Drift Angles at a Full Scale Speed of 20 Knots for the Strut Rudder at Design Draft

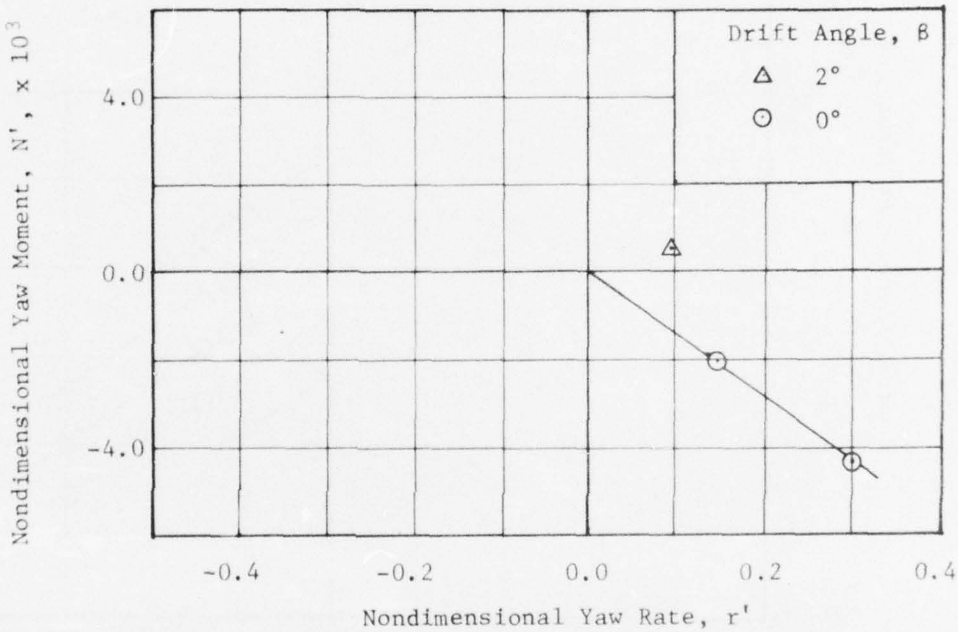

Figure 33 - Variation of Nondimensional Yaw Moment with Nondimensional Yaw Rate for Two Drift Angles at a Full Scale Speed of 22.5 Knots for the Strut Rudder at Design Draft

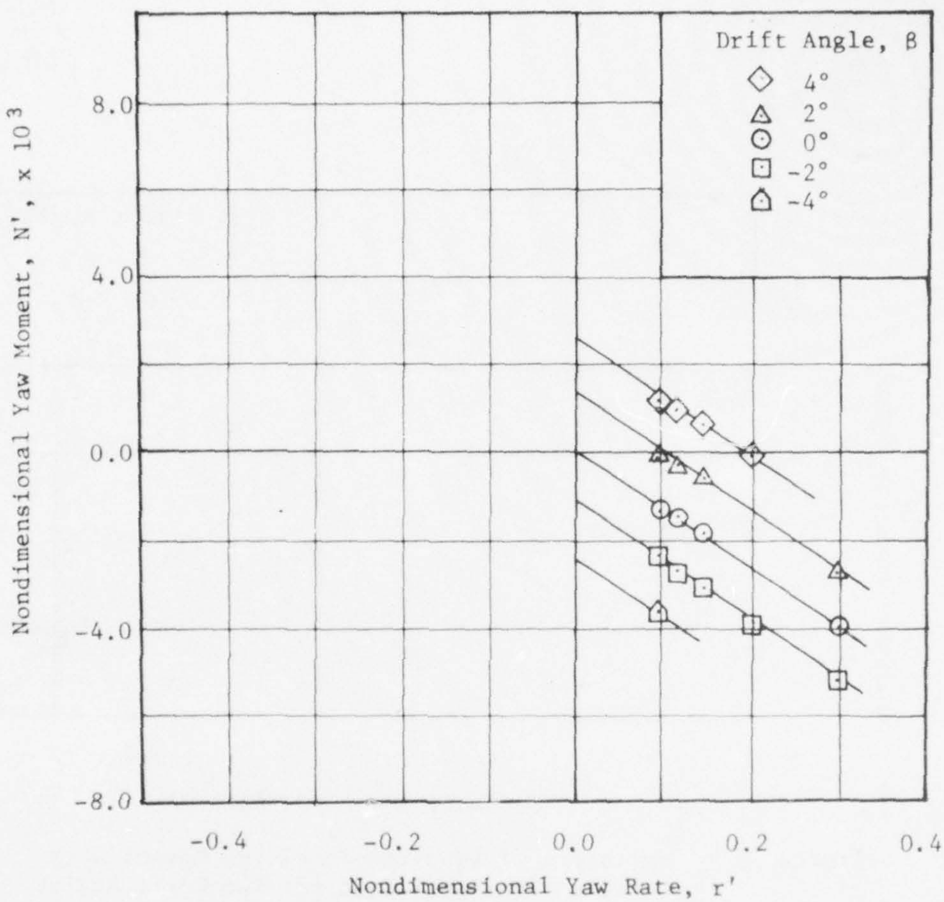

Figure 34 - Variation of Nondimensional Yaw Moment with Nondimensional Yaw Rate for a Series of Drift Angles at a Full Scale Speed of 25 Knots for the Strut Rudder at Design Draft

AD-A034 593 DAVID W TAYLOR NAVAL SHIP RESEARCH AND DEVELOPMENT CE--ETC F/G 13/10
ROTATING ARM EXPERIMENTS FOR SWATH 6A MANEUVERING PREDICTIONS.(U)
JUL 76 J A FEIN, R T WATERS

UNCLASSIFIED SPD-698-01 NL

2 OF 4
AD
A034593

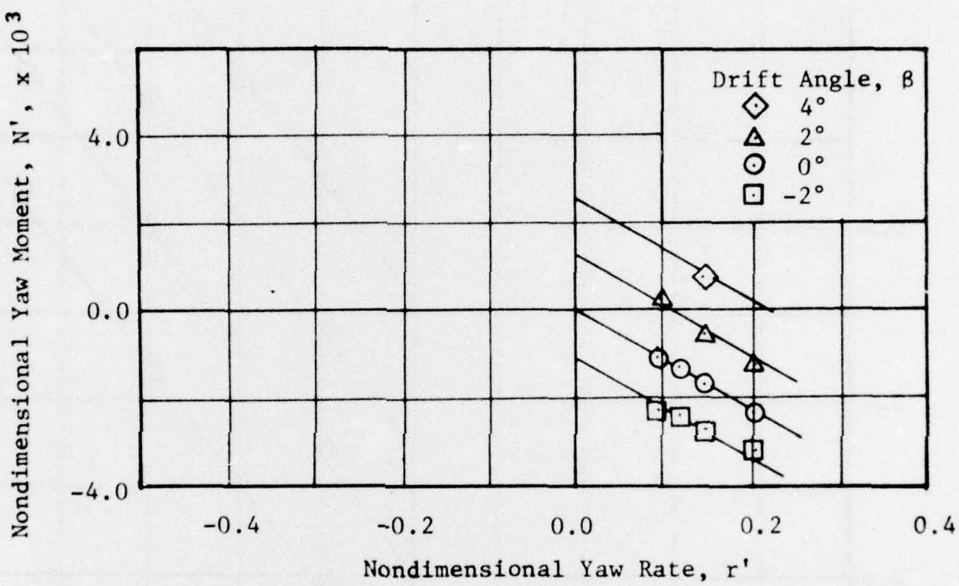

Figure 35 - Variation of Nondimensional Yaw Moment with Nondimensional Yaw Rate for a Series of Drift Angles at a Full Scale Speed of 28 Knots for the Strut Rudder at Design Draft

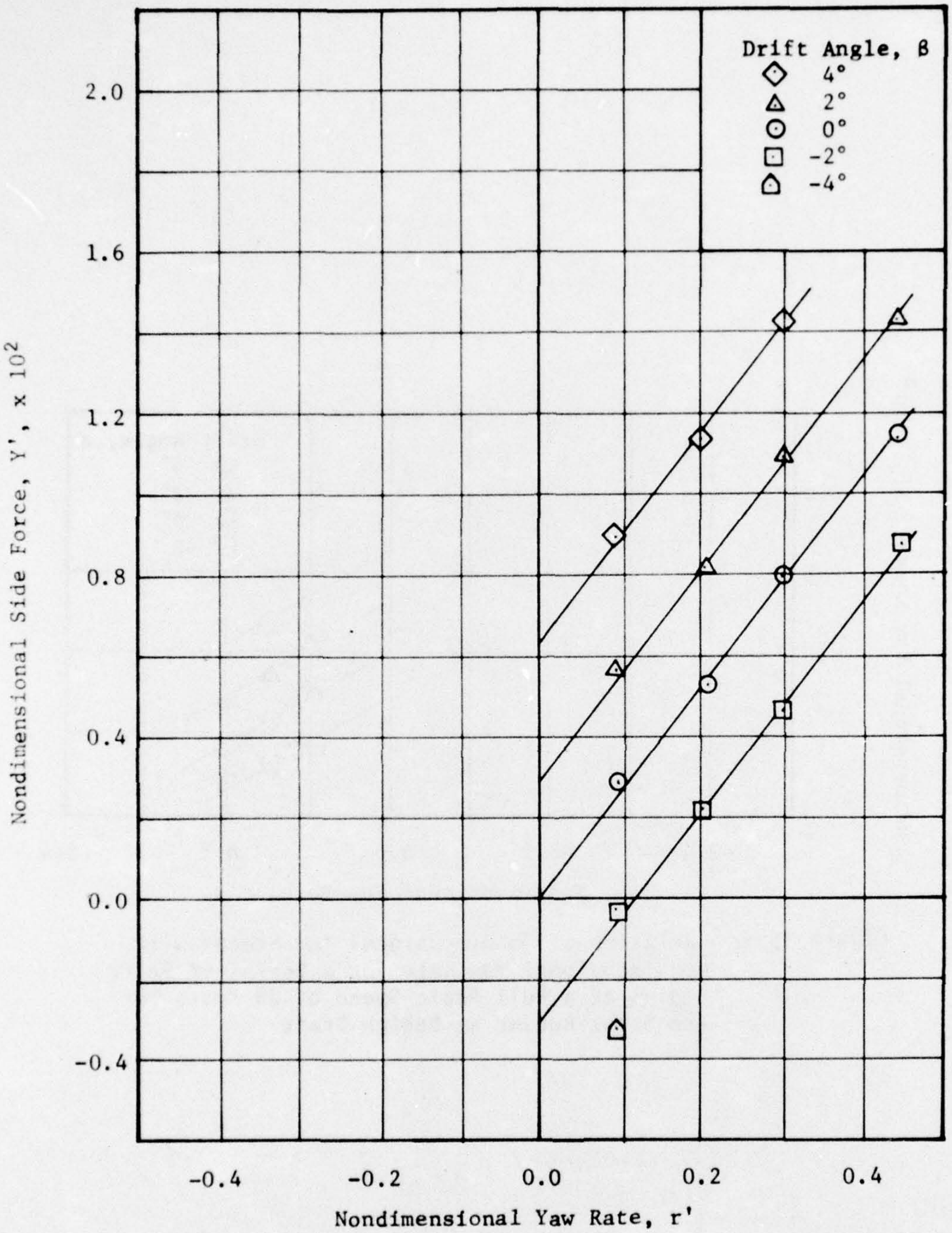

Figure 36 - Variation of Nondimensional Side Force with Nondimensional Yaw Rate for a Series of Drift Angles at a Full Scale Speed of 7 Knots for the Strut Rudder at Design Draft

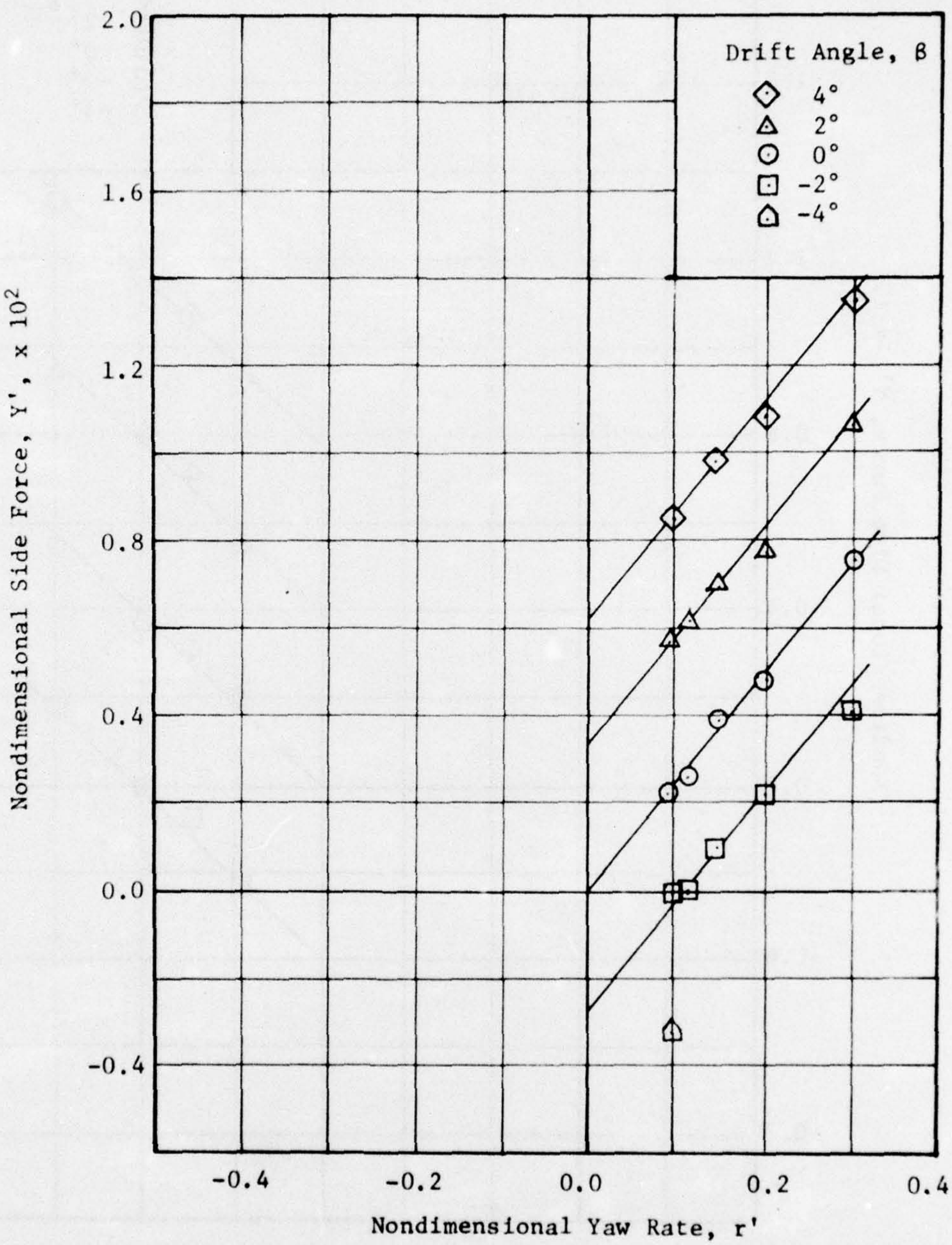

Figure 37 - Variation of Nondimentional Side Force with Nondimensional Yaw Rate for a Series of Drift Angles at a Full Scale Speed of 10 Knots for the Strut Rudder at Design Draft

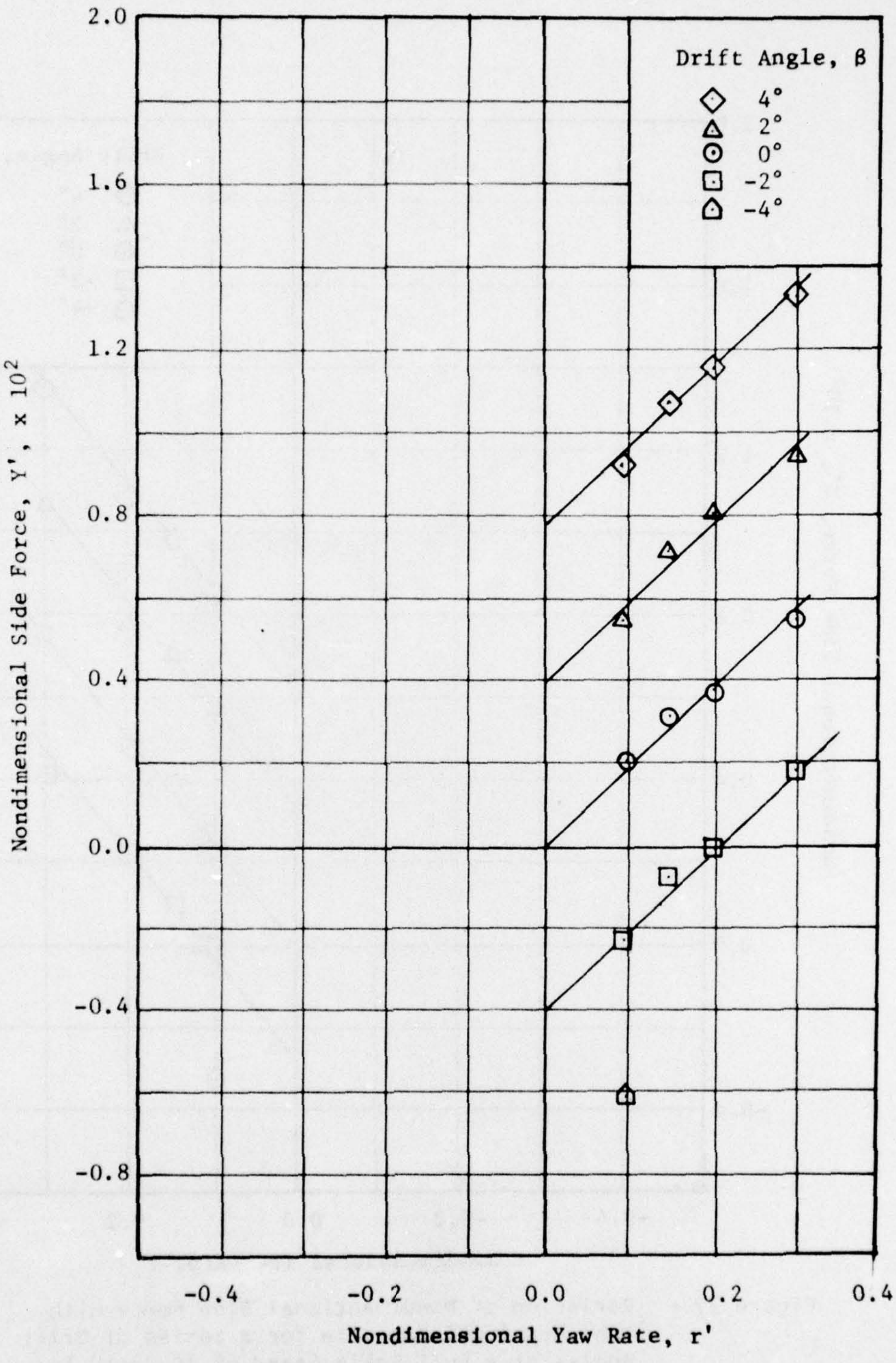

Figure 38 - Variation of Nondimensional Side Force with Nondimensional Yaw Rate for a Series of Drift Angles at a Full Scale Speed of 15 Knots for the Strut Rudder at Design Draft

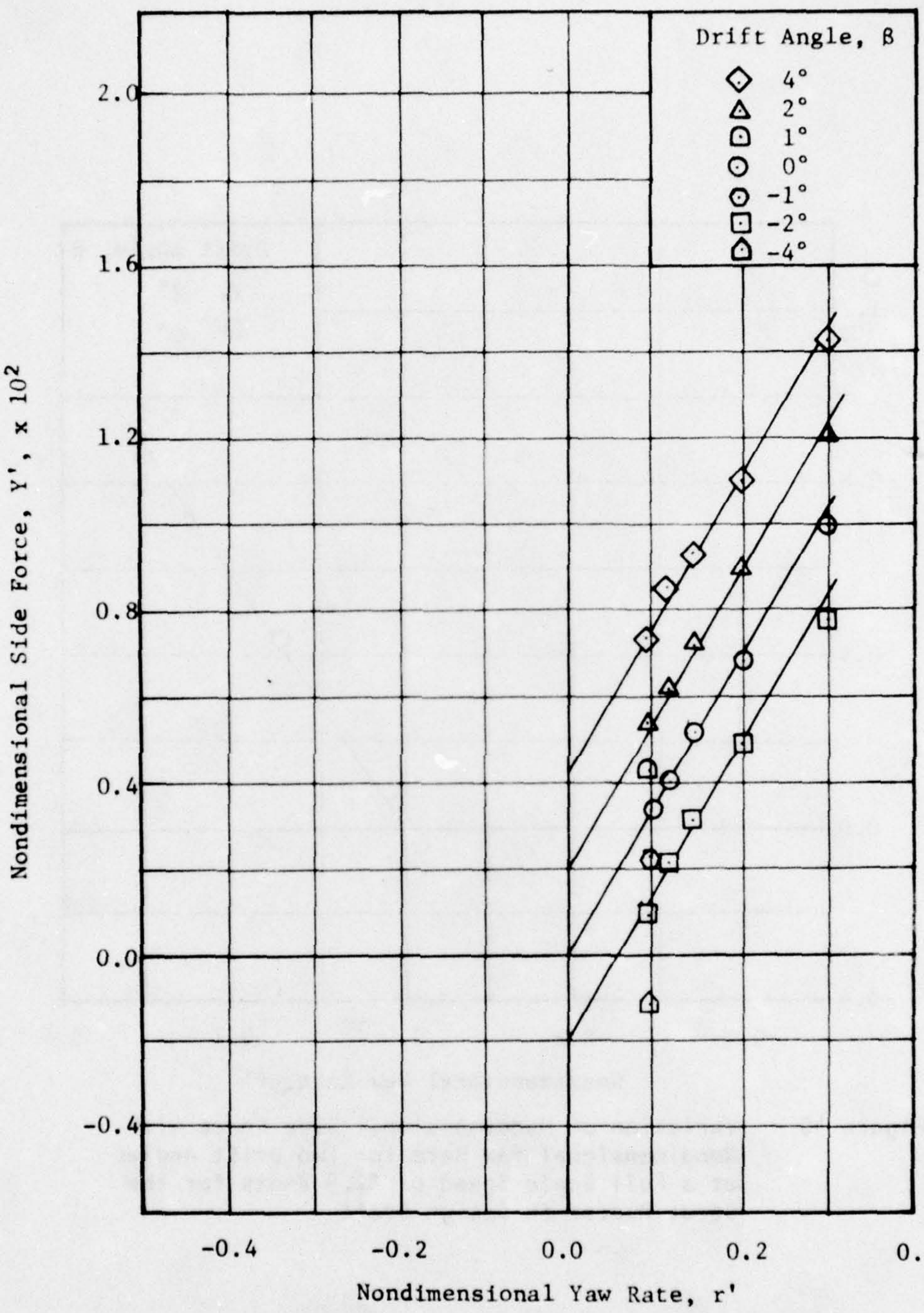

Figure 39 - Variation of Nondimensional Side Force with Nondimensional Yaw Rate for a Series of Drift Angles at a Full Scale Speed of 20 Knots for the Strut Rudder at Design Draft

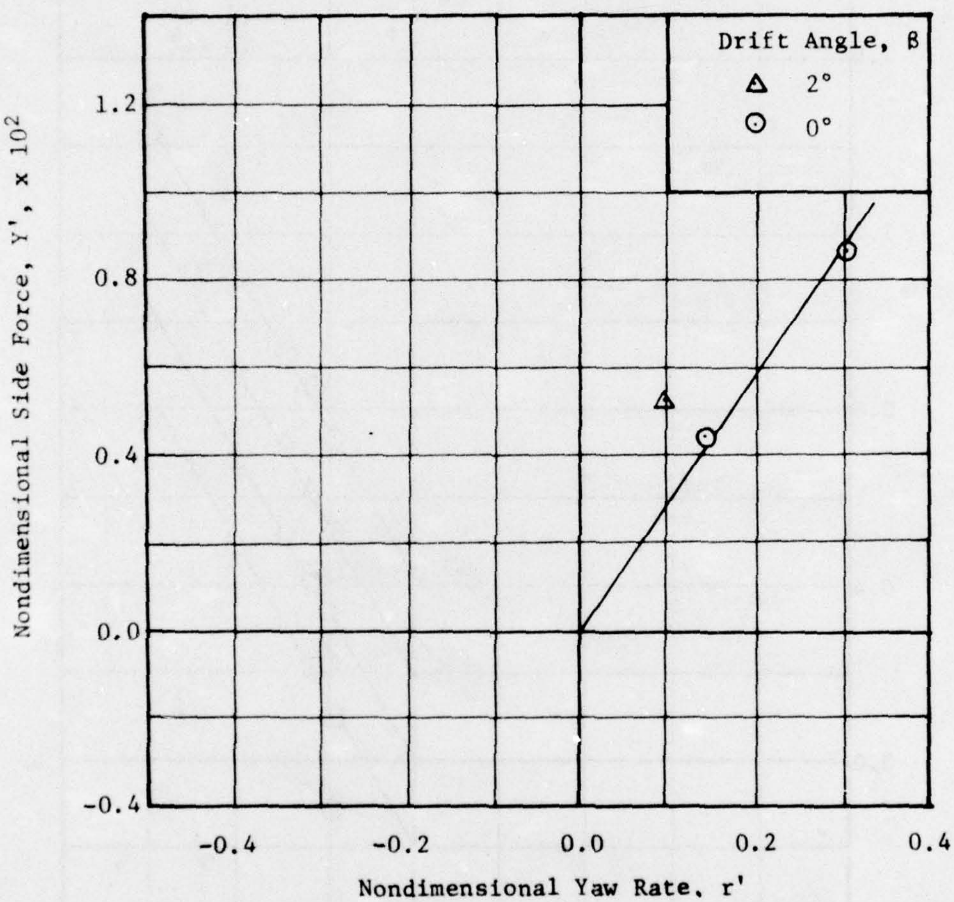

Figure 40 - Variation of Nondimensional Side Force with Nondimensional Yaw Rate for Two Drift Angles at a Full Scale Speed of 22.5 Knots for the Strut Rudder at Design Draft

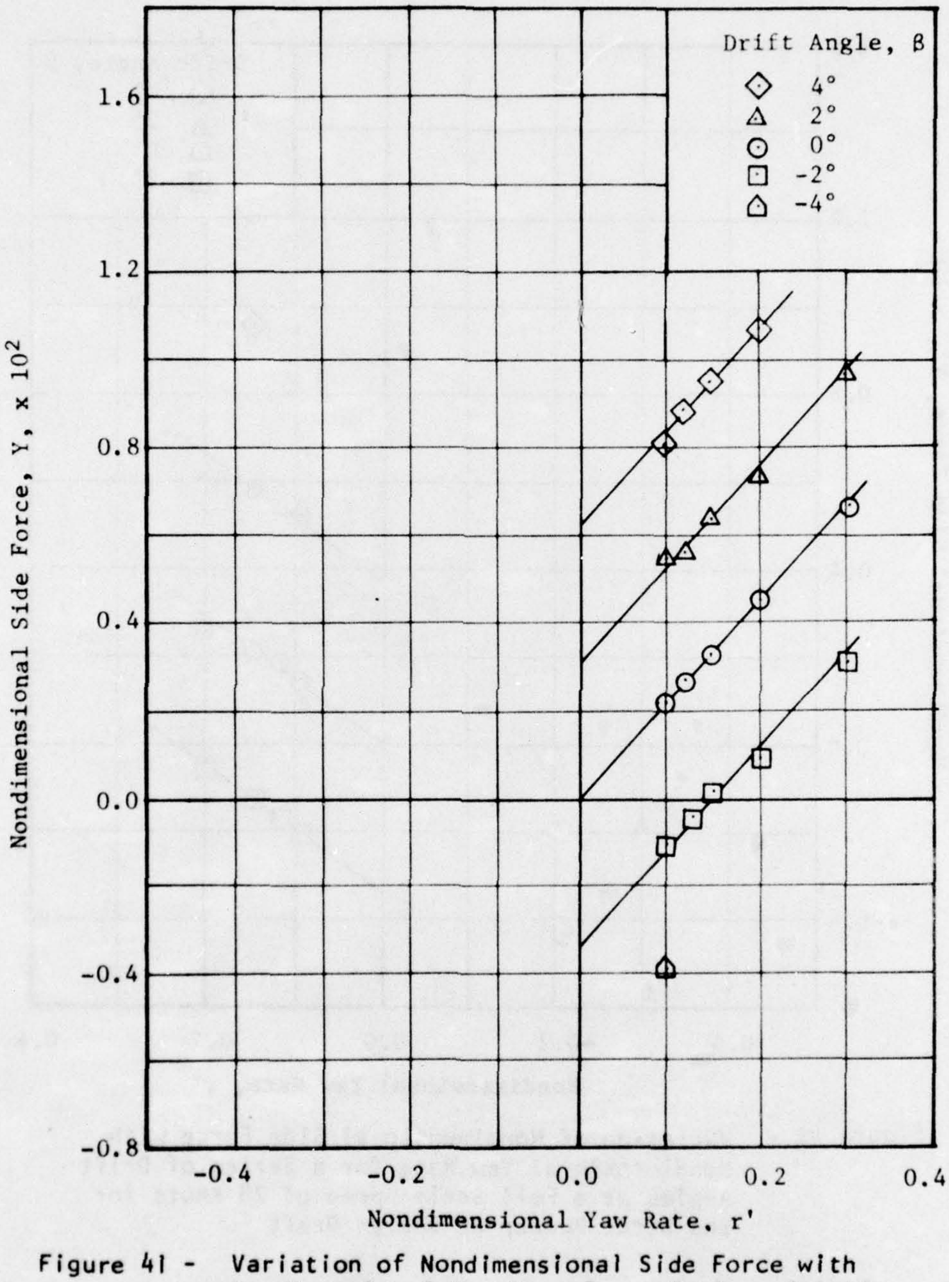

Figure 41 - Variation of Nondimensional Side Force with Nondimensional Yaw Rate for a Series of Drift Angles at a Full Scale Speed of 25 Knots for the Strut Rudder at Design Draft

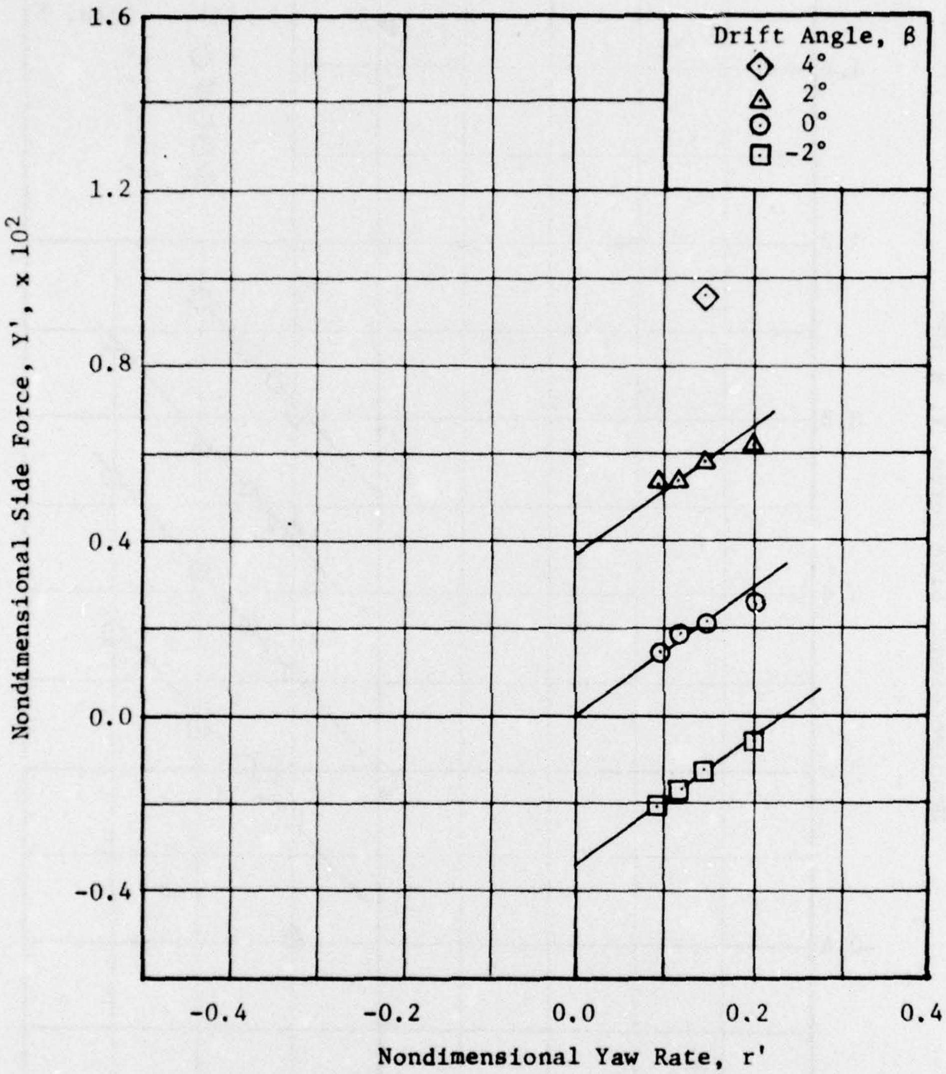

Figure 42 - Variation of Nondimensional Side Force with Nondimensional Yaw Rate for a Series of Drift Angles at a Full Scale Speed of 28 Knots for the Strut Rudder at Design Draft

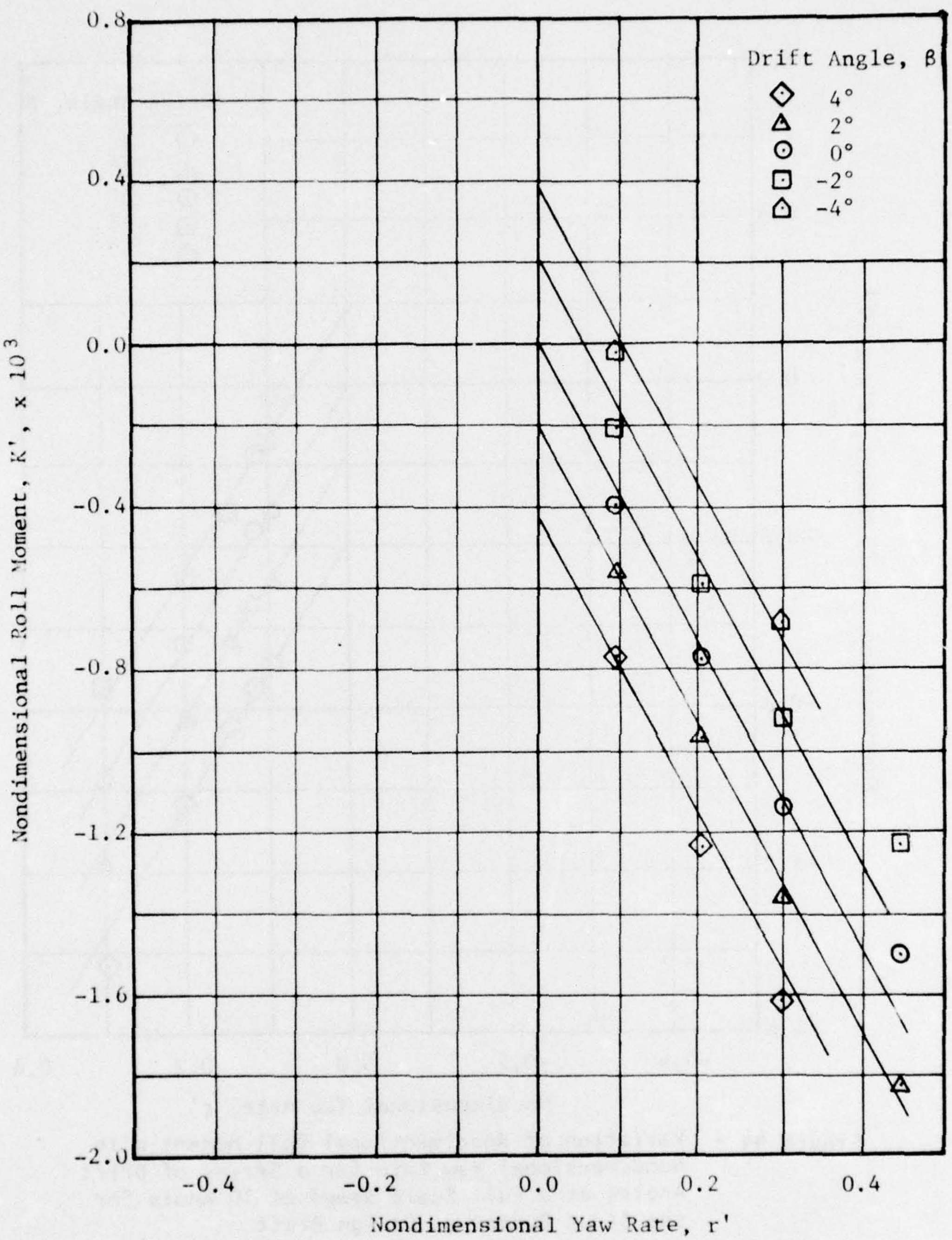

Figure 43 - Variation of Nondimensional Roll Moment with Nondimensional Yaw Rate for a Series of Drift Angles at a Full Scale Speed of 7 Knots for the Strut Rudder at Design Draft

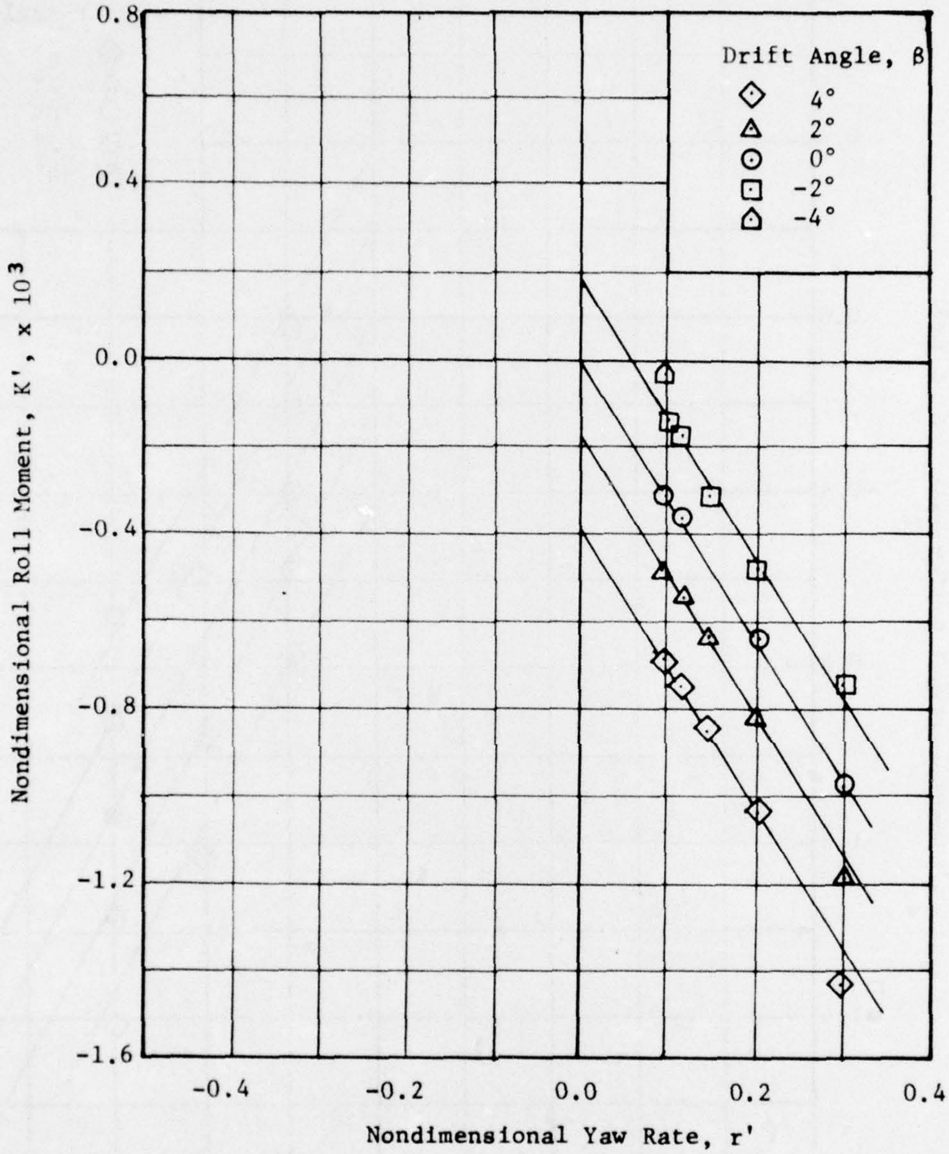

Figure 44 - Variation of Nondimensional Roll Moment with Nondimensional Yaw Rate for a Series of Drift Angles at a Full Scale Speed of 10 Knots for the Strut Rudder at Design Draft

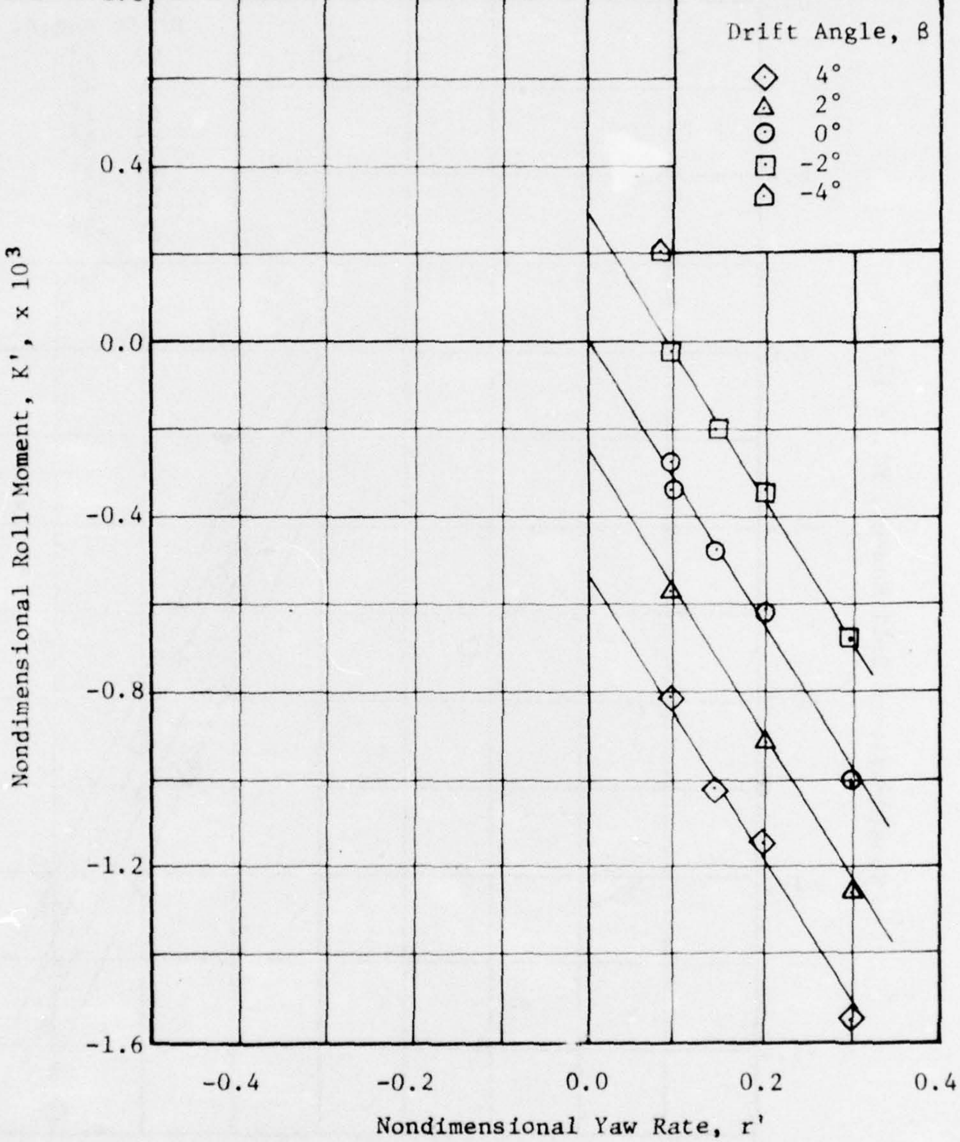

Figure 45 - Variation of Nondimensional Roll Moment with Nondimensional Yaw Rate for a Series of Drift Angles at a Full Scale Speed of 15 Knots for the Strut Rudder at Design Draft

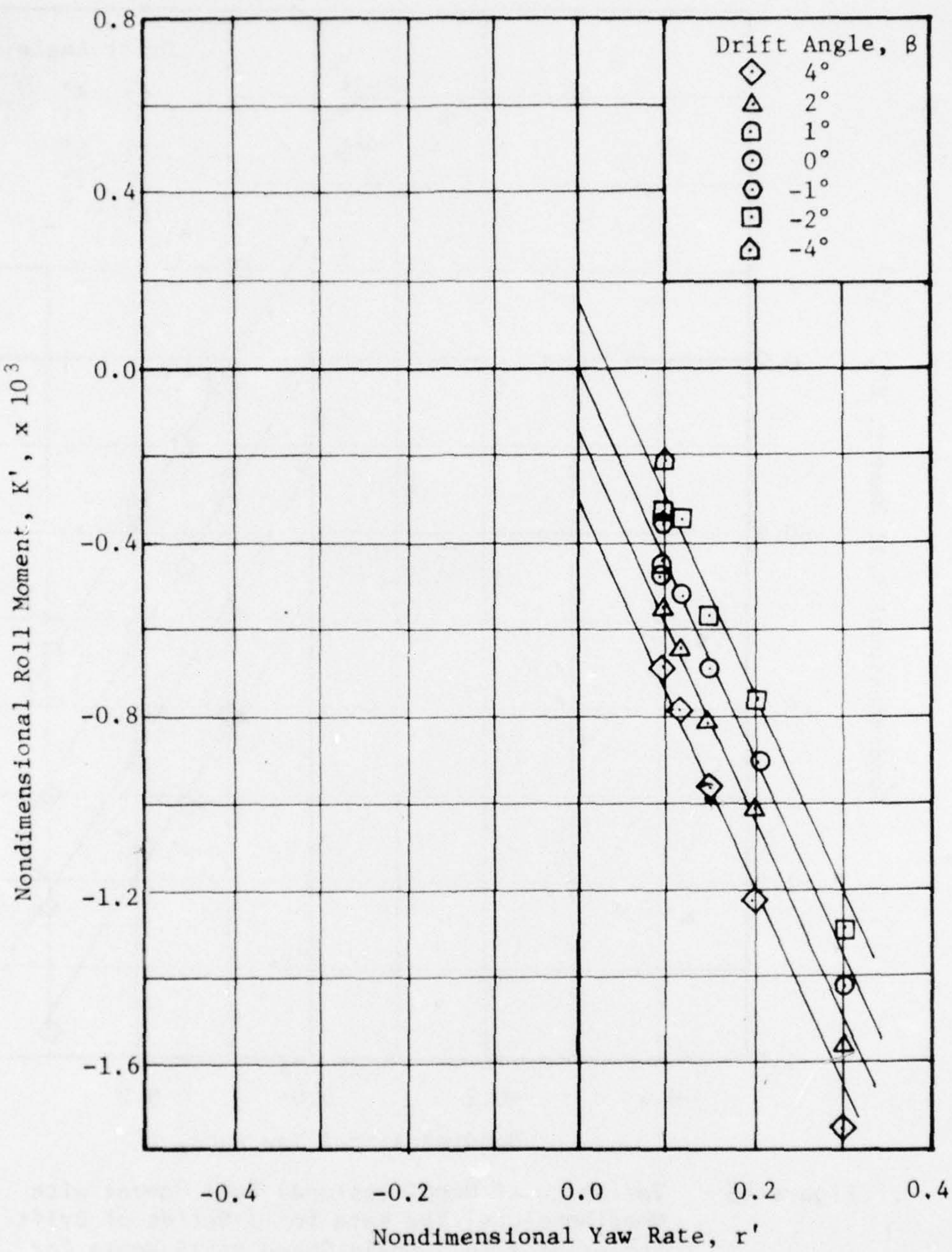

Figure 46 - Variation of Nondimensional Roll Moment with Nondimensional Yaw Rate for a Series of Drift Angles at a Full Scale Speed of 20 Knots for the Strut Rudder at Design Draft

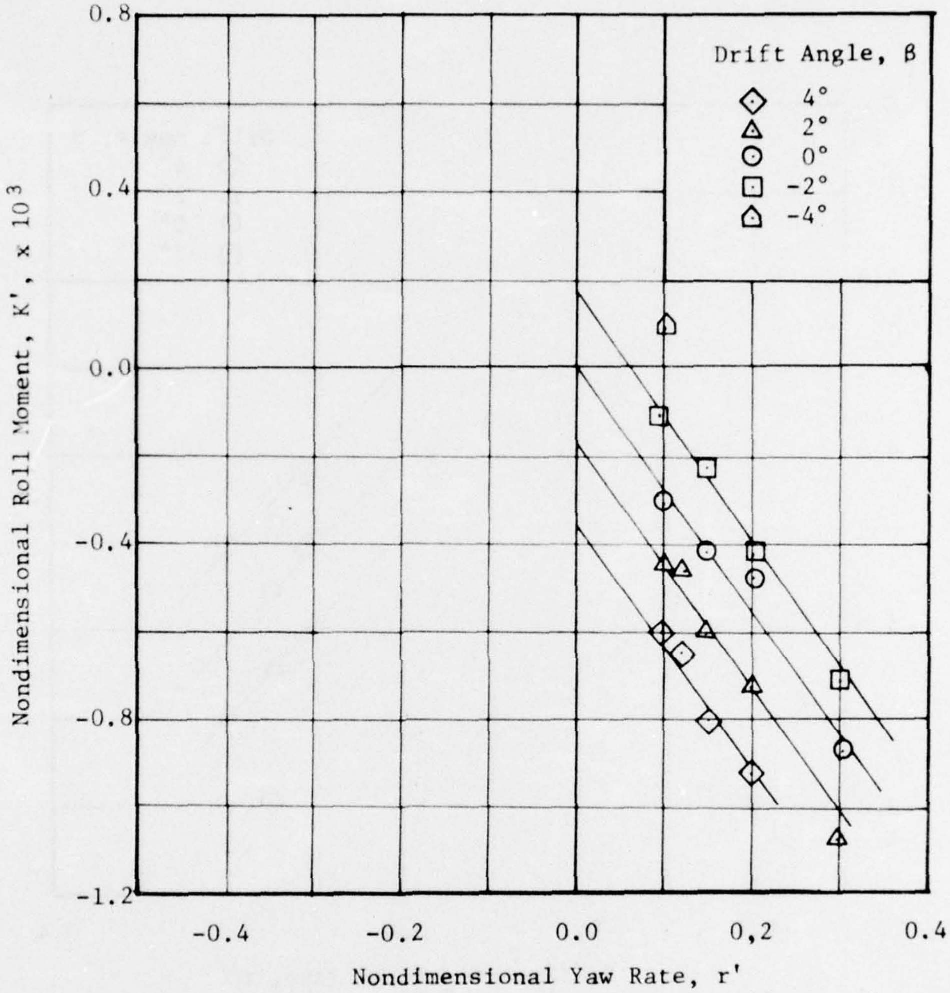

Figure 47 - Variation of Nondimensional Roll Moment with Nondimensional Yaw Rate for a Series of Drift Angles at a Full Scale Speed of 25 Knots for the Strut Rudder at Design Draft

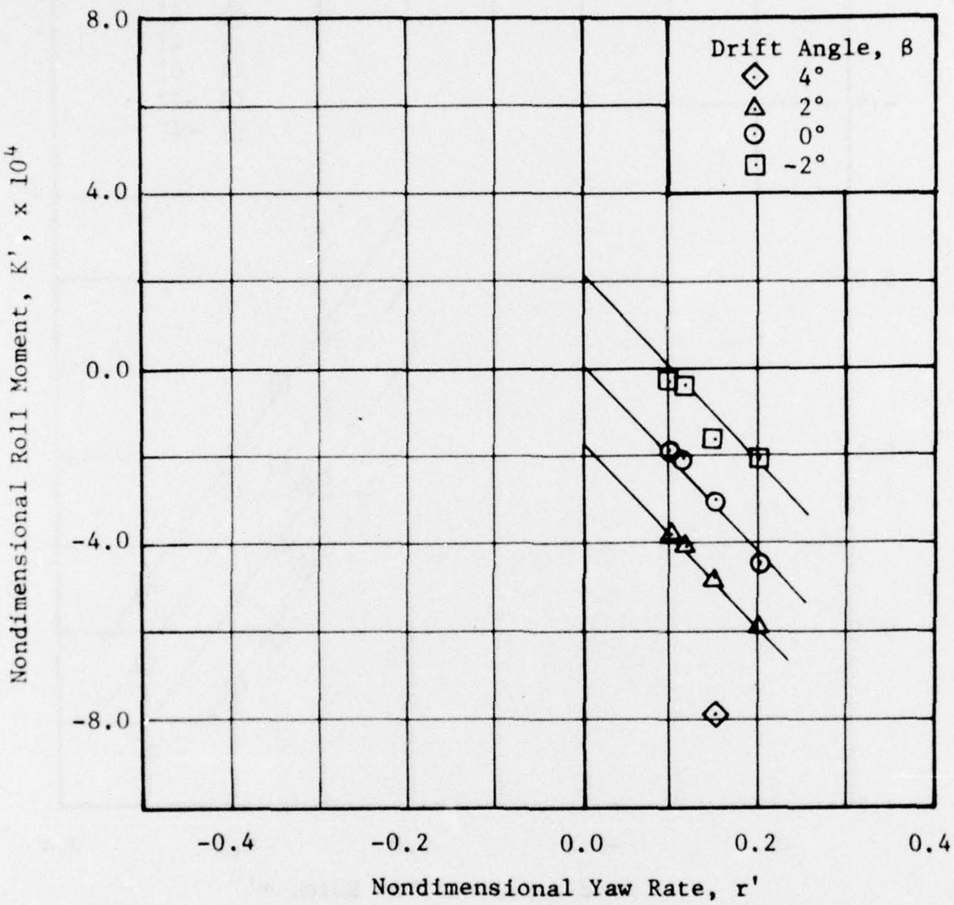

Figure 48 - Variation fo Nondimensional Roll Moment with Nondimensional Yaw Rate for a Series of Drift Angles at a Full Scale Speed of 28 Knots for the Strut Rudder at Design Draft

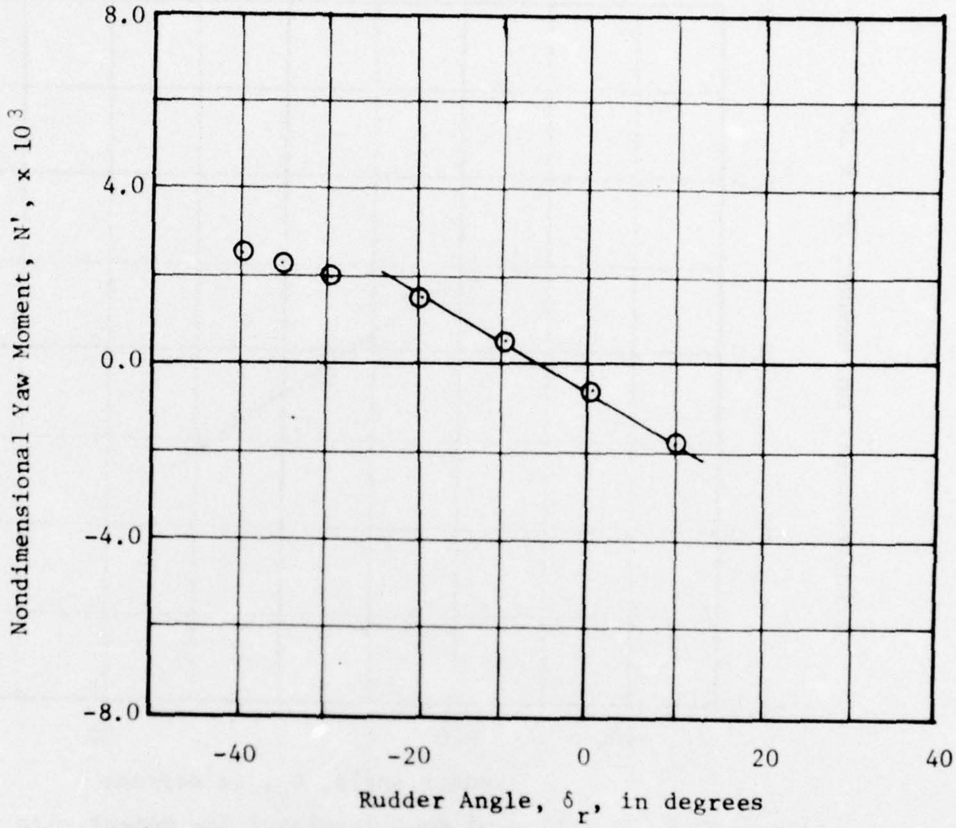

Figure 49 - Variation of Nondimensional Yaw Moment with Rudder Angle for a Nondimensional Yaw Rate of 0.093 at a Full Scale Speed of 5 Knots for the Strut Rudder at Design Draft

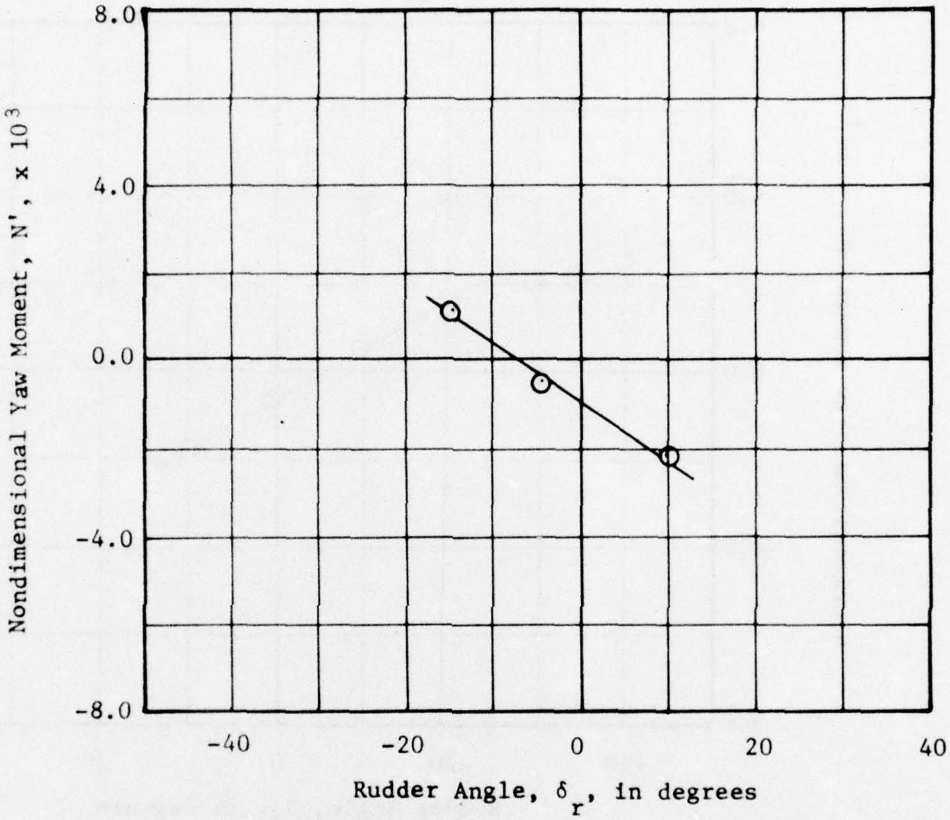

Figure 50 - Variation of Nondimensional Yaw Moment with Rudder Angle for a Nondimensional Yaw Rate of 0.093 at a Full Scale Speed of 10 Knots for the Strut Rudder at Design Draft

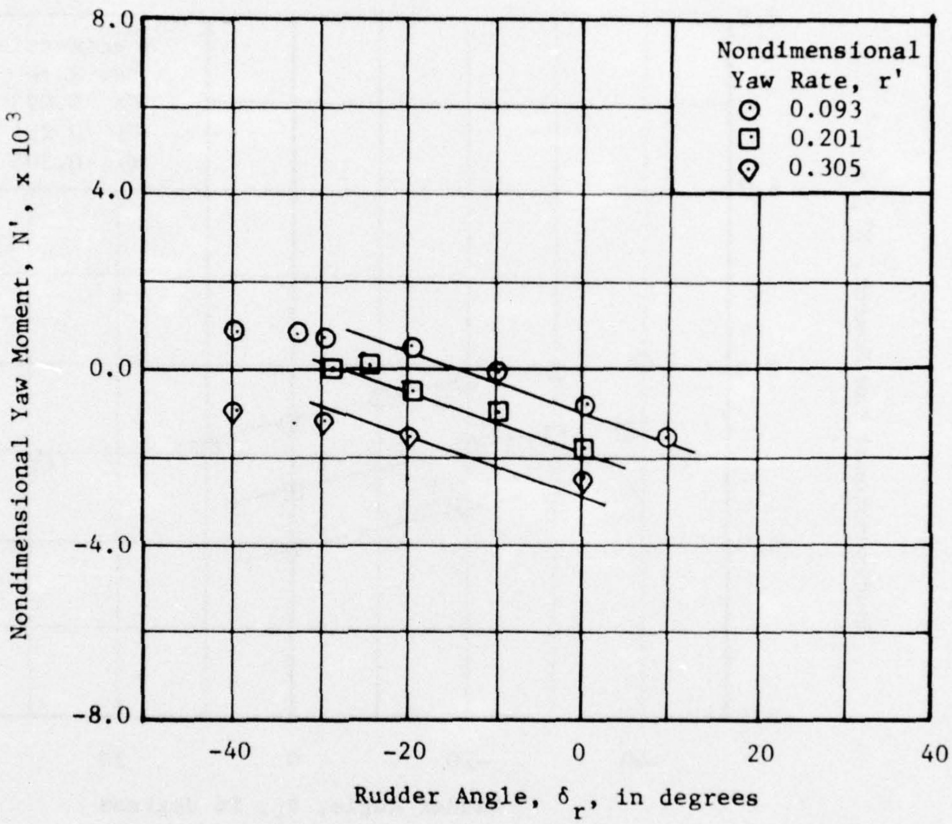

Figure 51 - Variation of Nondimensional Yaw Moment with Rudder Angle for a Series of Nondimensional Yaw Rates at a Full Scale Speed of 15 Knots for the Strut Rudder at Design Draft

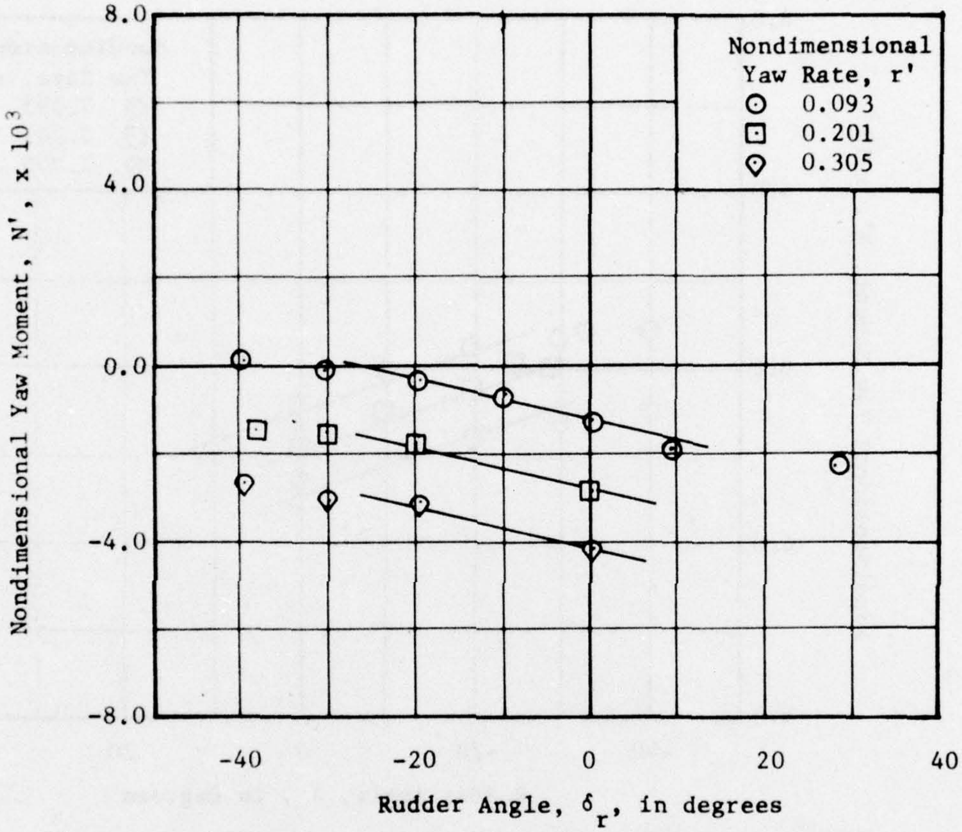

Figure 52 - Variation of Nondimensional Yaw Moment with Rudder Angle for a Series of Nondimensional Yaw Rates at a Full Scale Speed of 20 Knots for the Strut Rudder at Design Draft

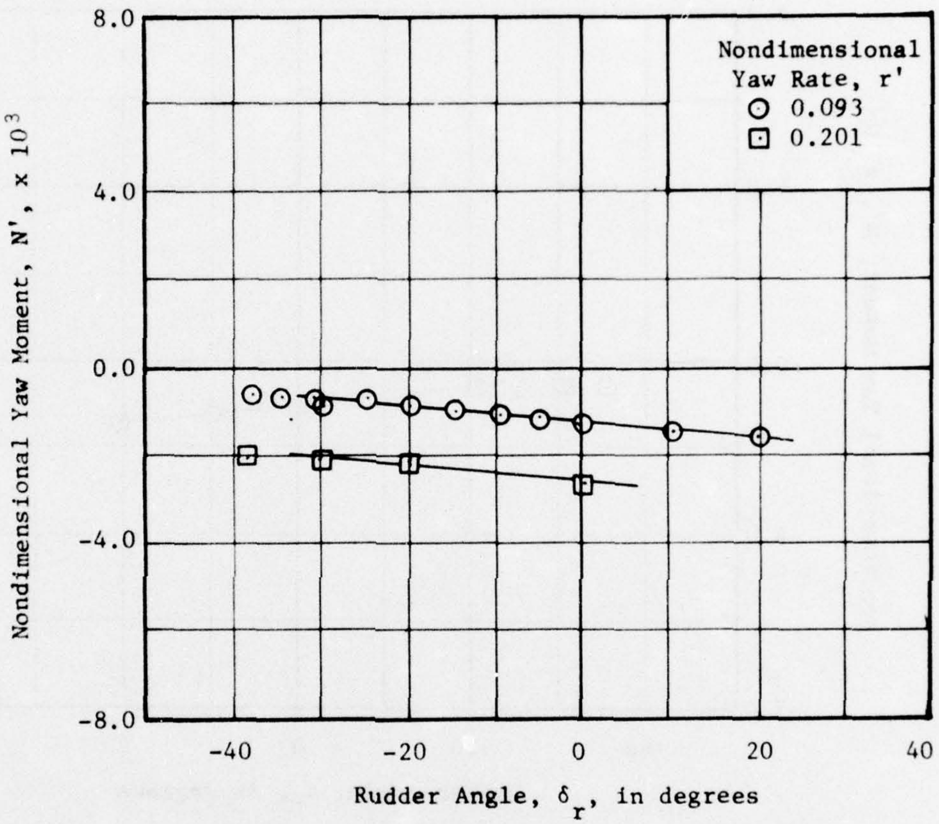

Figure 53 - Variation of Nondimensional Yaw Moment with Rudder Angle for Two Nondimensional Yaw Rates at a Full Scale Speed of 25 Knots for the Strut Rudder at Design Draft

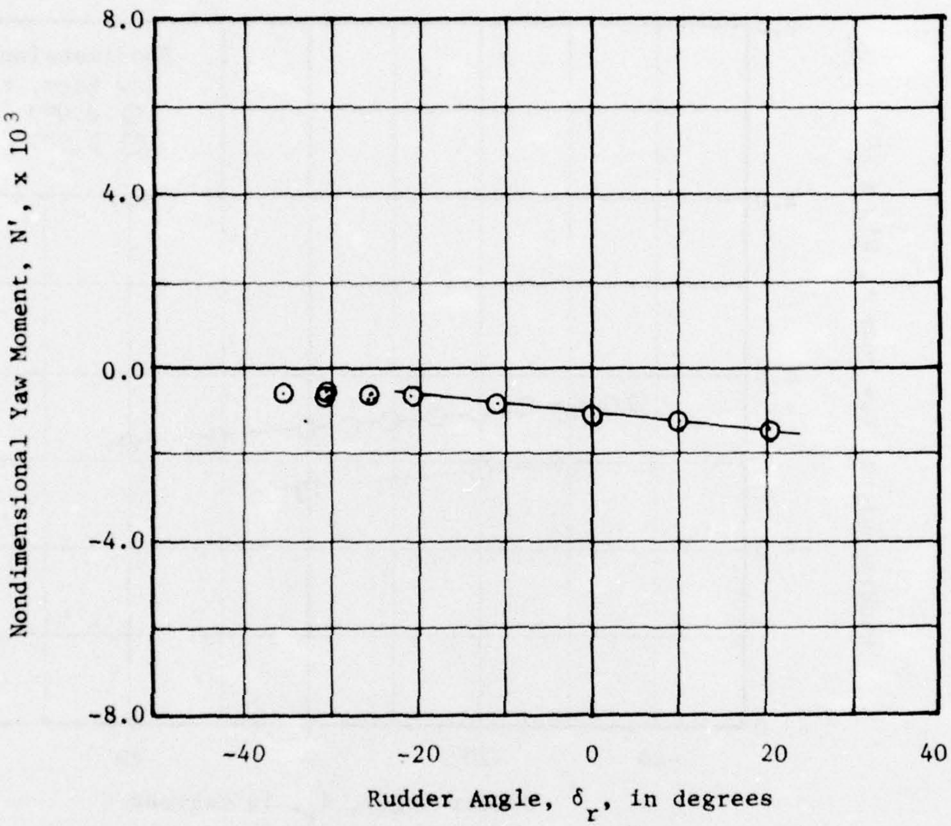

Figure 54 - Variation of Nondimensional Yaw Moment with Rudder Angle for a Nondimensional Yaw Rate of 0.093 at a Full Scale Speed of 28 Knots for the Strut Rudder at Design Draft

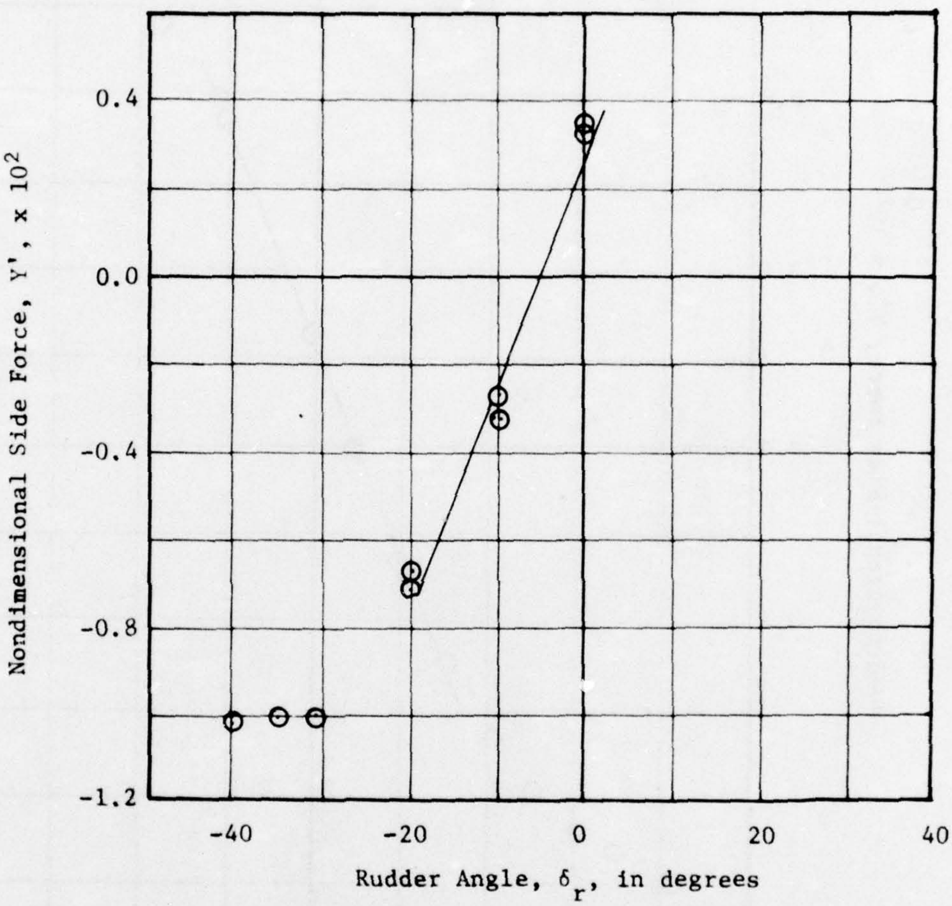

Figure 55 - Variation of Nondimensional Side Force with Rudder Angle for a Nondimensional Yaw Rate of 0.093 at a Full Scale Speed of 5 Knots for the Strut Rudder at Design Draft

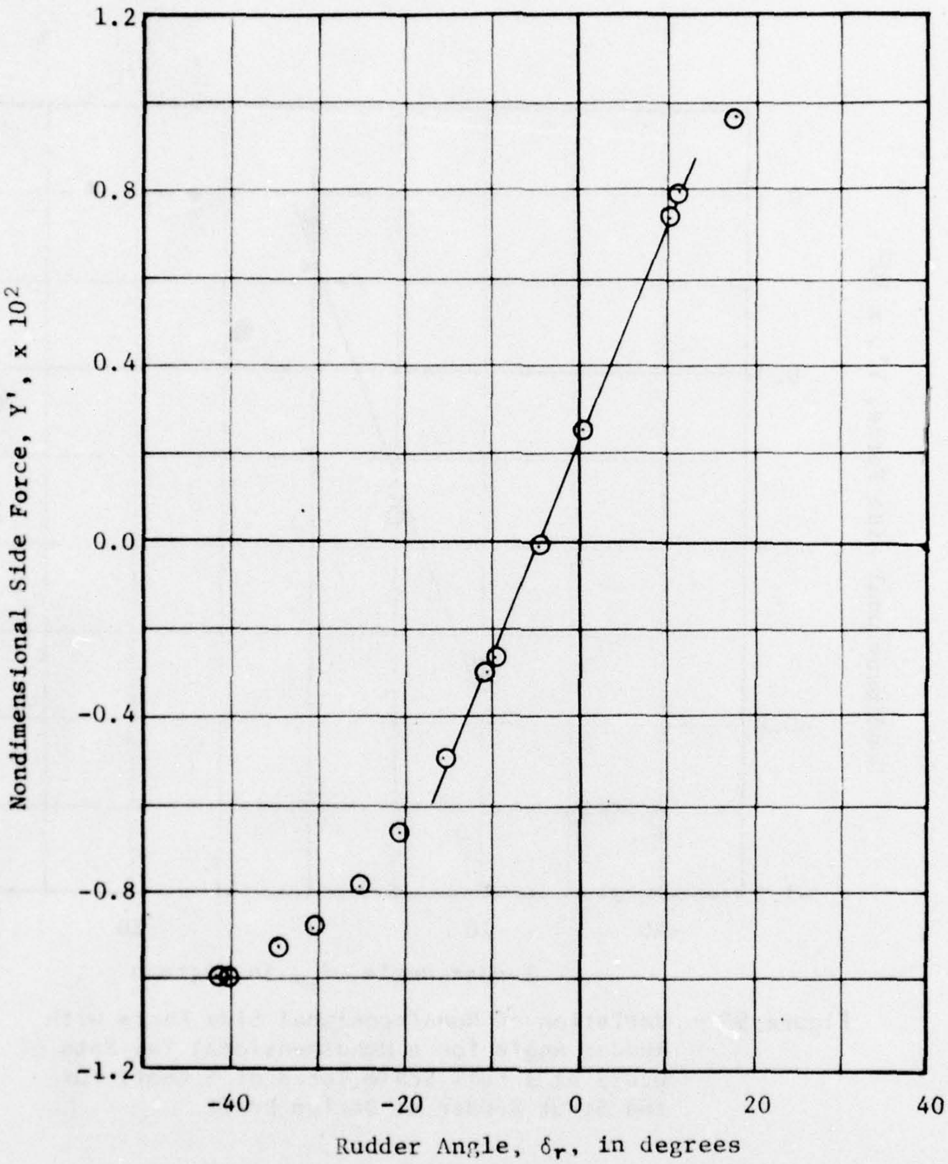

Figure 56 - Variation of Nondimensional Side Force with Rudder Angle for a Nondimensional Yaw Rate of 0.093 at a Full Scale Speed of 10 Knots for the Strut Rudder at Design Draft

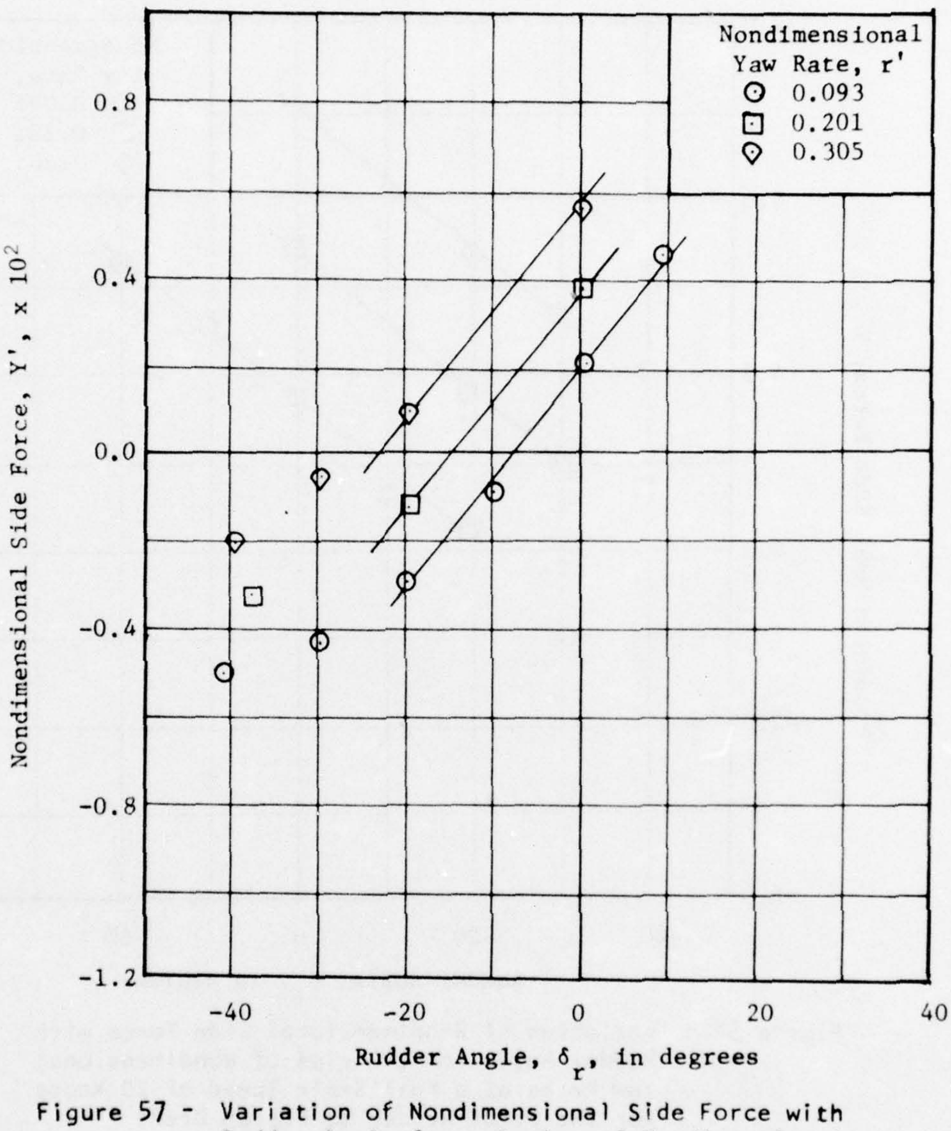

Figure 57 - Variation of Nondimensional Side Force with Rudder Angle for a Series of Nondimensional Yaw Rates at a Full Scale Speed of 15 Knots for the Strut Rudder at Design Draft

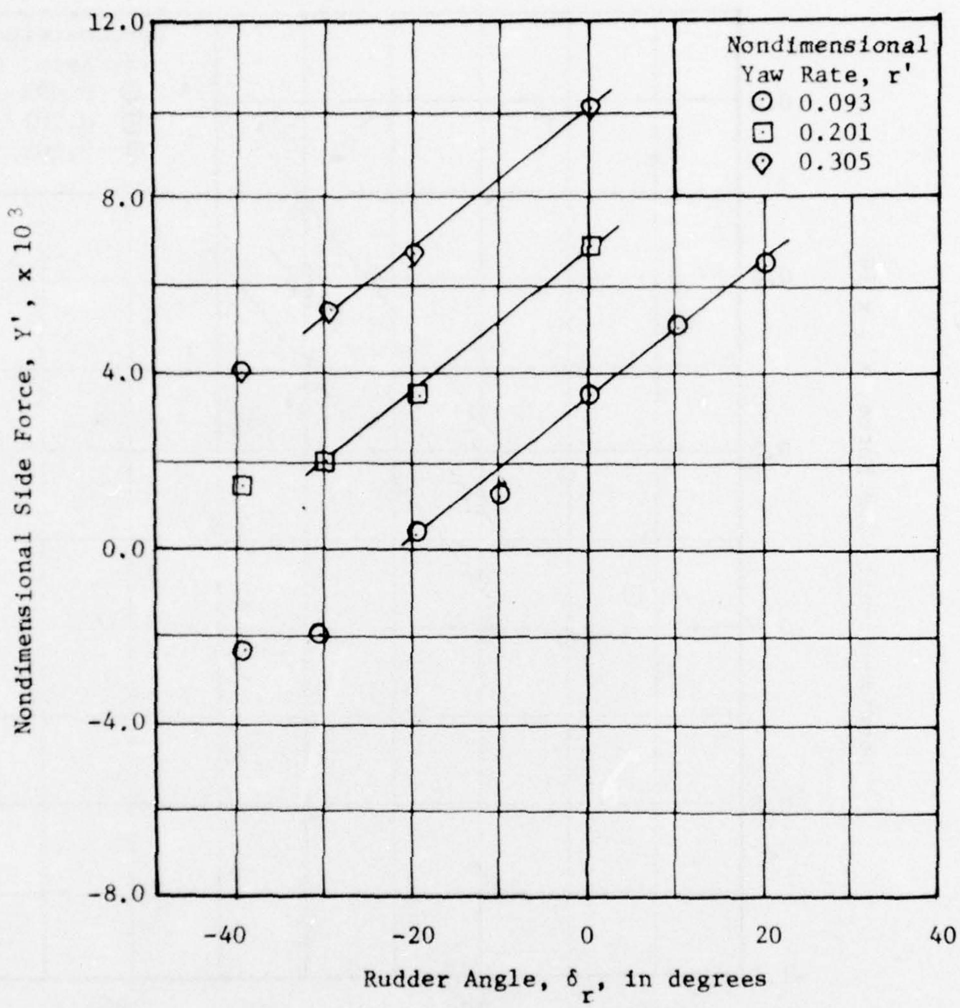

Figure 58 - Variation of Nondimensional Side Force with Rudder Angle for a Series of Nondimensional Yaw Rates at a Full Scale Speed of 20 Knots for the Strut Rudder at Design Draft

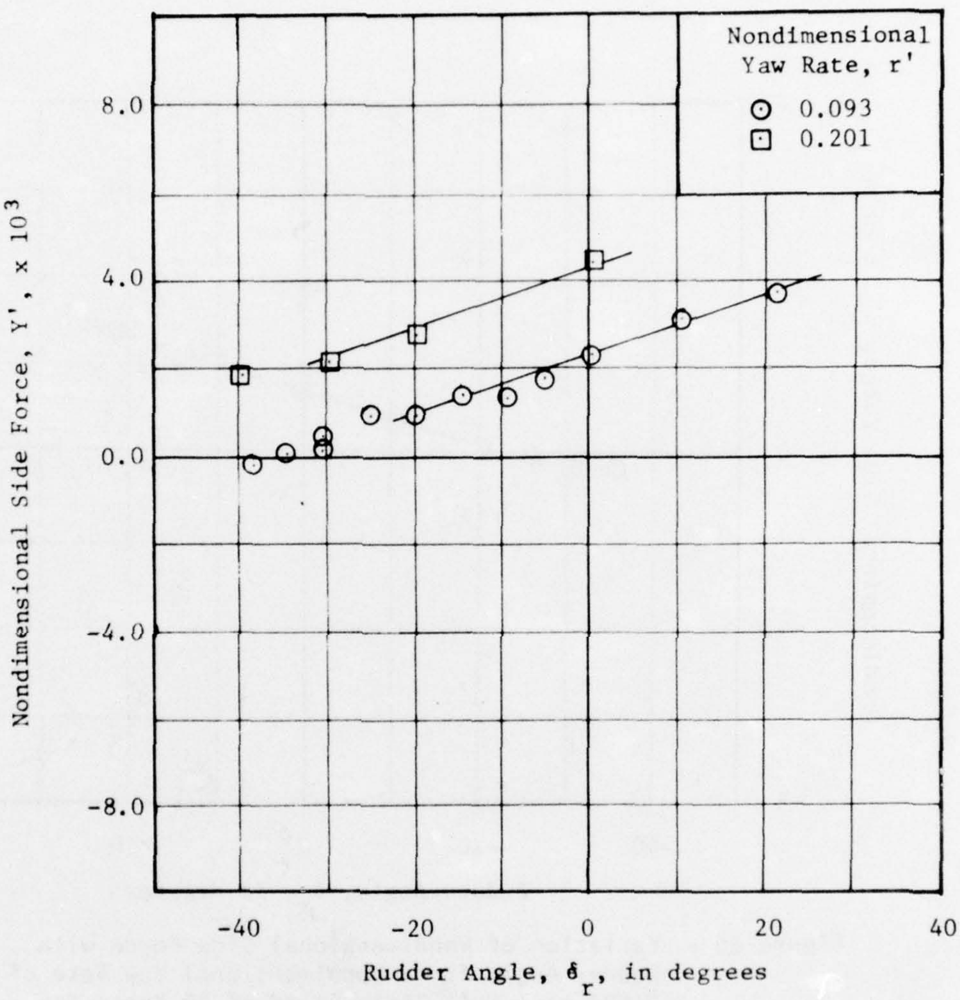

Figure 59 - Variation of Nondimensional Side Force with Rudder Angle for Two Nondimensional Yaw Rates at a Full Scale Speed of 25 Knots for the Strut Rudder at Design Draft

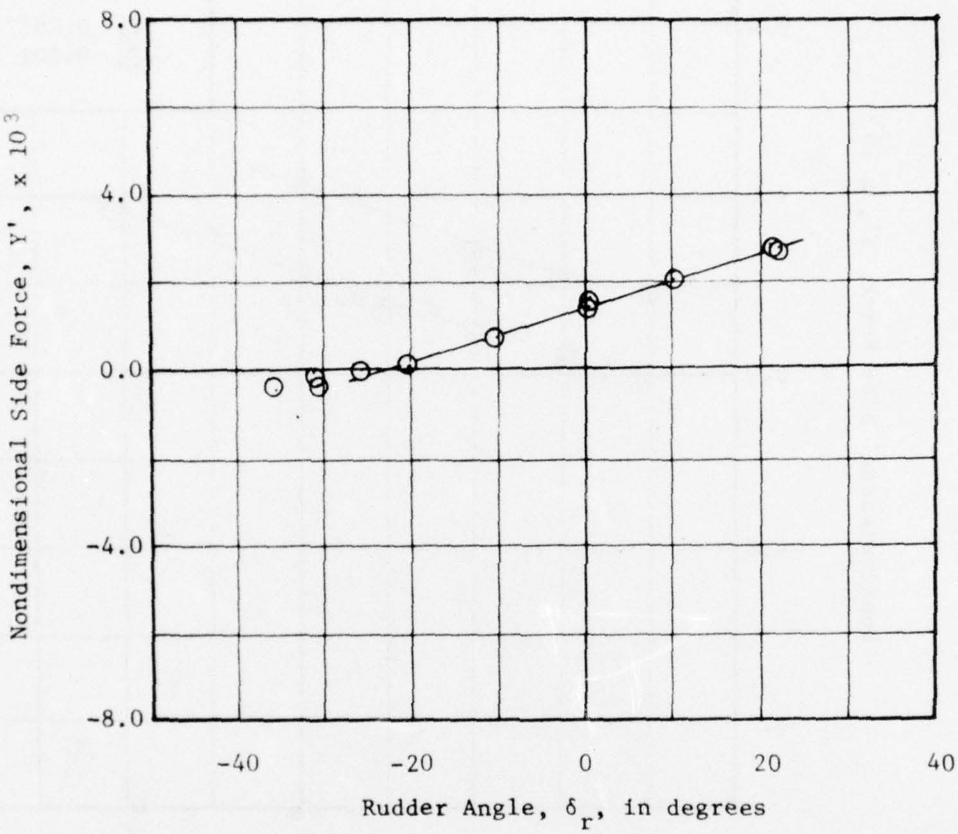

Figure 60 - Variation of Nondimensional Side Force with Rudder Angle for a Nondimensional Yaw Rate of 0.093 at a Full Scale Speed of 28 Knots for the Strut Rudder at Design Draft

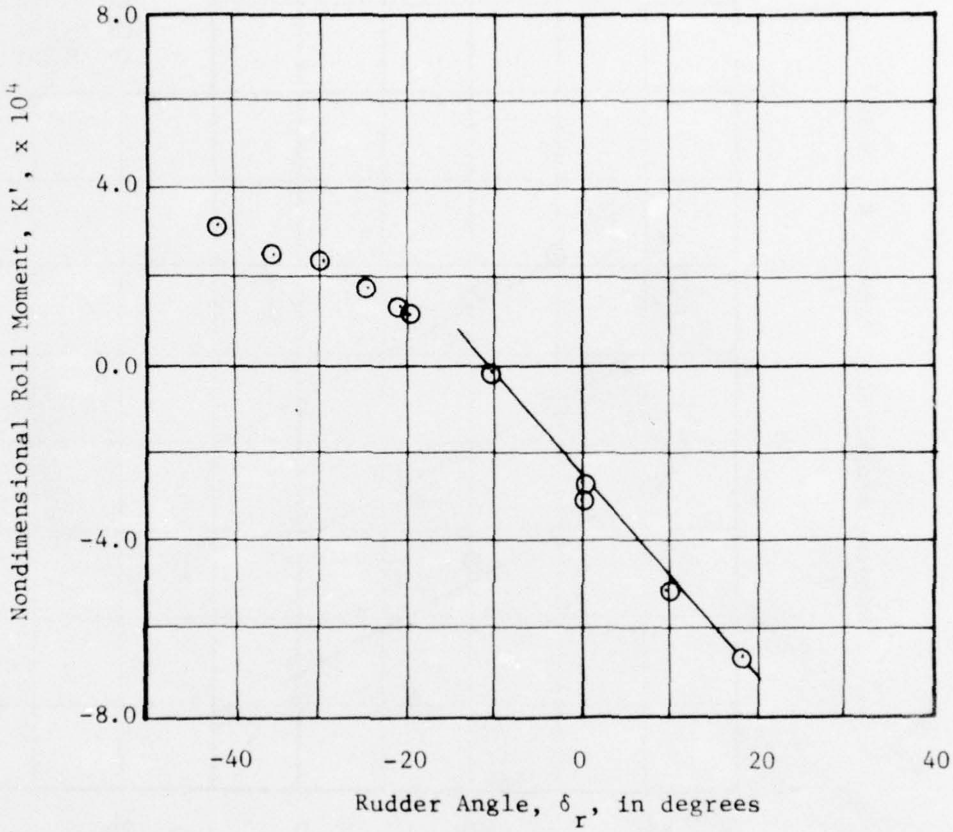

Figure 61 - Variation of Nondimensional Roll Moment with Rudder Angle for a Nondimensional Yaw Rate of 0.093 at a Full Scale Speed of 10 Knots for the Strut Rudder at Design Draft

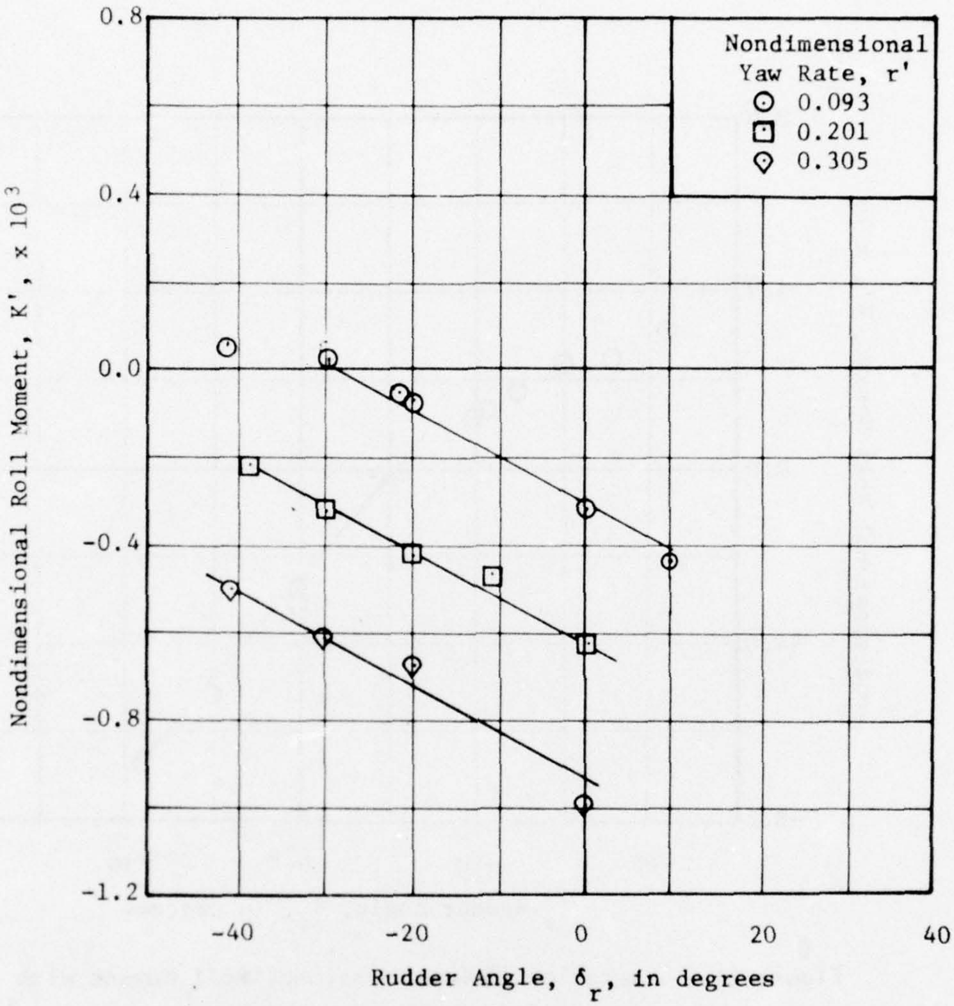

Figure 62 - Variation of Nondimensional Roll Moment with Rudder Angle for a Series of Nondimensional Yaw Rates at a Full Scale Speed of 15 Knots for the Strut Rudder at Design Draft

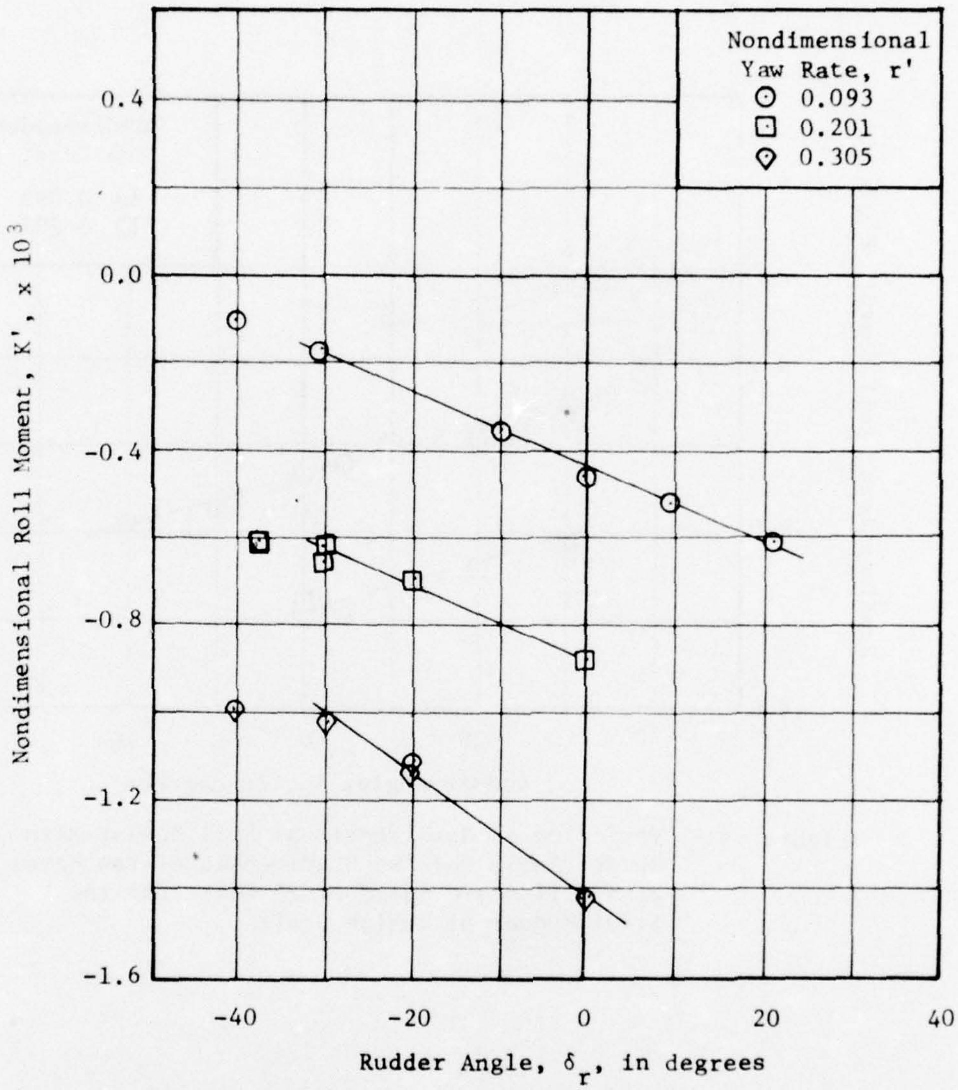

Figure 63 - Variation of Nondimensional Roll Moment with Rudder Angle for a Series of Nondimensional Yaw Rates at a Full Scale Speed of 20 Knots for the Strut Rudder at Design Draft

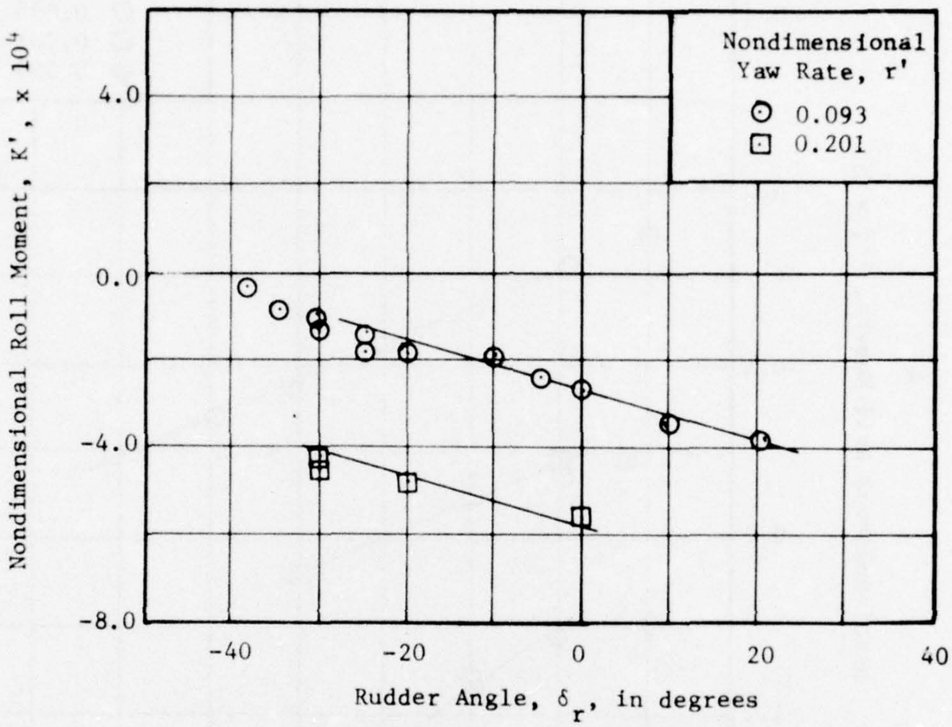

Figure 64 - Variation of Nondimensional Roll Moment with Rudder Angle for Two Nondimensional Yaw Rates at a Full Scale Speed of 25 Knots for the Strut Rudder at Design Draft

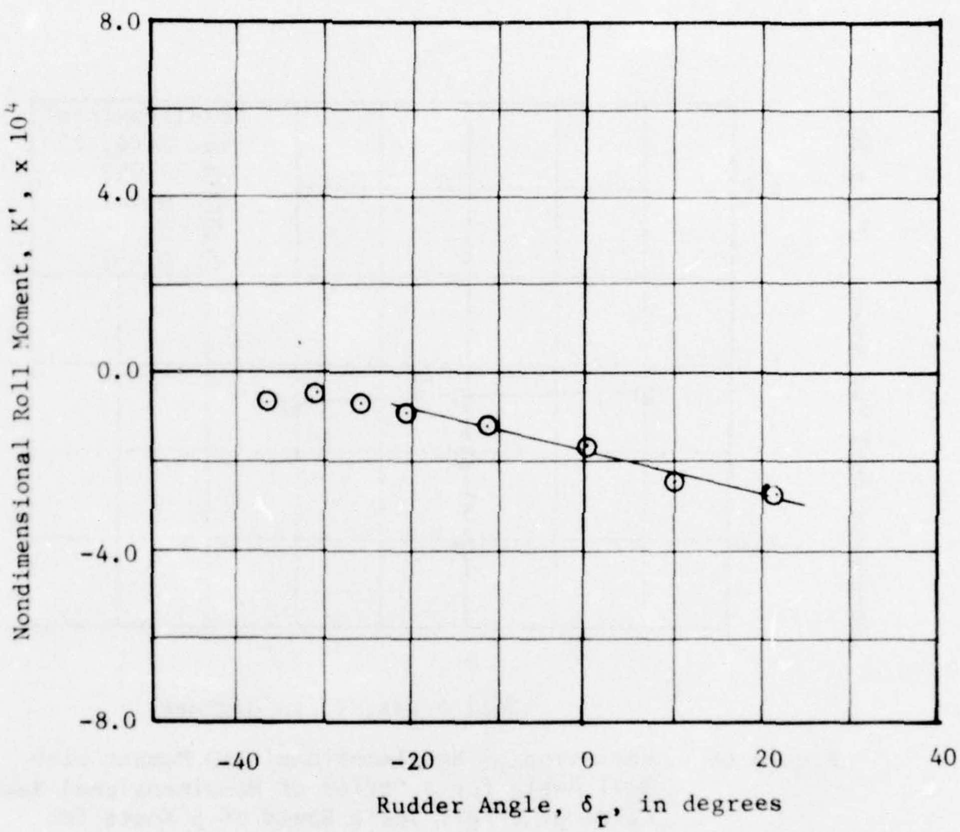

Figure 65 - Variation of Nondimensional Roll Moment with Rudder Angle for a Nondimensional Yaw Rate of 0.093 at a Full Scale Speed of 28 Knots for the Strut Rudder at Design Draft

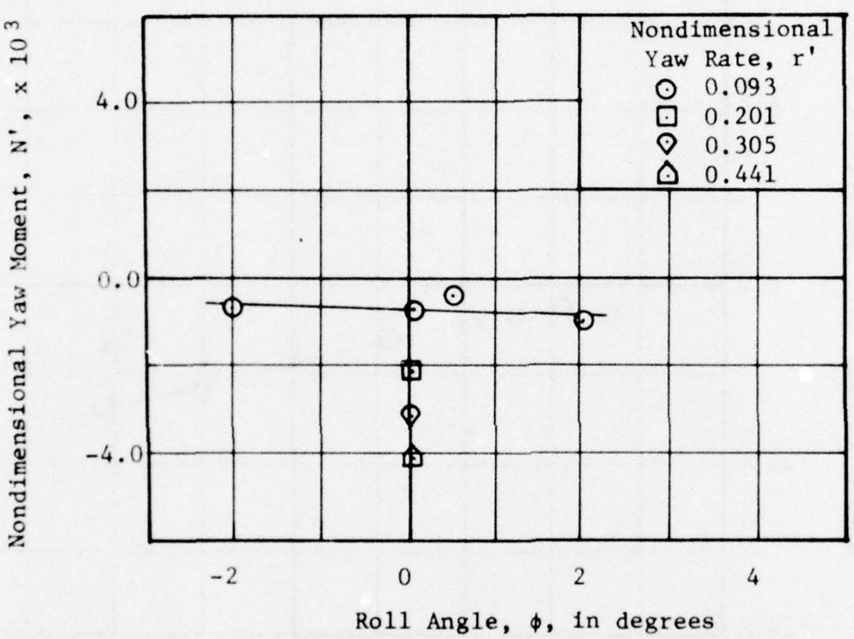

Figure 66 - Variation of Nondimensional Yaw Moment with Roll Angle for a Series of Nondimensional Yaw Rates at a Full Scale Speed of 5 Knots for the Strut Rudder at Design Draft

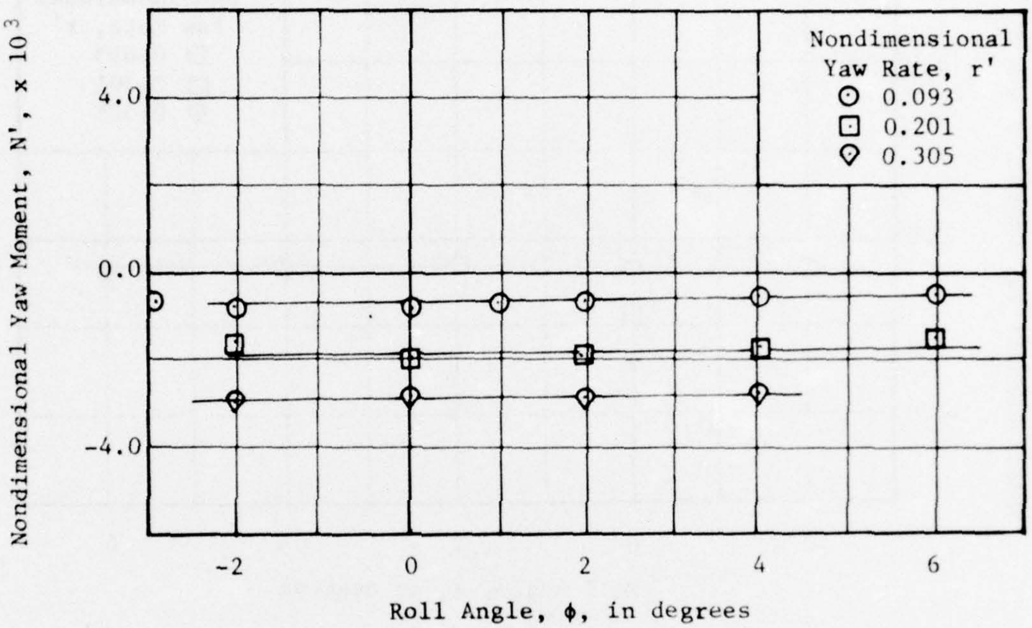

Figure 67 - Variation of Nondimensional Yaw Moment with Roll Angle for a Series of Nondimensional Yaw Rates at a Full Scale Speed of 10 Knots for the Strut Rudder at Design Draft

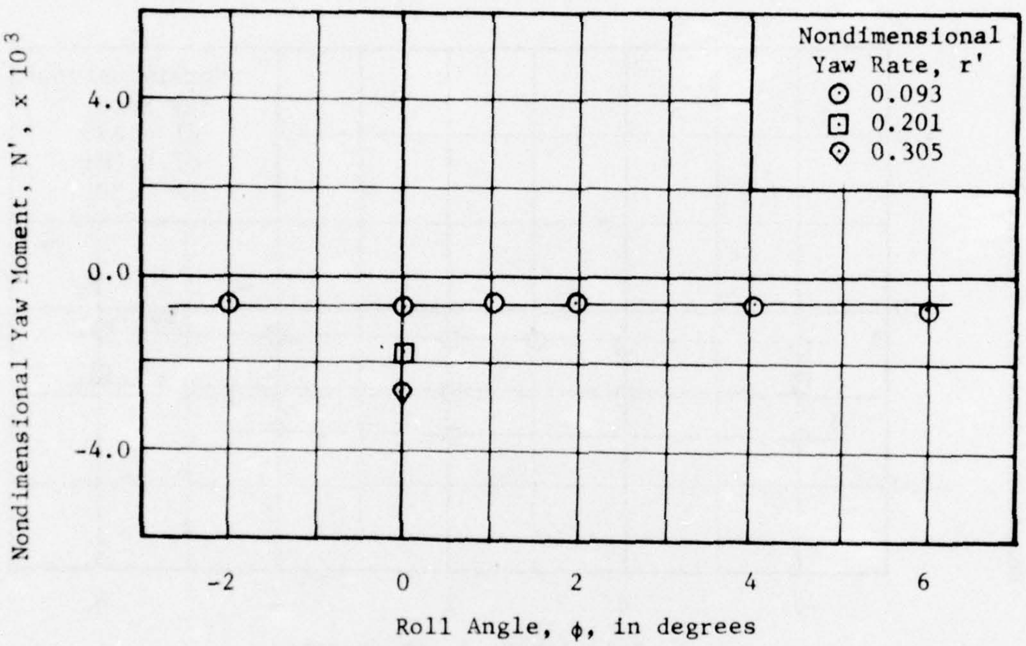

Figure 68 - Variation of Nondimensional Yaw Moment with Roll Angle for a Series of Nondimensional Yaw Rates at a Full Scale Speed of 15 Knots for the Strut Rudder at Design Draft

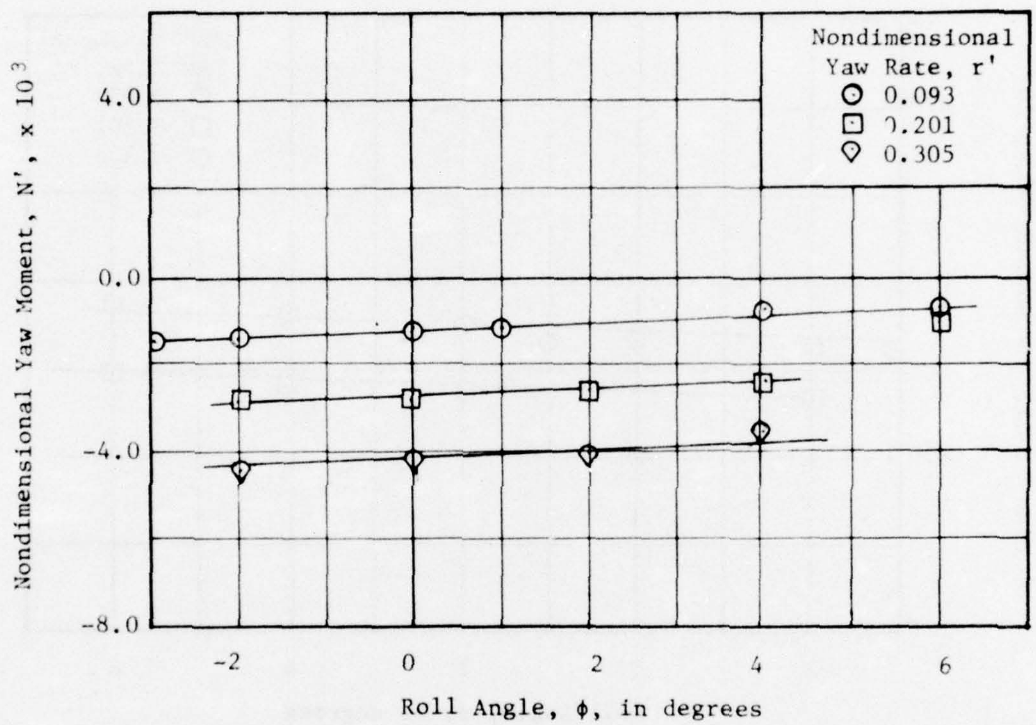

Figure 69 - Variation of Nondimensional Yaw Moment with Roll Angle for a Series of Nondimensional Yaw Rates at a Full Scale Speed of 20 Knots for the Strut Rudder at Design Draft

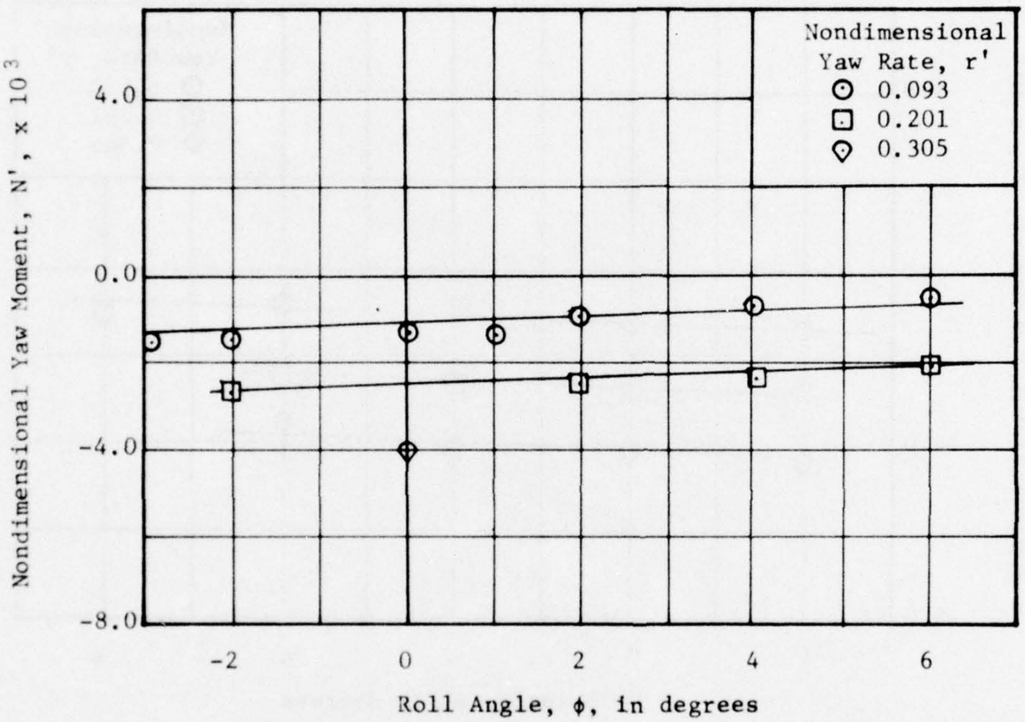

Figure 70 - Variation of Nondimensional Yaw Moment with Roll Angle for a Series of Nondimensional Yaw Rates at a Full Scale Speed of 25 Knots for the Strut Rudder at Design Draft

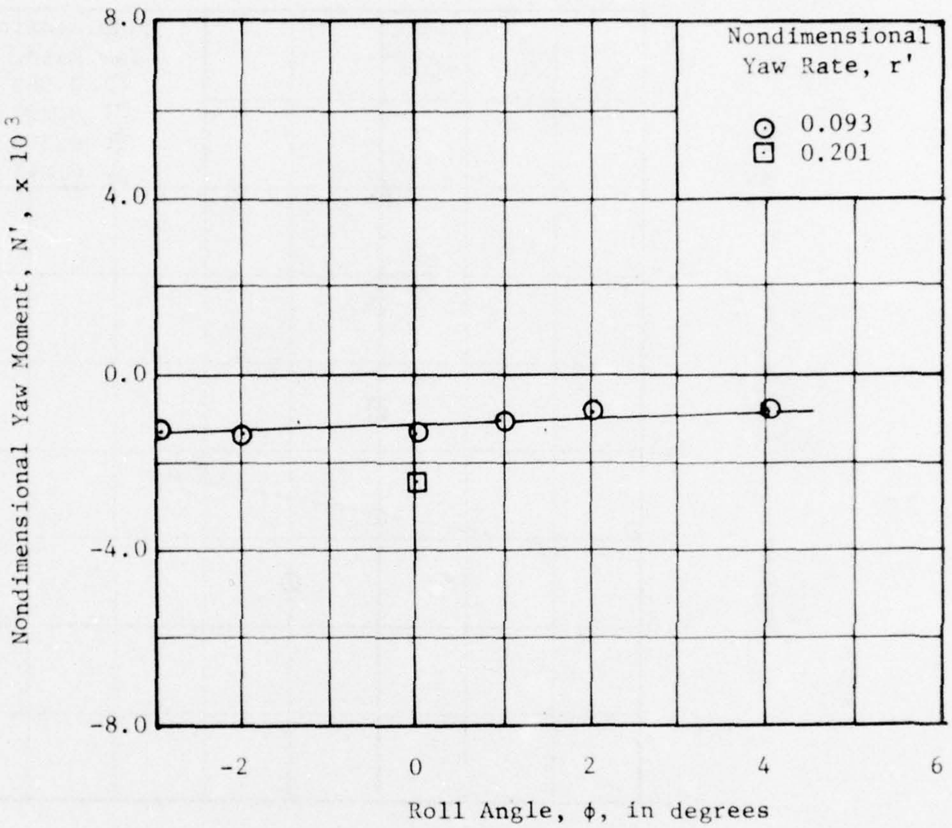

Figure 71 - Variation of Nondimensional Yaw Moment with Roll Angle for Two Nondimensional Yaw Rates at a Full Scale Speed of 28 Knots for the Strut Rudder at Design Draft

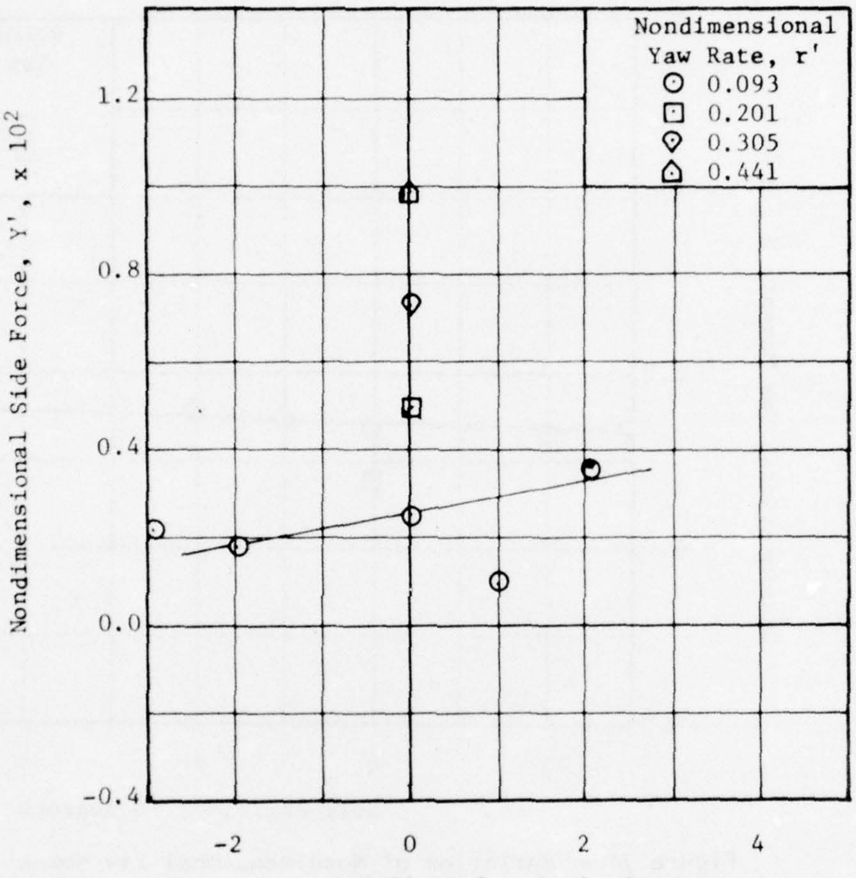

Figure 72 - Variation of Nondimensional Side Force with Roll Angle for a Series of Nondimensional Yaw Rates at a Full Scale Speed of 5 Knots for the Strut Rudder at Design Draft

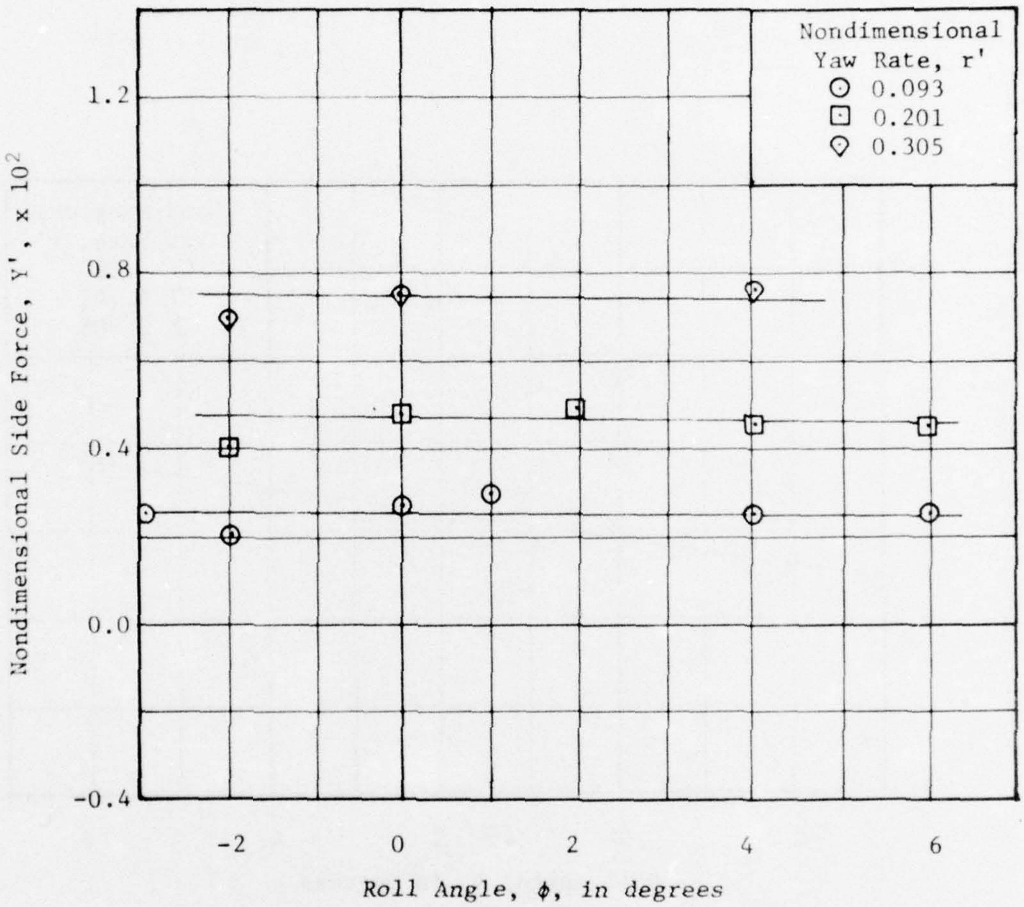

Figure 73 - Variation of Nondimensional Side Force with Roll Angle for a Series of Nondimensional Yaw Rates at a Full Scale Speed of 10 Knots for the Strut Rudder at Design Draft

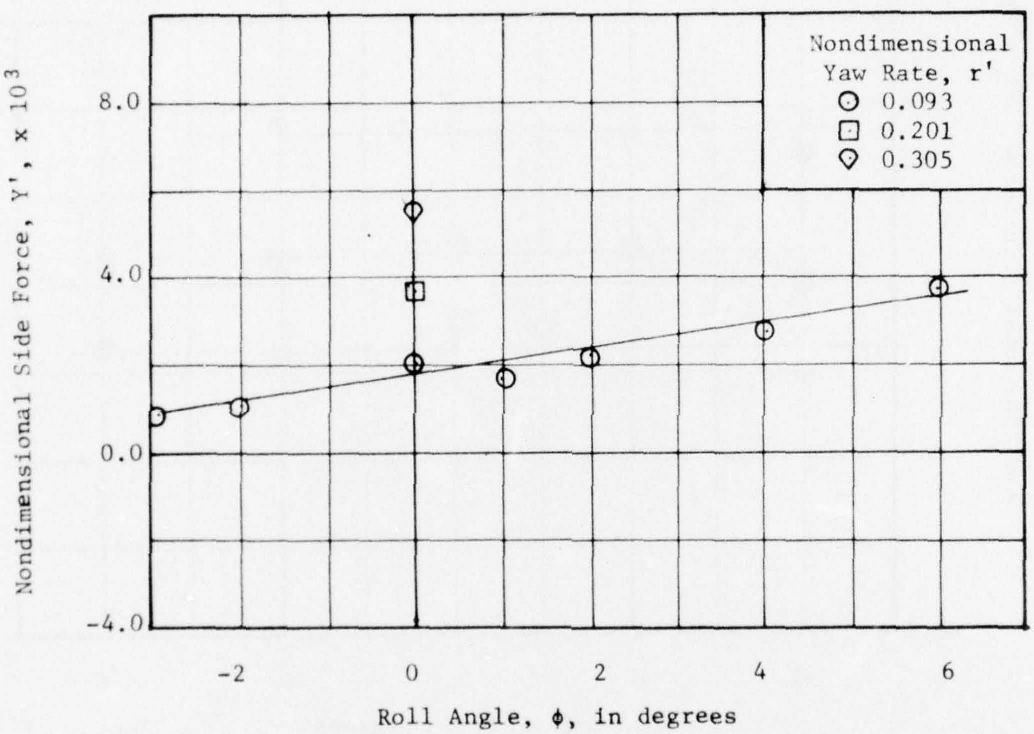

Figure 74 - Variation of Nondimensional Side Force with Roll Angle for a Series of Nondimensional Yaw Rates at a Full Scale Speed of 15 Knots for the Strut Rudder at Design Draft

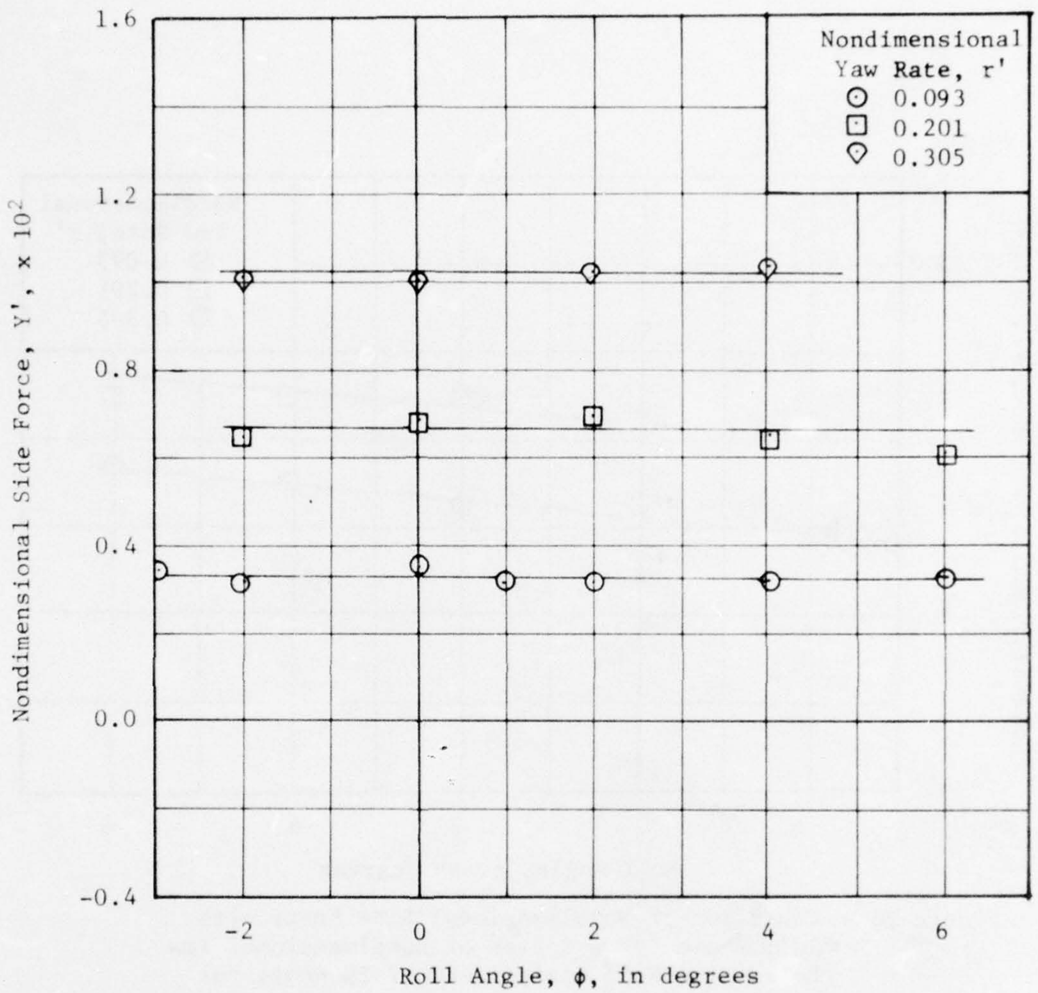

Figure 75 - Variation of Nondimensional Side Force with Roll Angle for a Series of Nondimensional Yaw Rates at a Full Scale Speed of 20 Knots for the Strut Rudder at Design Draft

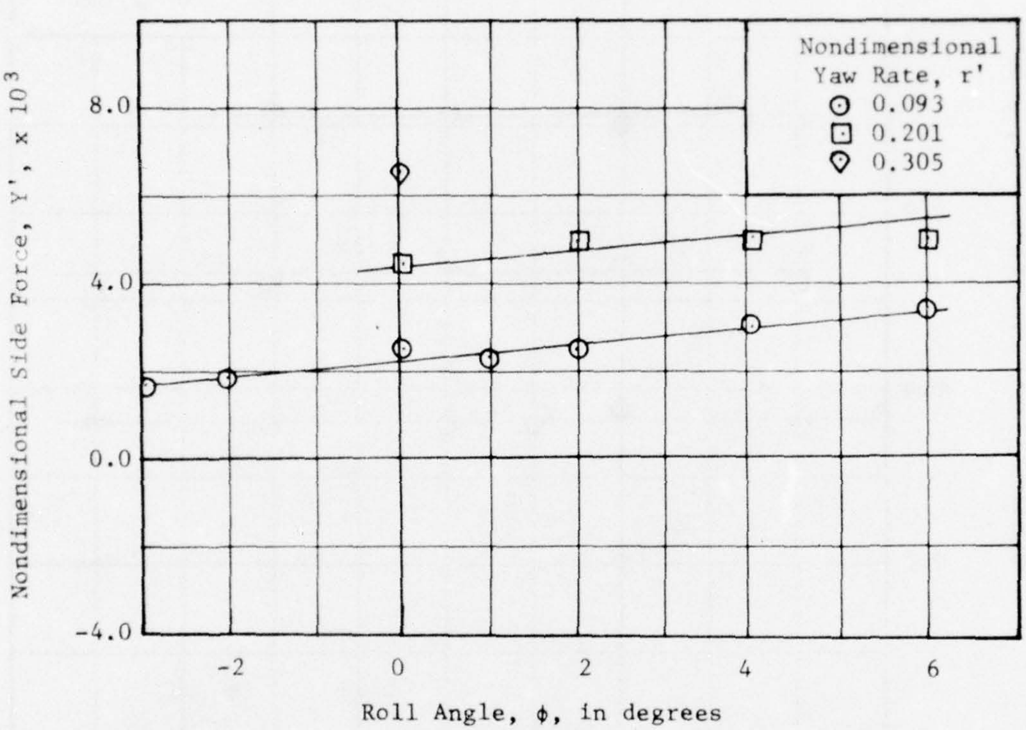

Figure 76 - Variation of Nondimensional Side Force with Roll Angle for a Series of Nondimensional Yaw Rates at a Full Scale Speed of 25 Knots for the Strut Rudder at Design Draft

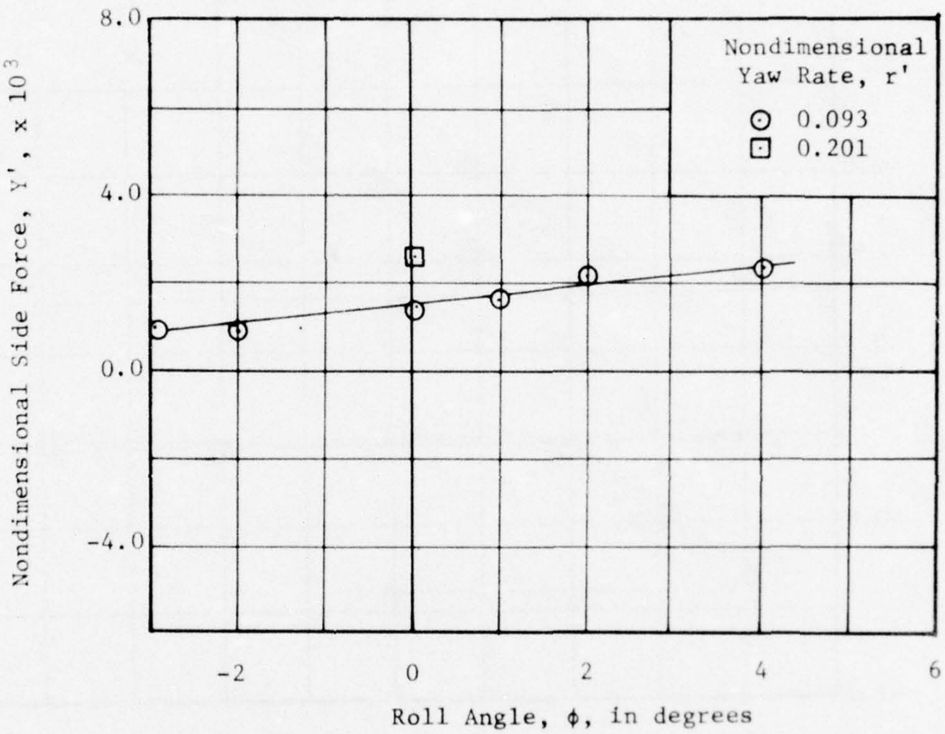

Figure 77 - Variation of Nondimensional Side Force with Roll Angle for Two Nondimensional Yaw Rates at a Full Scale Speed of 28 Knots for the Strut Rudder at Design Draft

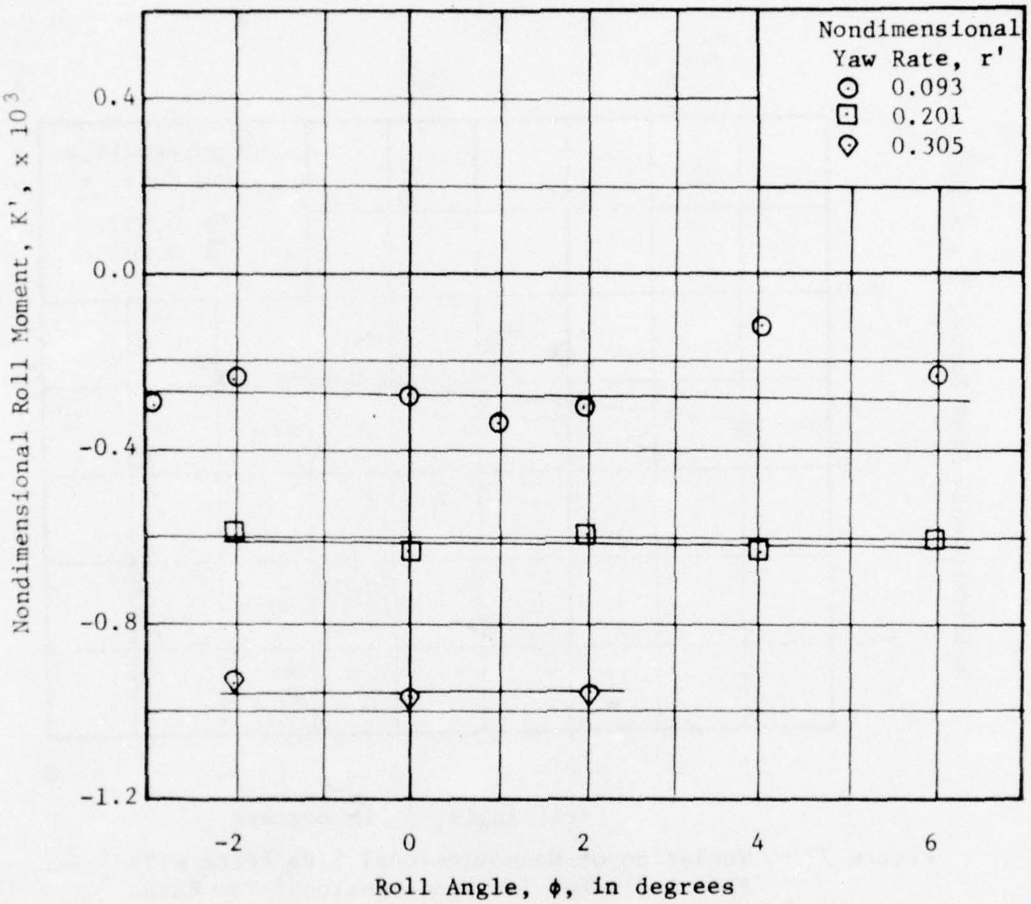

Figure 78 - Variation of Nondimensional Roll Moment with Roll Angle for a Series of Nondimensional Yaw Rates at a Full Scale Speed of 10 Knots for the Strut Rudder at Design Draft

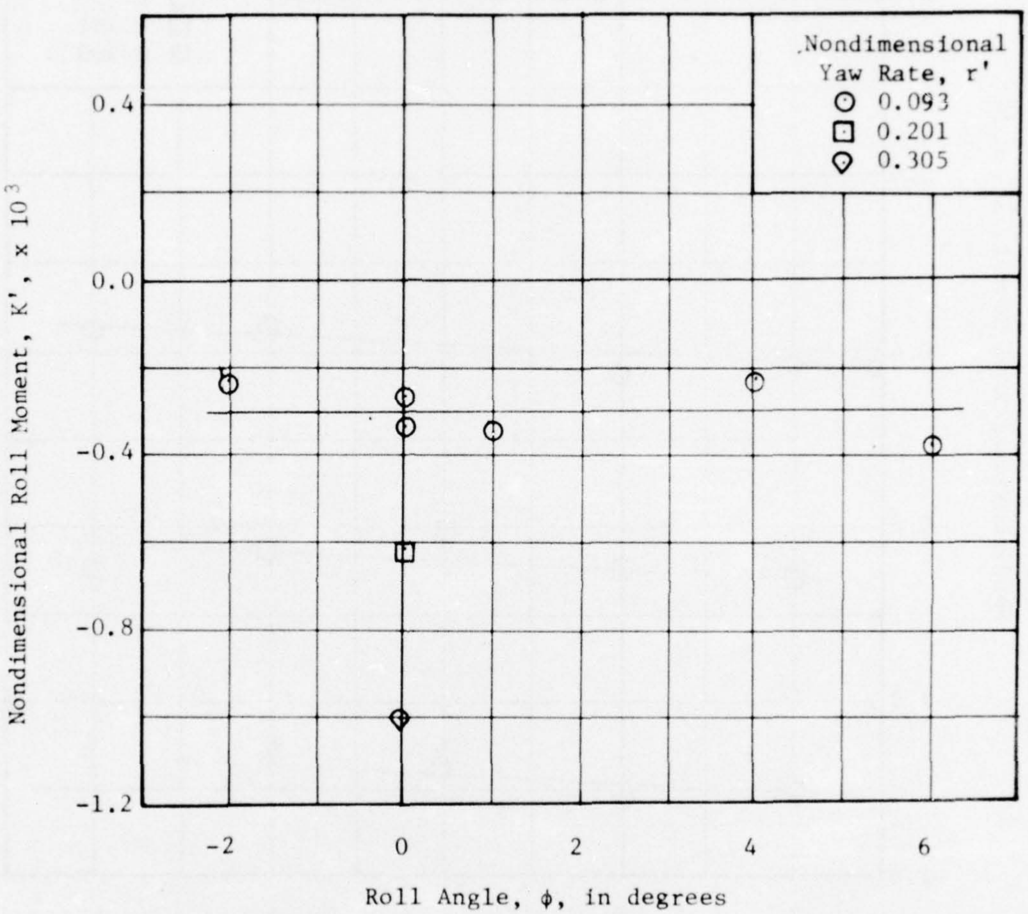

Figure 79 - Variation of Nondimensional Roll Moment with Roll Angle for a Series of Nondimensional Yaw Rates at a Full Scale Speed of 15 Knots for the Strut Rudder at Design Draft

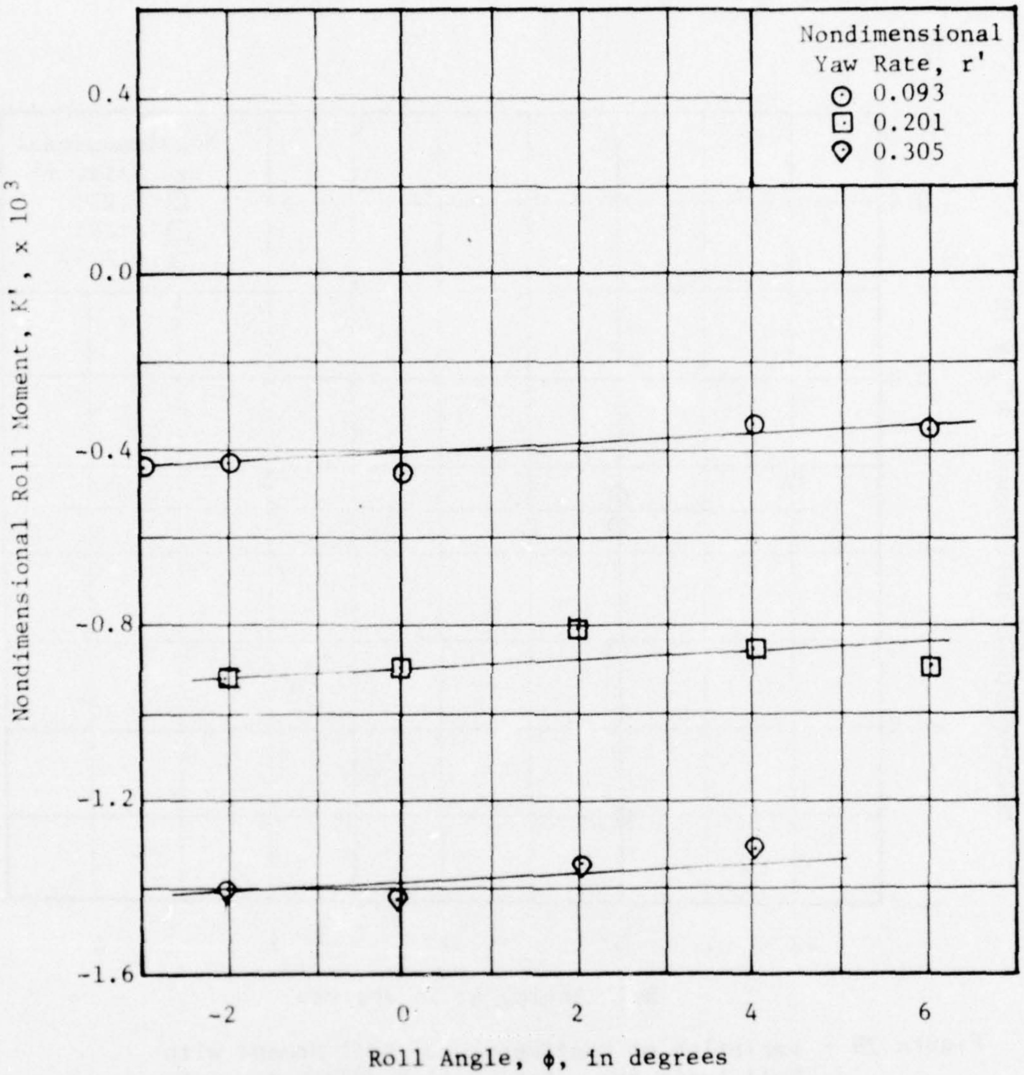

Figure 80 - Variation of Nondimensional Roll Moment with Roll Angle for a Series of Nondimensional Yaw Rates at a Full Scale Speed of 20 Knots for the Strut Rudder at Design Draft

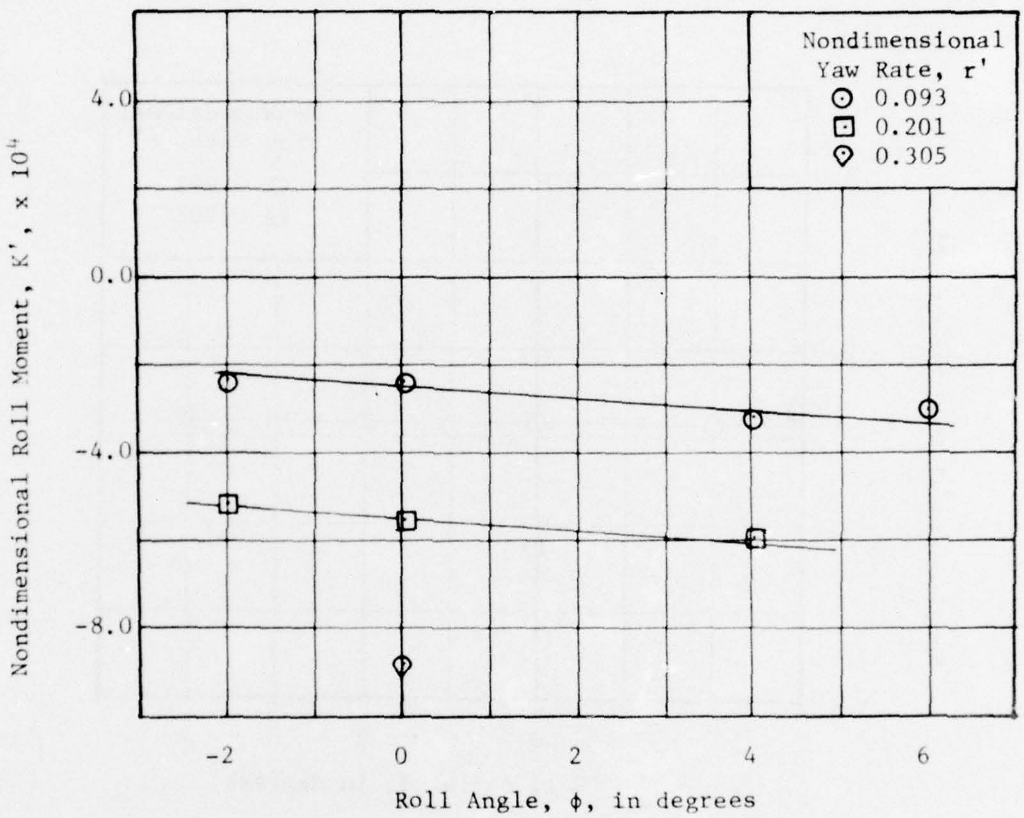

Figure 81 - Variation of Nondimensional Roll Moment with Roll Angle for a Series of Nondimensional Yaw Rates at a Full Scale Speed of 25 Knots for the Strut Rudder at Design Draft

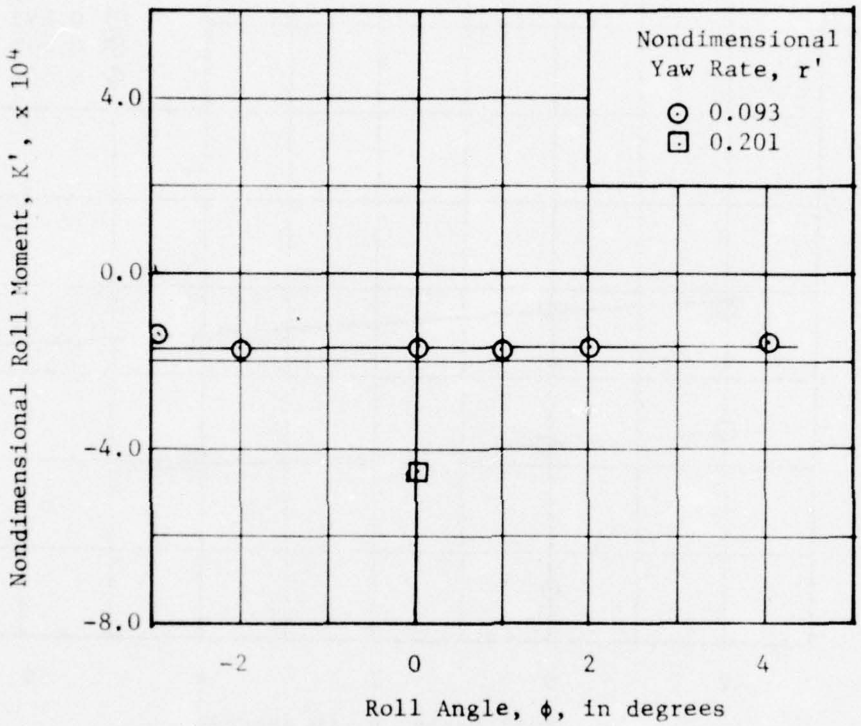

Figure 82 - Variation of Nondimensional Roll Moment with Roll Angle for Two Nondimensional Yaw Rates at a Full Scale Speed of 28 Knots for the Strut Rudder at Design Draft

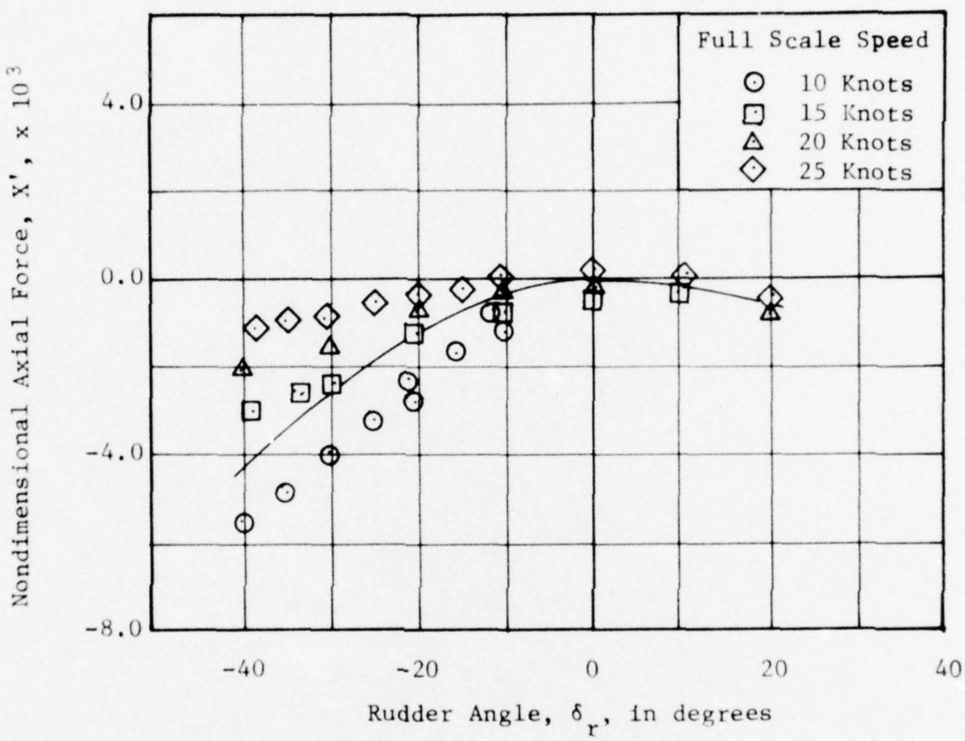

Figure 83 - Variation of Nondimensional Axial Force with Rudder Angle for a Series of Full Scale Speeds at a Nondimensional Yaw Rate of 0.093 for the Strut Rudder at Design Draft

Appendix B

(Figures 84 to 120)
Nondimensional Data Curves for
the Strut Rudder at Deep Draft

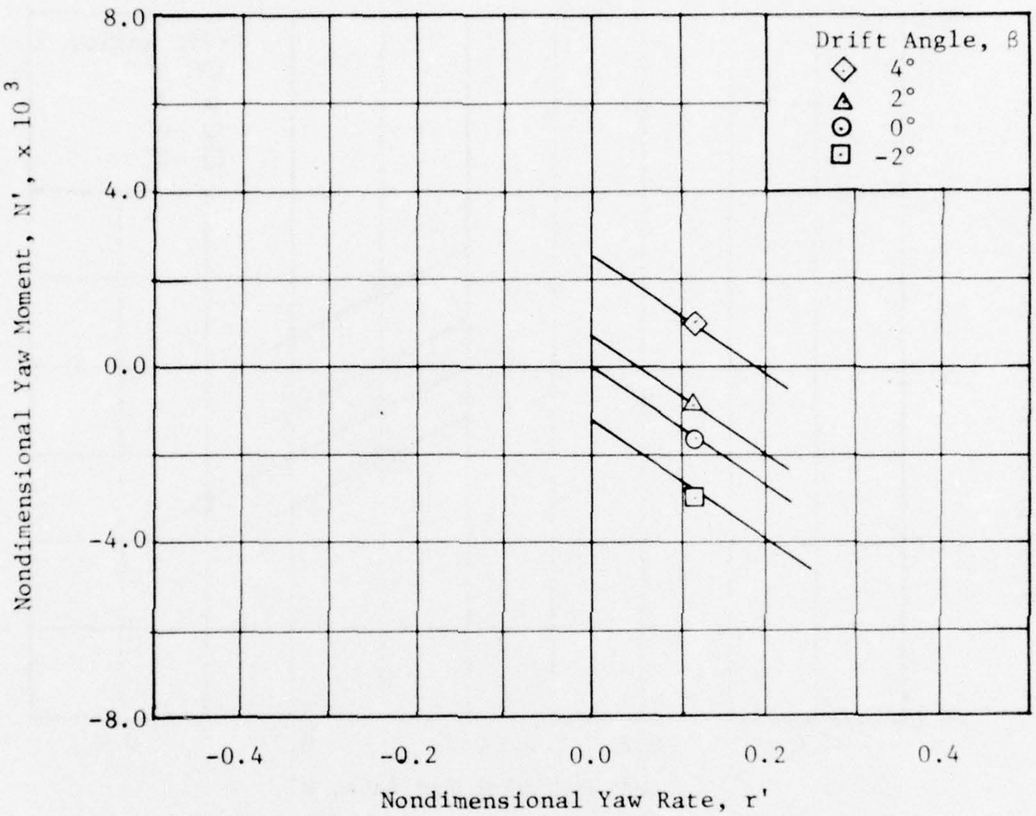

Figure 84 - Variation of Nondimensional Yaw Moment with Nondimensional Yaw Rate for a Series of Drift Angles at a Full Scale Speed of 5 Knots for the Strut Rudder at Deep Draft

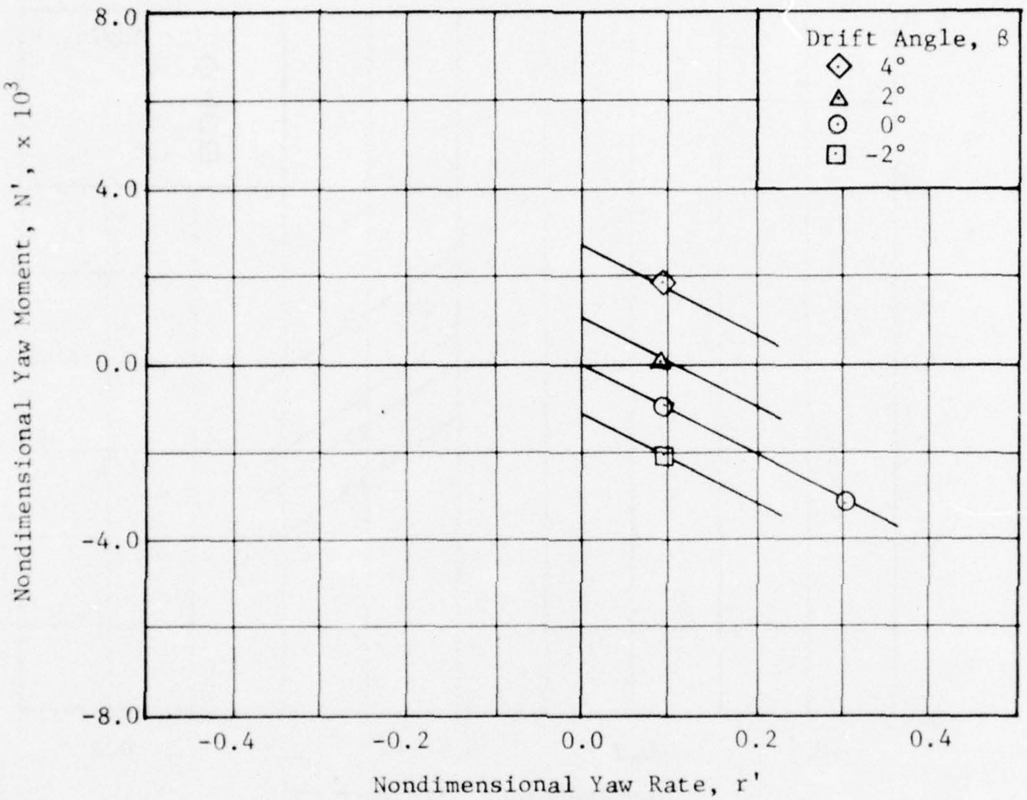

Figure 85 - Variation of Nondimensional Yaw Moment with Nondimensional Yaw Rate for a Series of Drift Angles at a Full Scale Speed of 10 Knots for the Strut Rudder at Deep Draft

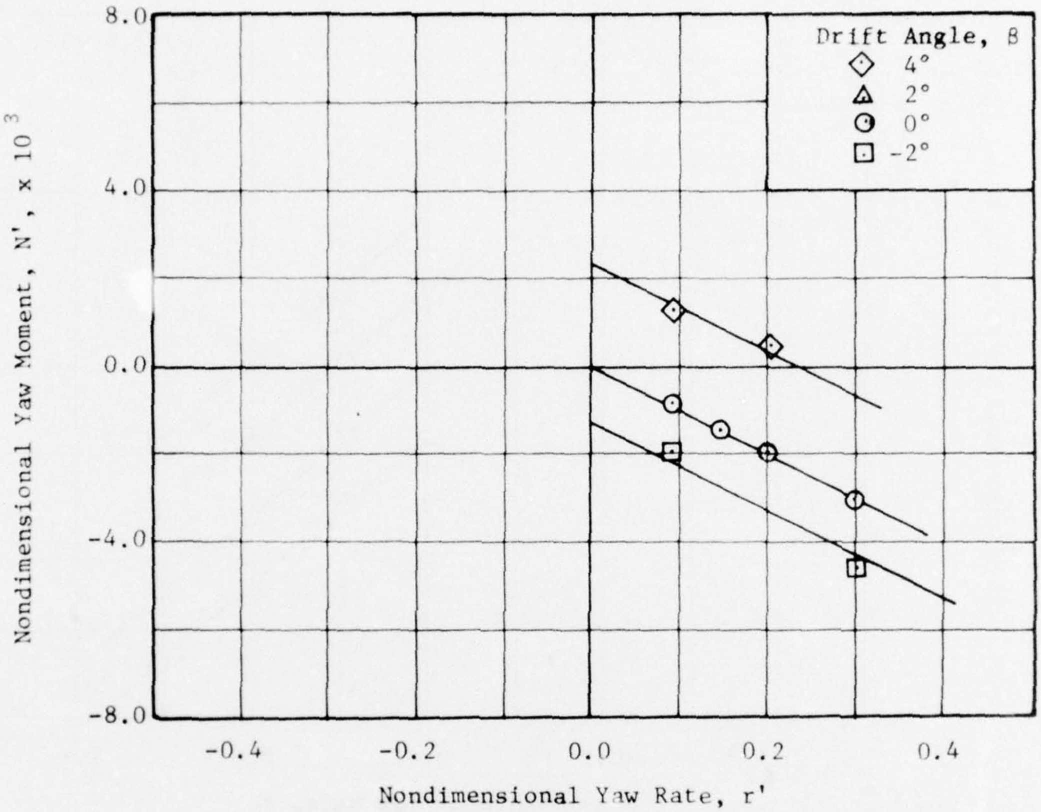

Figure 86 - Variation of Nondimensional Yaw Moment with Nondimensional Yaw Rate for a Series of Drift Angles at a Full Scale Speed of 15 Knots for the Strut Rudder at Deep Draft

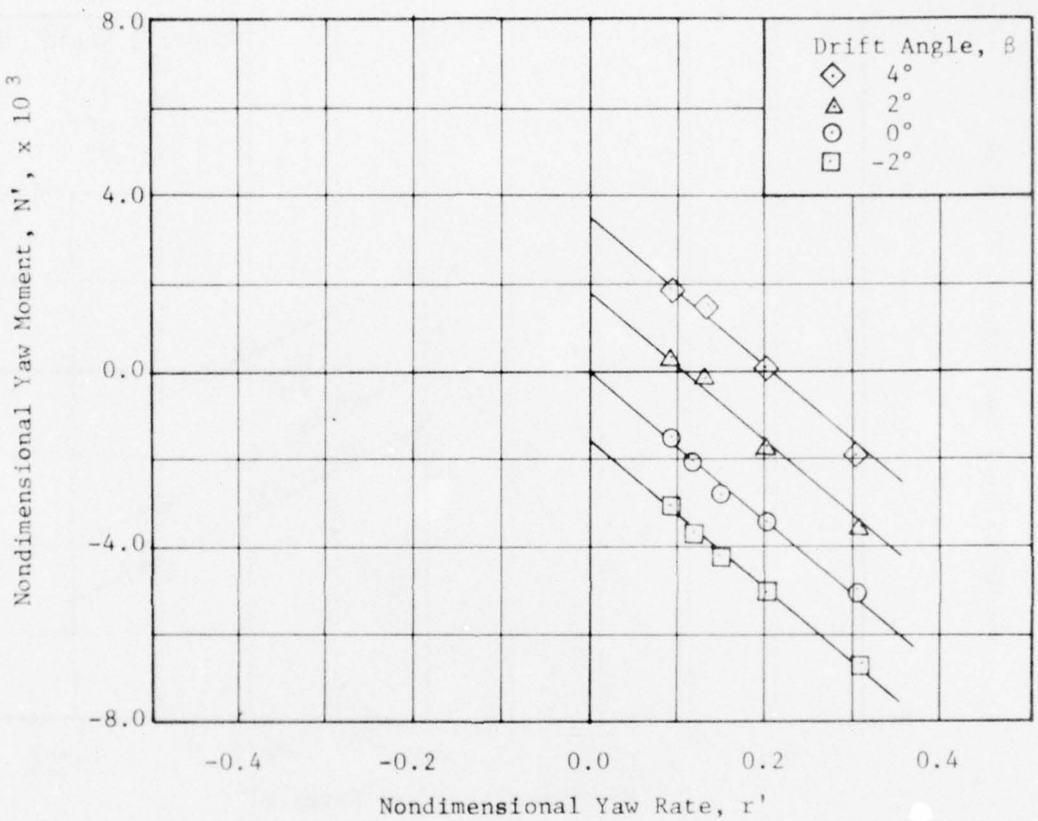

Figure 87 - Variation of Nondimensional Yaw Moment with Nondimensional Yaw Rate for a Series of Drift Angles at a Full Scale Speed of 20 Knots for the Strut Rudder at Deep Draft

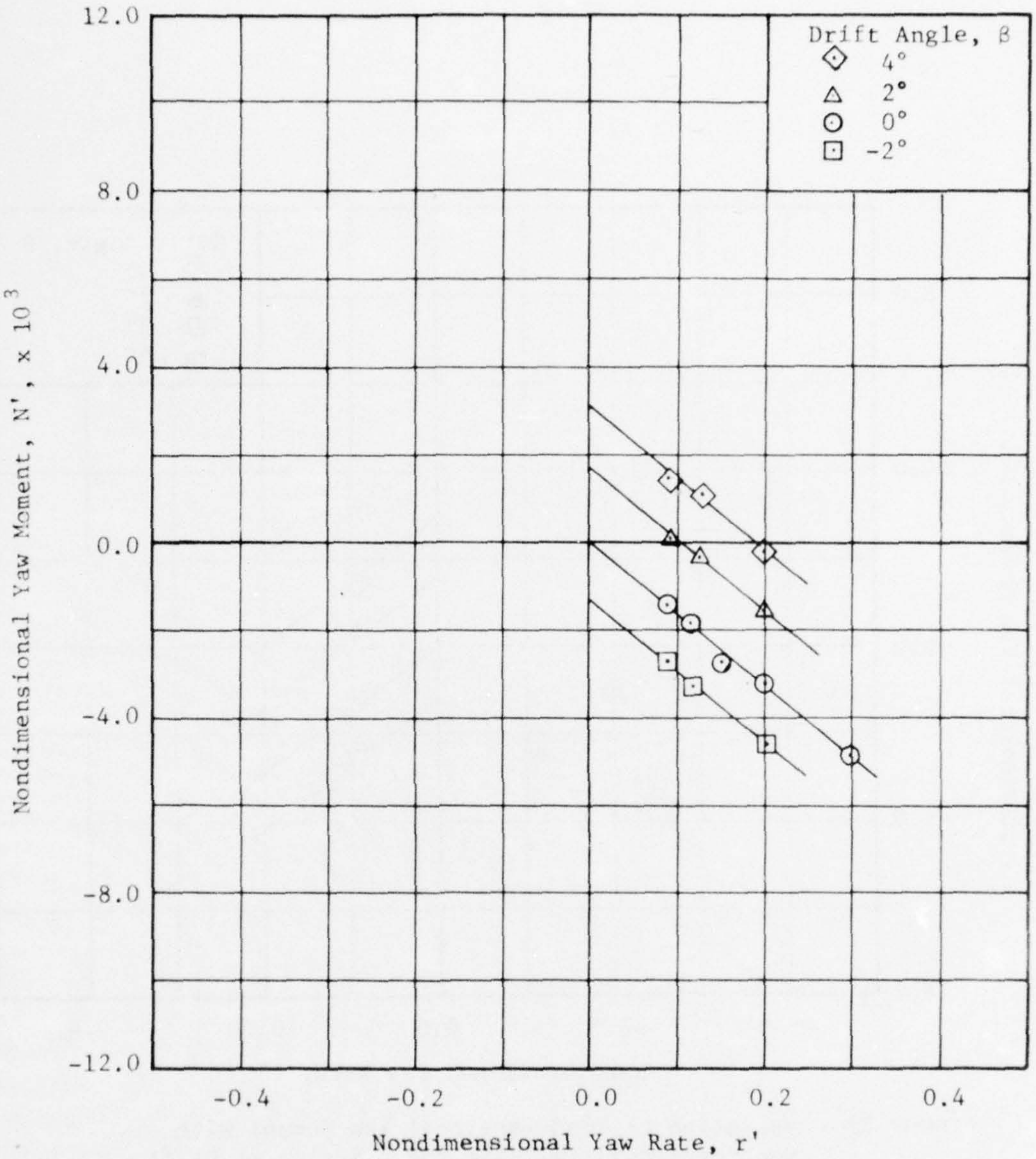

Figure 88 - Variation of Nondimensional Yaw Moment with Nondimensional Yaw Rate for a Series of Drift Angles at a Full Scale Speed of 25 Knots for the Strut Rudder at Deep Draft

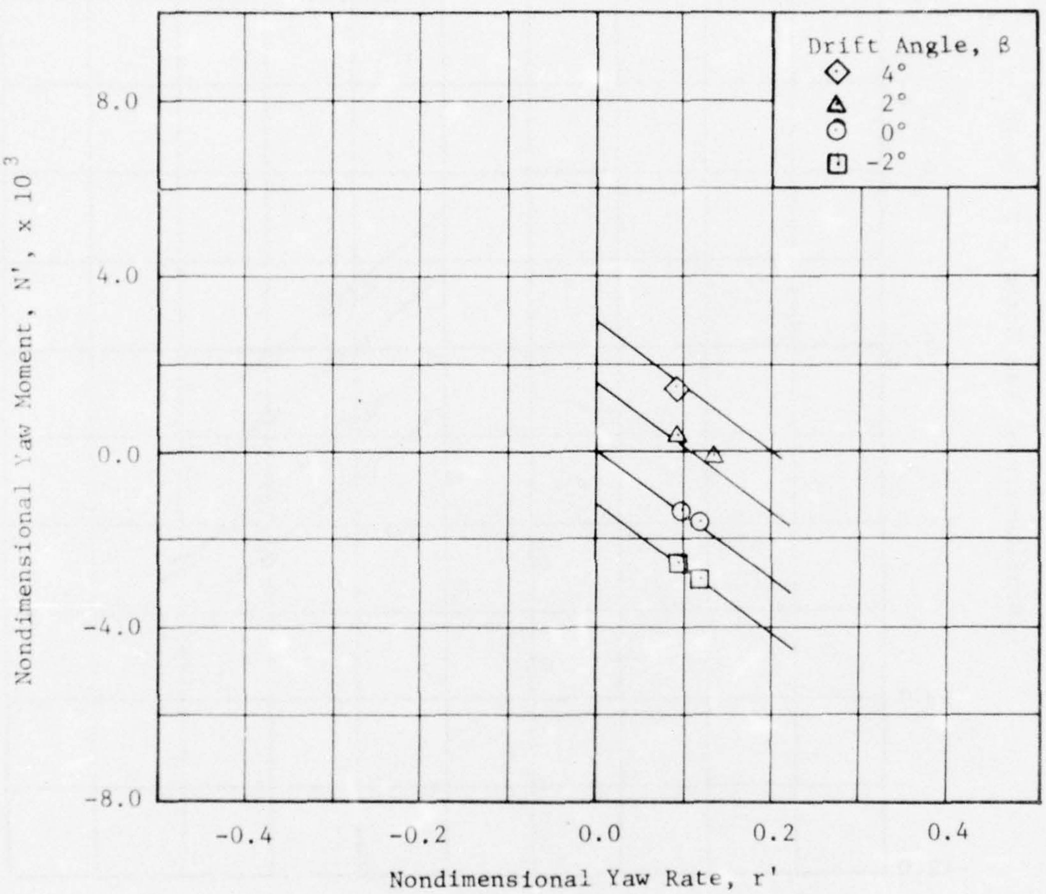

Figure 89 - Variation of Nondimensional Yaw Moment with Nondimensional Yaw Rate for a Series of Drift Angles at a Full Scale Speed of 28 Knots for the Strut Rudder at Deep Draft

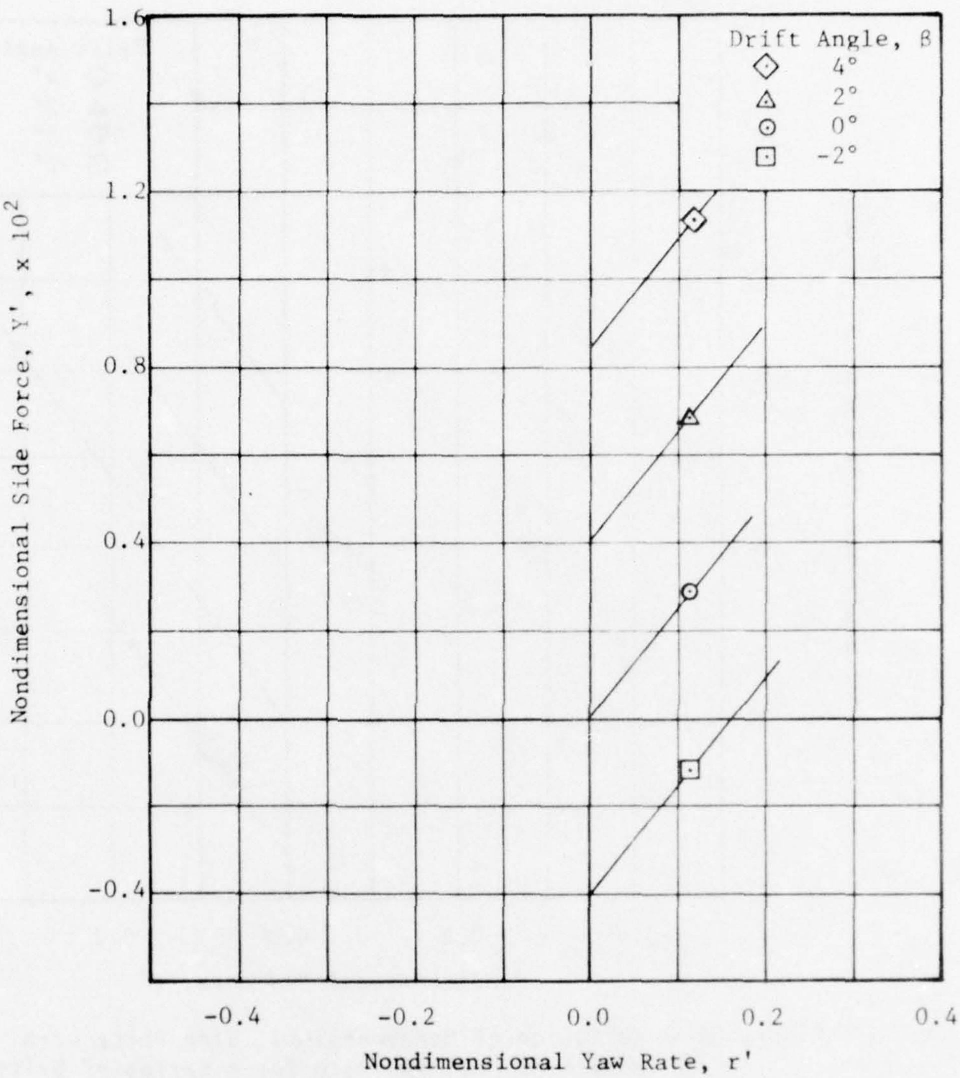

Figure 90 - Variation of Nondimensional Side Force with Nondimensional Yaw Rate for a Series of Drift Angles at a Full Scale Speed of 5 Knots for the Strut Rudder at Deep Draft

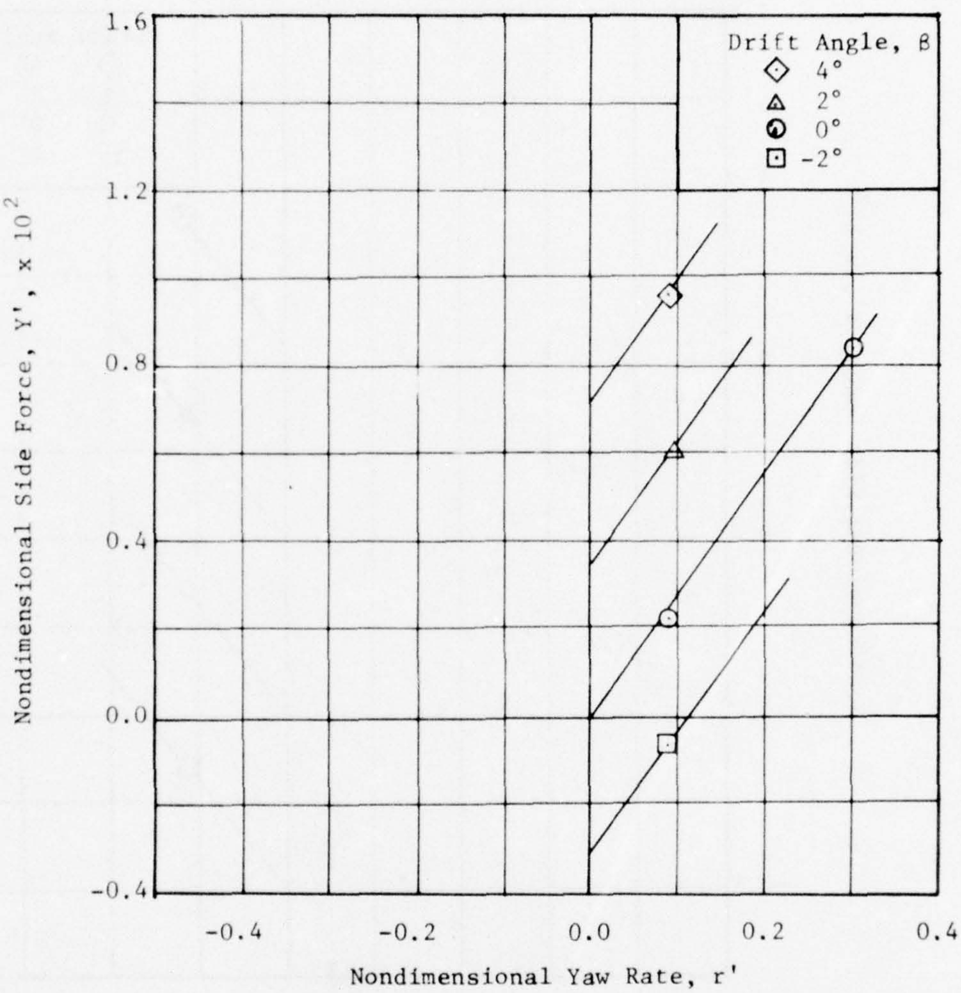

Figure 91 - Variation of Nondimensional Side Force with Nondimensional Yaw Rate for a Series of Drift Angles at a Full Scale Speed of 10 Knots for the Strut Rudder at Deep Draft

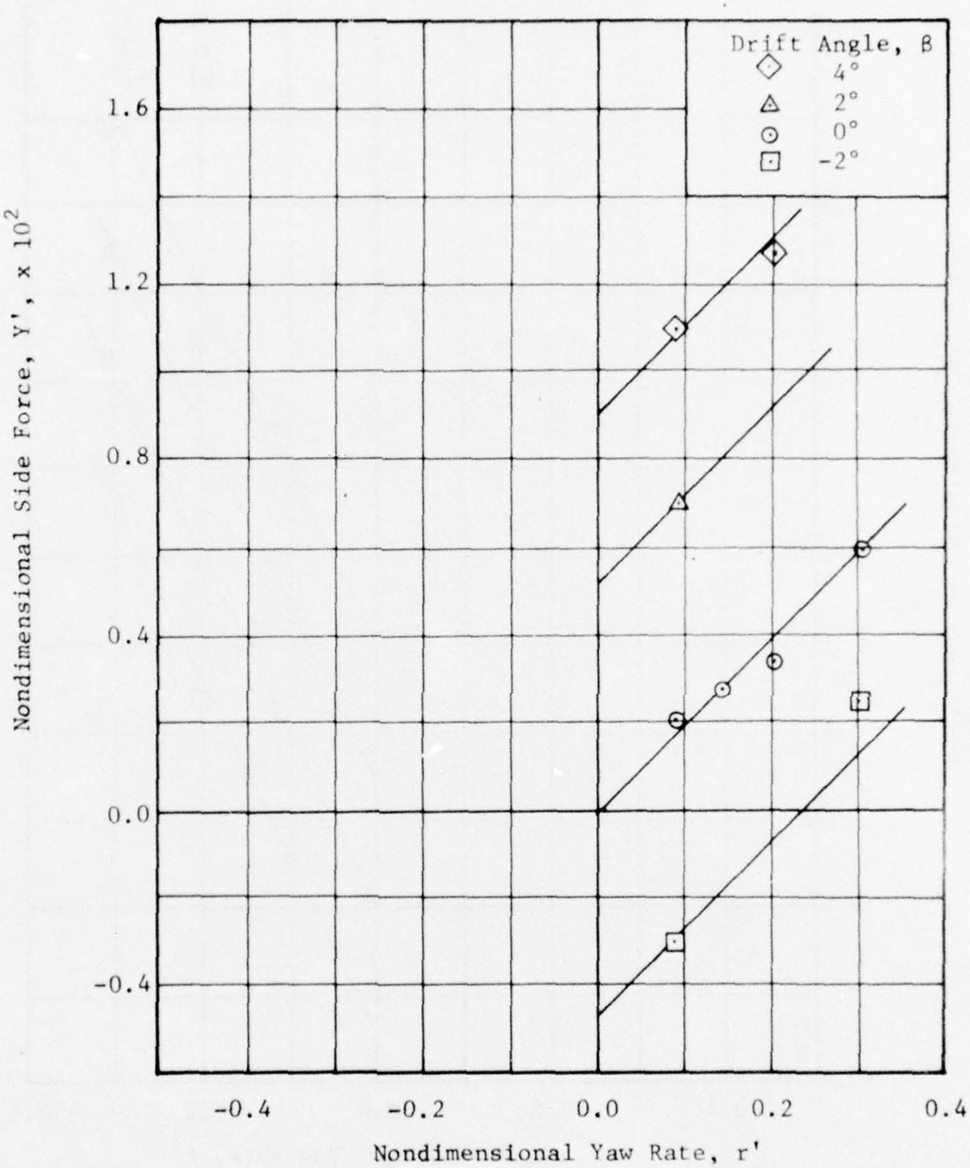

Figure 92 - Variation of Nondimensional Side Force with Nondimensional Yaw Rate for a Series of Drift Angles at a Full Scale Speed of 15 Knots for the Strut Rudder at Deep Draft

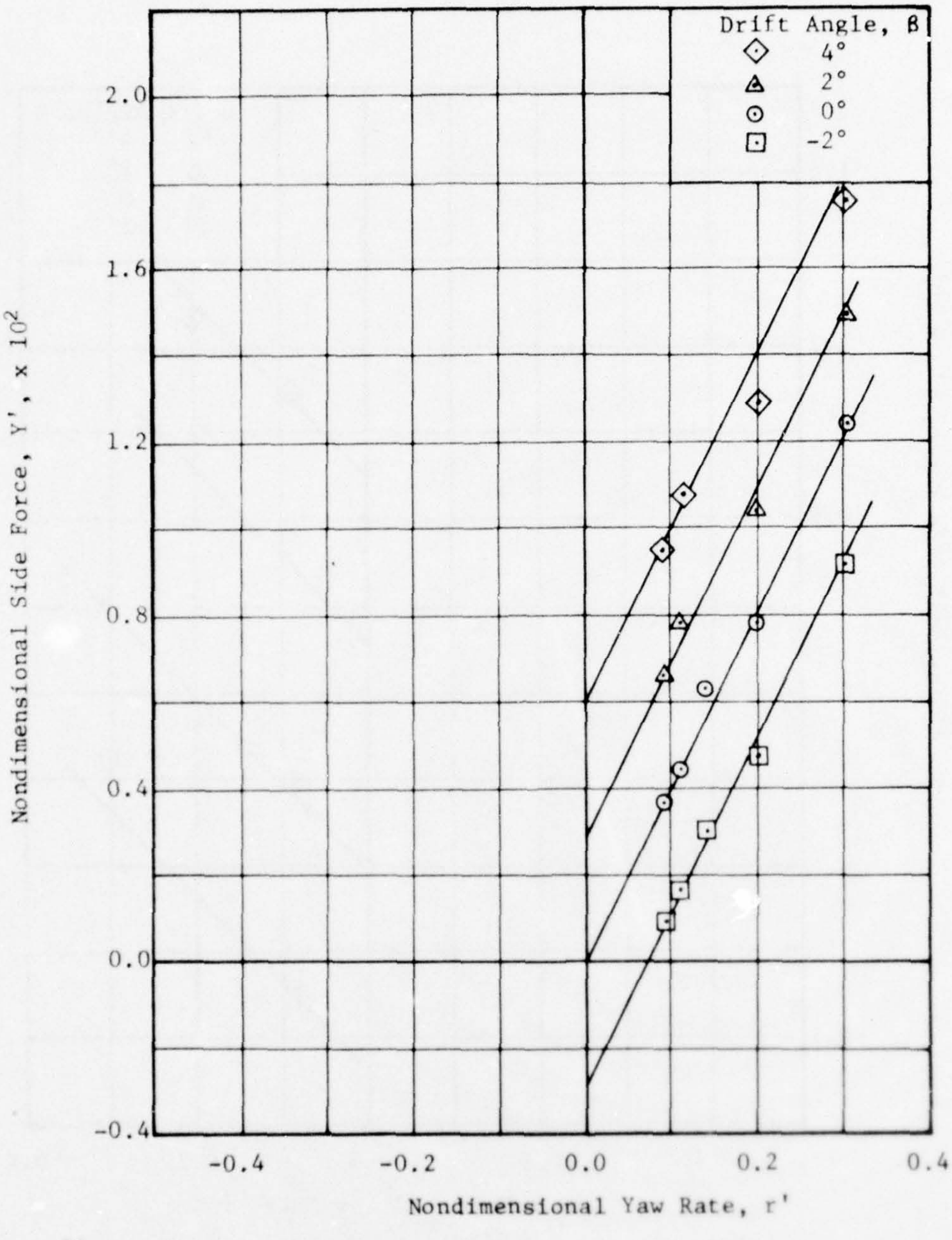

Figure 93 - Variation of Nondimensional Side Force with Nondimensional Yaw Rate for a Series of Drift Angles at a Full Scale Speed of 20 Knots for the Strut Rudder at Deep Draft

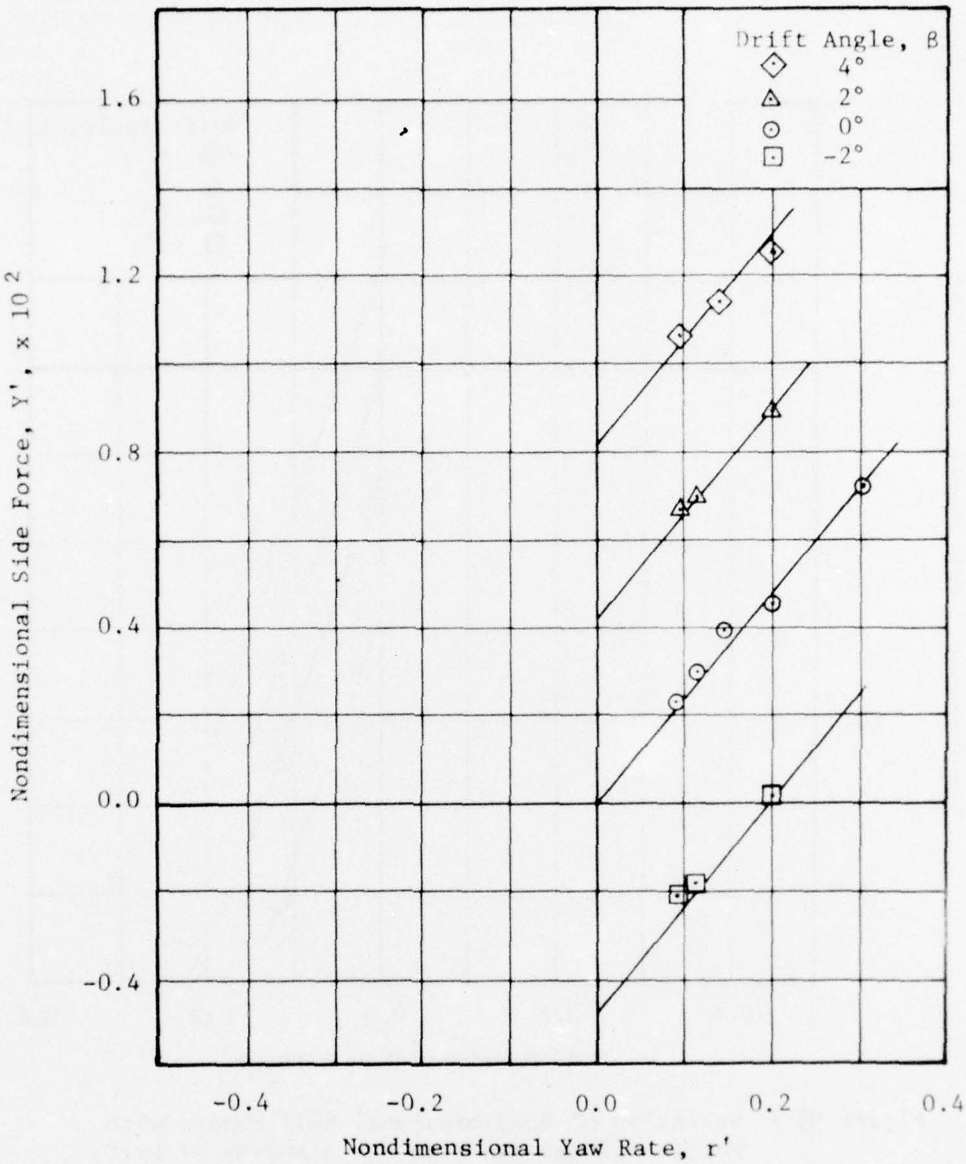

Figure 94 - Variation of Nondimensional Side Force with Nondimensional Yaw Rate for a Series of Drift Angles at a Full Scale Speed of 25 Knots for the Strut Rudder at Deep Draft

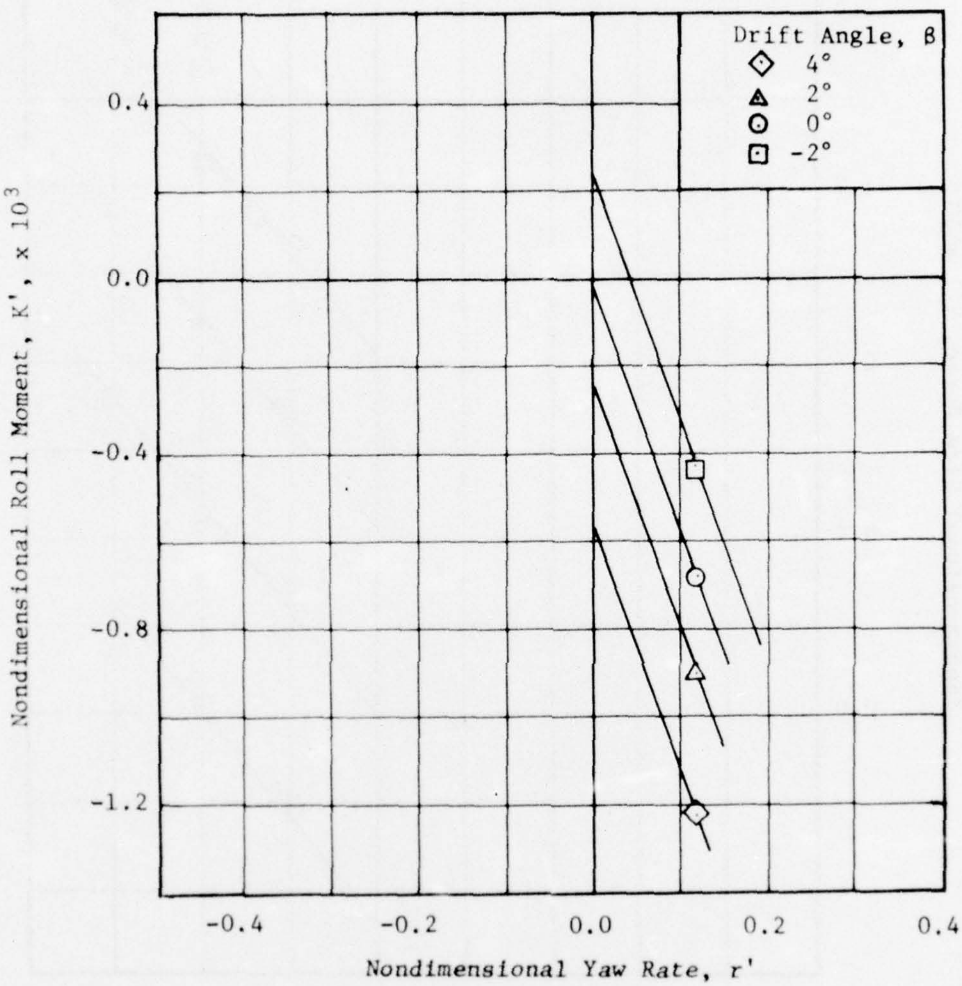

Figure 95 - Variation of Nondimensional Roll Moment with Nondimensional Yaw Rate for a Series of Drift An ,es at a Full Scale Speed of 5 Knots for the Strut Rudder at Deep Draft

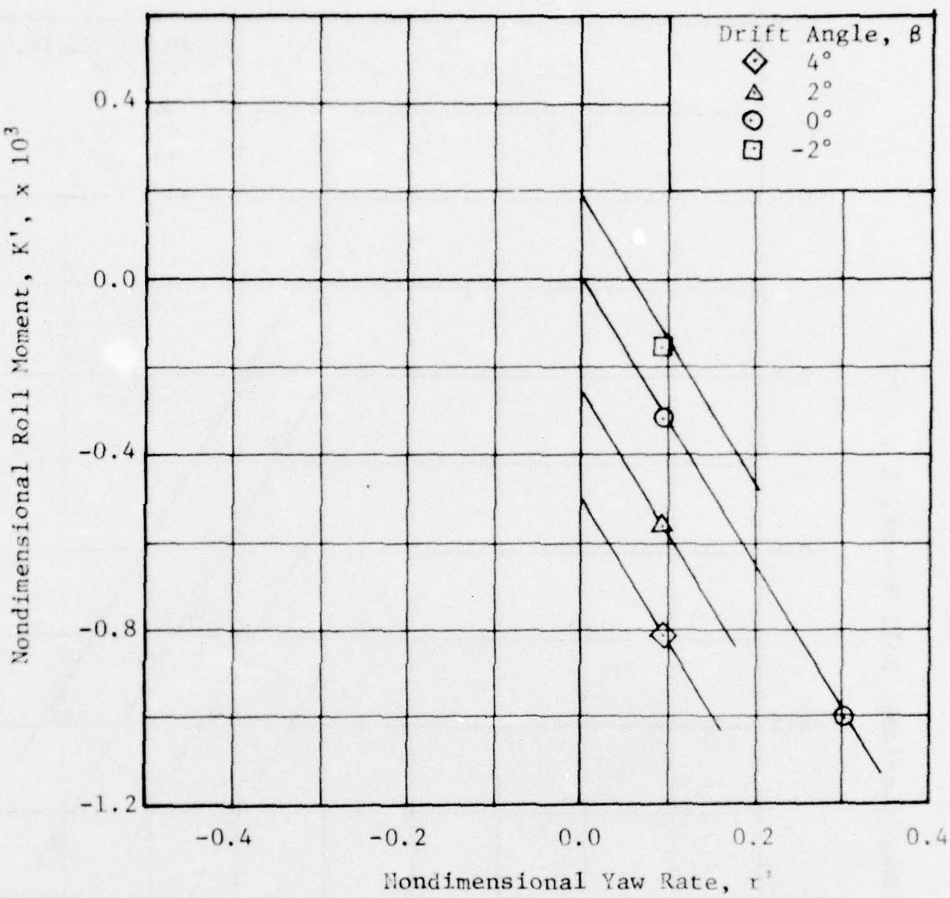

Figure 96 - Variation of Nondimensional Roll Moment with Nondimensional Yaw Rate for a Series of Drift Angles at a Full Scale Speed of 10 Knots for the Strut Rudder at Deep Draft

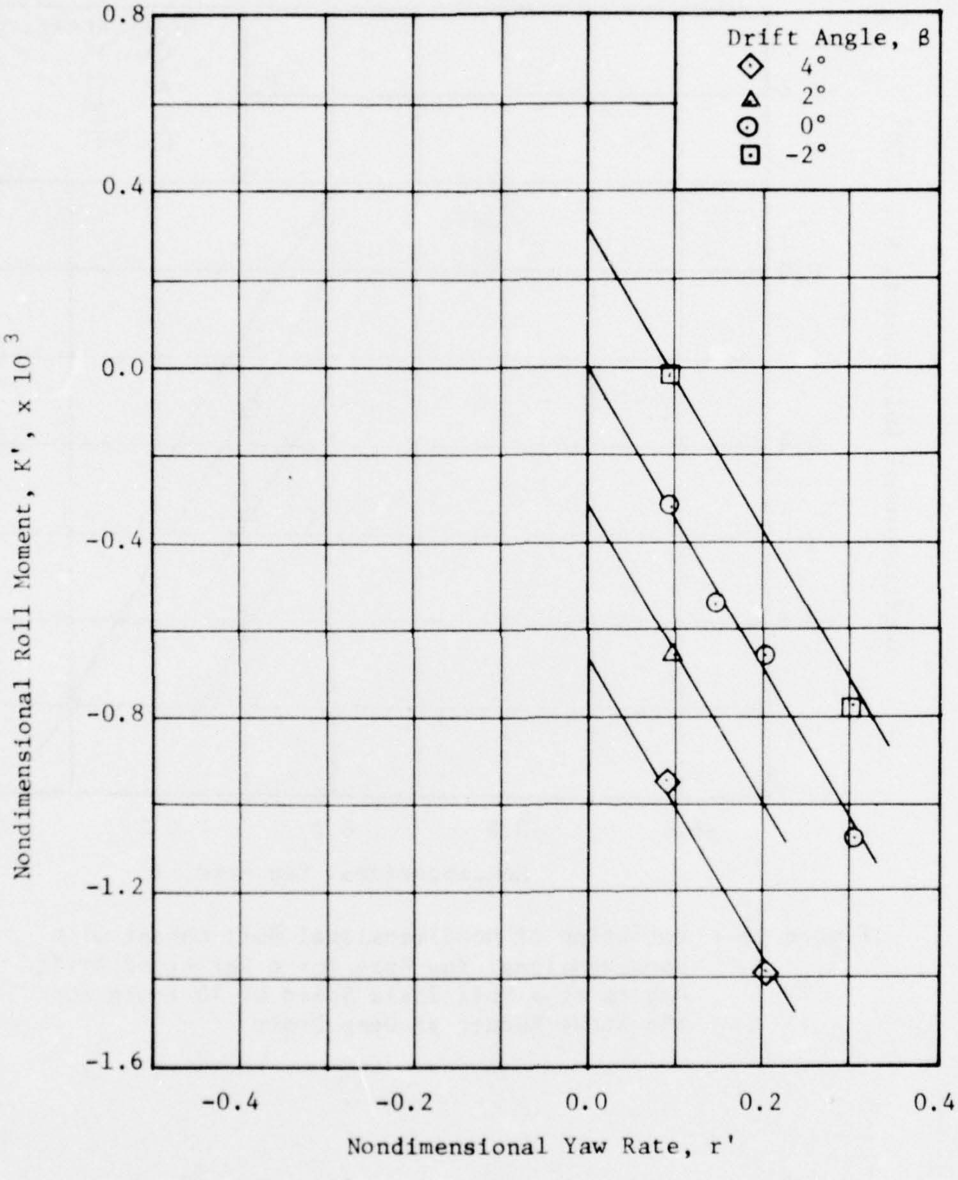

Figure 97 - Variation of Nondimensional Roll Moment with Nondimensional Yaw Rate for a Series of Drift Angles at a Full Scale Speed of 15 Knots for the Strut Rudder at Deep Draft

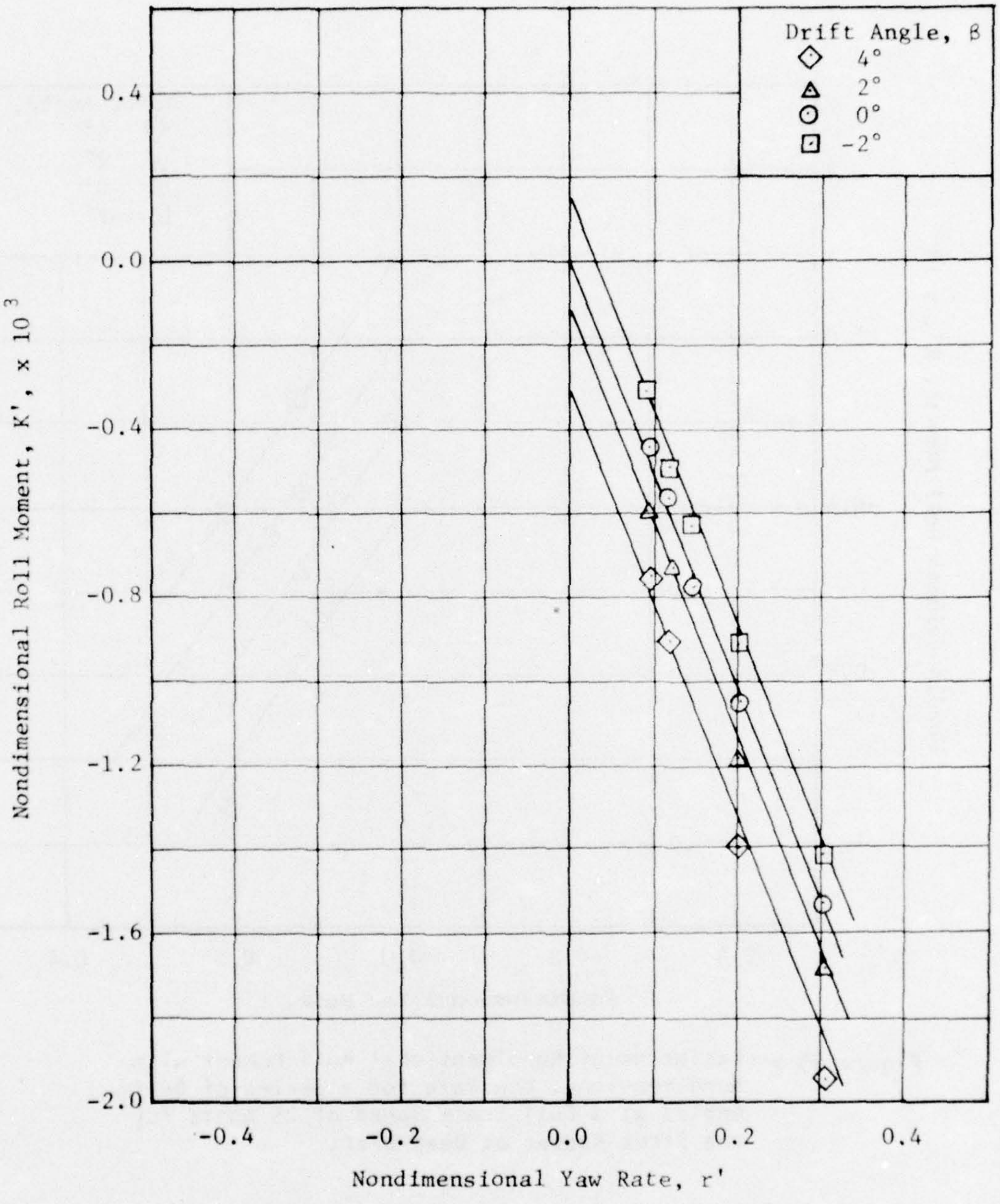

Figure 98 - Variation of Nondimensional Roll Moment with Nondimensional Yaw Rate for a Series of Drift Angles at a Full Scale Speed of 20 Knots for the Strut Rudder at Deep Draft

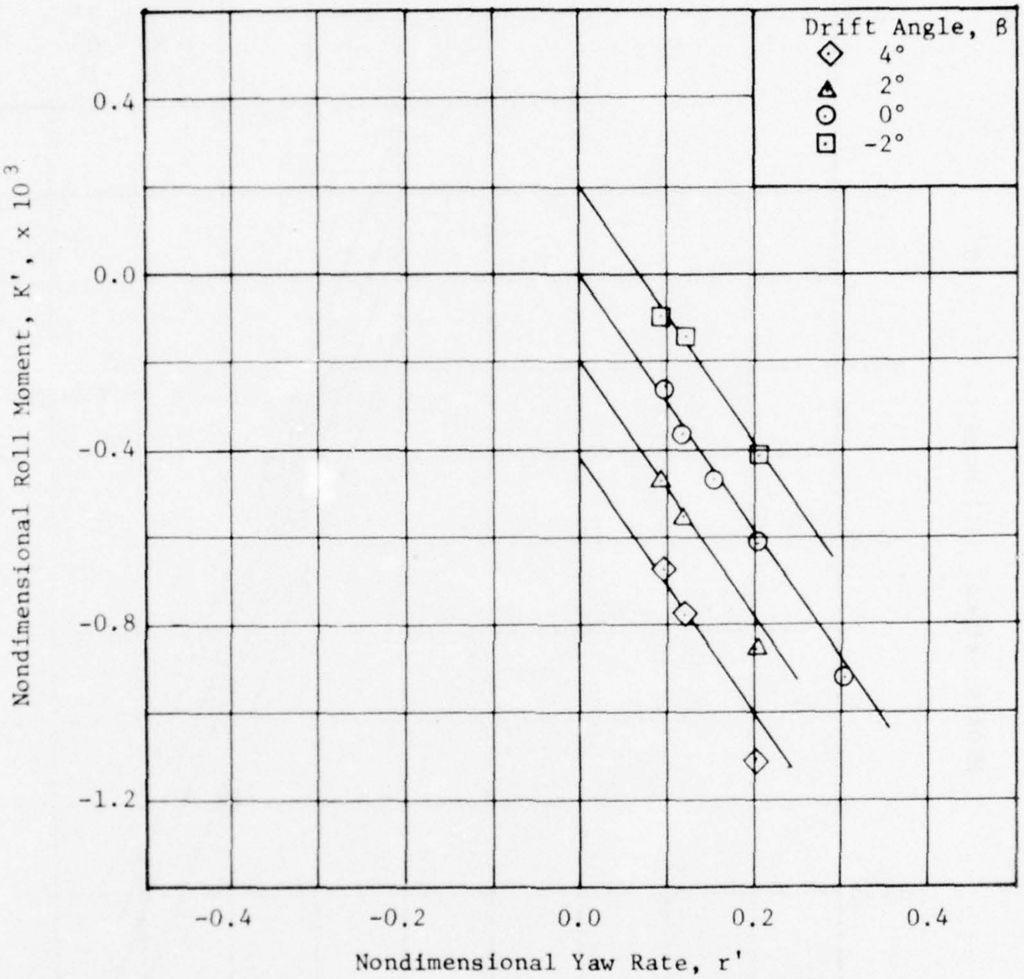

Figure 99 - Variation of Nondimensional Roll Moment with Nondimensional Yaw Rate for a Series of Drift Angles at a Full Scale Speed of 25 Knots for the Strut Rudder at Deep Draft

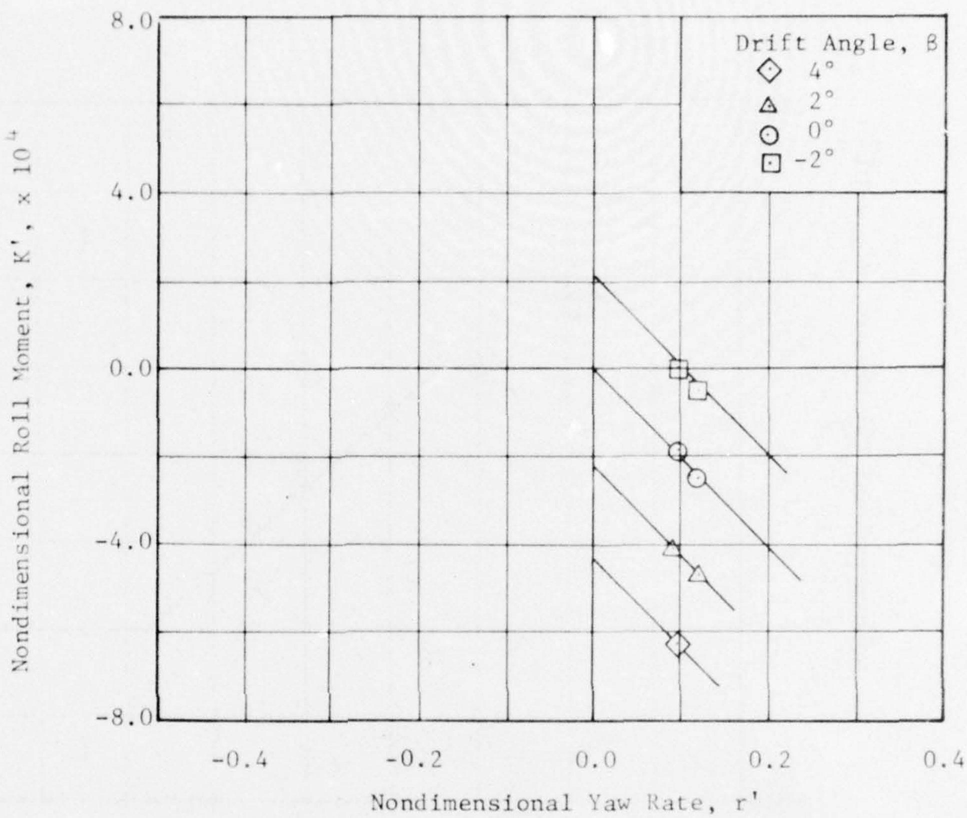

Figure 100 - Variation of Nondimensional Roll Moment with Nondimensional Yaw Rate for a Series of Drift Angles at a Full Scale Speed of 28 Knots for the Strut Rudder at Deep Draft

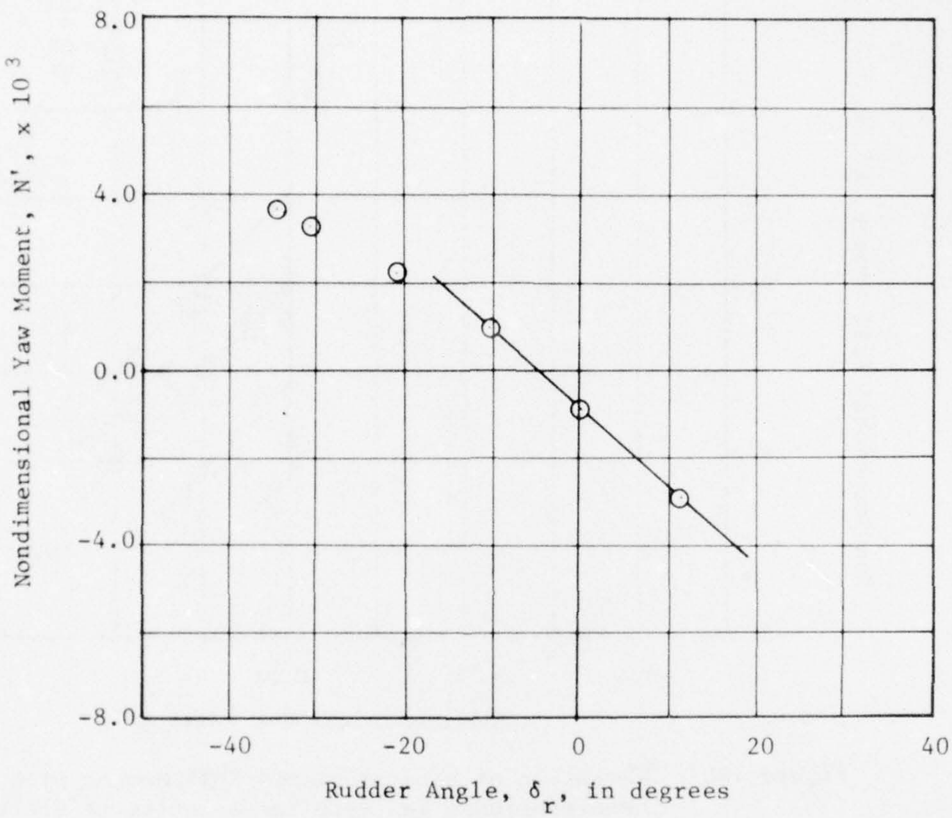

Figure 101 - Variation of Nondimensional Yaw Moment with Rudder Angle for a Nondimensional Yaw Rate of 0.093 at a Full Scale Speed of 10 Knots for the Strut Rudder at Deep Draft

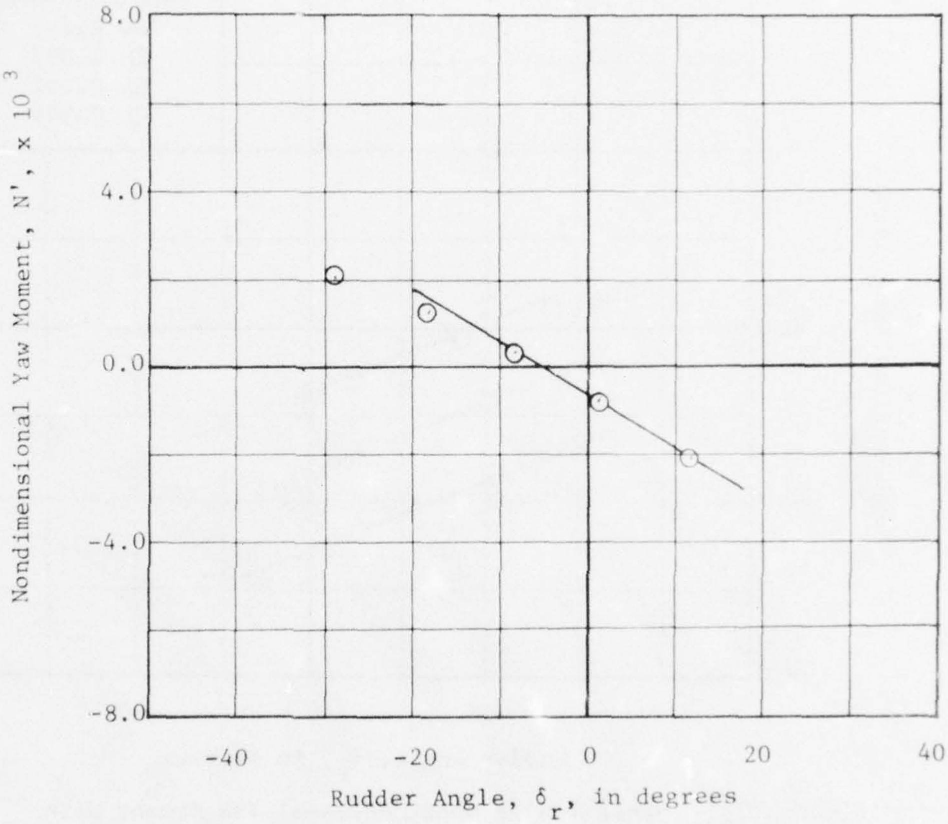

Figure 102 - Variation of Nondimensional Yaw Moment with Rudder Angle for a Nondimensional Yaw Rate of 0.093 at a Full Scale Speed of 15 Knots for the Strut Rudder at Deep Draft

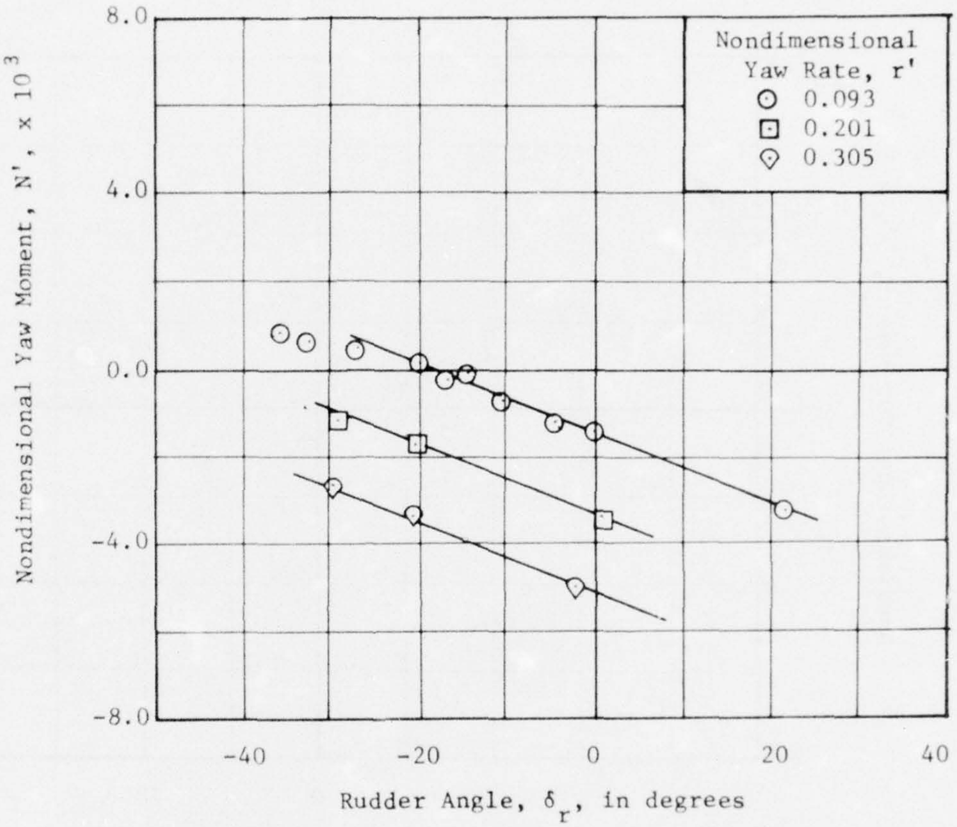

Figure 103 - Variation of Nondimensional Yaw Moment with Rudder Angle for a Series of Nondimensional Yaw Rates at a Full Scale Speed of 20 Knots for the Strut Rudder at Deep Draft

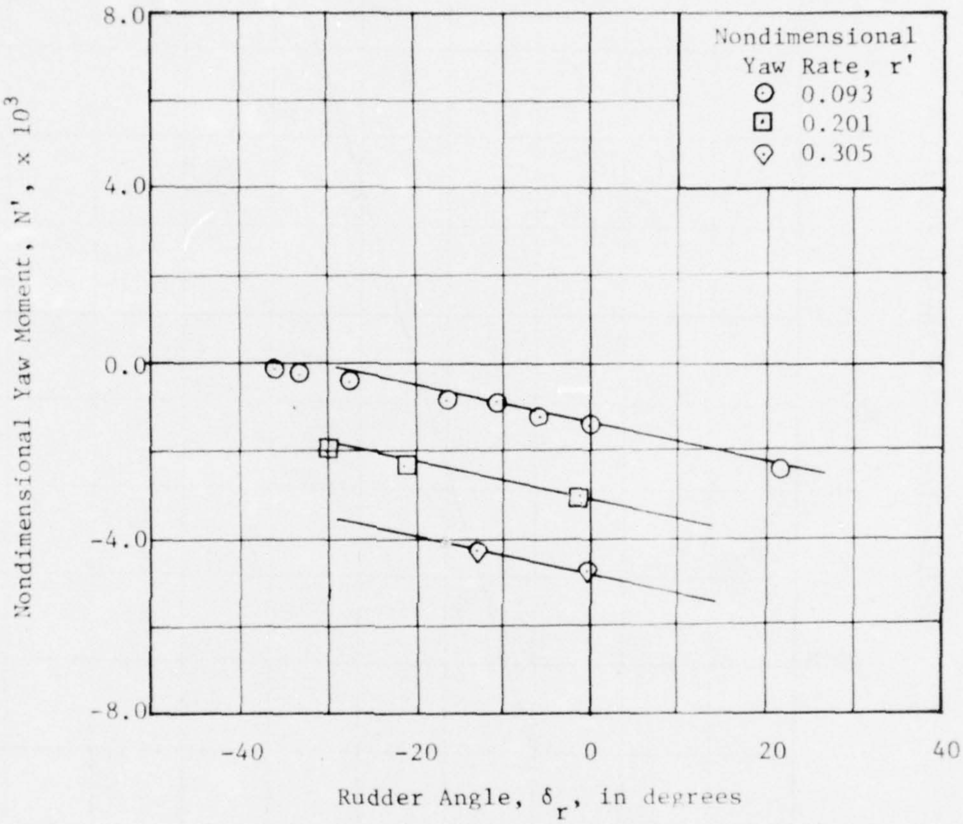

Figure 104 - Variation of Nondimensional Yaw Moment with Rudder Angle for a Series of Nondimensional Yaw Rates at a Full Scale Speed of 25 Knots for the Strut Rudder at Deep Draft

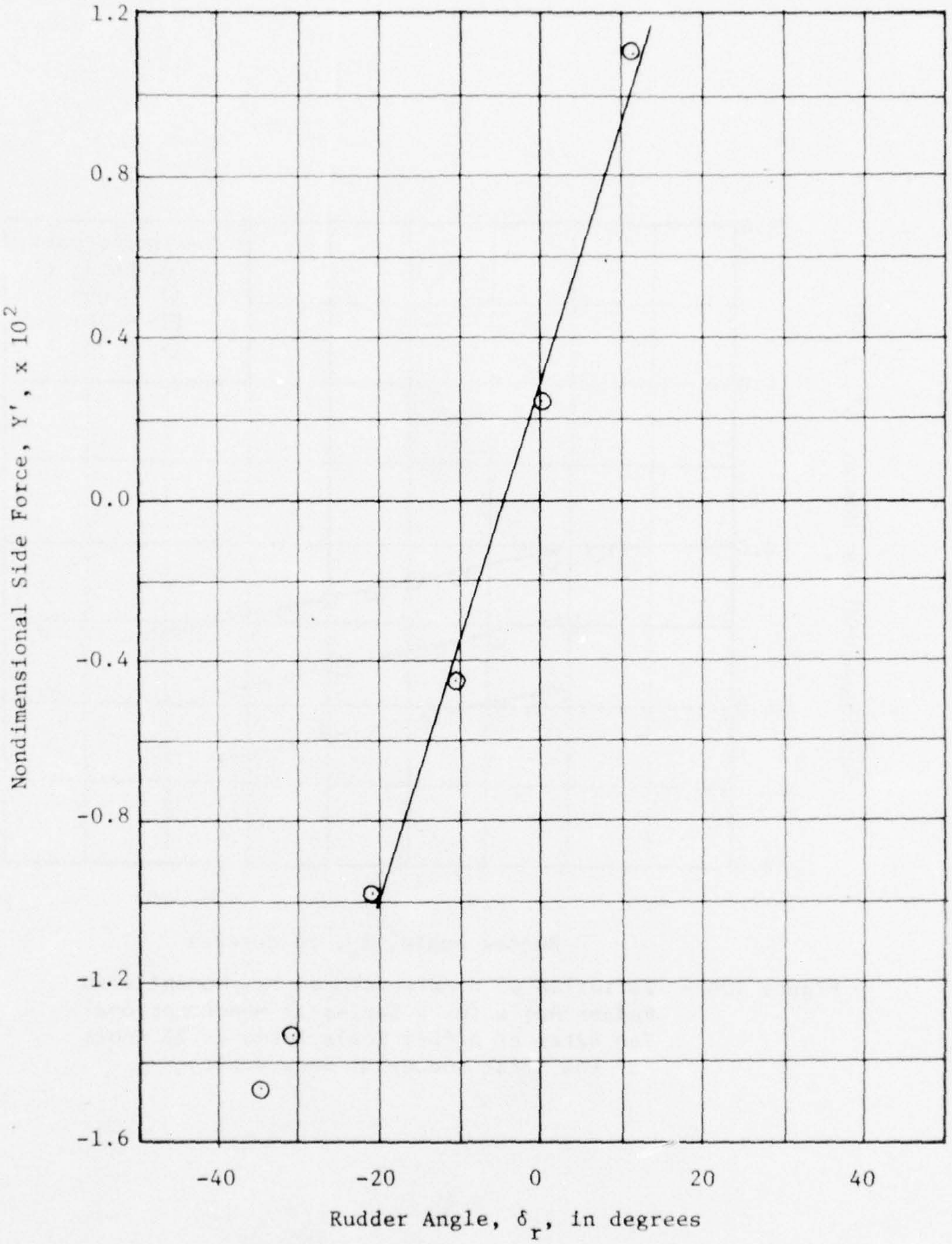

Figure 105 - Variation of Nondimensional Side Force with Rudder Angle for a Nondimensional Yaw Rate of 0.093 at a Full Scale Speed of 10 Knots for the Strut Rudder at Deep Draft

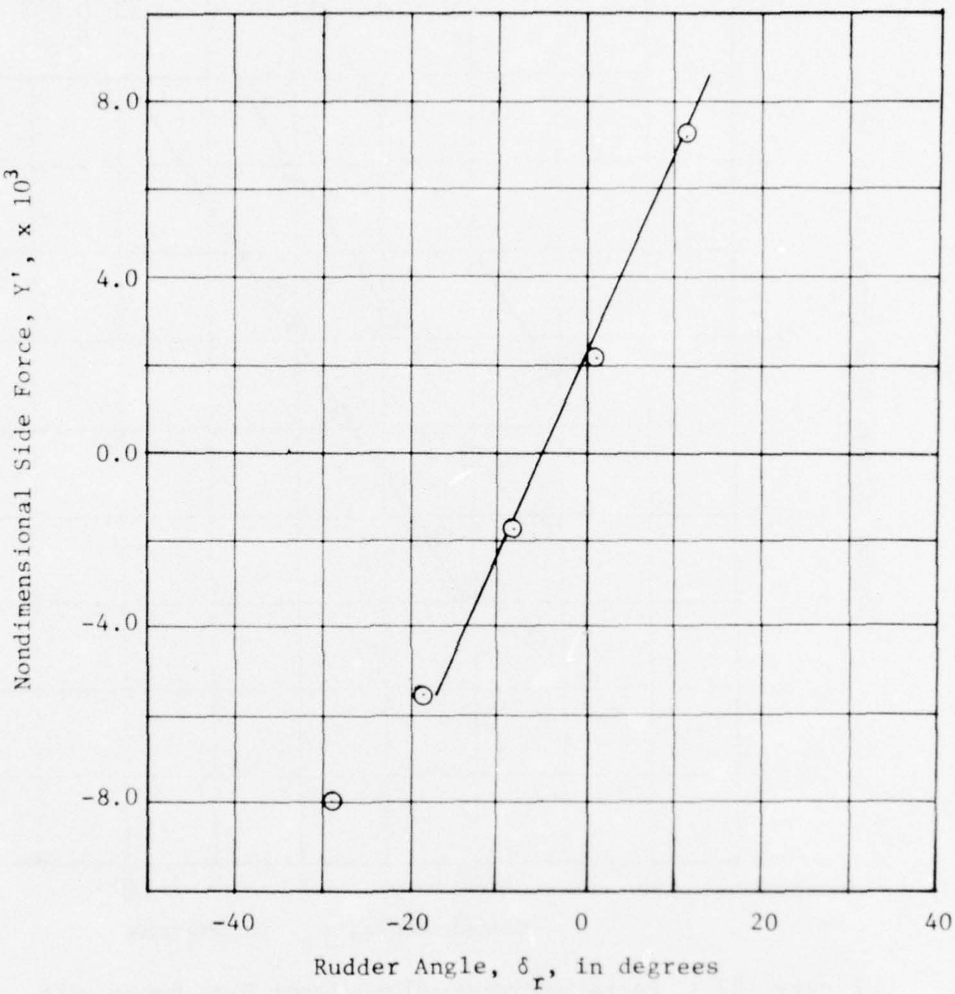

Figure 106 - Variation of Nondimensional Side Force with Rudder Angle for a Nondimensional Yaw Rate of 0.093 at a Full Scale Speed of 15 Knots for the Strut Rudder at Deep Draft

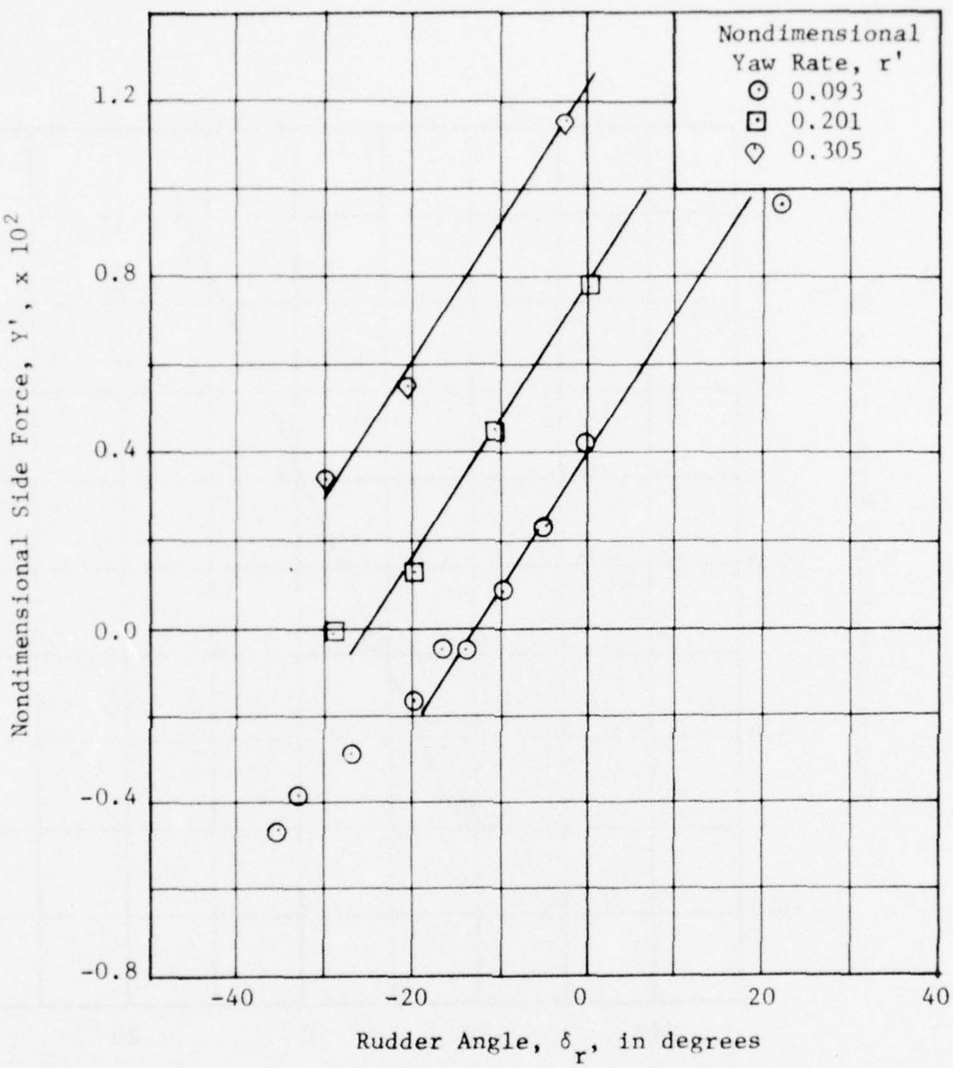

Figure 107 - Variation of Nondimensional Side Force with Rudder Angle for a Series of Nondimensional Yaw Rates at a Full Scale Speed of 20 Knots for the Strut Rudder at Deep Draft

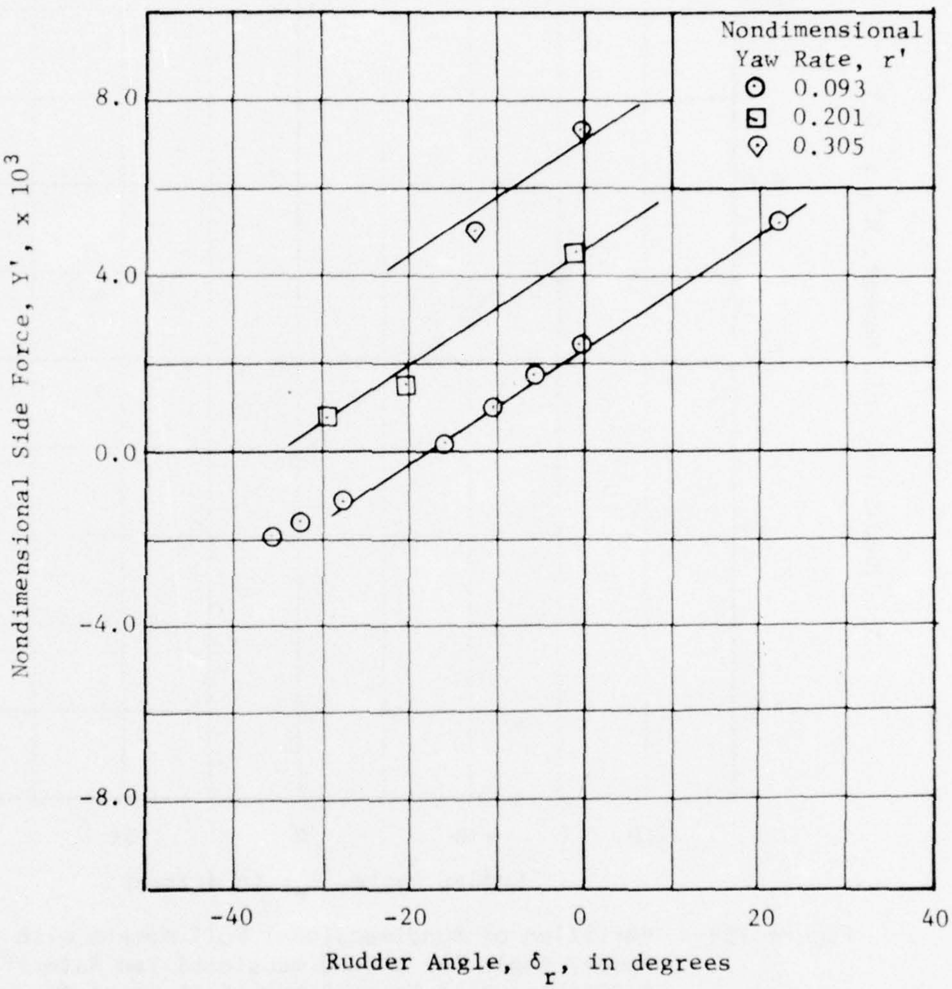

Figure 108 - Variation of Nondimensional Side Force with Rudder Angle for a Series of Nondimensional Yaw Rates at a Full Scale Speed of 25 Knots for the Strut Rudder at Deep Draft

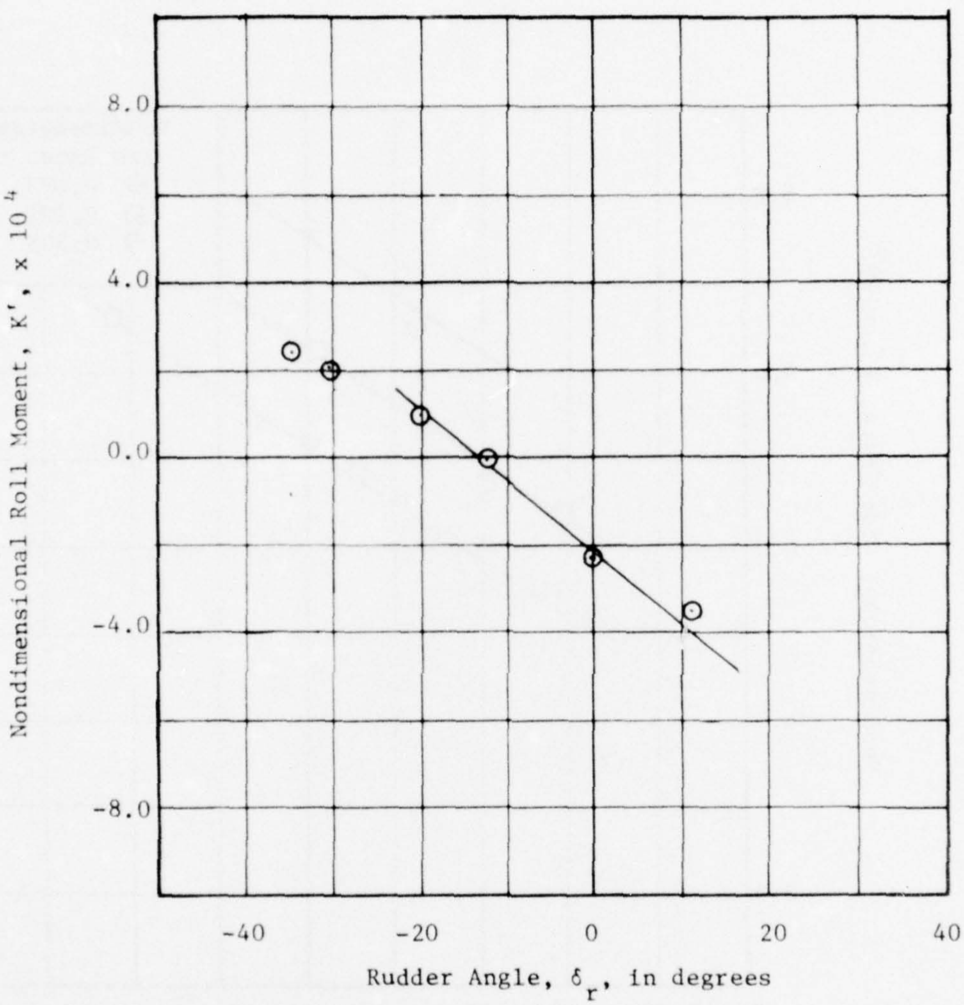

Figure 109 - Variation of Nondimensional Roll Moment with Rudder Angle for a Nondimensional Yaw Rate of 0.093 at a Full Scale Speed of 10 Knots for the Strut Rudder at Deep Draft

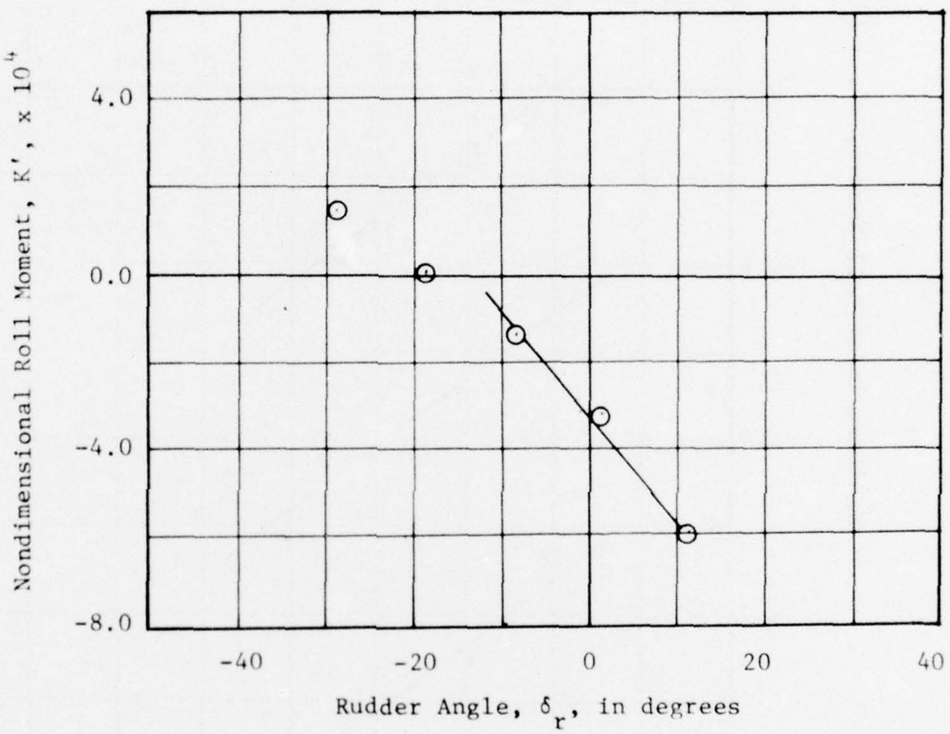

Figure 110 - Variation of Nondimensional Roll Moment with Rudder Angle for a Nondimensional Yaw Rate of 0.093 at a Full Scale Speed of 15 Knots for the Strut Rudder at Deep Draft

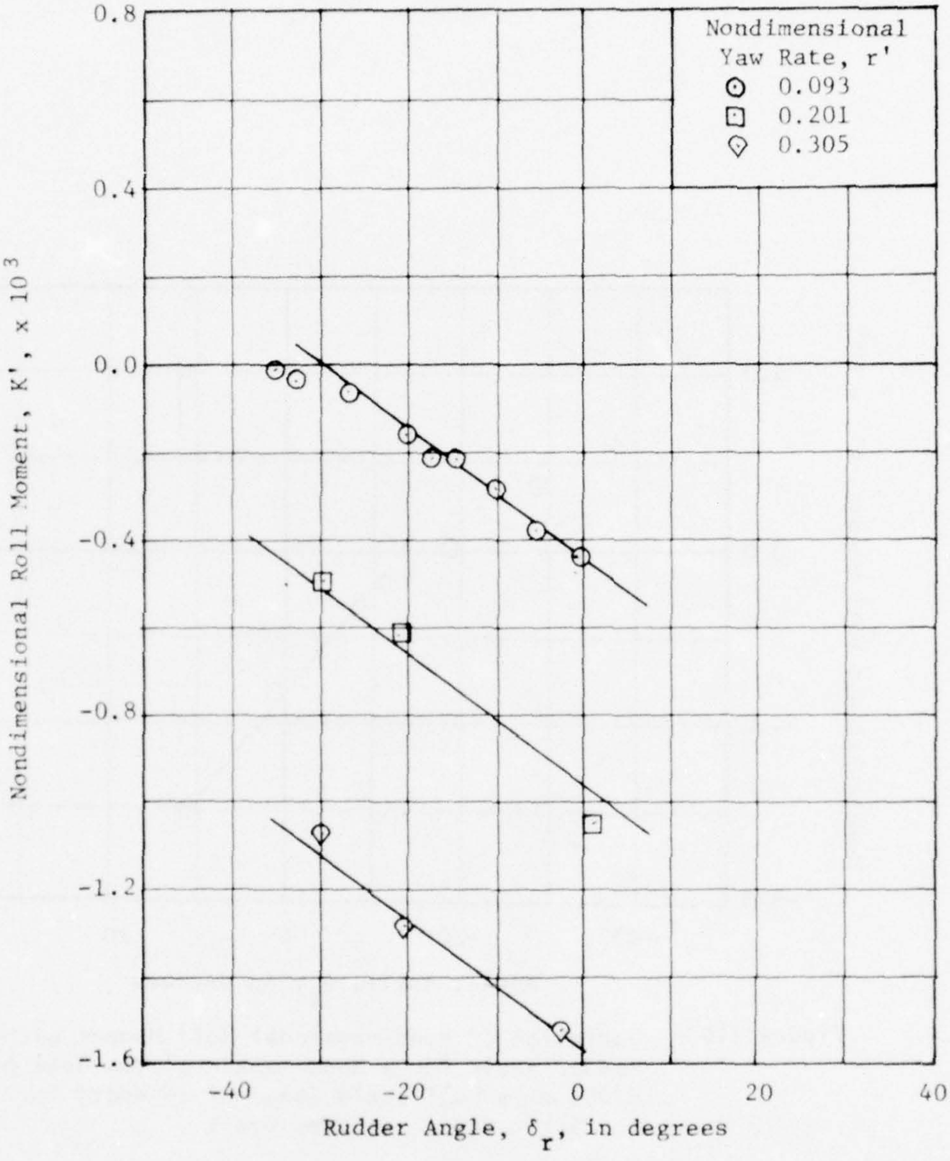

Figure 111 - Variation of Nondimensional Roll Moment with Rudder Angle for a Series of Nondimensional Yaw Rates at a Full Scale Speed of 20 Knots for the Strut Rudder at Deep Draft

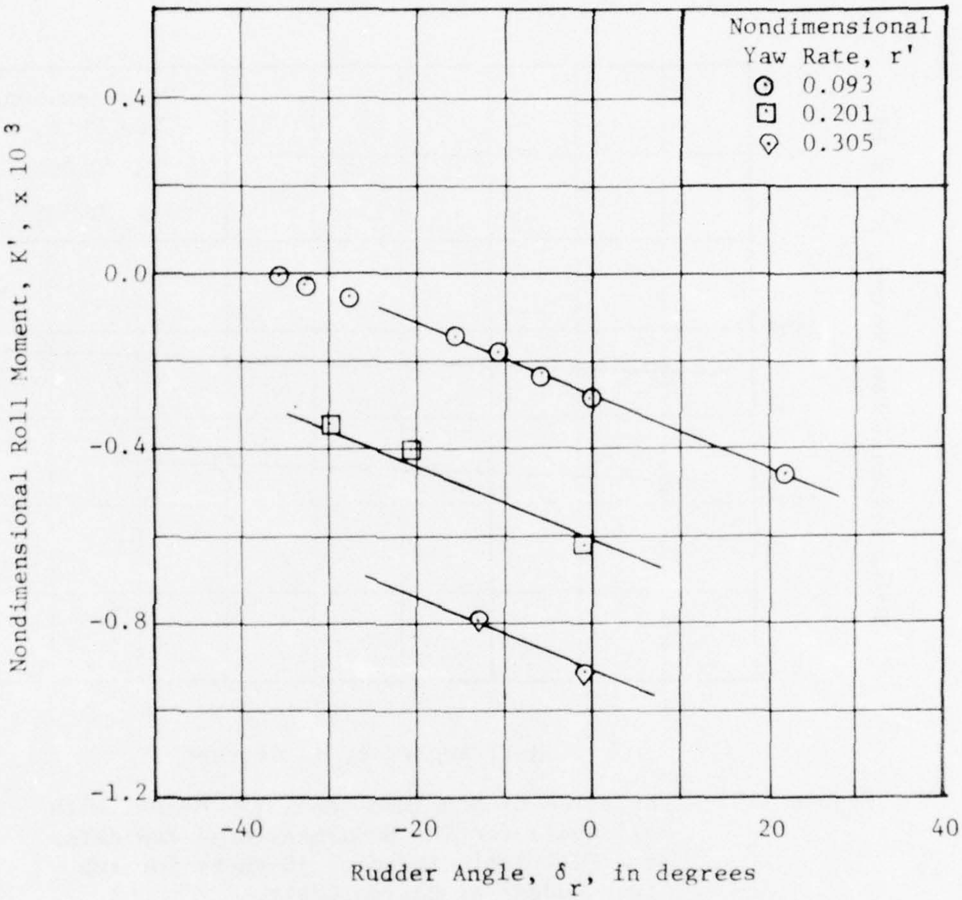

Figure 112 - Variation of Nondimensional Roll Moment with Rudder Angle for a Series of Nondimensional Yaw Rates at a Full Scale Speed of 25 Knots for the Strut Rudder at Deep Draft

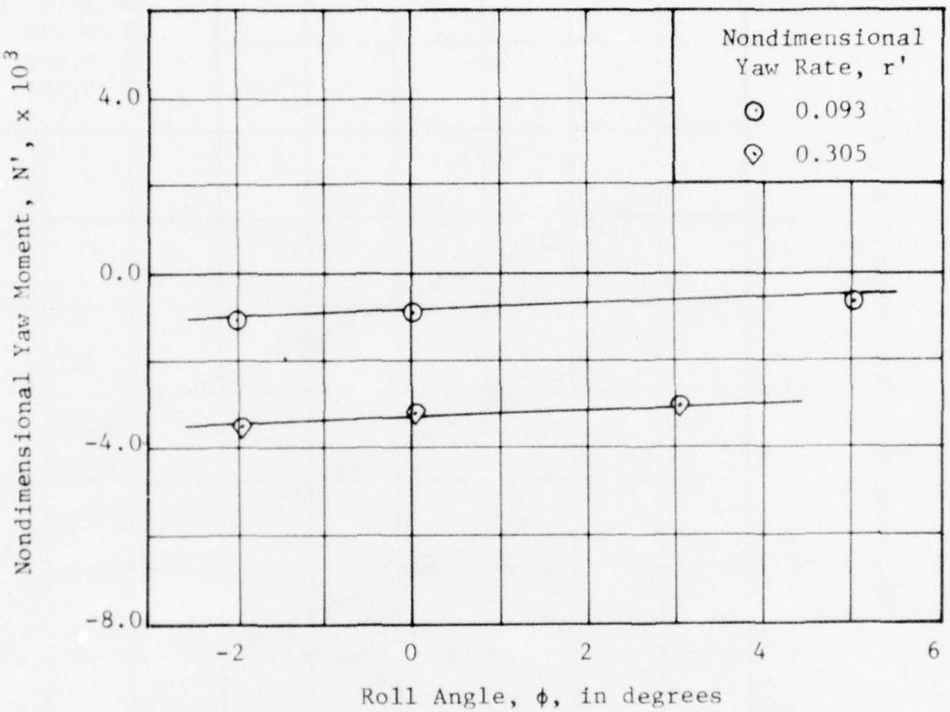

Figure 113 - Variation of Nondimensional Yaw Moment with Roll Angle for Two Nondimensional Yaw Rates at a Full Scale Speed of 10 Knots for the Strut Rudder at Design Draft

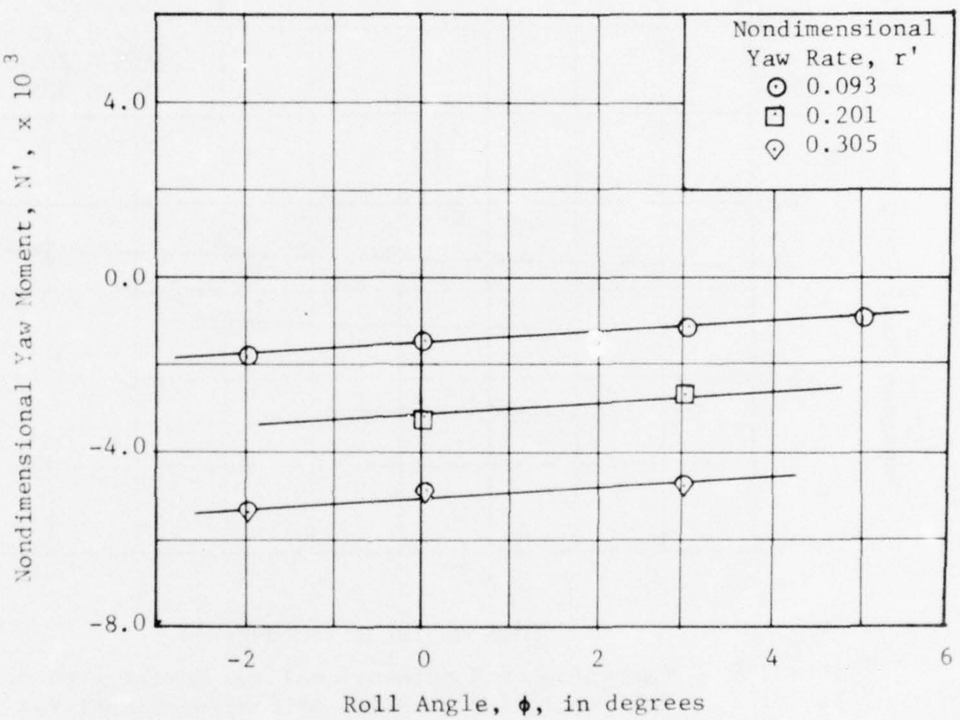

Figure 114 - Variation of Nondimensional Yaw Moment with Roll Angle for a Series of Nondimensional Yaw Rates at a Full Scale Speed of 20 Knots for the Strut Rudder at Deep Draft

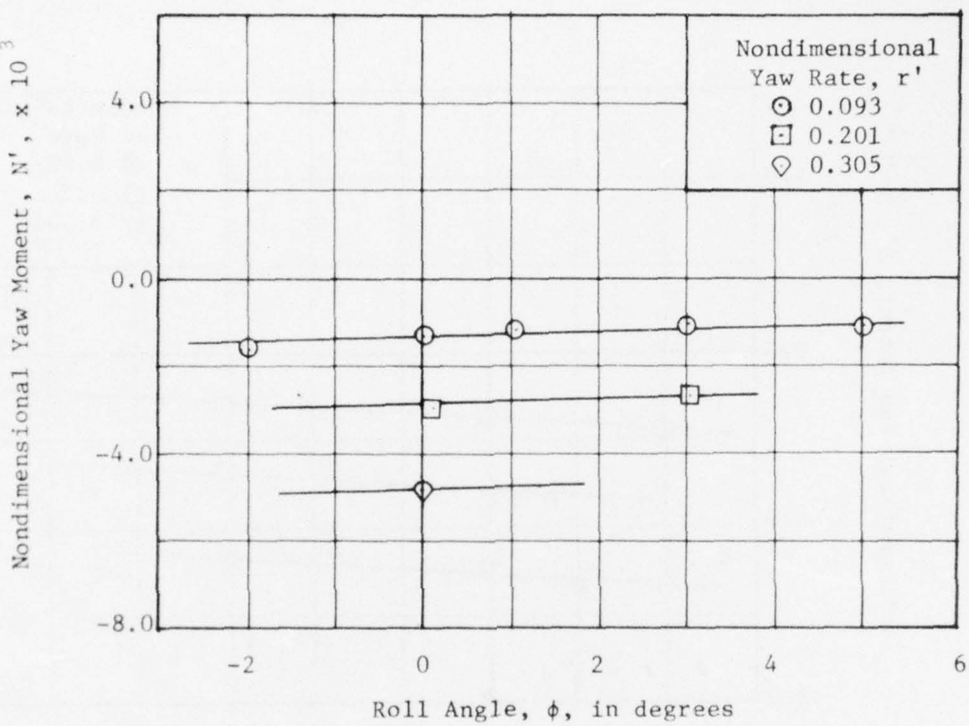

Figure 115 - Variation of Nondimensional Yaw Moment with Roll Angle for a Series of Nondimensional Yaw Rates at a Full Scale Speed of 25 Knots for the Strut Rudder at Deep Draft

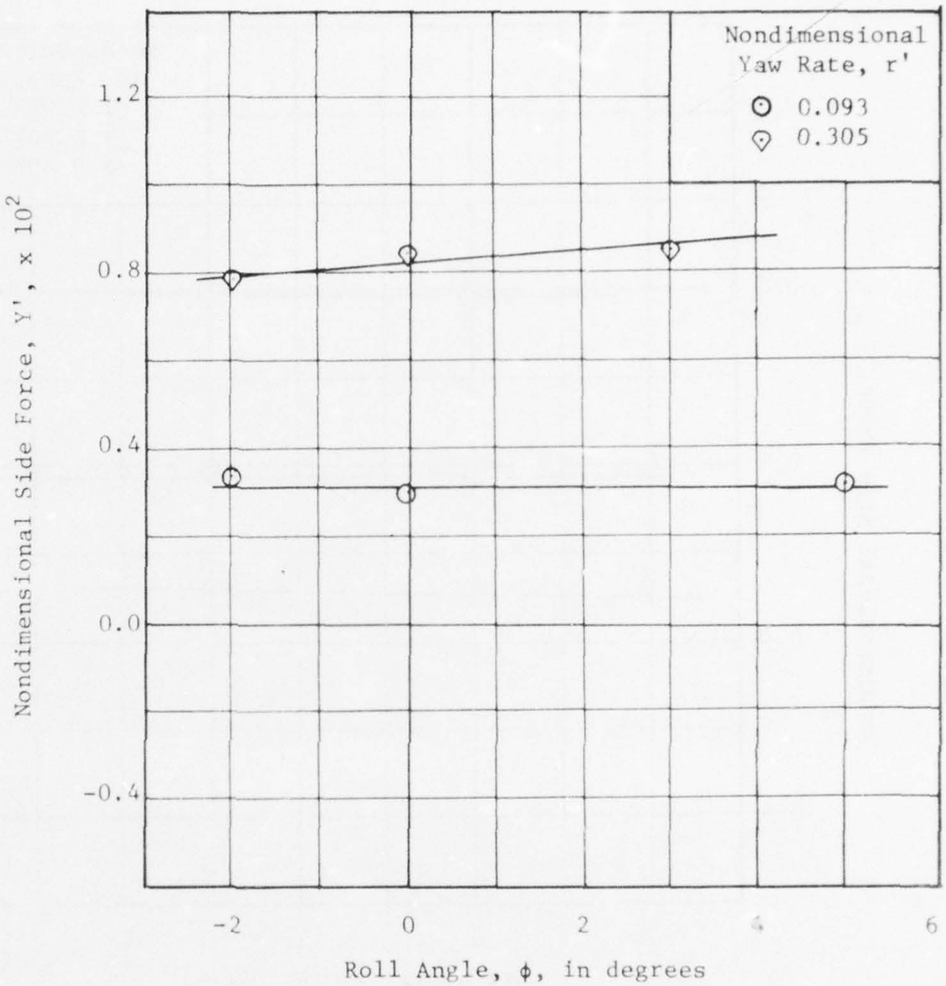

Figure 116 - Variation of Nondimensional Side Force with Roll Angle for Two Nondimensional Yaw Rates at a Full Scale Speed of 10 Knots for the Strut Rudder at Deep Draft

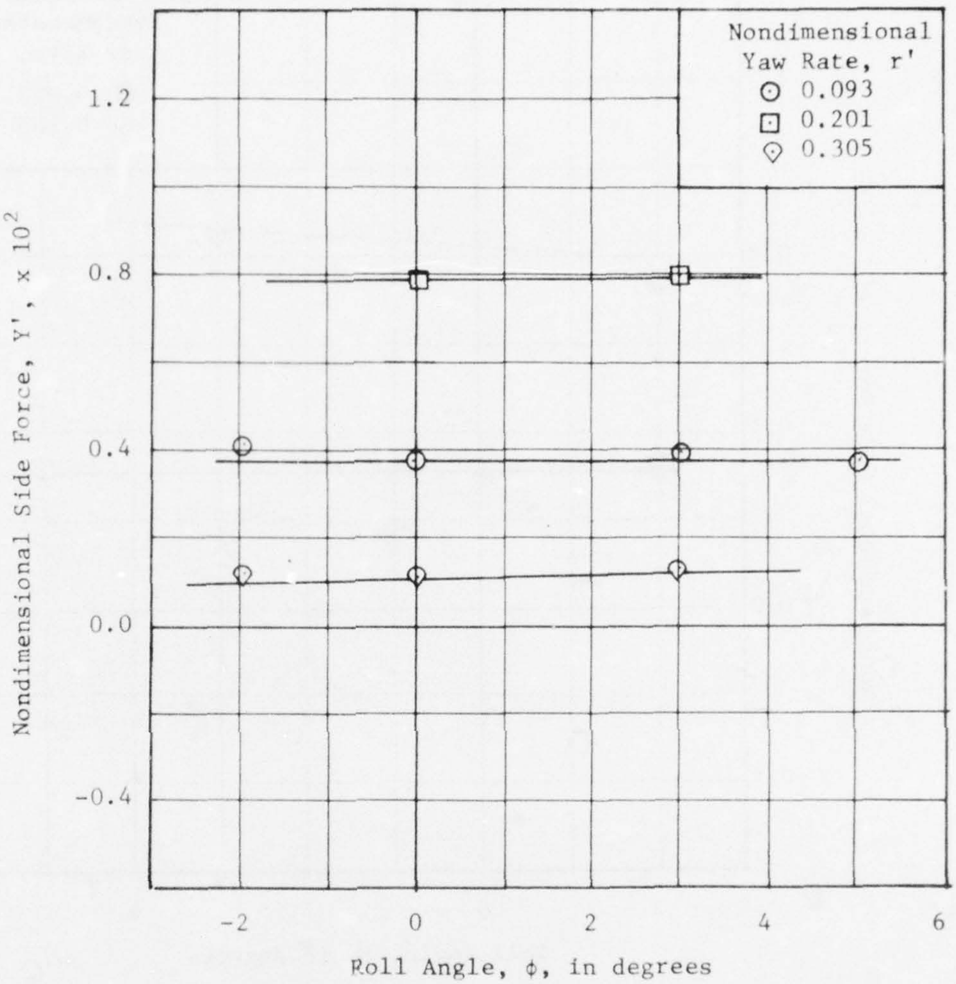

Figure 117 - Variation of Nondimensional Side Force with Roll Angle for a Series of Nondimensional Yaw Rates at a Full Scale Speed of 20 Knots for the Strut Rudder at Deep Draft

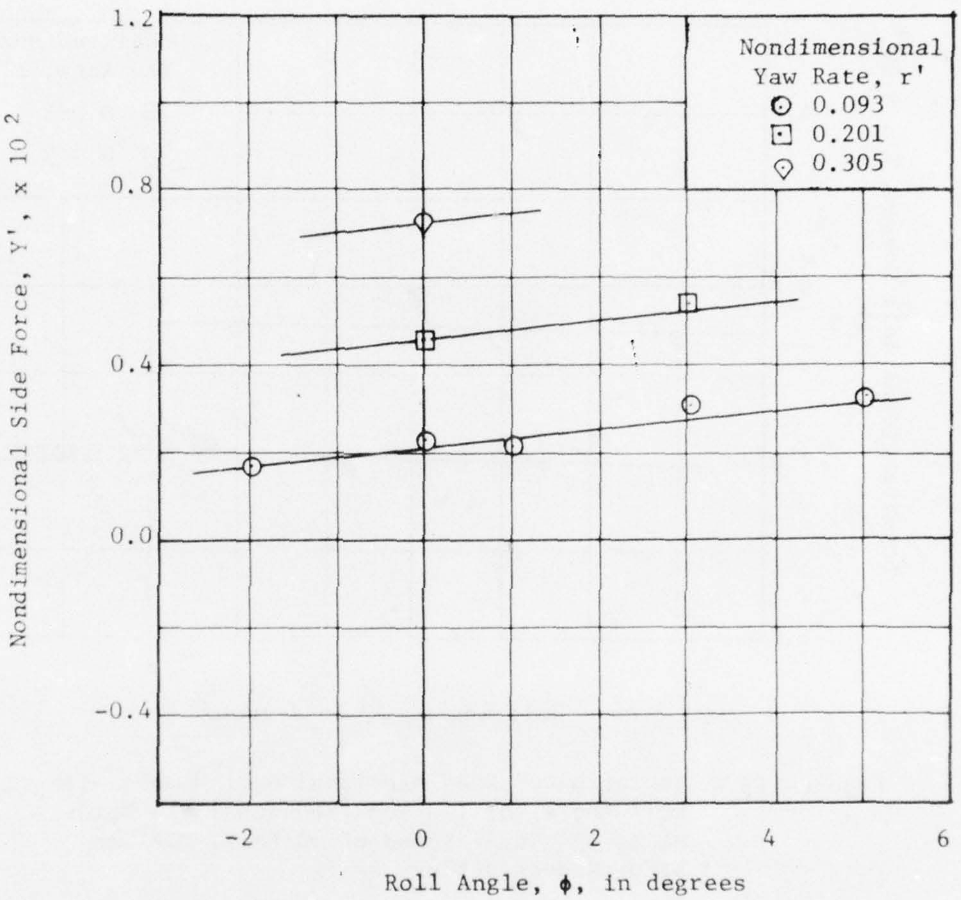

Figure 118 - Variation of Nondimensional Side Force with Roll Angle for a Series of Nondimensional Yaw Rates at a Full Scale Speed of 25 Knots for the Strut Rudder at Deep Draft

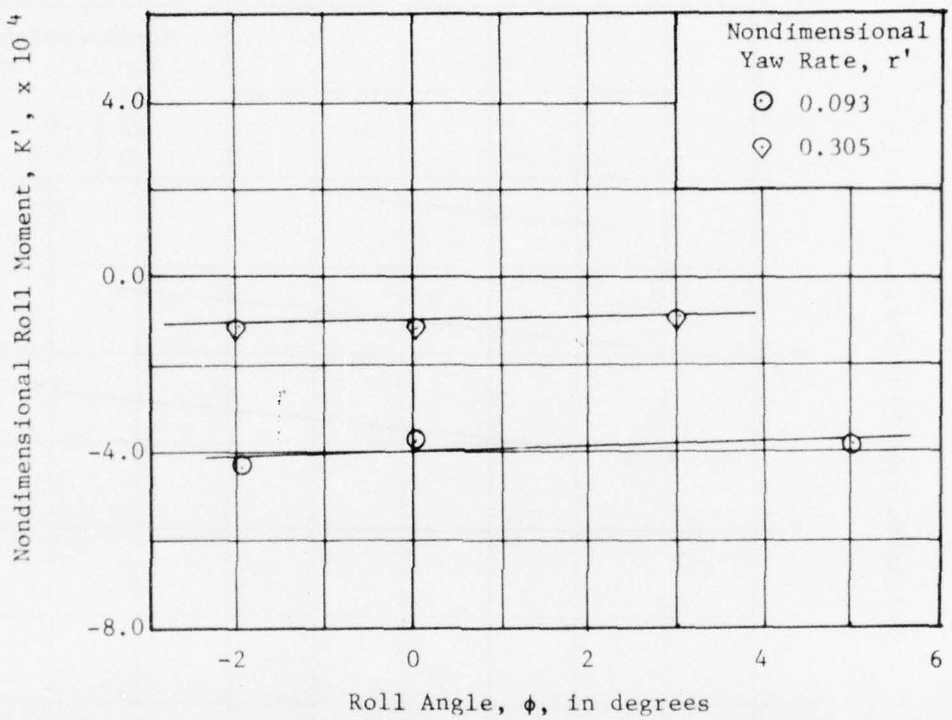

Figure 119 - Variation of Nondimensional Roll Moment with Roll Angle for Two Nondimensional Yaw Rates at a Full Scale Speed of 10 Knots for the Strut Rudder at Deep Draft

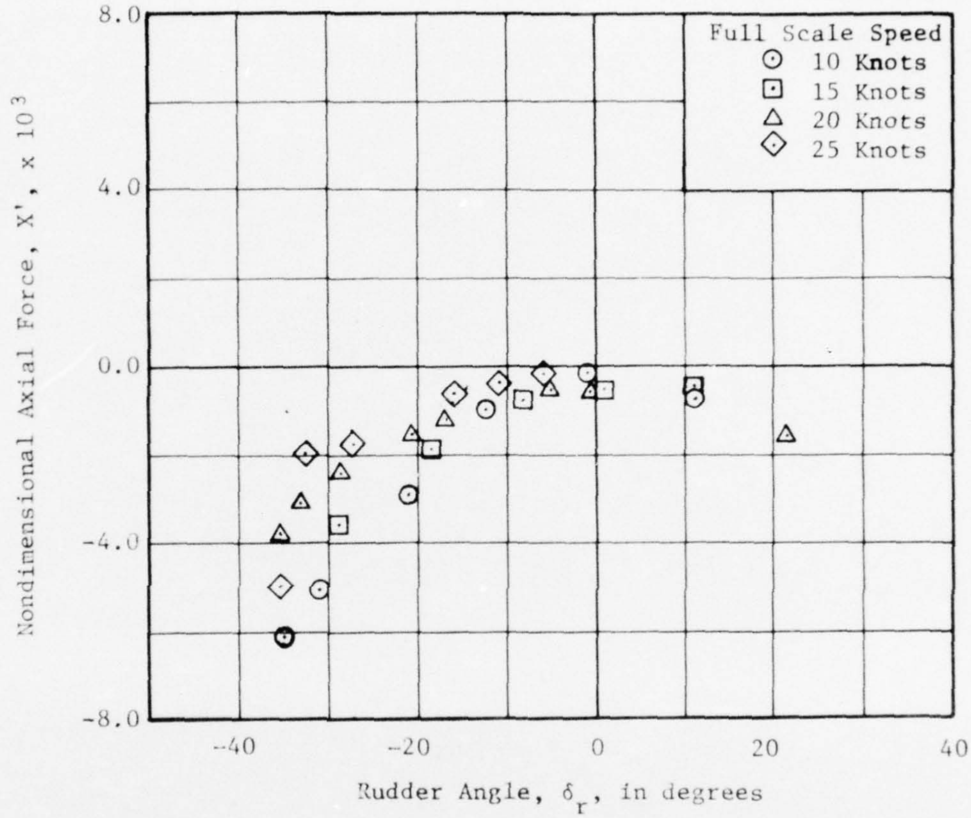

Figure 120 - Variation of Nondimensional Axial Force with Rudder Angle for a Series of Speeds at a Nondimensional Yaw Rate of 0.093 for the Strut Rudder at Deep Draft

Appendix C

(Figures 121 to 162)
Nondimensional Data Curves for
the Spade Rudder at Design Draft

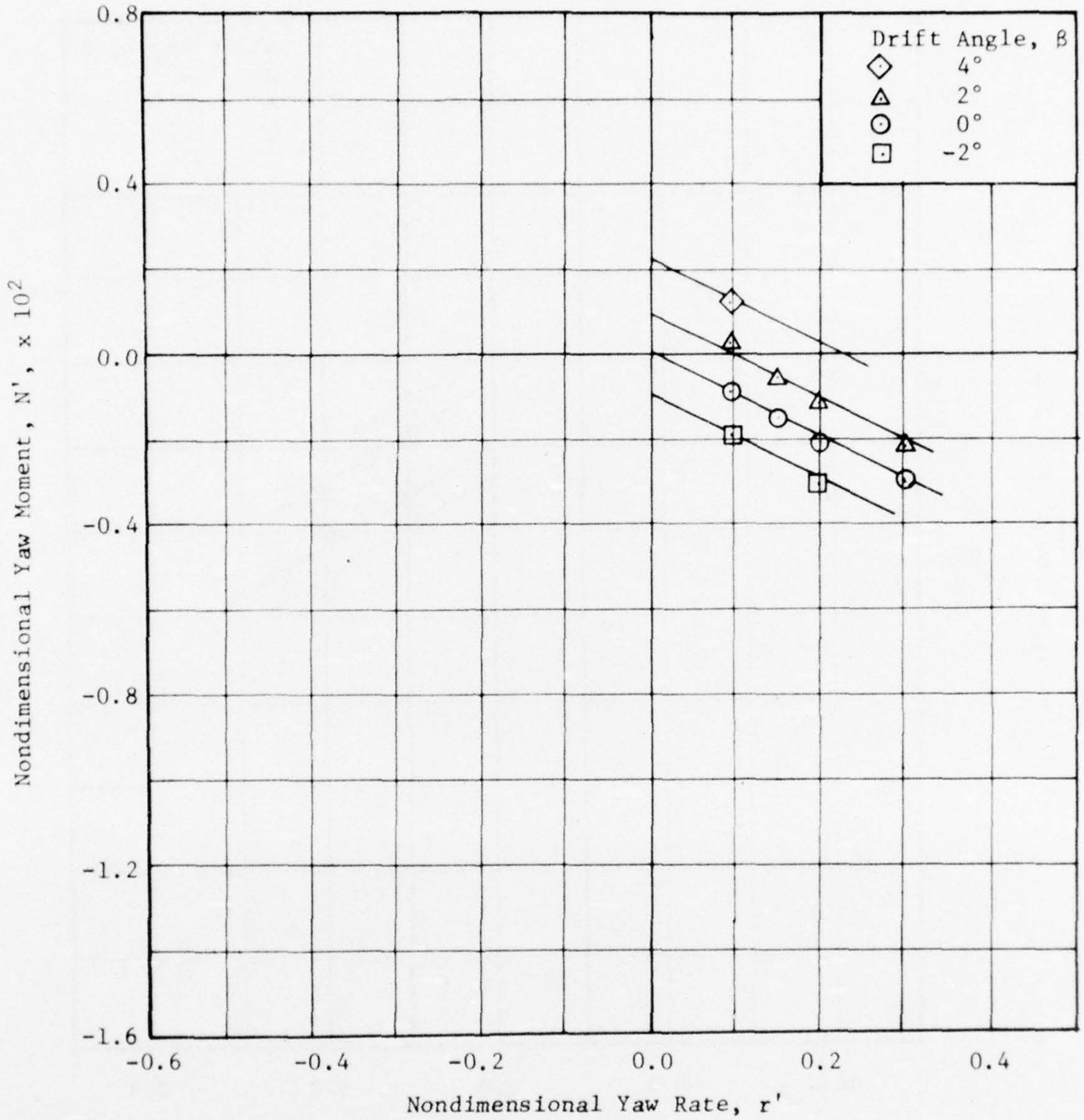

Figure 121 - Variation of Nondimensional Yaw Moment with Nondimensional Yaw Rate for a Series of Drift Angles at a Full Scale Speed of 10 Knots for the Spade Rudder at Design Draft

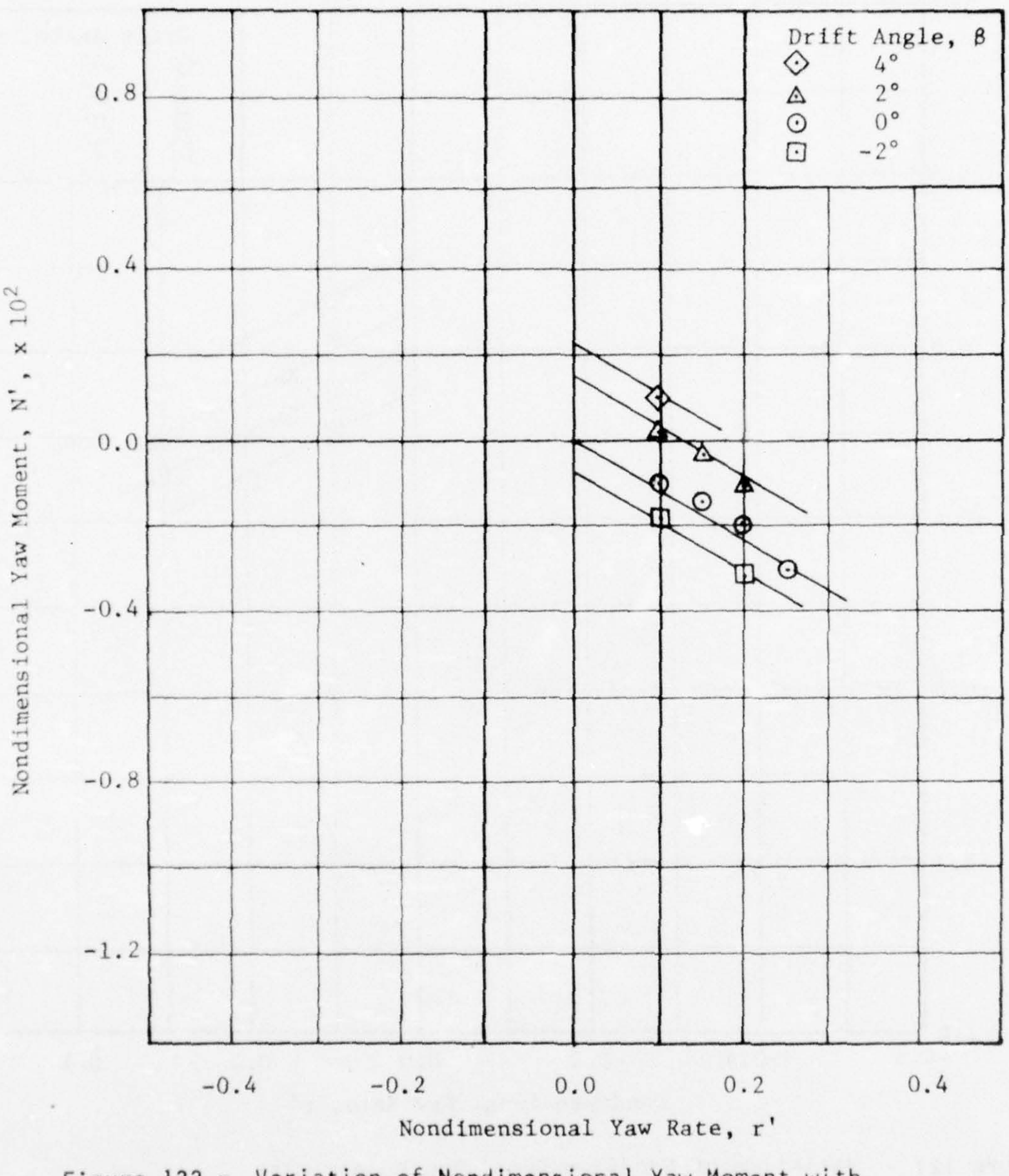

Figure 122 - Variation of Nondimensional Yaw Moment with Nondimensional Yaw Rate for a Series of Drift Angles at a Full Scale Speed of 15 Knots for the Spade Rudder at Design Draft

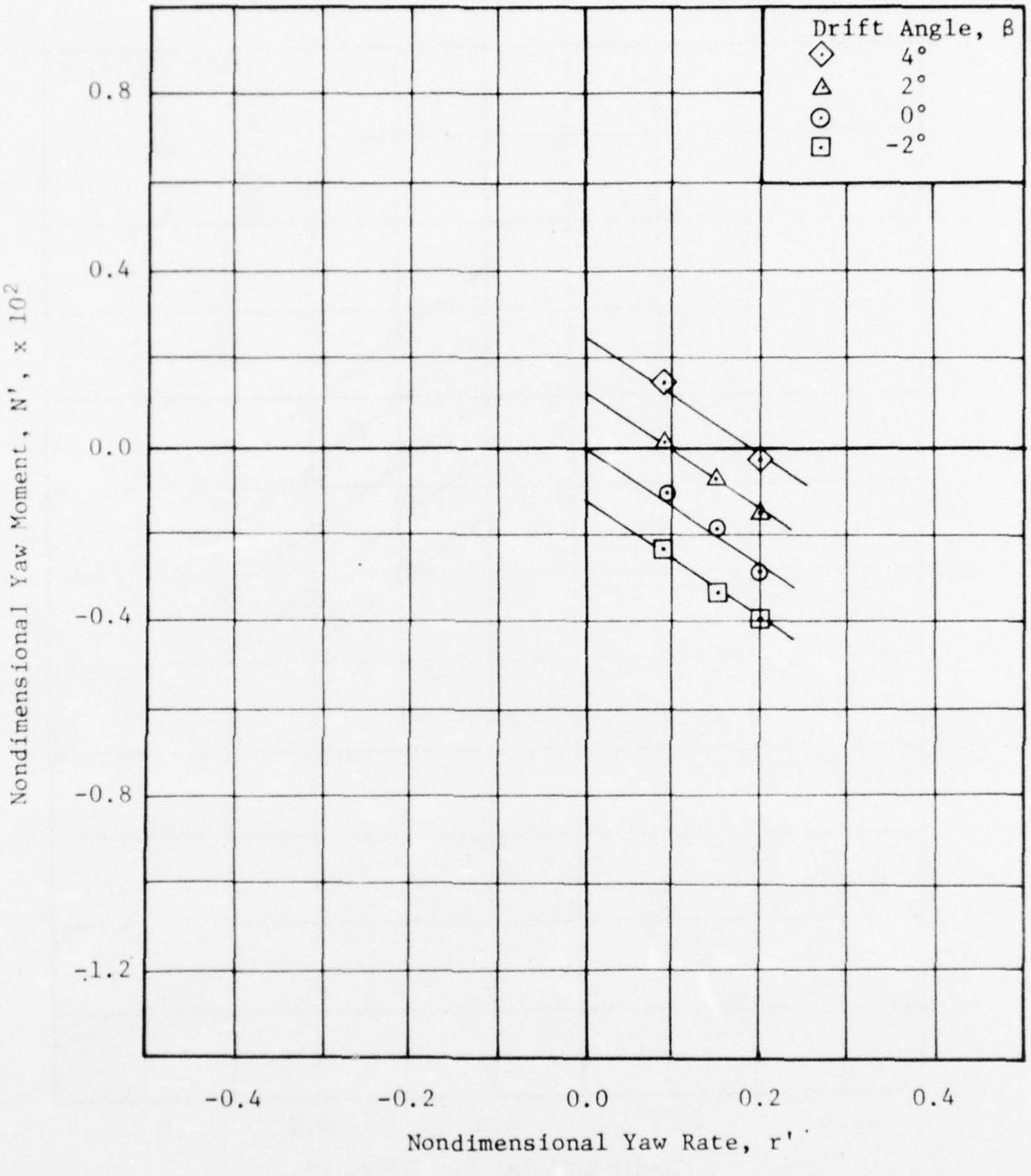

Figure 123 - Variation of Nondimensional Yaw Moment with Nondimensional Yaw Rate for a Series of Drift Angles at a Full Scale Speed of 20 Knots for the Spade Rudder at Design Draft

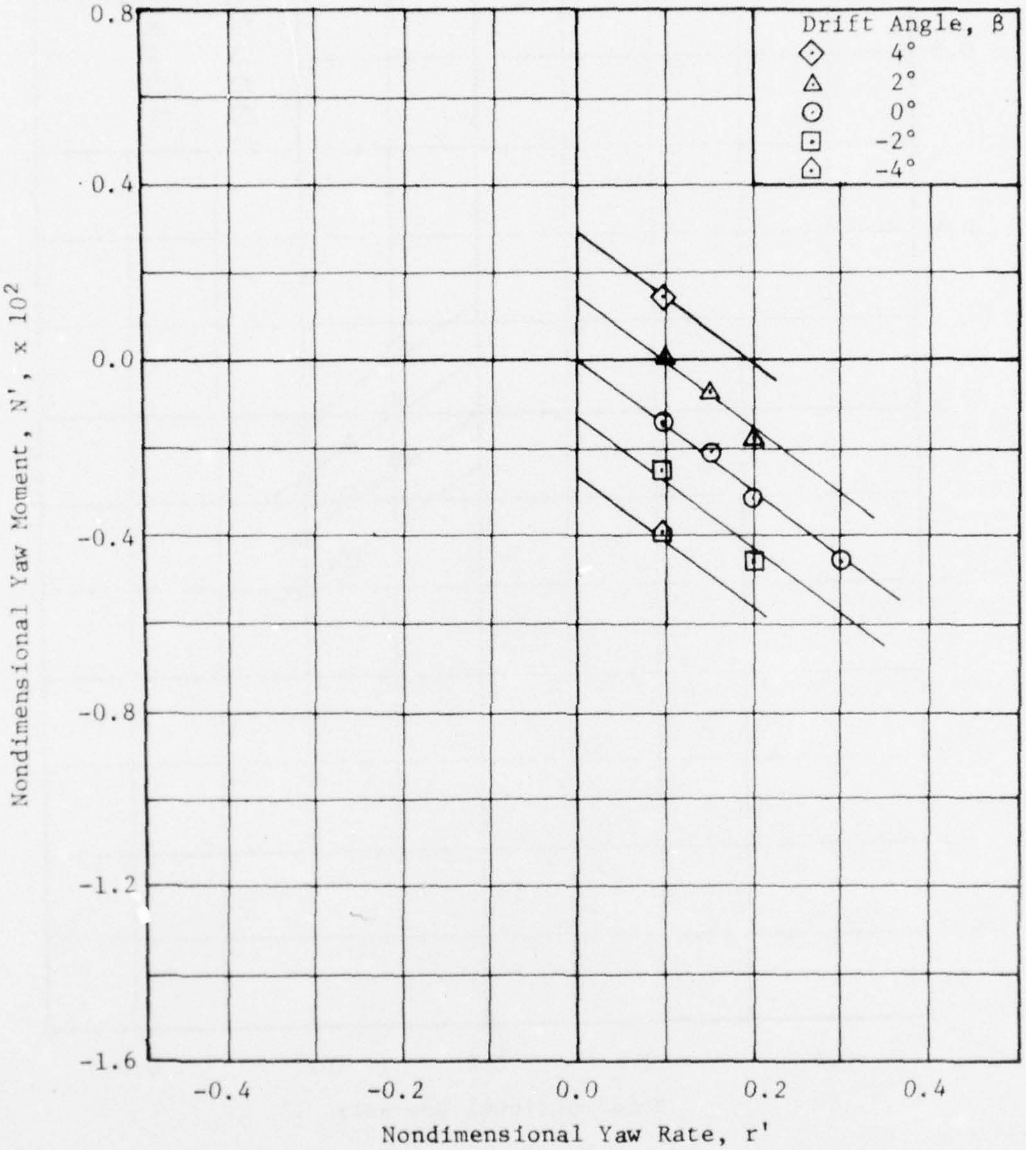

Figure 124 - Variation of Nondimensional Yaw Moment with Nondimensional Yaw Rate for a Series of Drift Angles at a Full Scale Speed of 25 Knots for the Spade Rudder at Design Draft

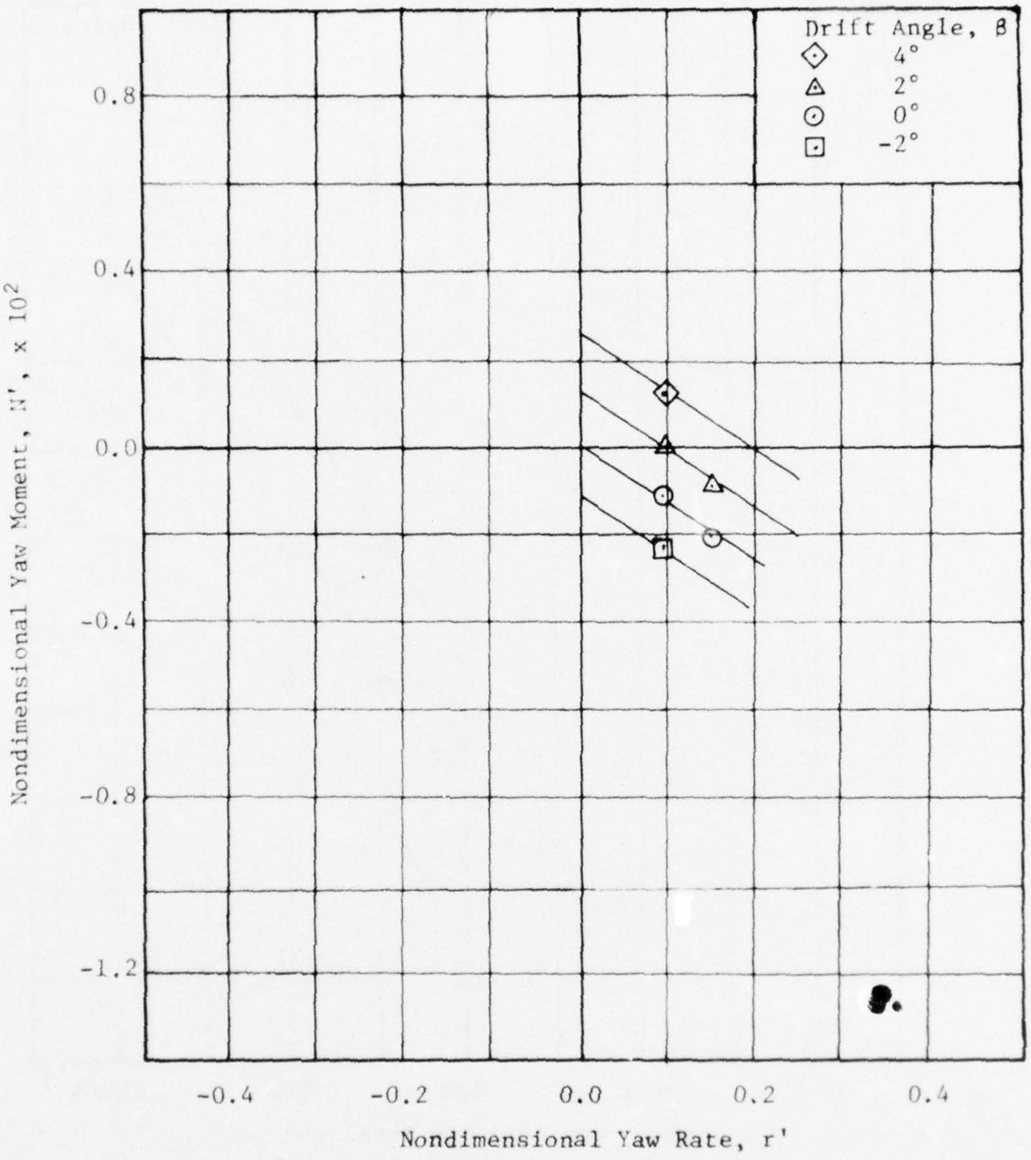

Figure 125 - Variation of Nondimensional Yaw Moment with Nondimensional Yaw Rate for a Series of Drift Angles at a Full Scale Speed of 28 Knots for the Spade Rudder at Design Draft

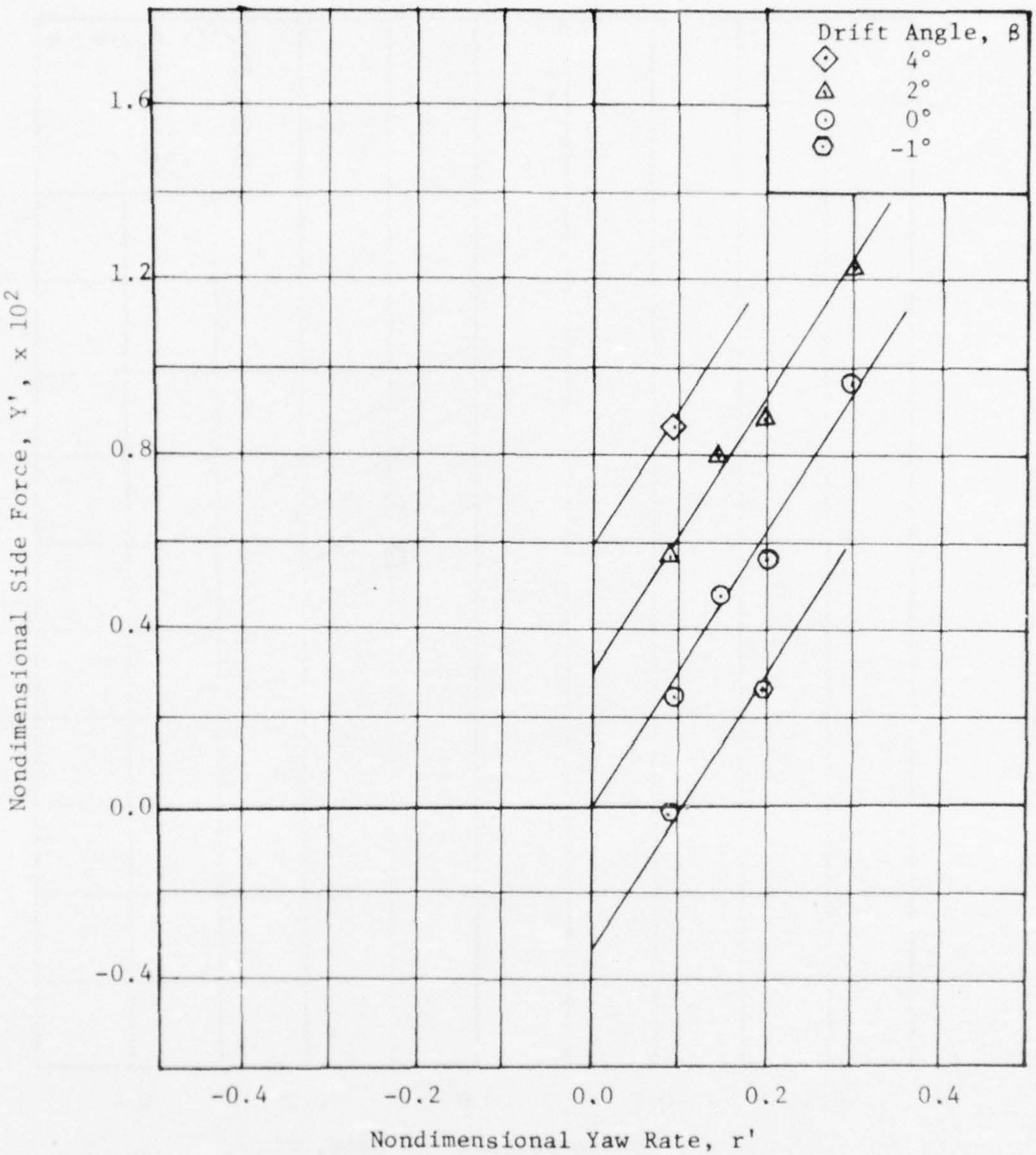

Figure 126 - Variation of Nondimensional Side Force with Nondimensional Yaw Rate for a Series of Drift Angles at a Full Scale Speed of 10 Knots for the Spade Rudder at Design Draft

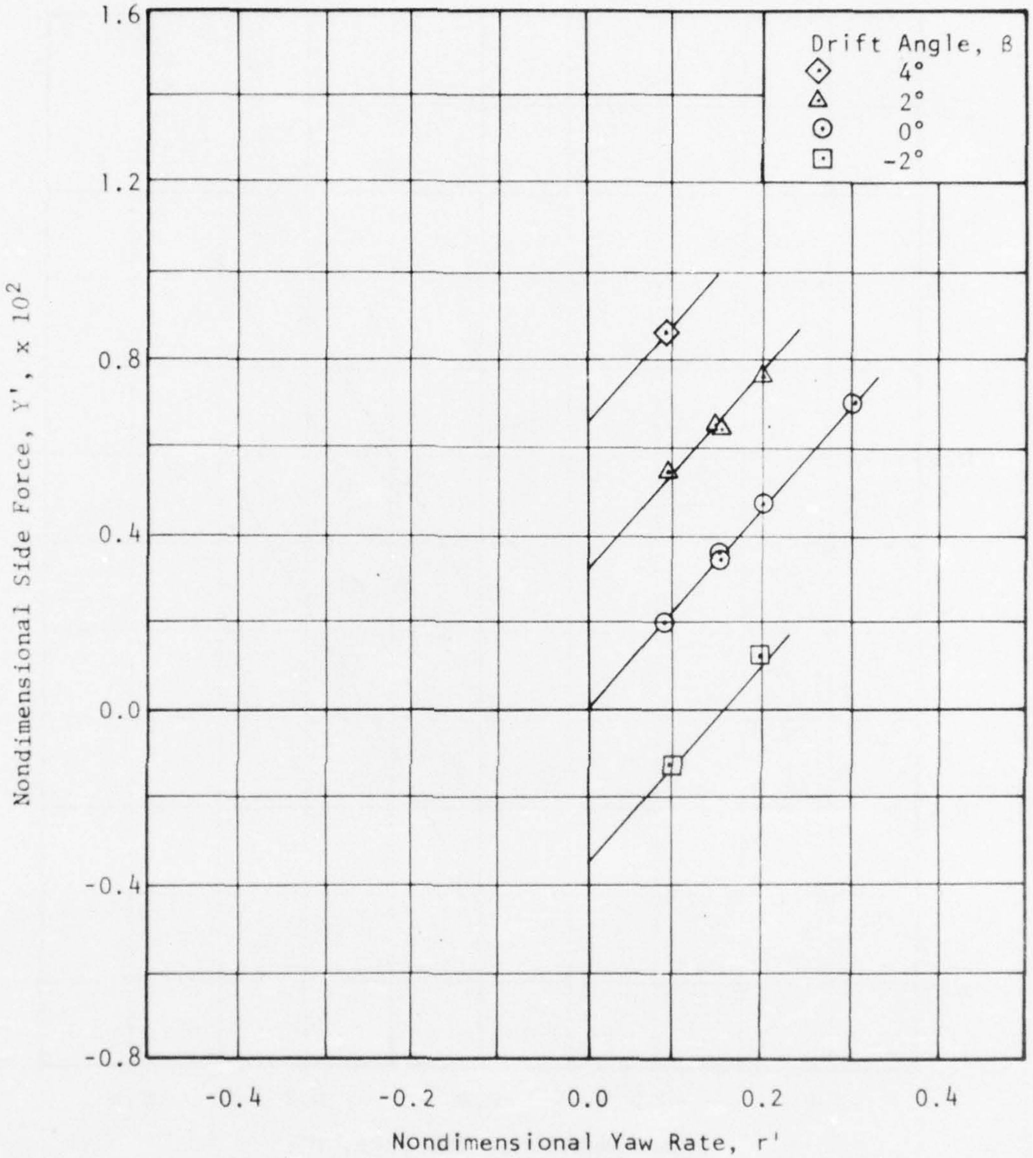

Figure 127 - Variation of Nondimensional Side Force with Nondimensional Yaw Rate for a Series of Drift Angles at a Full Scale Speed of 15 Knots for the Spade Rudder at Design Draft

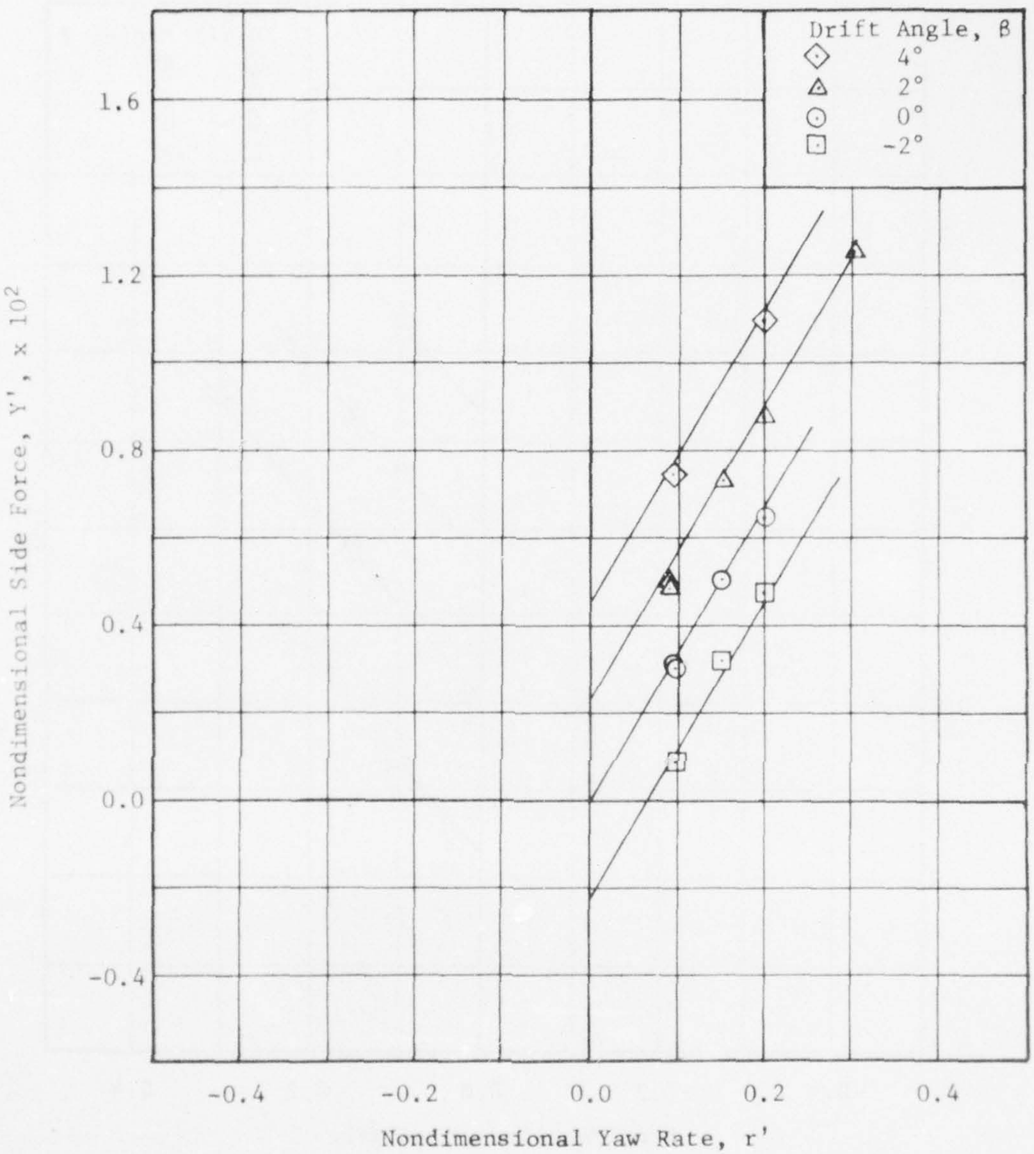

Figure 128 - Variation of Nondimensional Side Force with Nondimensional Yaw Rate for a Series of Drift Angles at a Full Scale Speed of 20 Knots for the Spade Rudder at Design Draft

AD-A034 593 DAVID W TAYLOR NAVAL SHIP RESEARCH AND DEVELOPMENT CE--ETC F/G 13/10
ROTATING ARM EXPERIMENTS FOR SWATH 6A MANEUVERING PREDICTIONS.(U)
JUL 76 J A FEIN, R T WATERS

UNCLASSIFIED SPD-698-01 NL

3 OF 4
AD
A034593

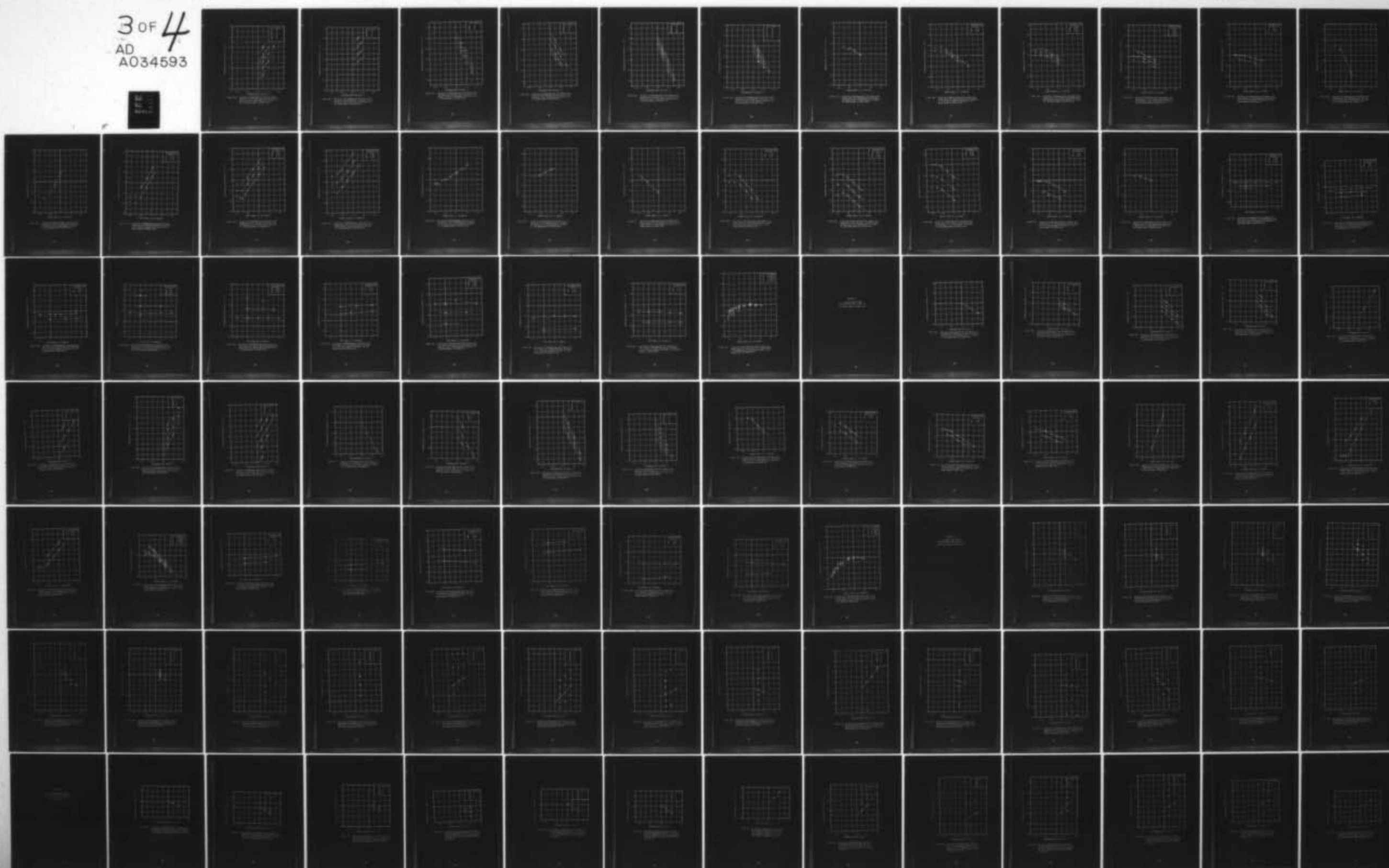

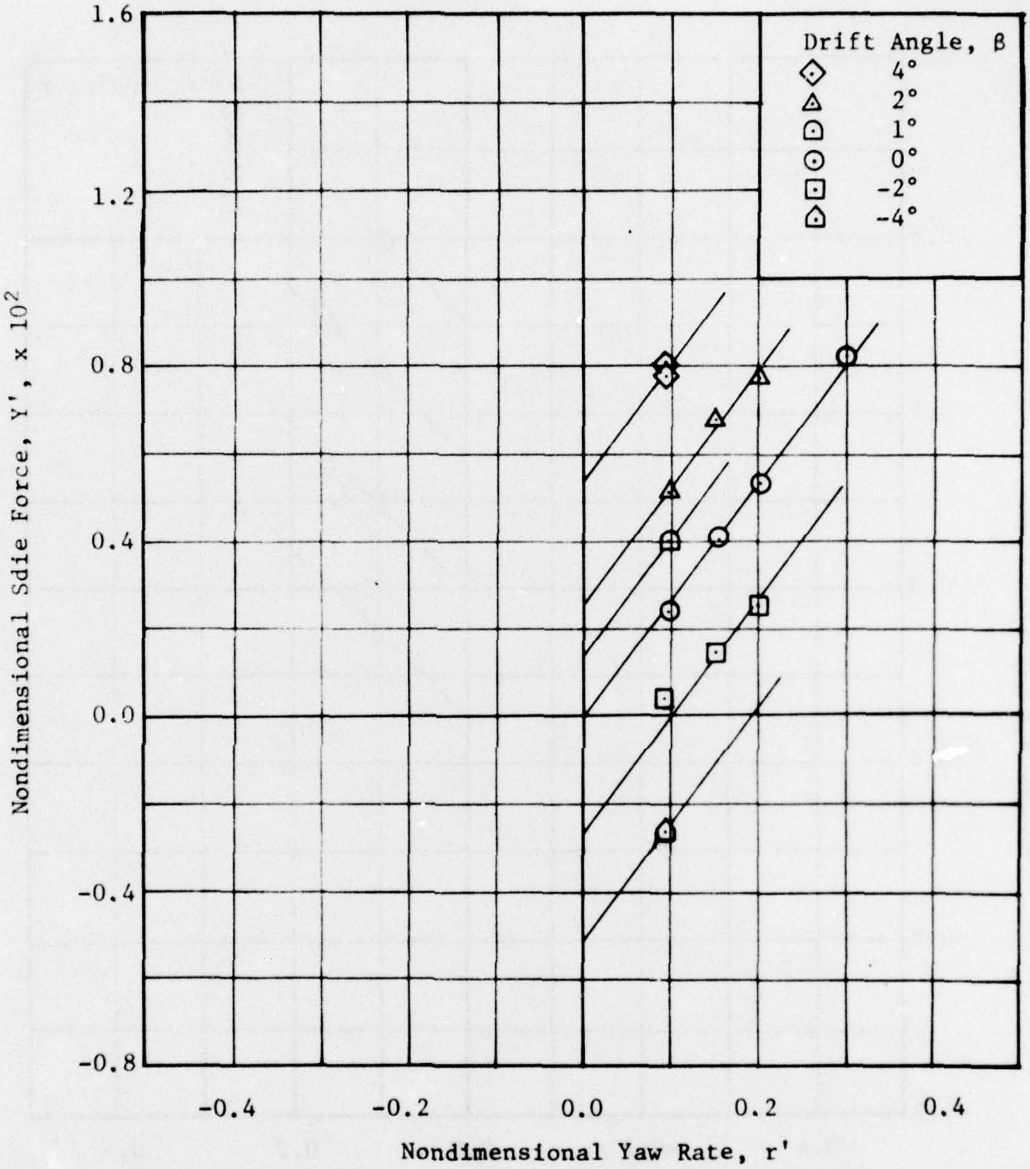

Figure 129 - Variation of Nondimensional Side Force with Nondimensional Yaw Rate for a Series of Drift Angles at a Full Scale Speed of 25 Knots for the Spade Rudder at Design Draft

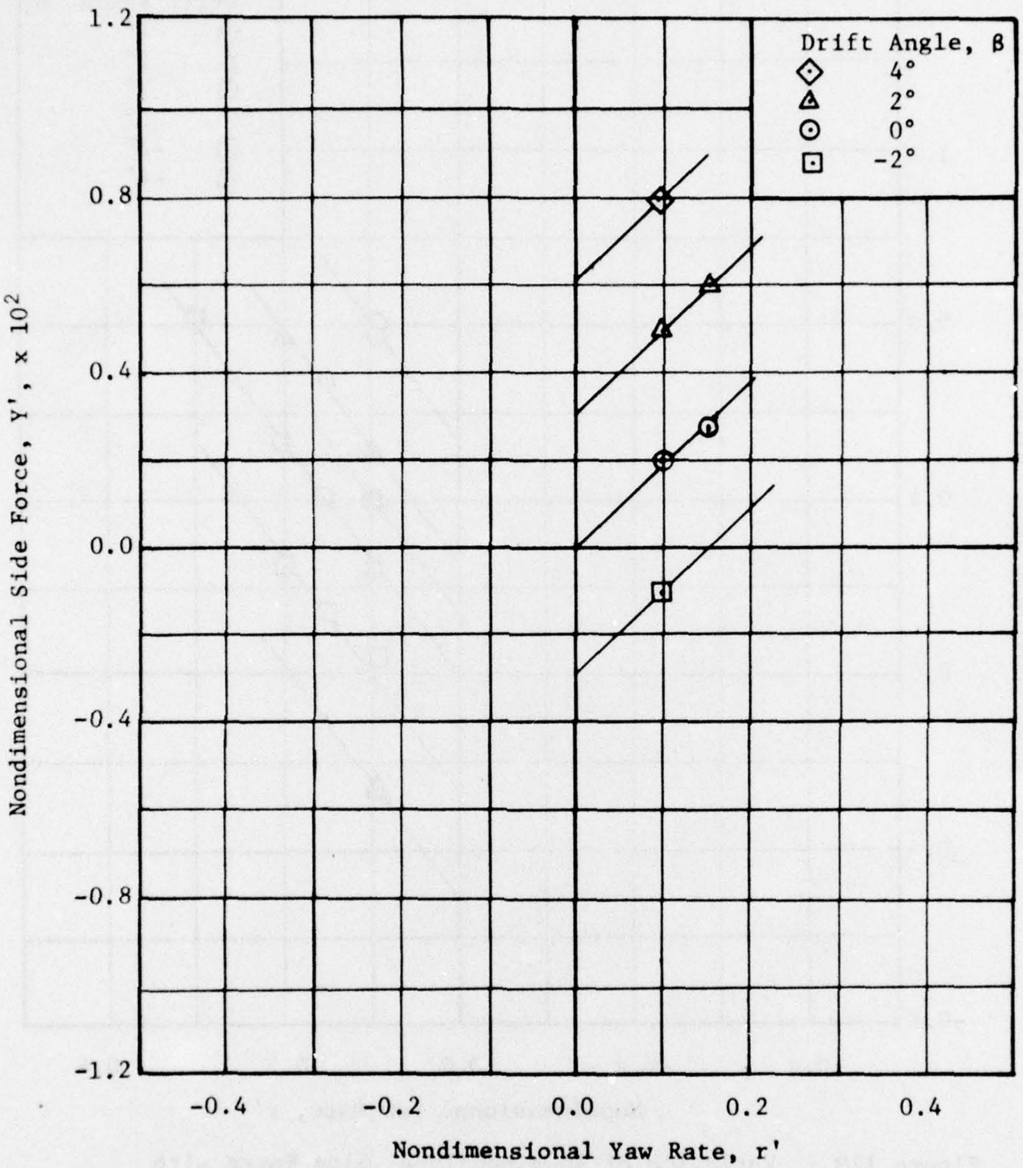

Figure 130 - Variation of Nondimensional Side Force with Nondimensional Yaw Rate for a Series of Drift Angles at a Full Scale Speed of 28 Knots for the Spade Rudder at Design Draft

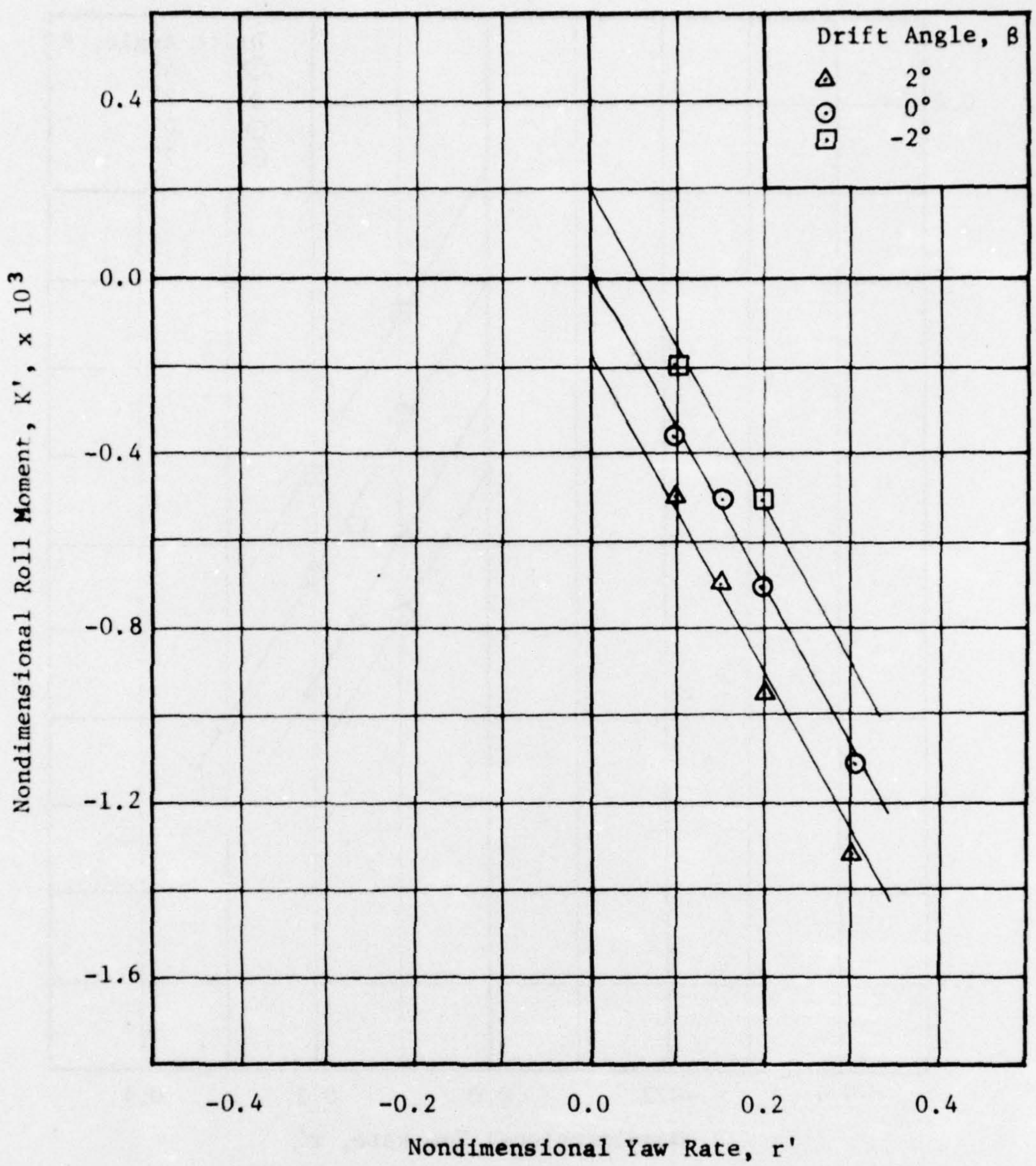

Figure 131 - Variation of Nondimensional Roll Moment with Nondimensional Yaw Rate for a Series of Drift Angles at a Full Scale Speed of 10 Knots for the Spade Rudder at Design Draft

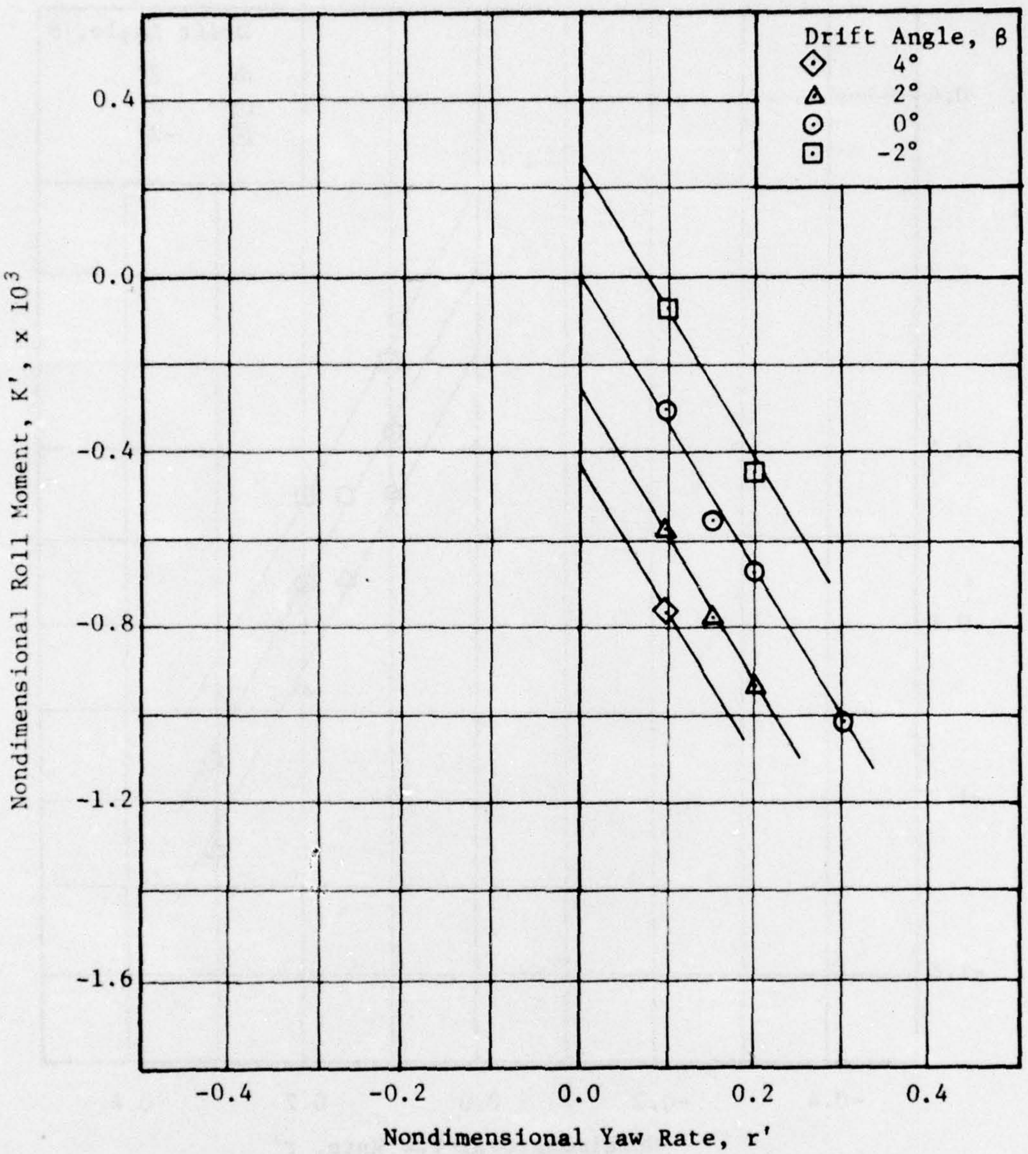

Figure 132 - Variation of Nondimensional Roll Moment with Nondimensional Yaw Rate for a Series of Drift Angles at a Full Scale Speed of 15 Knots for the Spade Rudder at Design Draft

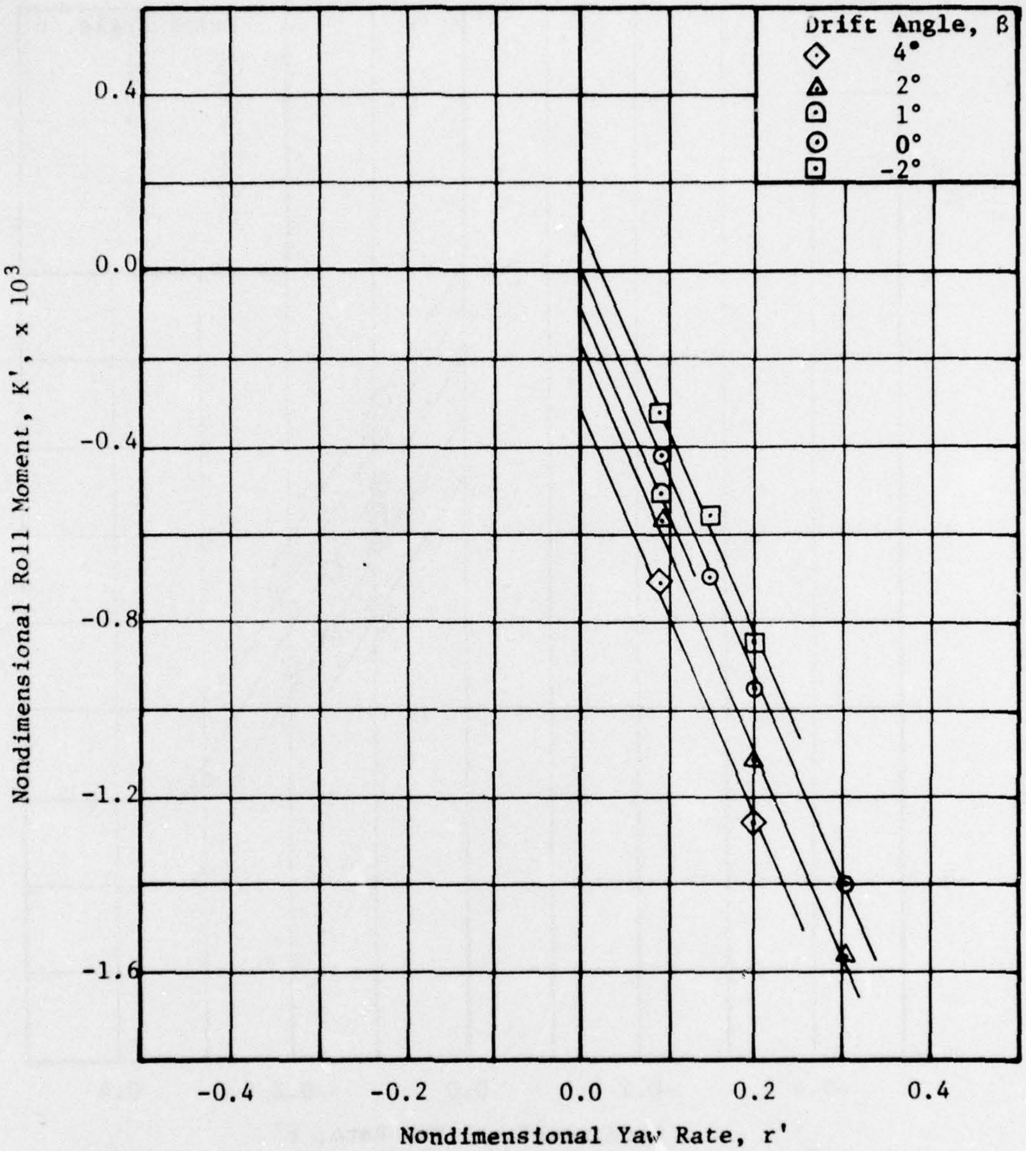

Figure 133 - Variation of Nondimensional Roll Moment with Nondimensional Yaw Rate for a Series of Drift Angles at a Full Scale Speed of 20 Knots for the Spade Rudder at Design Draft

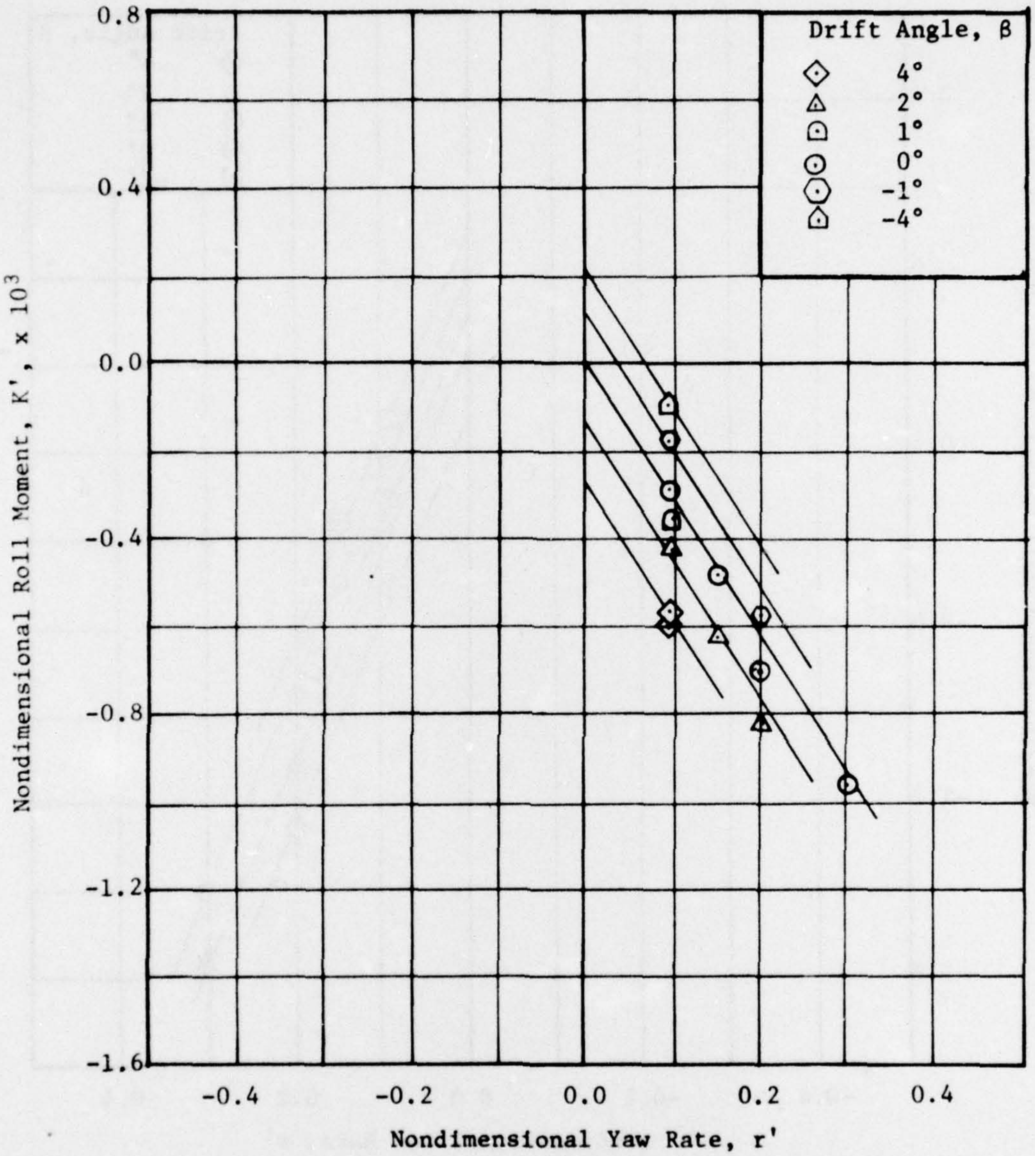

Figure 134 - Variation of Nondimensional Roll Moment with Nondimensional Yaw Rate for a Series of Drift Angles at a Full Scale Speed of 25 Knots for the Spade Rudder at Design Draft

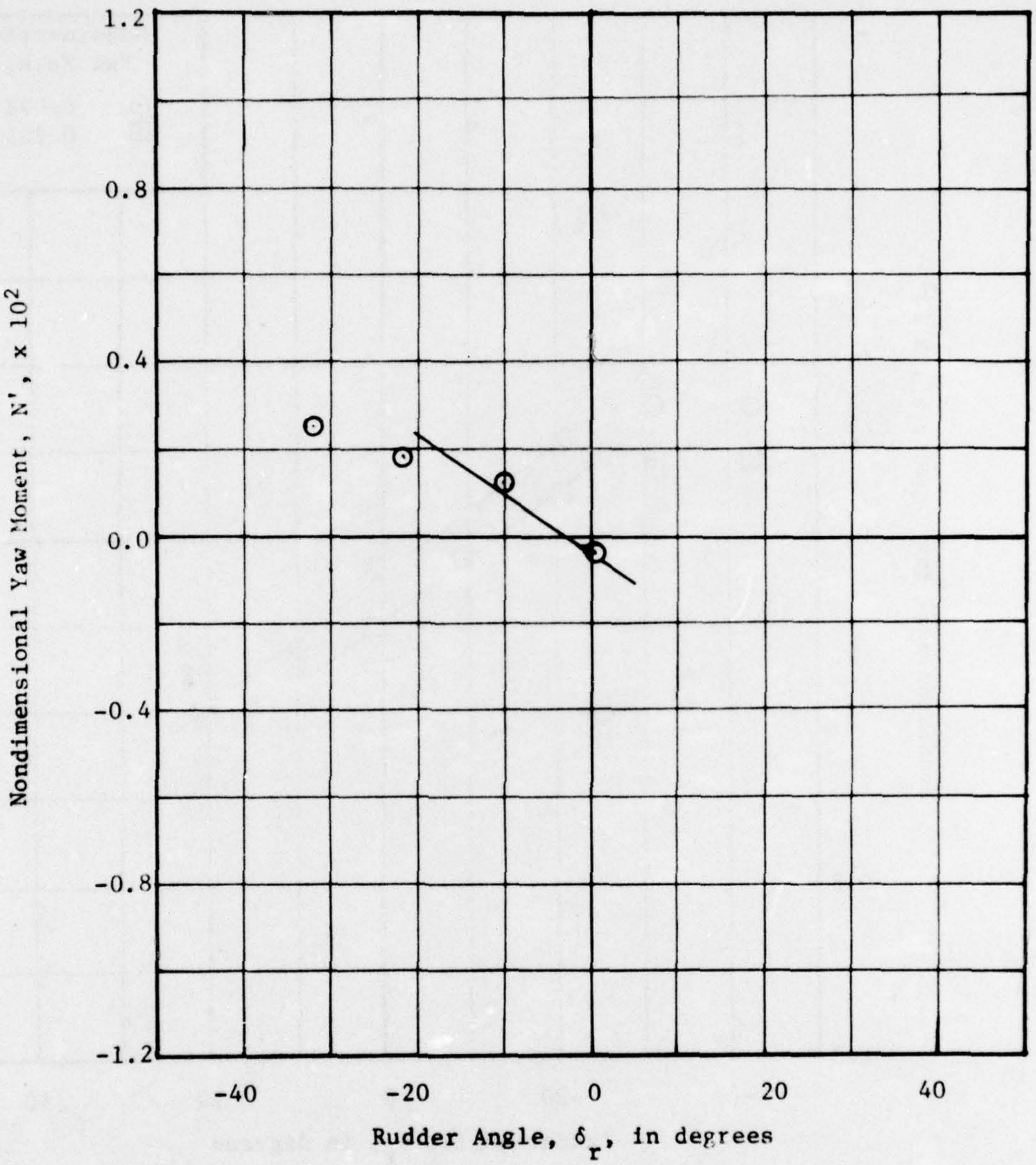

Figure 135 - Variation of Nondimensional Yaw Moment with Rudder Angle for a Nondimensional Yaw Rate of 0.093 at a Full Scale Speed of 5 Knots for the Spade Rudder at Design Draft

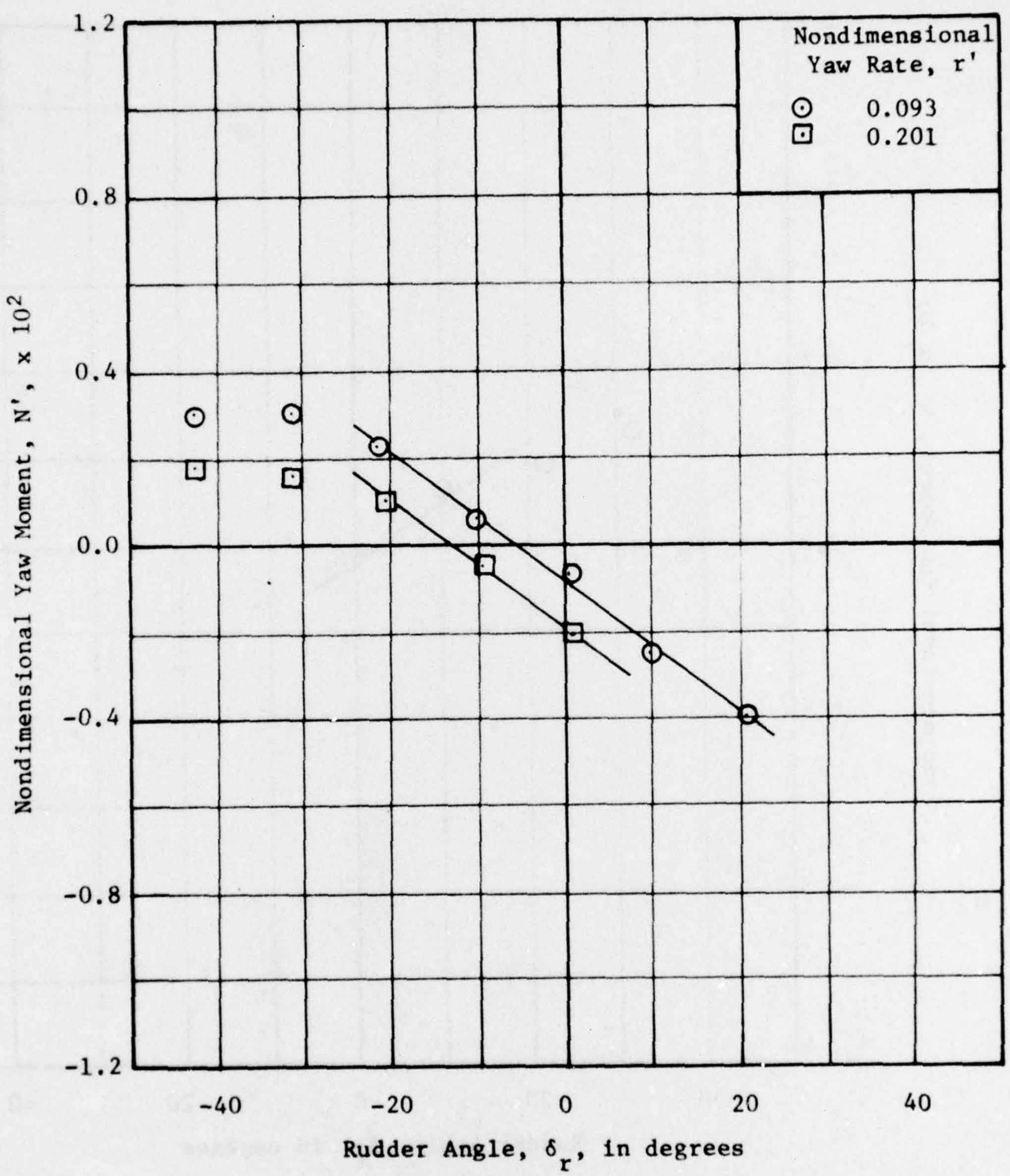

Figure 136 - Variation of Nondimensional Yaw Moment with Rudder Angle for Two Nondimensional Yaw Rates at a Full Scale Speed of 10 Knots for the Spade Rudder at Design Draft

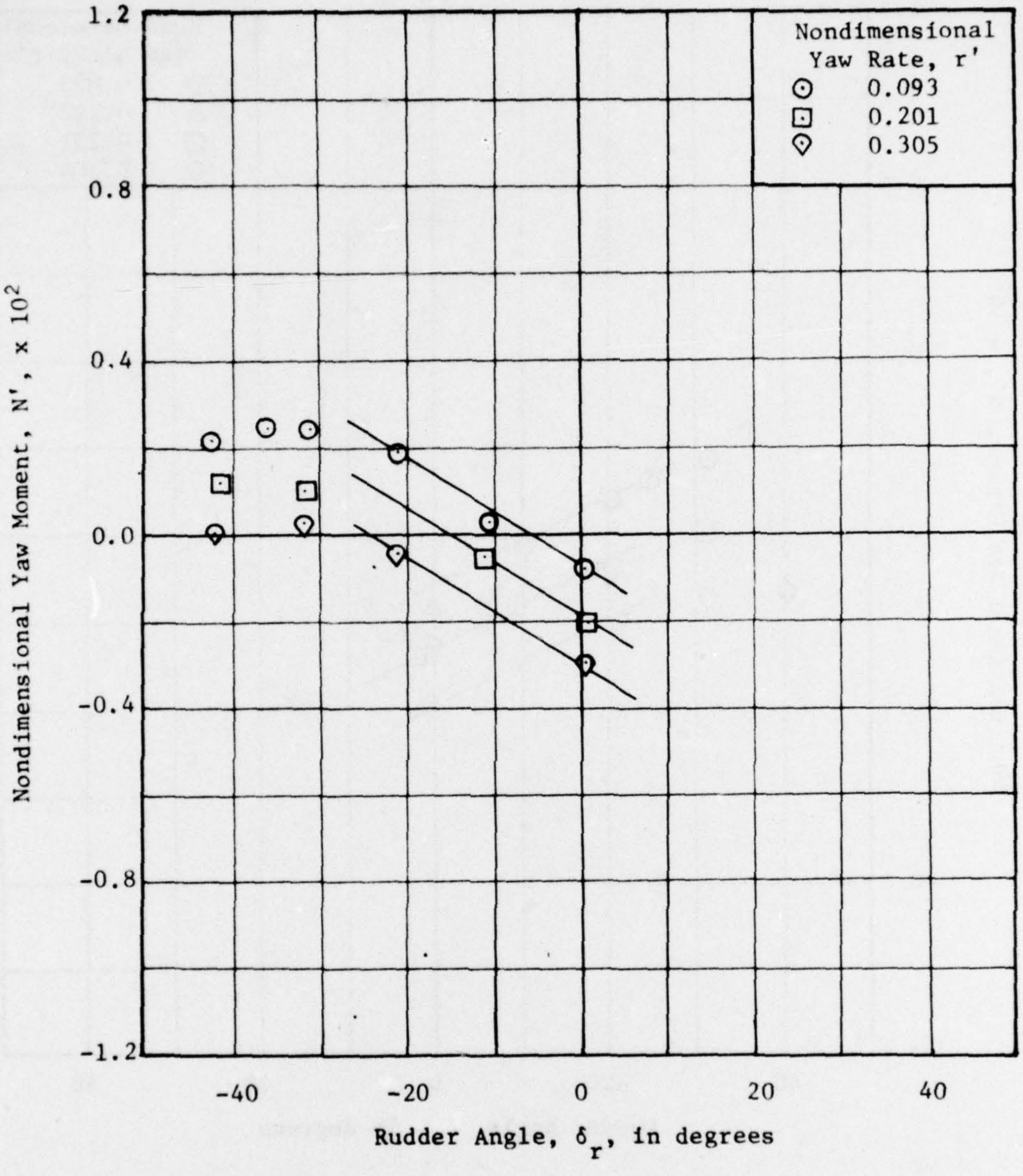

Figure 137 - Variation of Nondimensional Yaw Moment with Rudder Angle for a Series of Nondimensional Yaw Rates at a Full Scale Speed of 15 Knots for the Spade Rudder at Design Draft

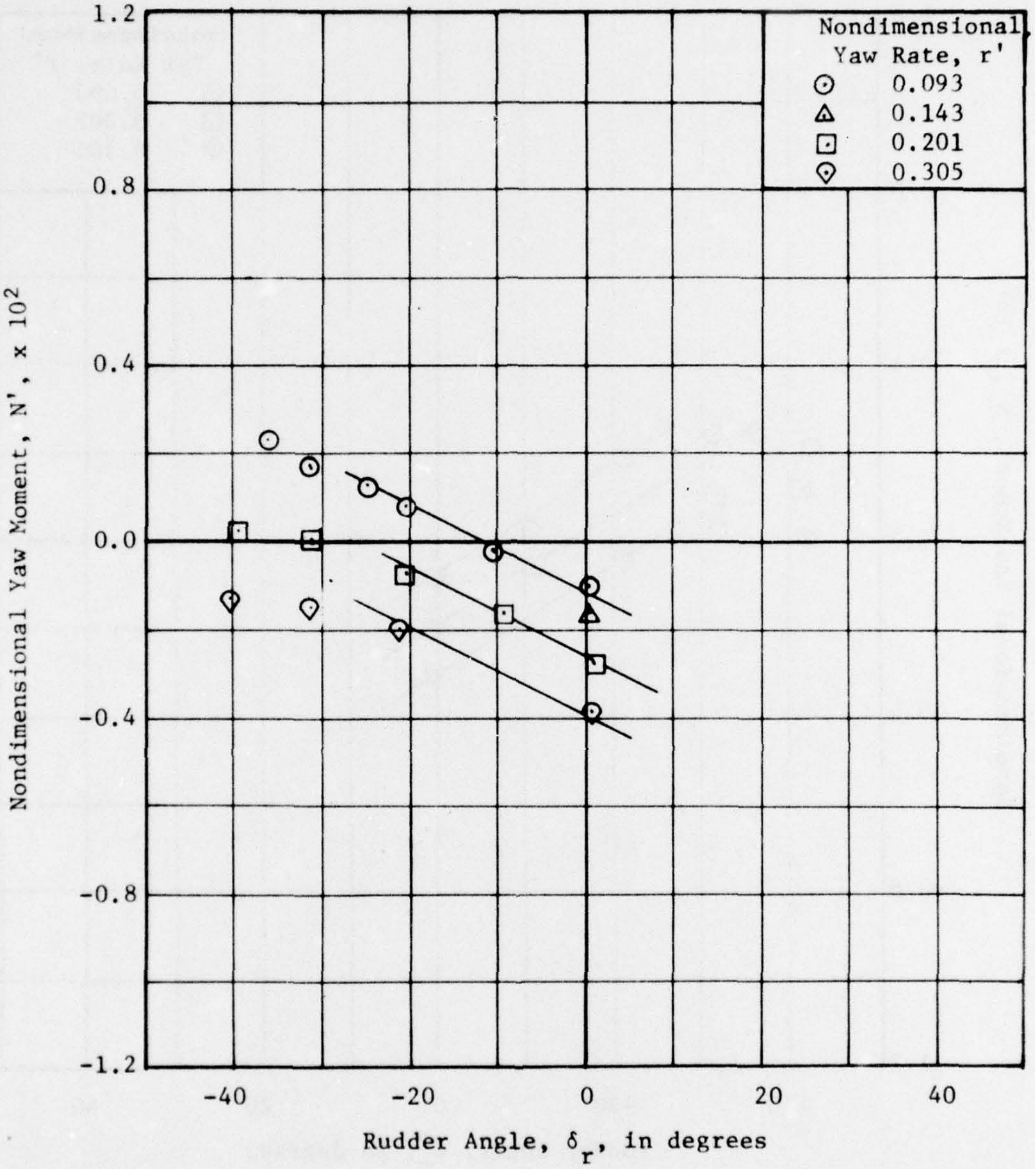

Figure 138 - Variation of Nondimensional Yaw Moment with Rudder Angle for a Series of Nondimensional Yaw Rates at a Full Scale Speed of 20 Knots for the Spade Rudder at Design Draft

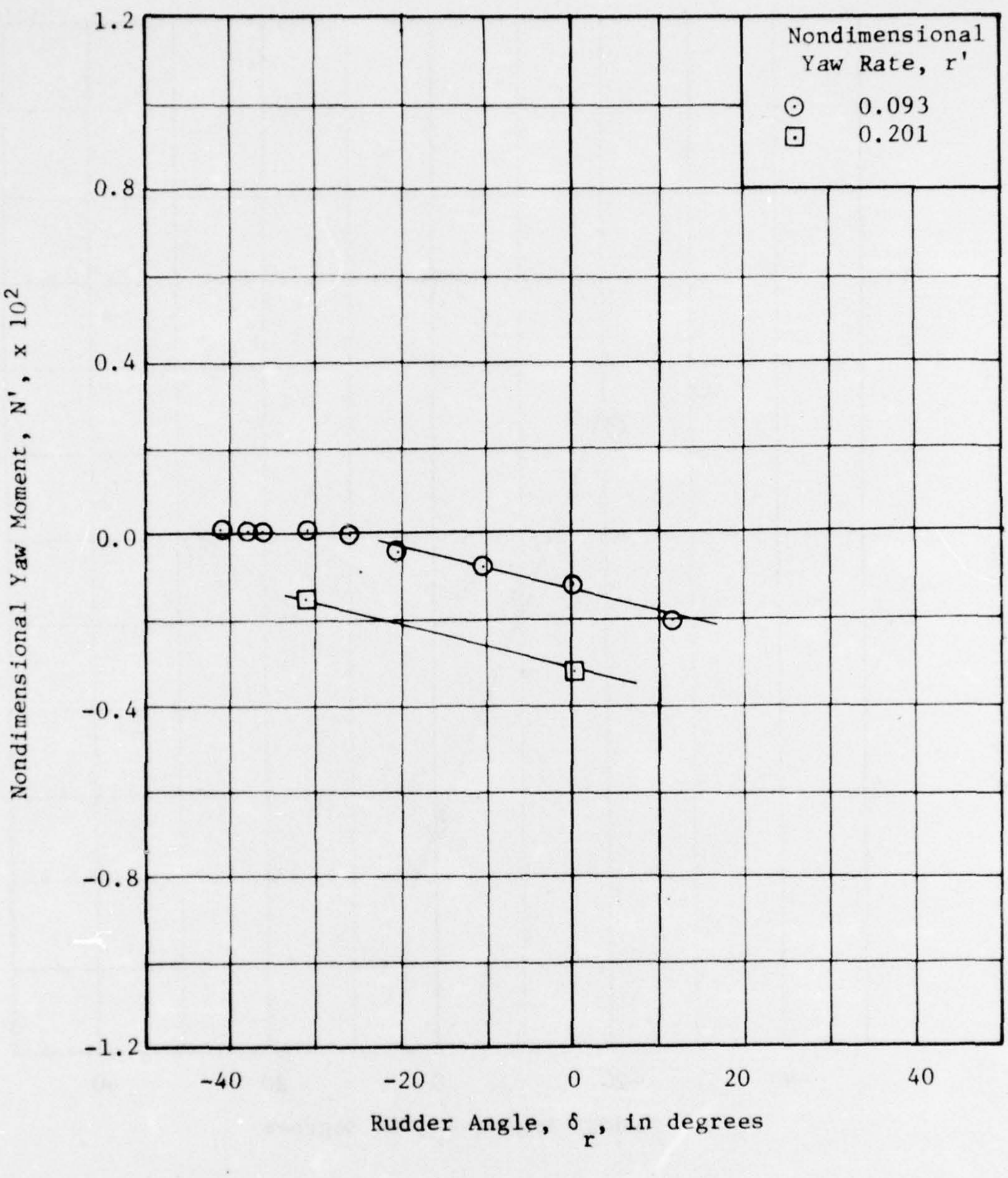

Figure 139 - Variation of Nondimensional Yaw Moment with Rudder Angle for Two Nondimensional Yaw Rates at a Full Scale Speed of 25 Knots for the Spade Rudder at Design Draft

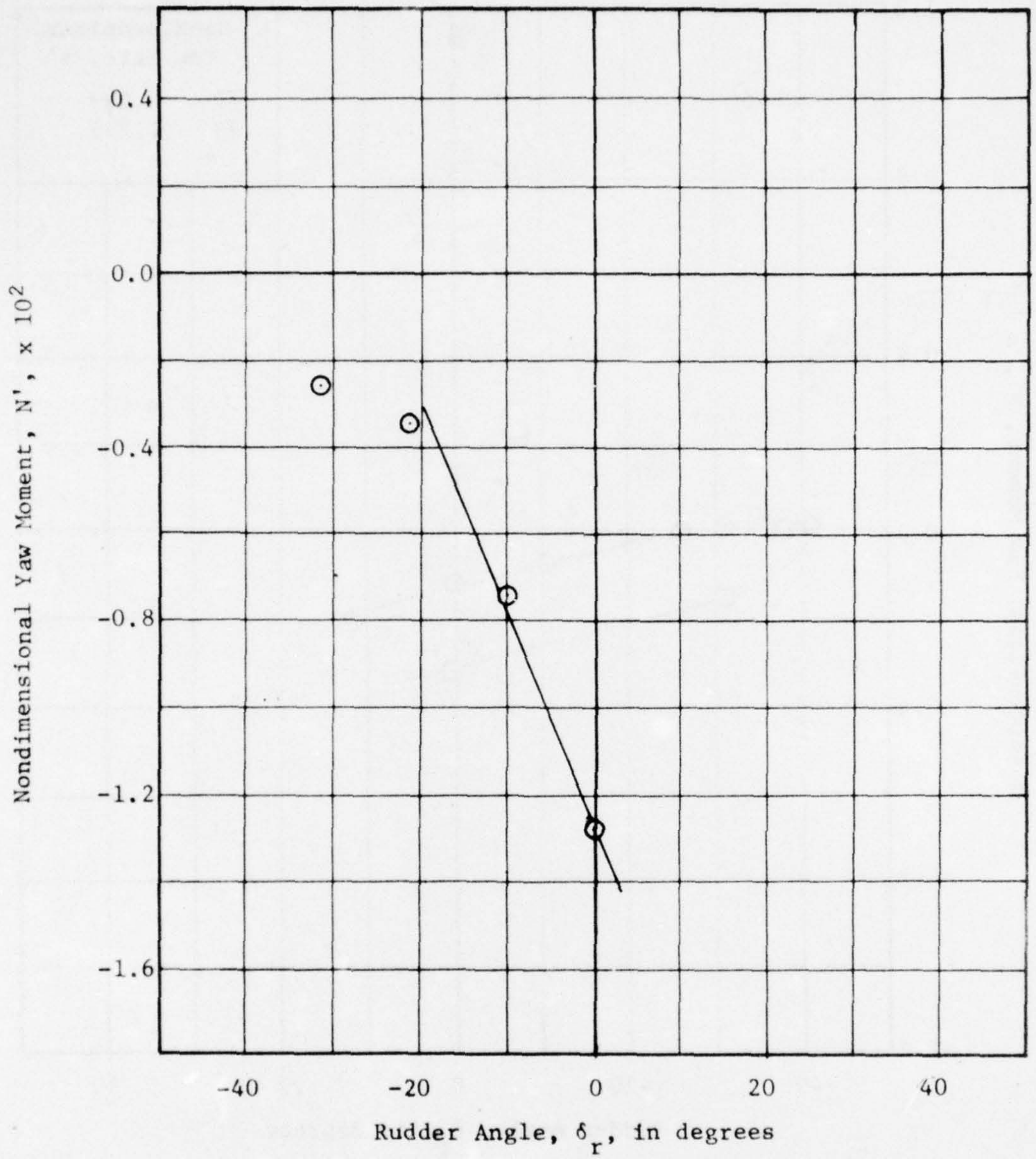

Figure 140 - Variation of Nondimensional Yaw Moment with Rudder Angle for a Nondimensional Yaw Rate of 0.093 at a Full Scale Speed of 28 Knots for the Spade Rudder at Design Draft

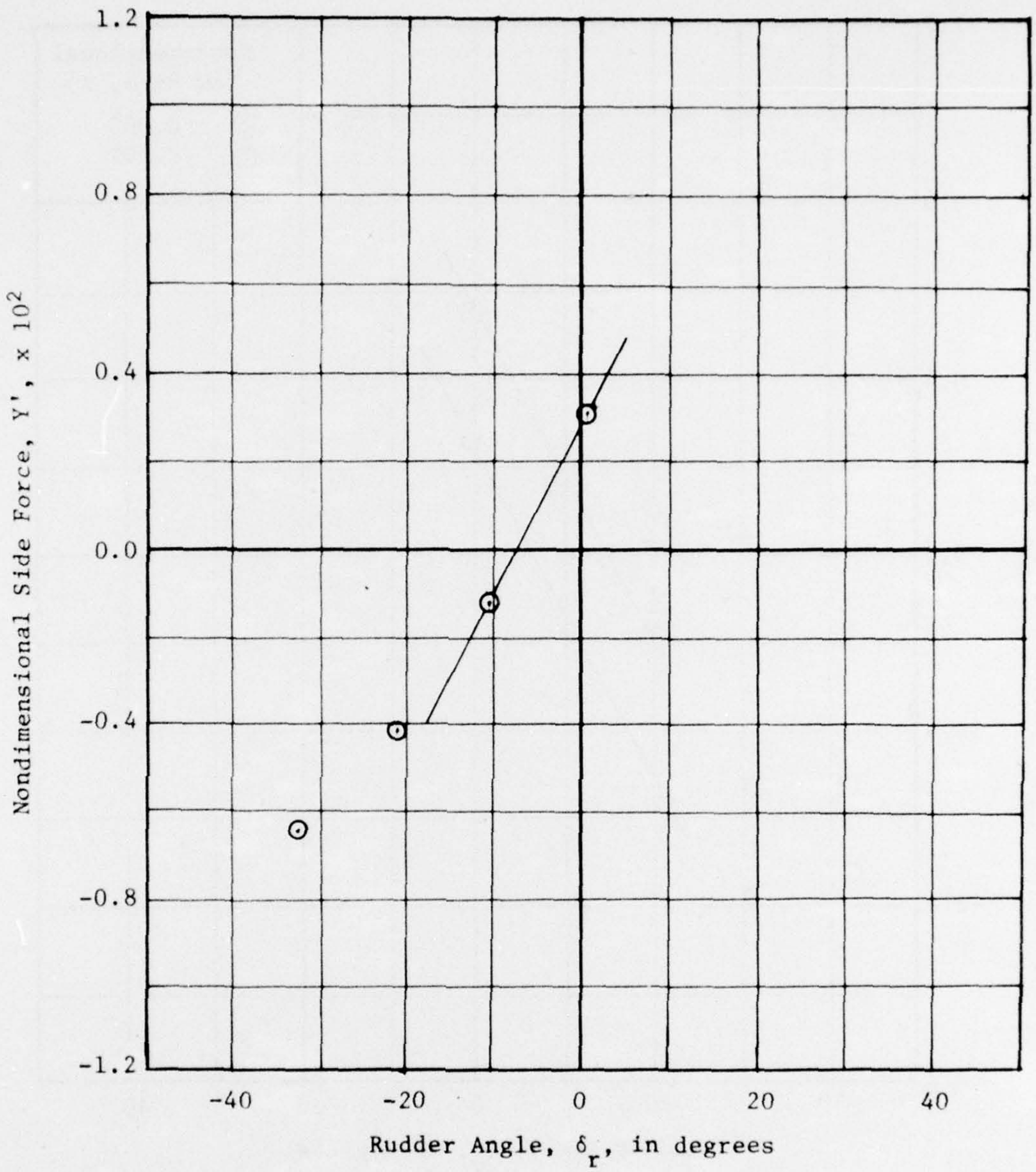

Figure 141 - Variation of Nondimensional Side Force with Rudder Angle for a Nondimensional Yaw Rate of 0.093 at a Full Scale Speed of 5 Knots for the Spade Rudder at Design Draft

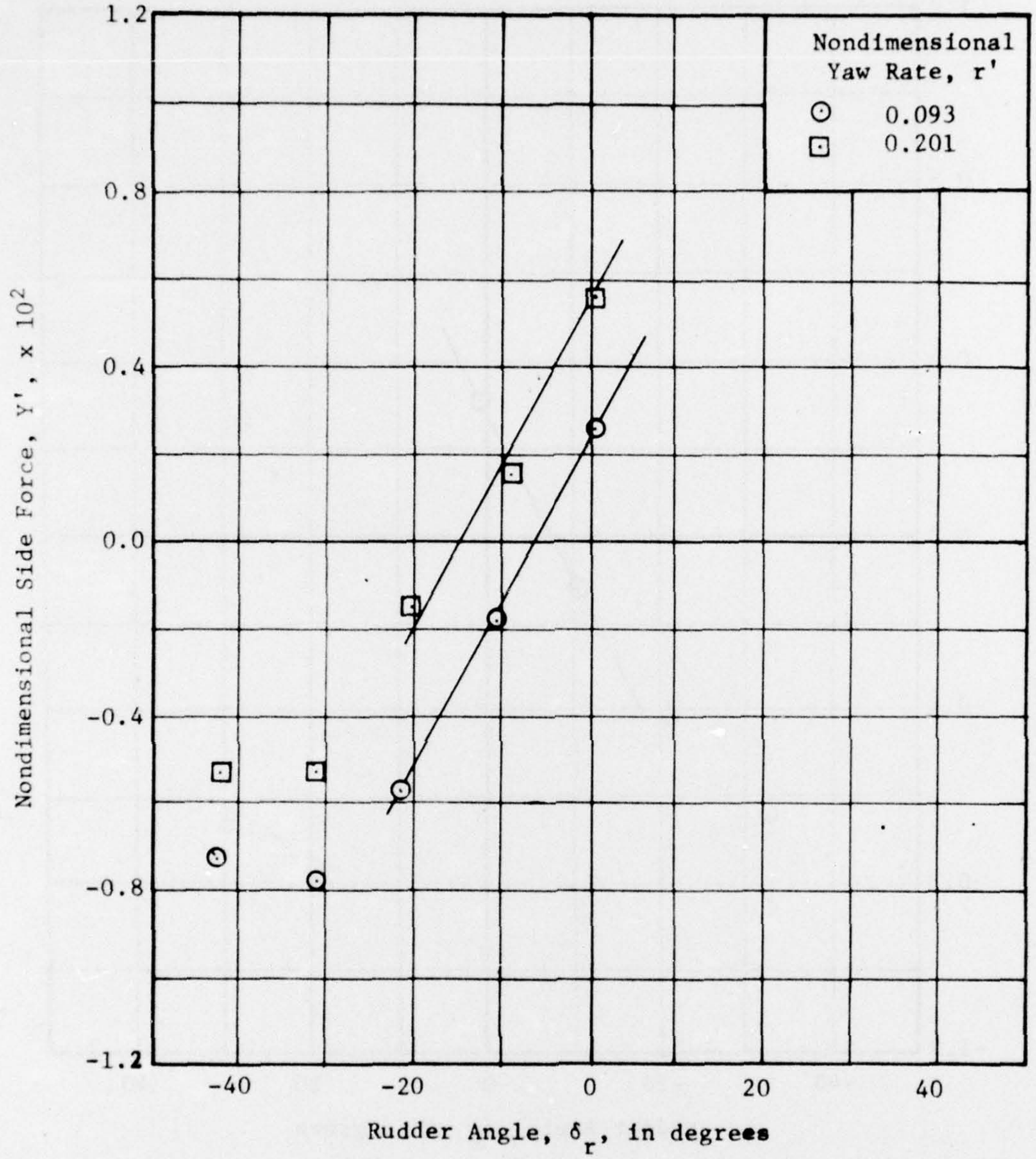

Figure 142 - Variation of Nondimensional Side Force with Rudder Angle for Two Nondimensional Yaw Rates at a Full Scale Speed of 10 Knots for the Spade Rudder at Design Draft

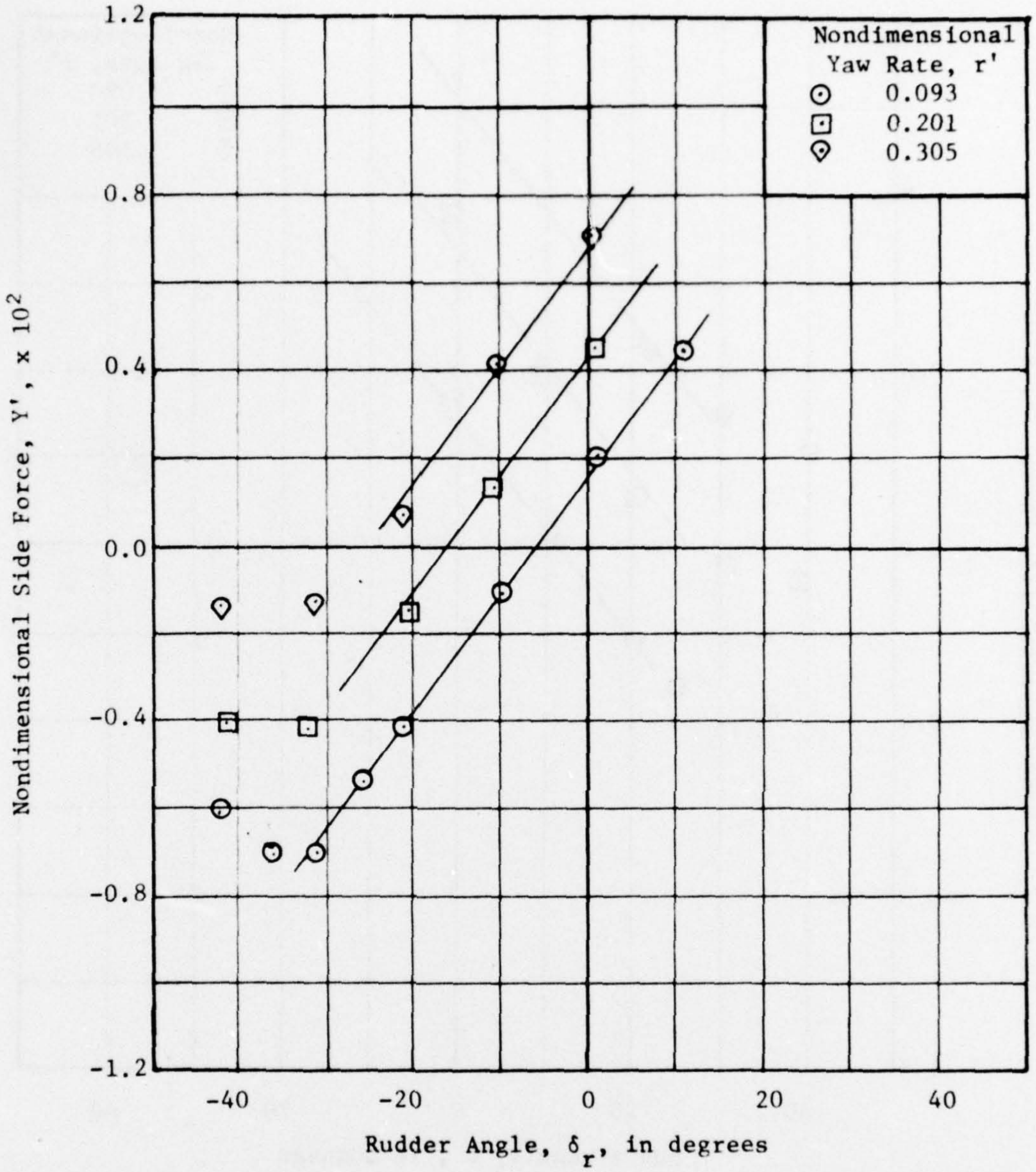

Figure 143 - Variation of Nondimensional Side Force with Rudder Angle for a Series of Nondimensional Yaw Rates at a Full Scale Speed of 15 Knots for the Spade Rudder at Design Draft

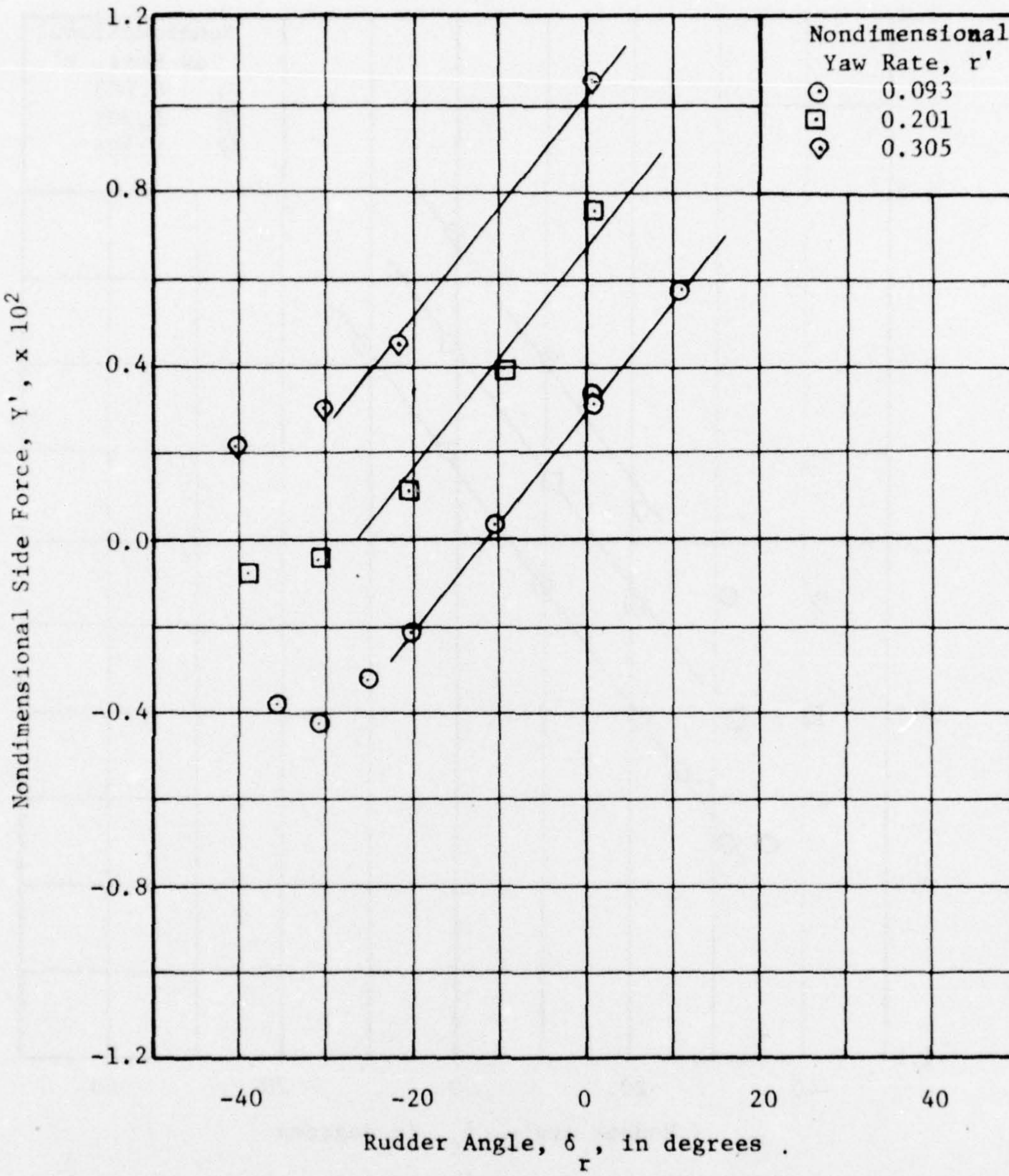

Figure 144 - Variation of Nondimensional Side Force with Rudder Angle for a Series of Nondimensional Yaw Rates at a Full Scale Speed of 20 Knots for the Spade Rudder at Design Draft

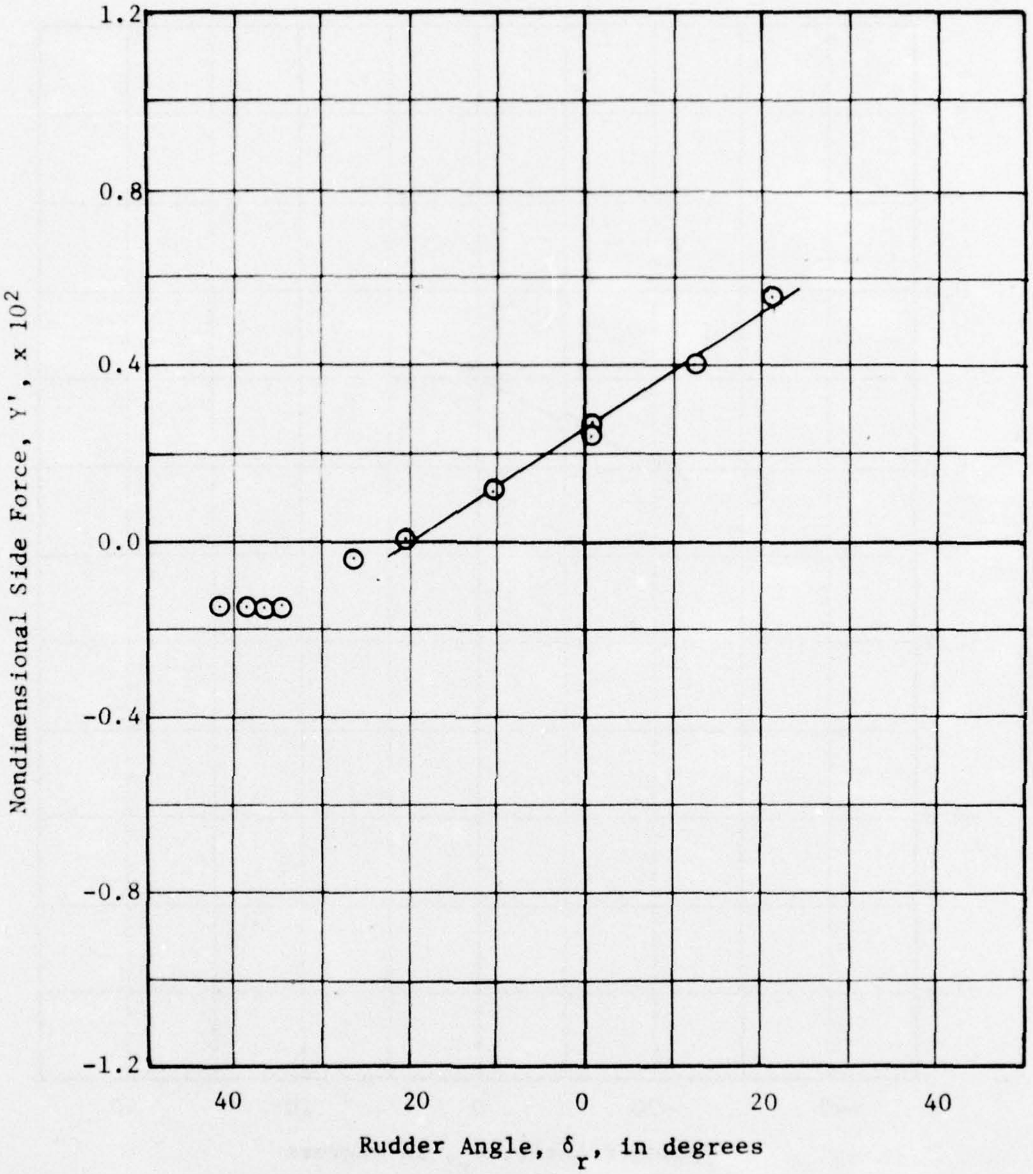

Figure 145 - Variation of Nondimensional Side Force with Rudder Angle for a Nondimensional Yaw Rate of 0.093 at a Full Scale Speed of 25 Knots for the Spade Rudder at Design Draft

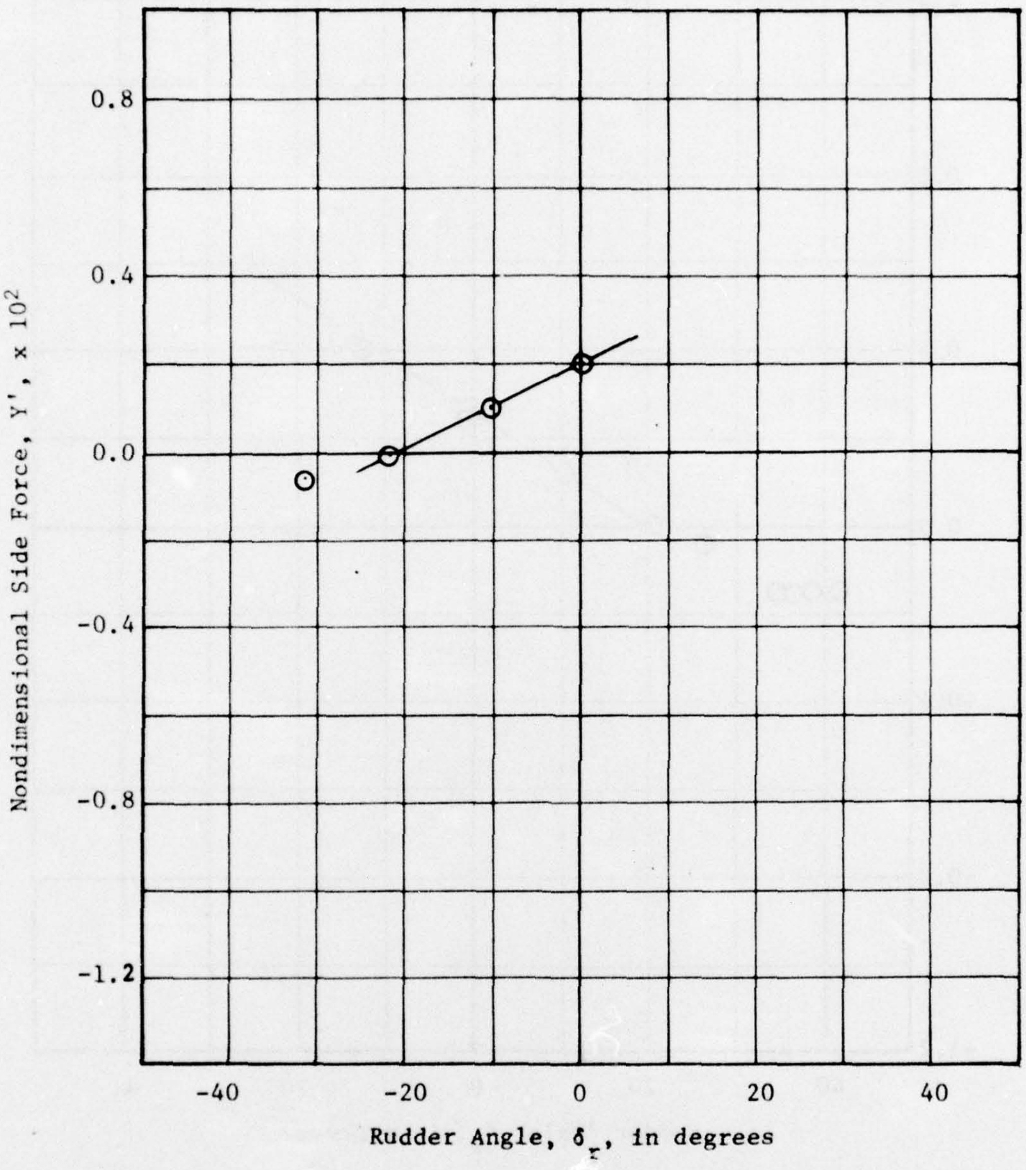

Figure 146 - Variation of Nondimensional Side Force with Rudder Angle for a Nondimensional Yaw Rate of 0.093 at a Full Scale Speed of 28 Knots for the Spade Rudder at Design Draft

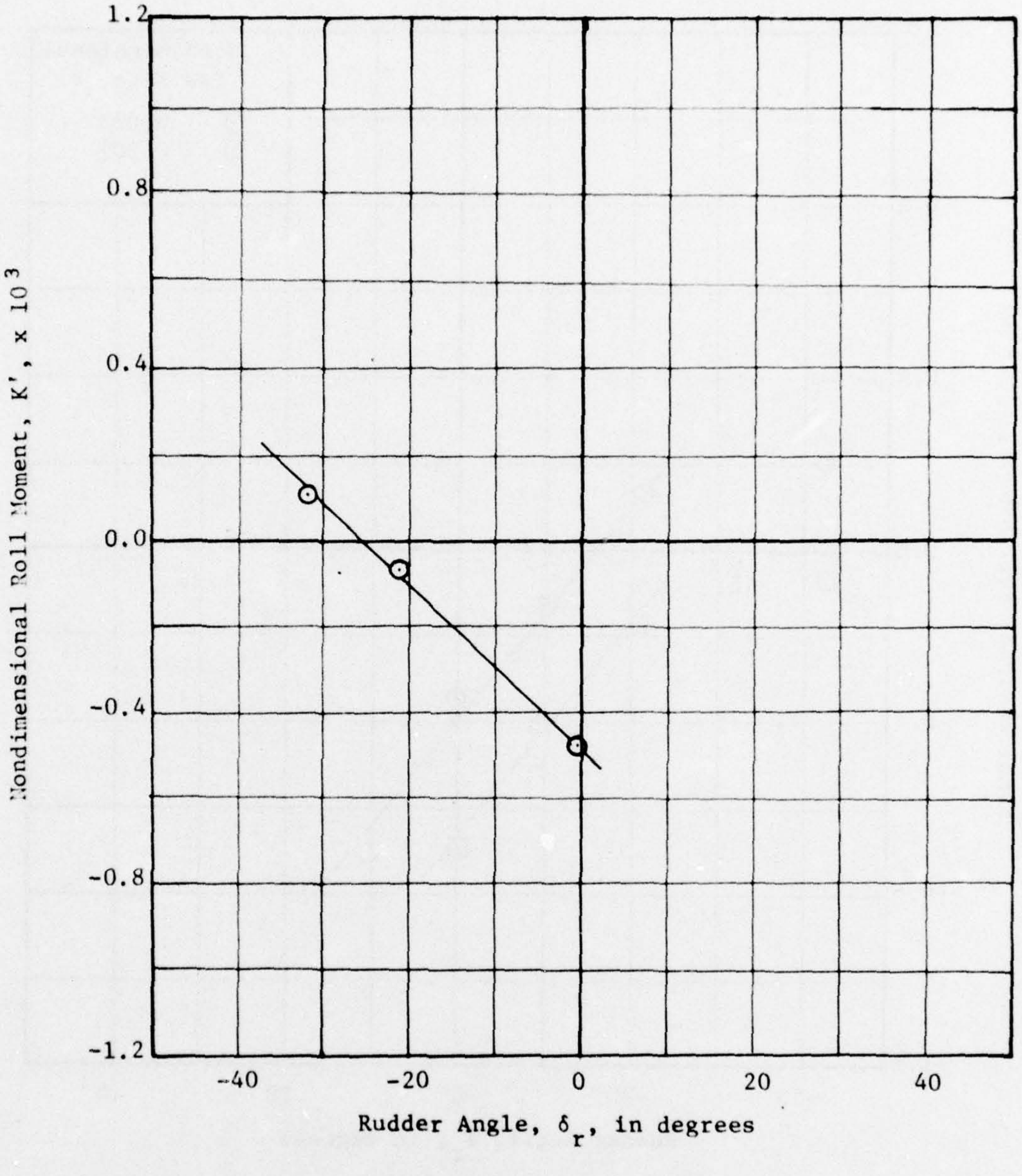

Figure 147 - Variation of Nondimensional Roll Moment with Rudder Angle for a Nondimensional Yaw rate of 0.093 at a Full Scale Speed of 5 Knots for the Spade Rudder at Design Draft

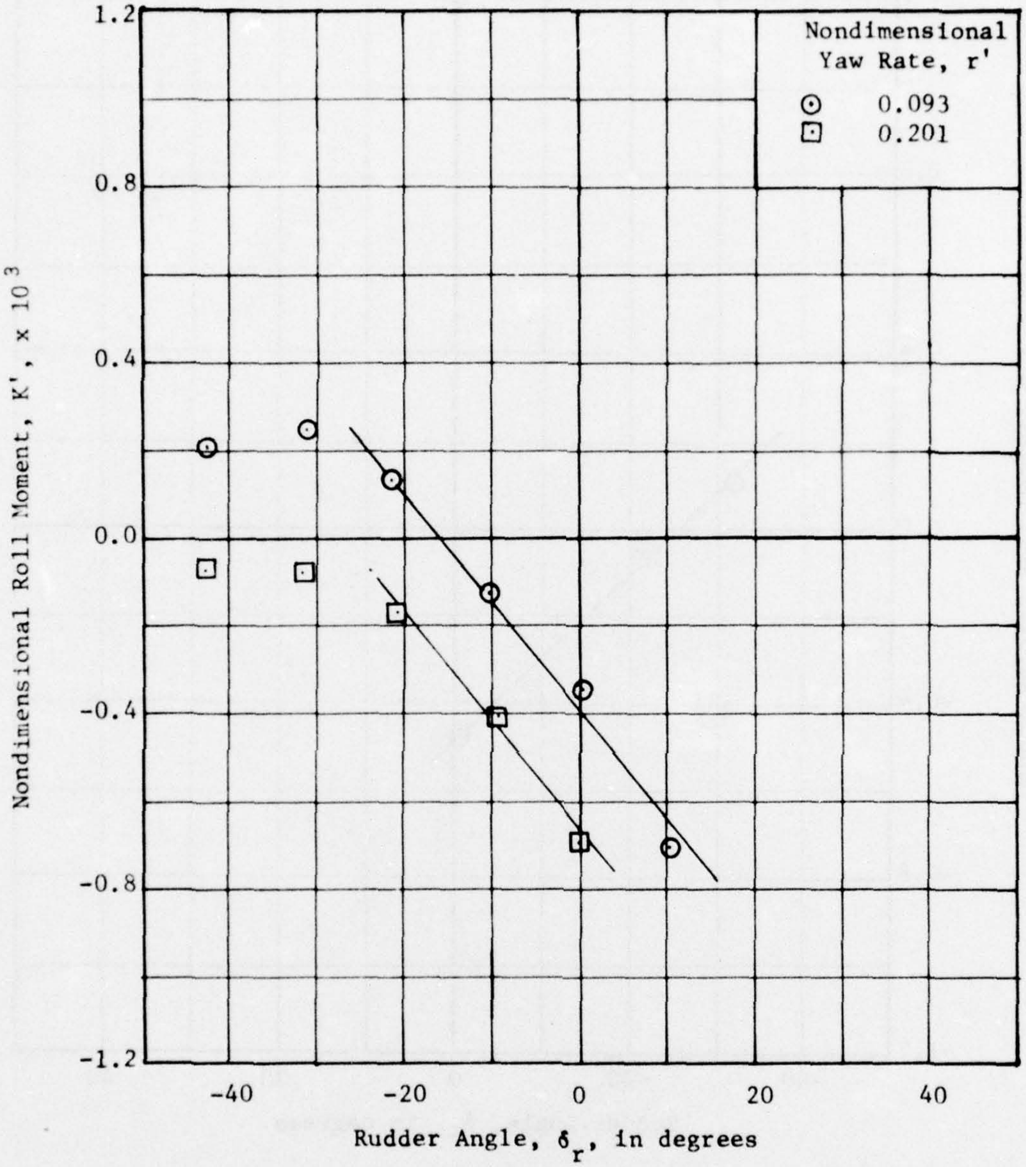

Figure 148 - Variation of Nondimensional **Roll Moment** with Rudder Angle for Two Nondimensional Yaw Rates at a Full Scale Speed of 10 Knots for the Spade Rudder at Design Draft

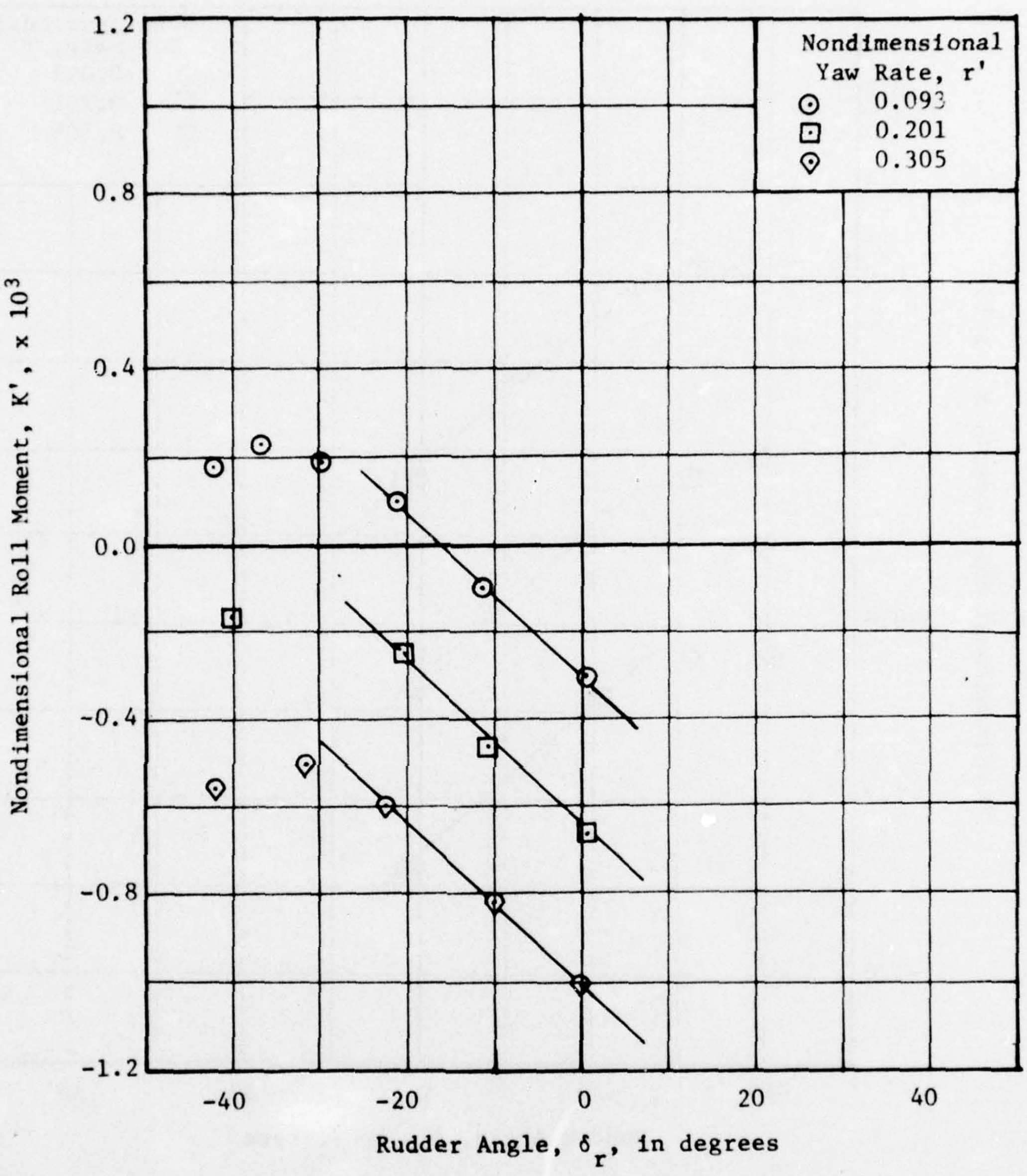

Figure 149 - Variation of Nondimensional Roll Moment with Rudder Angle for a Series of Nondimensional Yaw Rates at a Full Scale Speed of 15 Knots for the Spade Rudder at Design Draft

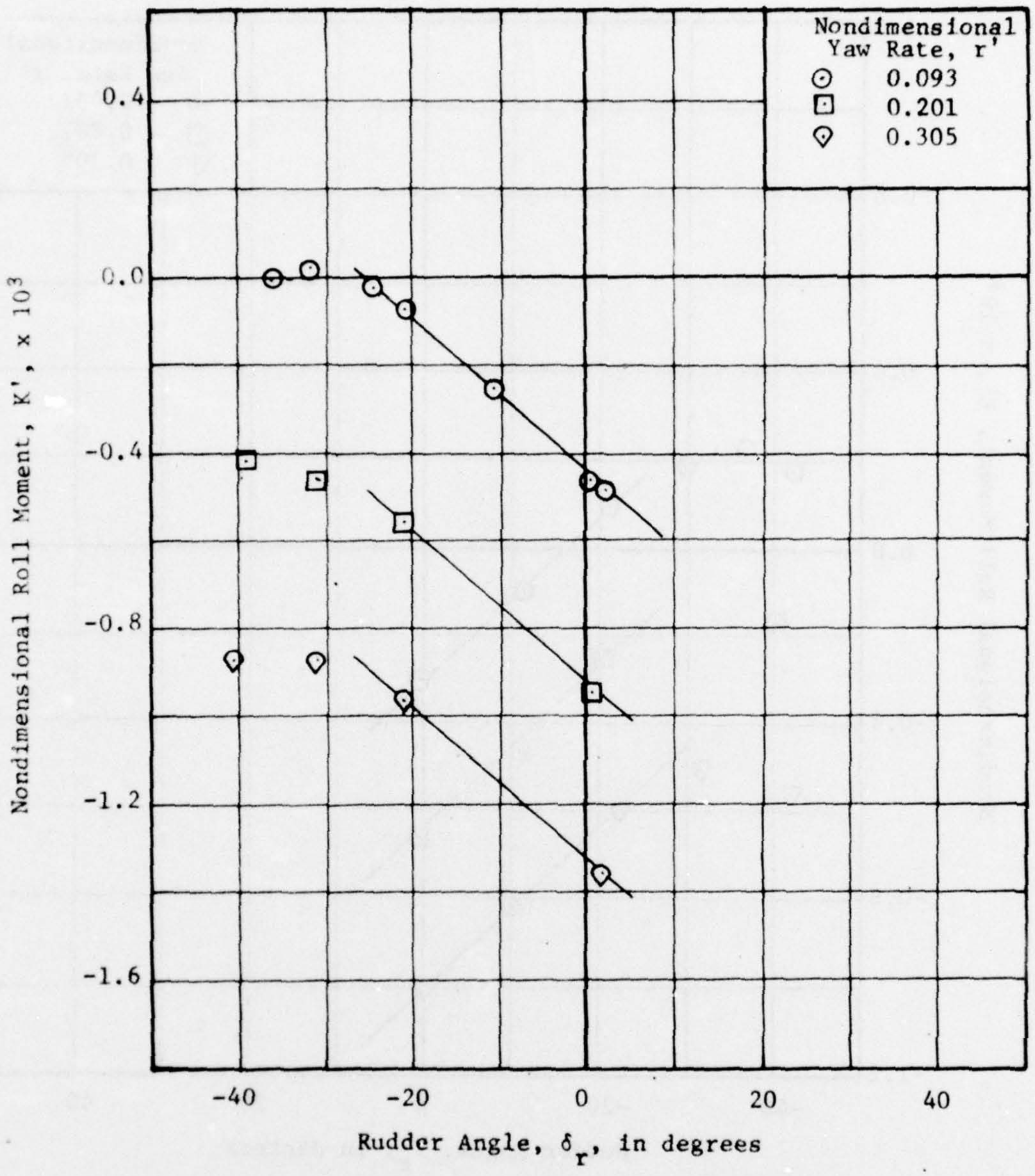

Figure 150 - Variation of Nondimensional Roll Moment with Rudder Angle for a Series of Nondimensional Yaw Rates at a Full Scale Speed of 20 Knots for the Spade Rudder at Design Draft

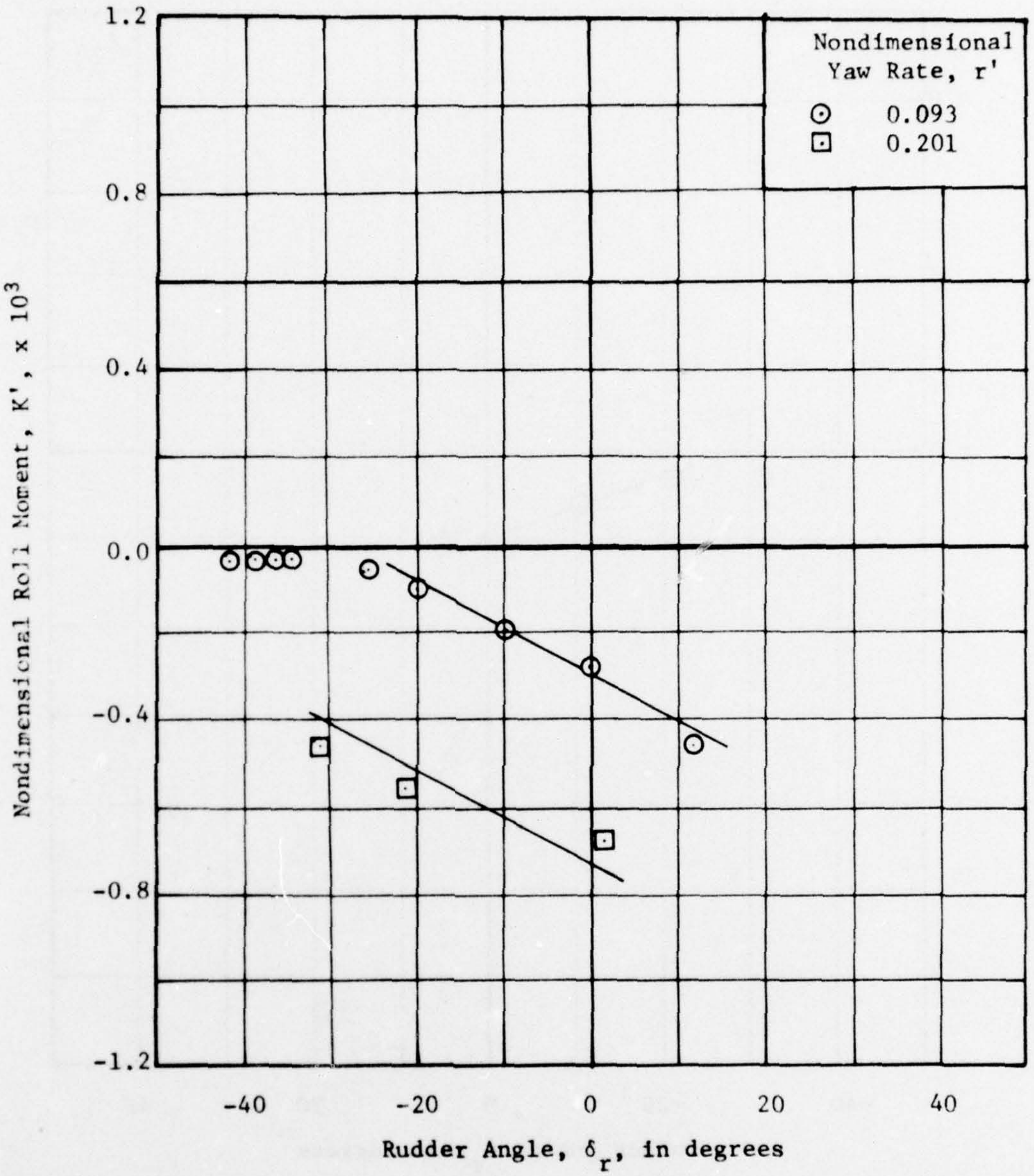

Figure 151 - Variation of Nondimensional Roll Moment with Rudder Angle for Two Nondimensional Yaw Rates at a Full Scale Speed of 25 Knots for the Spade Rudder at Design Draft

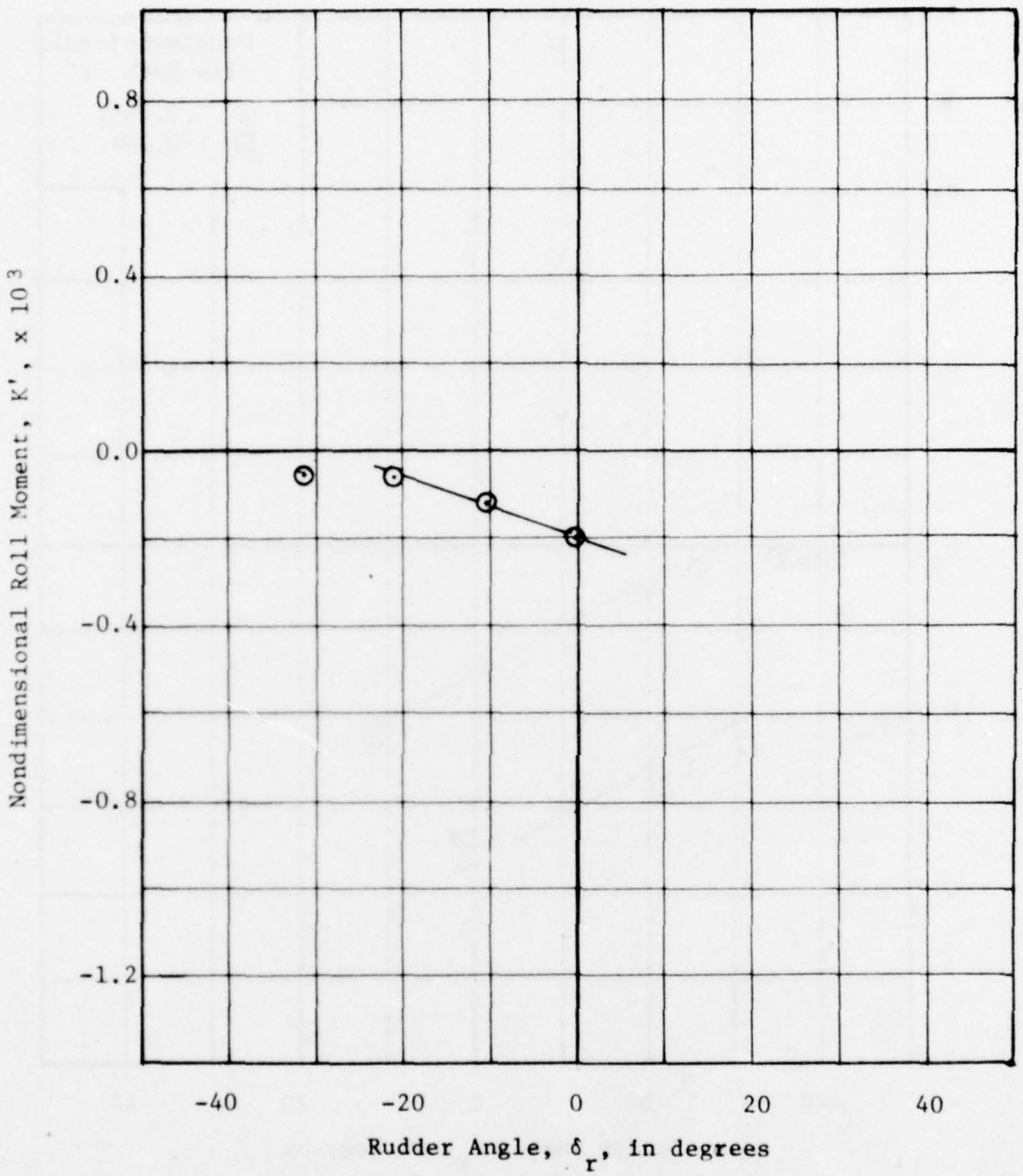

Figure 152 - Variation of Nondimensional Roll Moment with Rudder Angle for a Nondimensional Yaw Rate of 0.093 at a Full Scale Speed of 28 Knots for the Spade Rudder at Design Draft

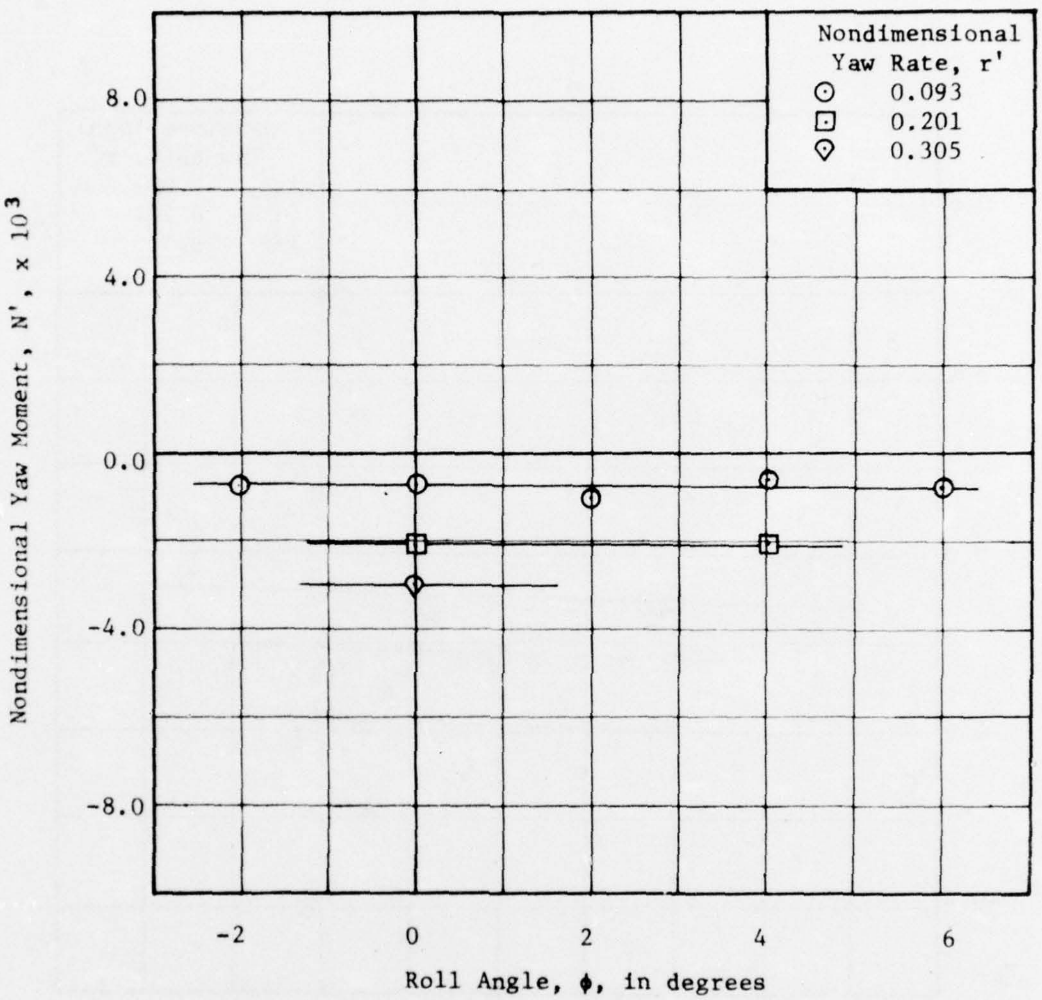

Figure 153 - Variation of Nondimensional Yaw Moment with Roll Angle for a Series of Nondimensional Yaw Rates at a Full Scale Speed of 10 Knots for the Spade Rudder at Design Draft

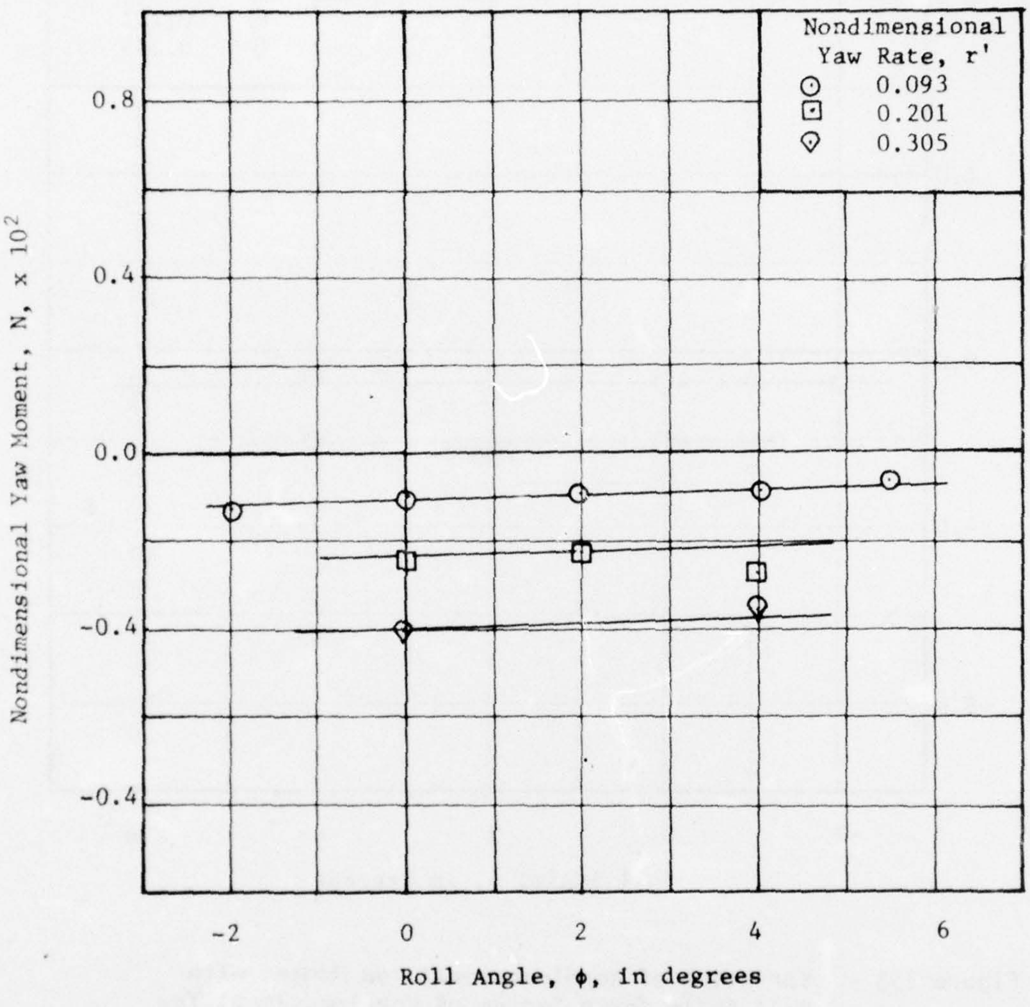

Figure 154 - Variation of Nondimensional Yaw Moment with Roll Angle for a Series of Nondimensional Yaw Rates at a Full Scale Speed of 20 Knots for the Spade Rudder at Design Draft

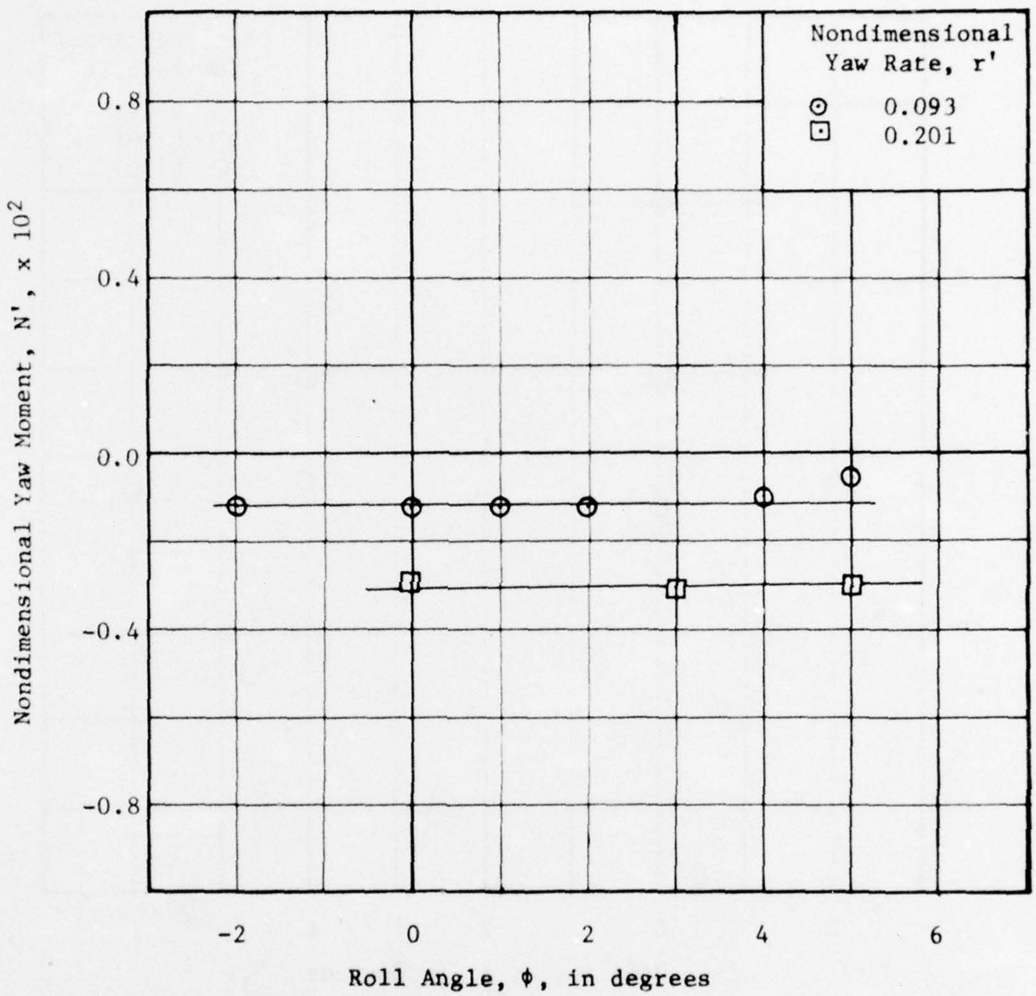

Figure 155 - Variation of Nondimensional Yaw Moment with Roll Angle for Two Nondimensional Yaw Rates at a Full Scale Speed of 25 Knots for the Spade Rudder at Design Draft

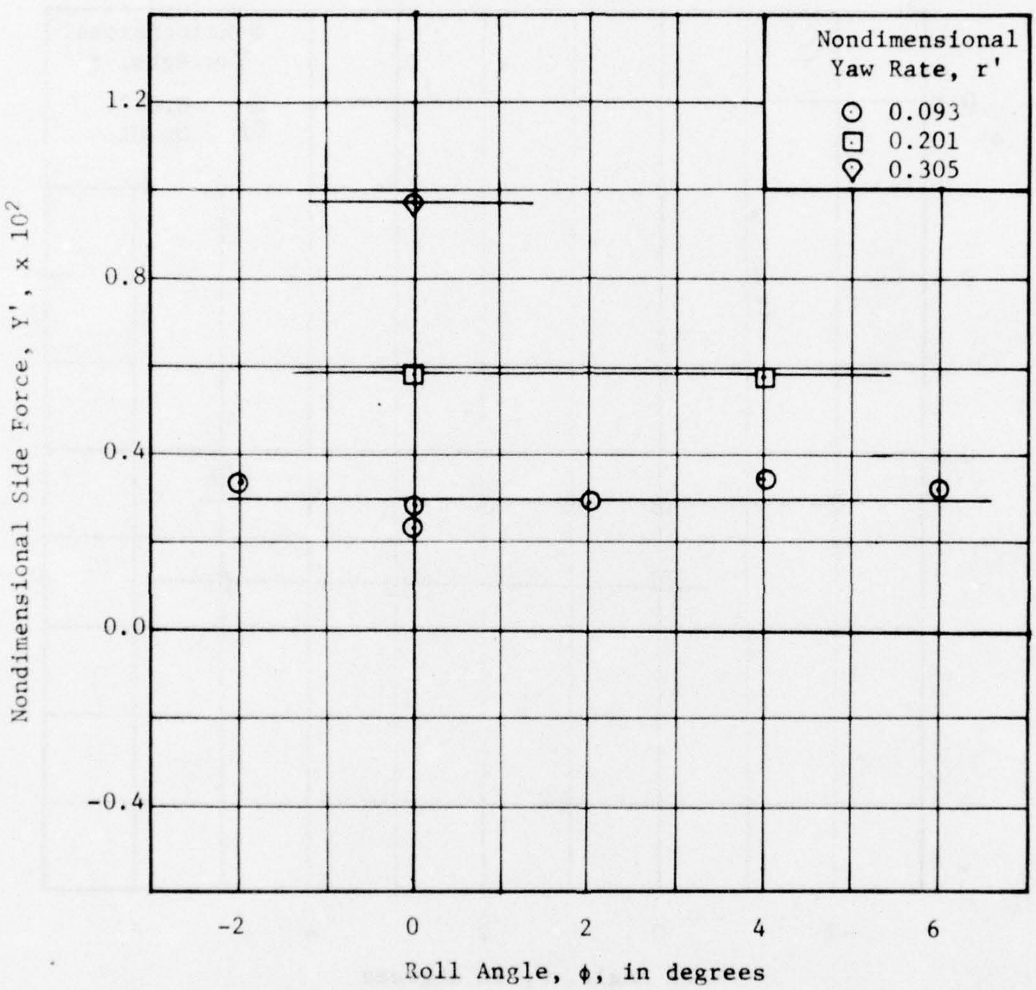

Figure 156 - Variation of Nondimensional Side Force with Roll Angle for a Series of Nondimensional Yaw Rates at a Full Scale Speed of 10 Knots for the Spade Rudder at Design Draft

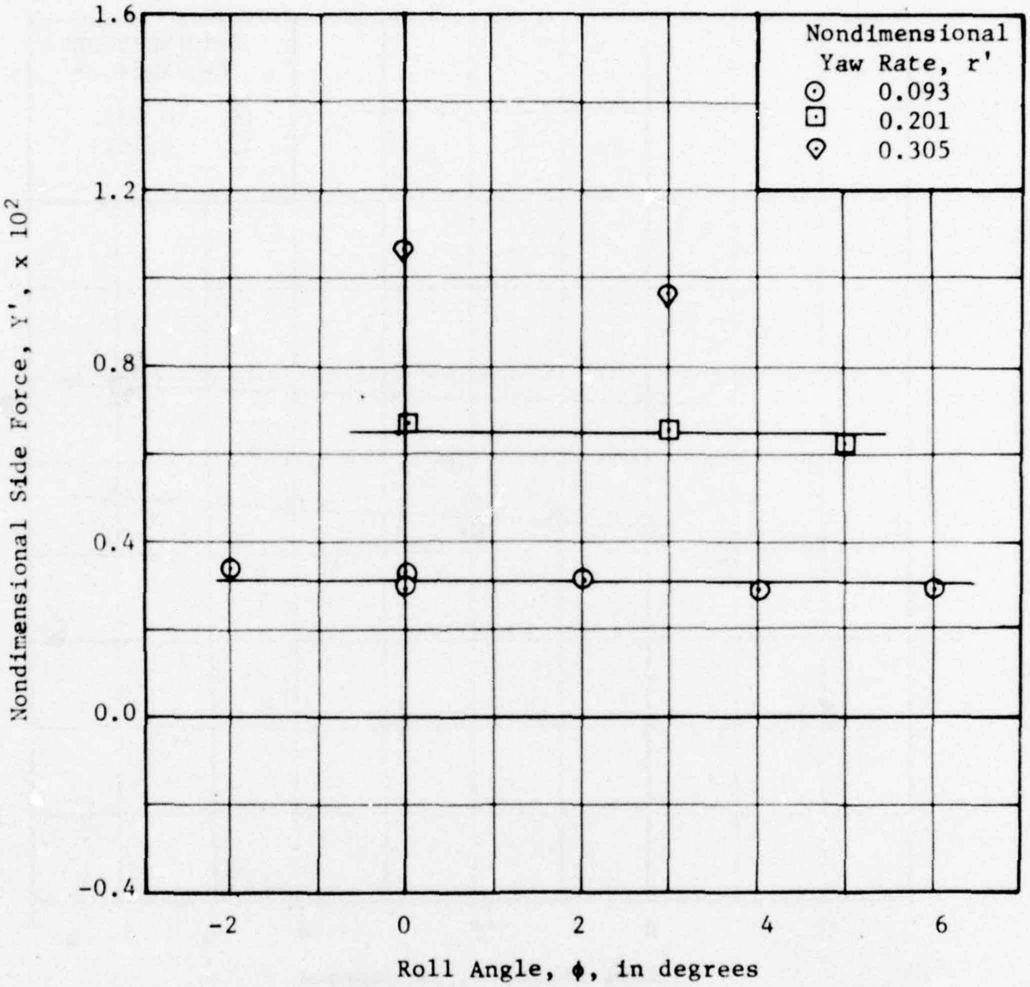

Figure 157 - Variation of Nondimensional Side Force with Roll Angle for a Series of Nondimensional Yaw Rates at a Full Scale Speed of 20 Knots for the Spade Rudder at Design Draft

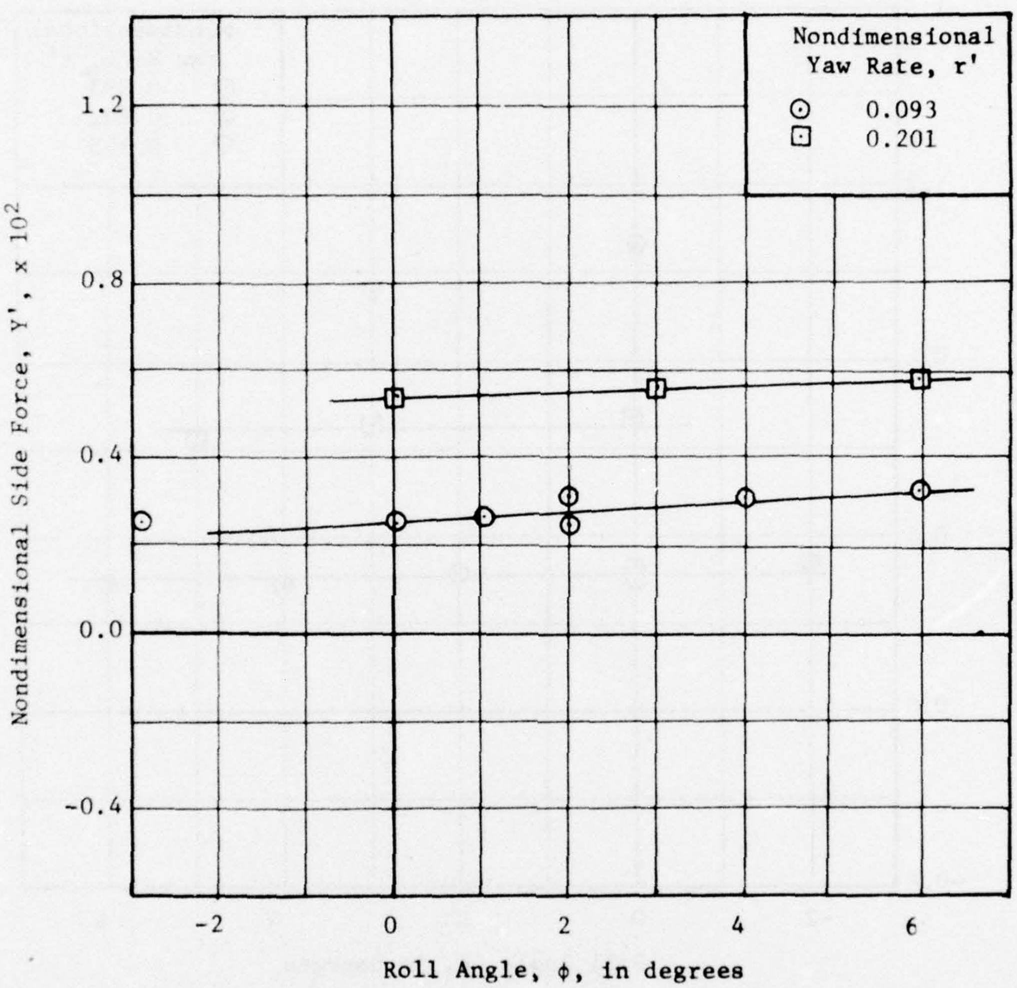

Figure 158 - Variation of Nondimensional Side Force with Roll Angle for Two Nondimensional Yaw Rates at a Full Scale Speed of 25 Knots for the Spade Rudder at Design Draft

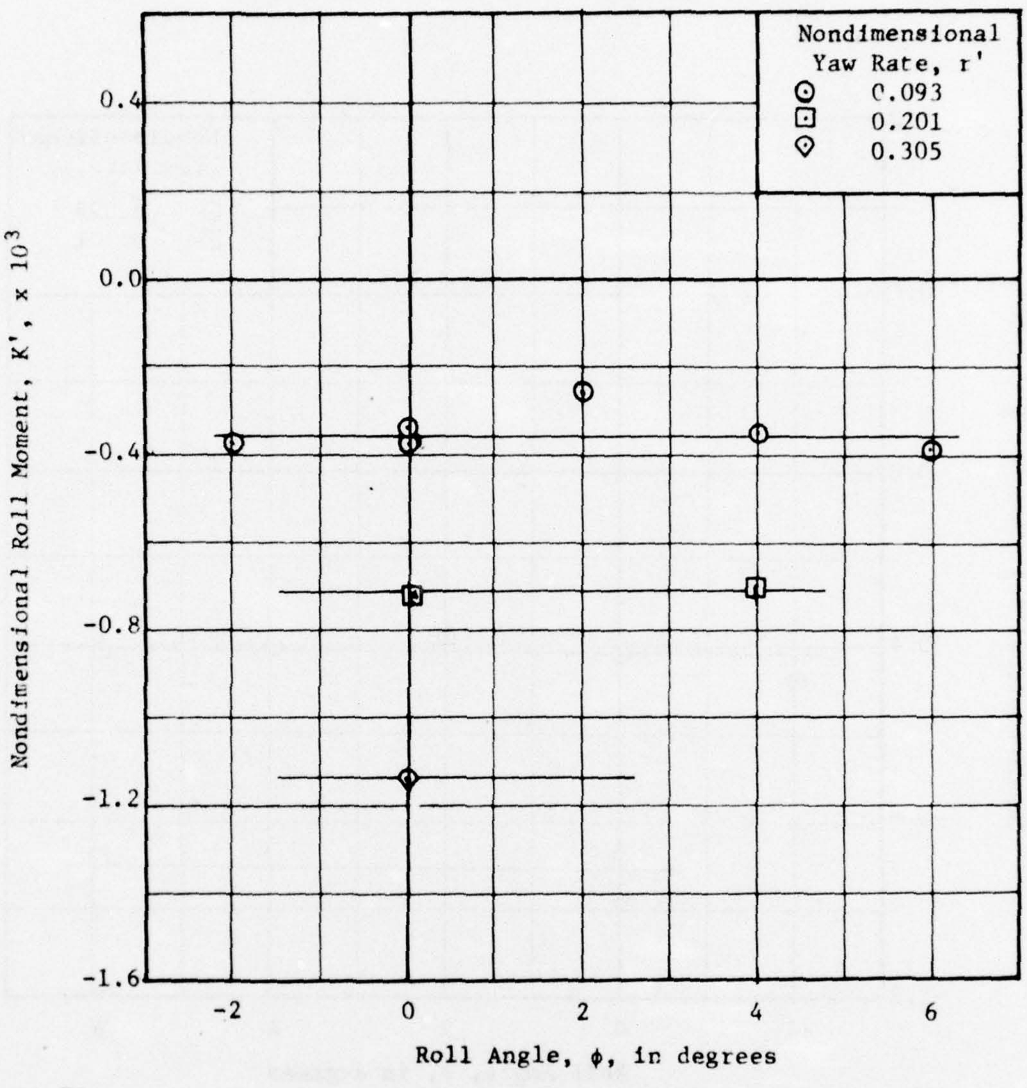

Figure 159 - Variation of Nondimensional Roll Moment with Roll Angle for a Series of Nondimensional Yaw Rates at a Full Scale Speed of 10 Knots for the Spade Rudder at Design Draft

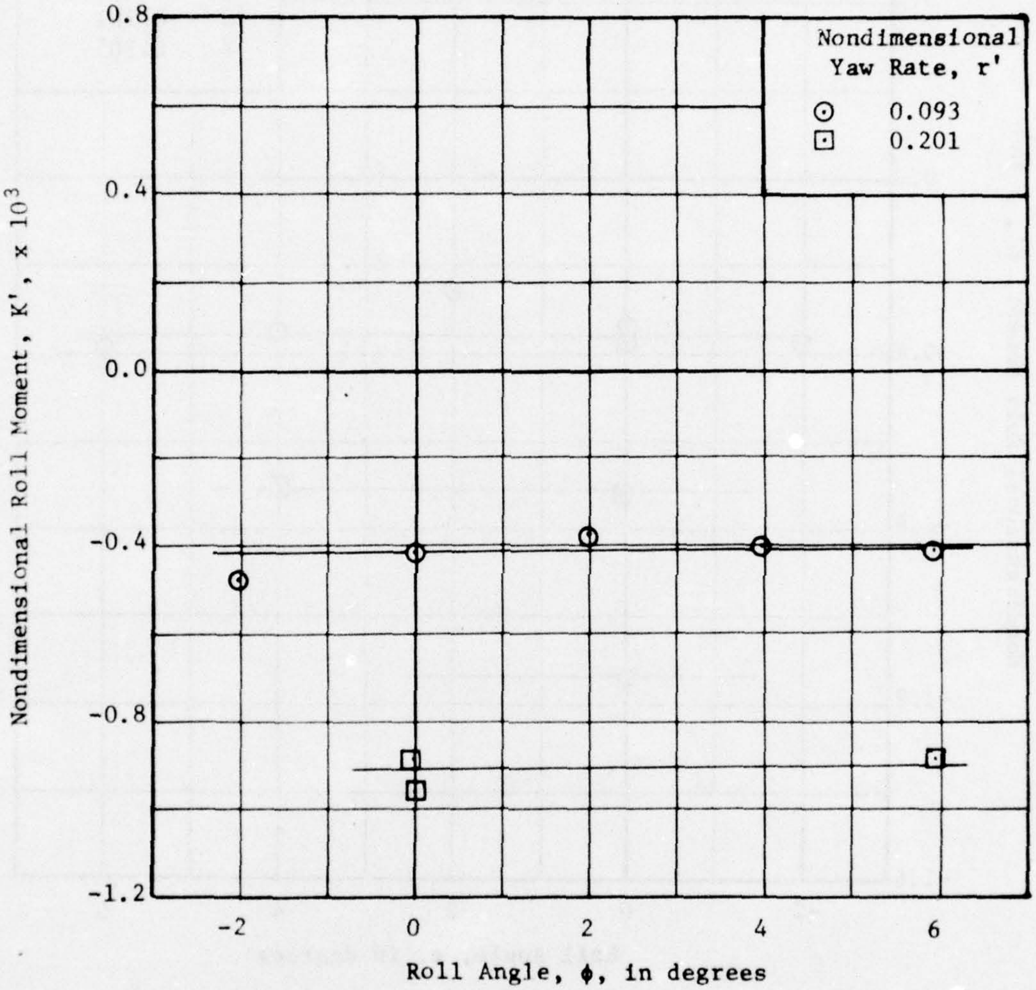

Figure 160 - Variation of Nondimensional Roll Moment with Roll Angle for Two Nondimensional Yaw Rates at a Full Scale Speed of 20 Knots for the Spade Rudder at Design Draft

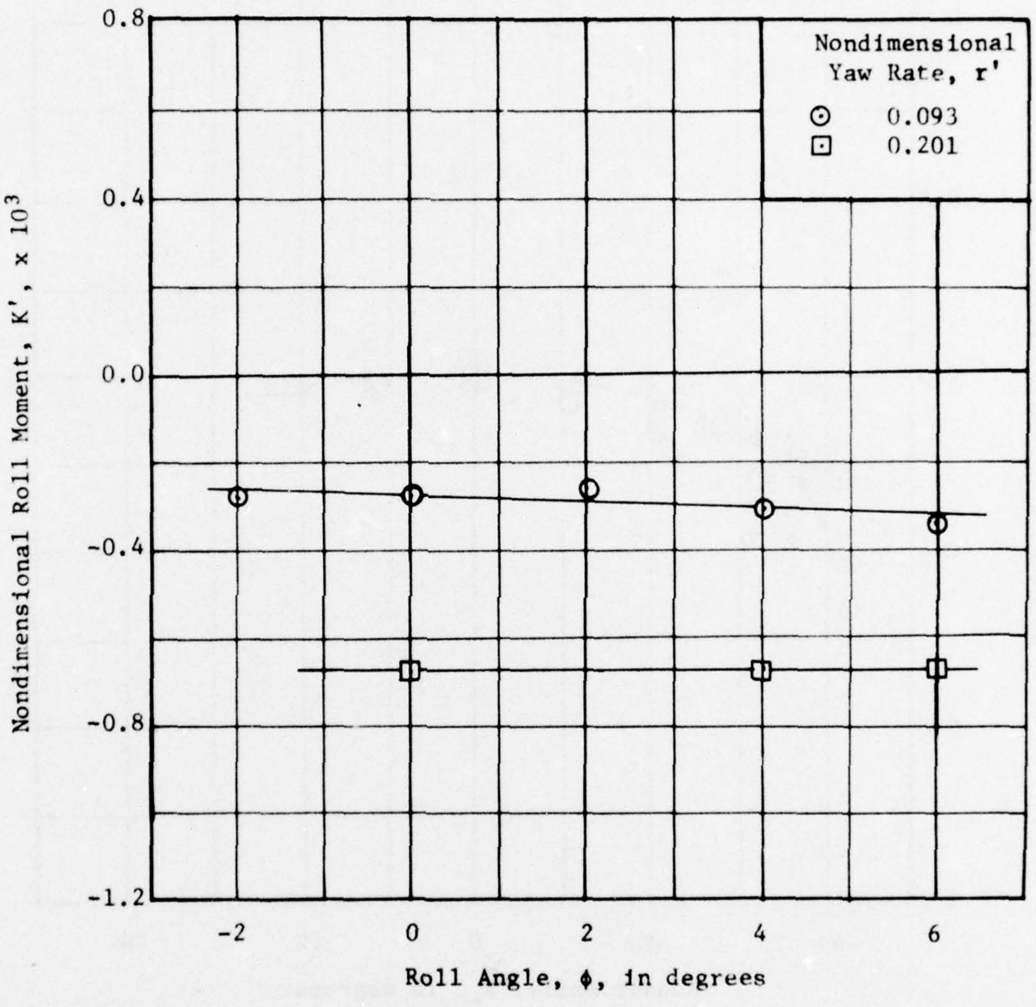

Figure 161 - Variation of Nondimensional Roll Moment with Roll Angle for Two Nondimensional Yaw Rates at a Full Scale Speed of 25 Knots for the Spade Rudder at Design Draft

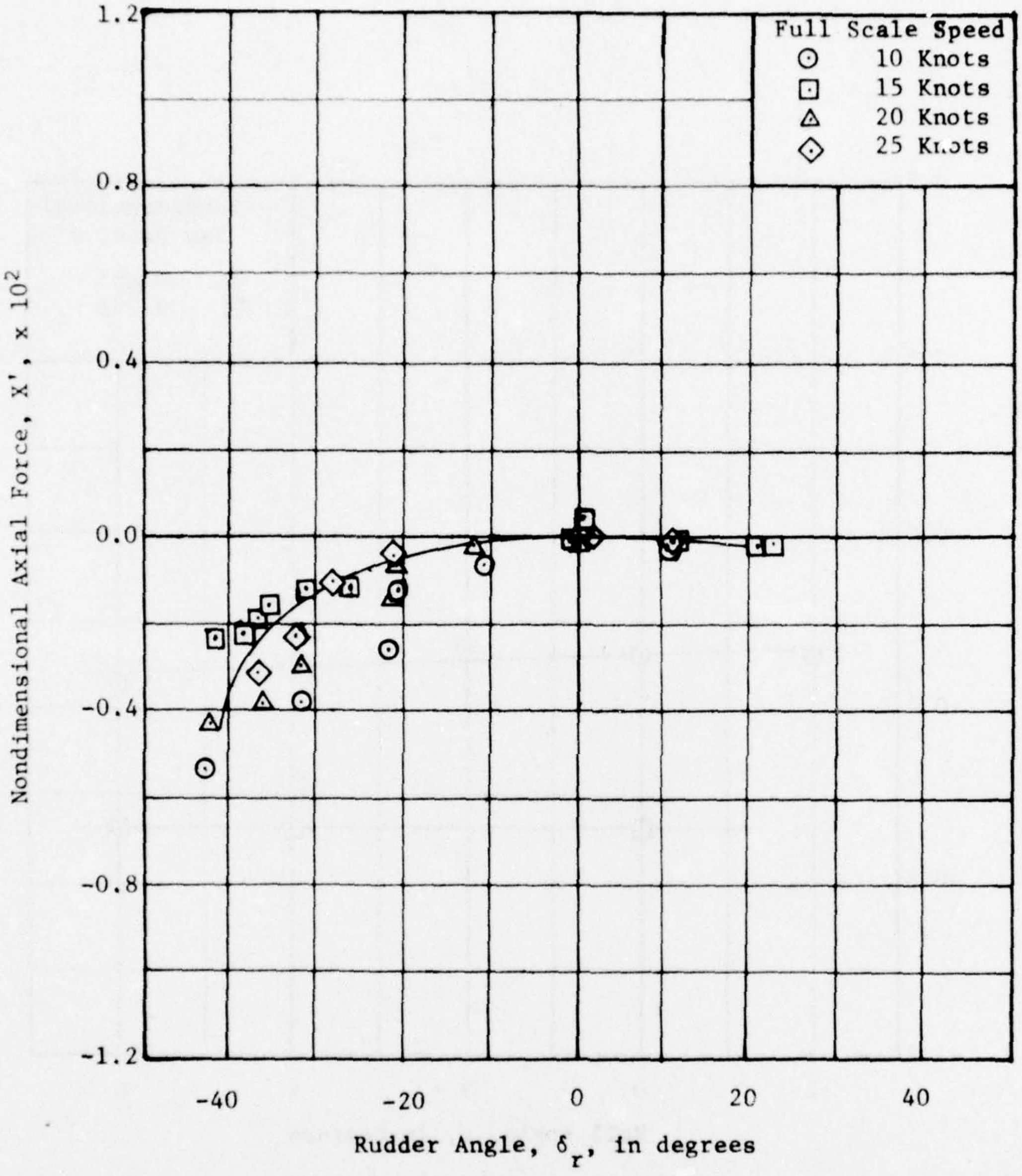

Figure 162 - Variation of Nondimensional Axial Force with Rudder Angle for a Series of Full Scale Speeds at a Nondimensional Yaw Rate of 0.093 for the Spade Rudder at Design Draft

Appendix D

(Figures 163 to 190)
Nondimensional Data Curves for
the Spade Rudder at Deep Draft

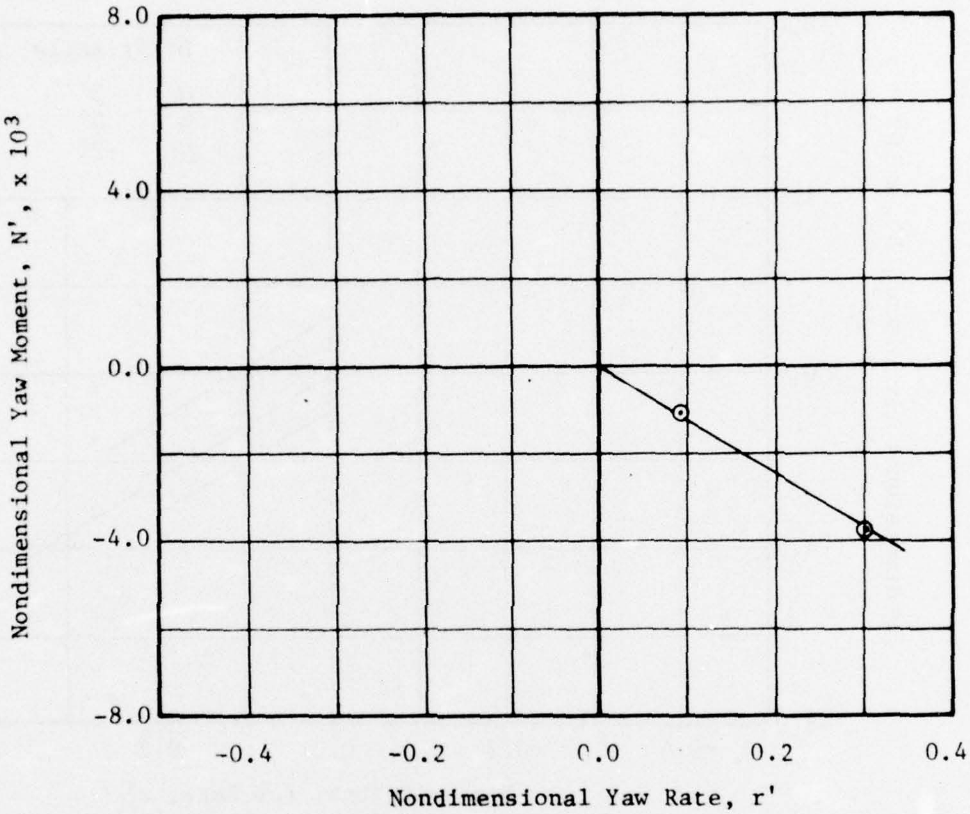

Figure 163 - Variation of Nondimensional Yaw Moment with Nondimensional Yaw Rate for a Drift Angle of 0 Degrees at a Full Scale Speed of 10 Knots for the Spade Rudder at Deep Draft

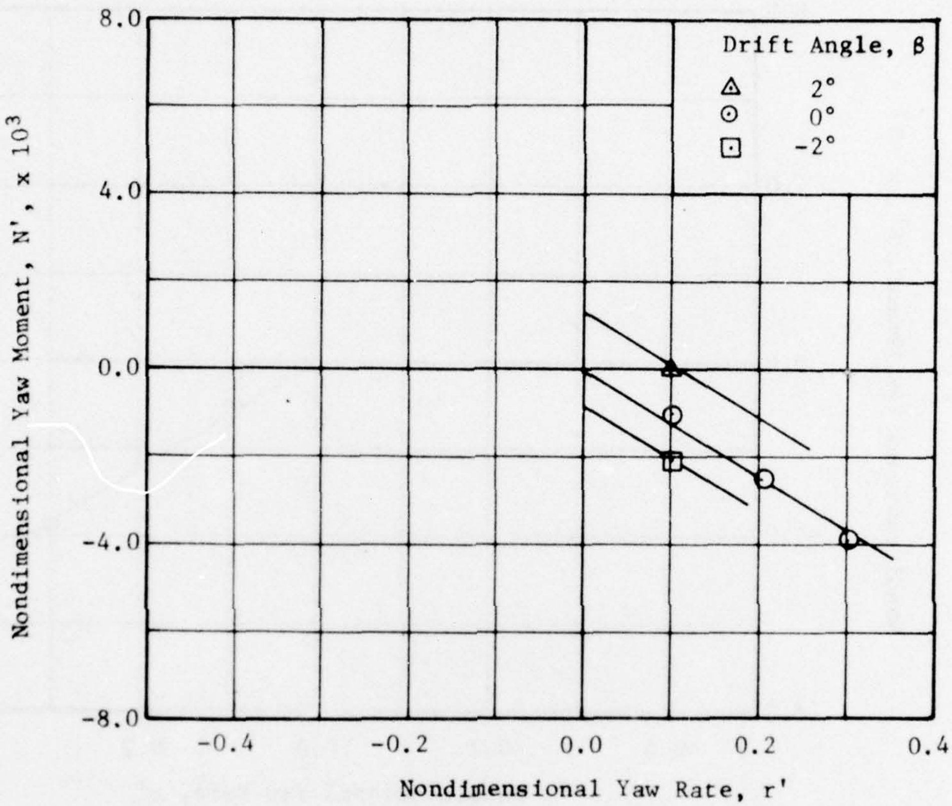

Figure 164 - Variation of Nondimensional Yaw Moment with Nondimensional Yaw Rate for a Series of Drift Angles at a Full Scale Speed of 15 Knots for the Spade Rudder at Deep Draft

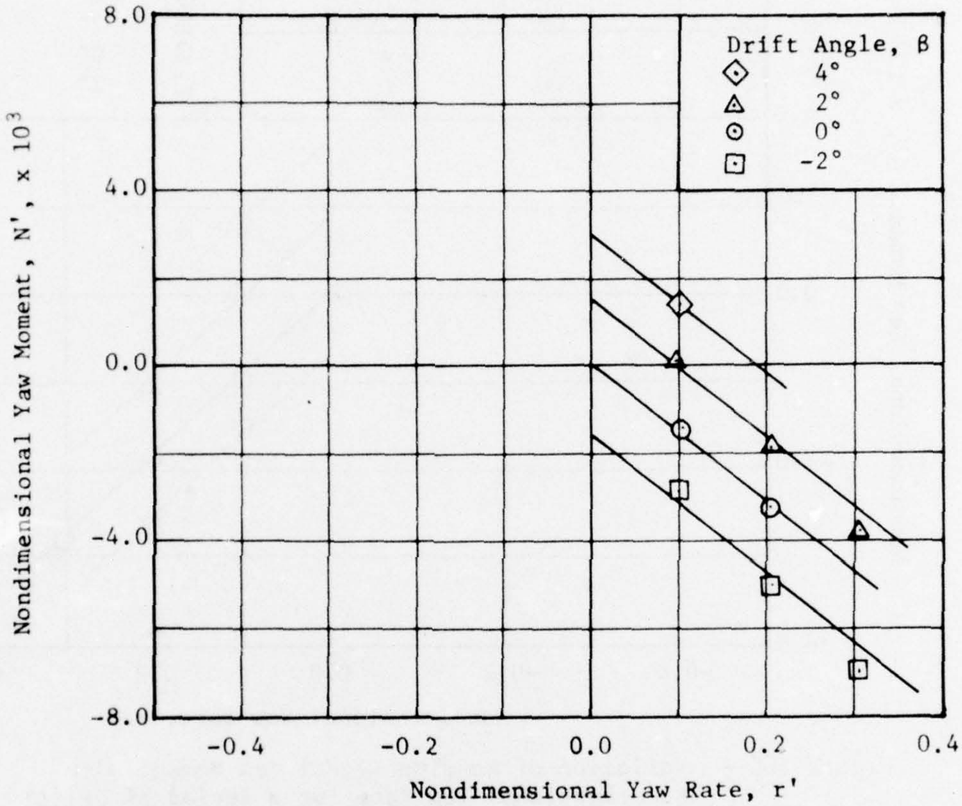

Figure 165 - Variation of Nondimensional Yaw Moment with Nondimensional Yaw Rate for a Series of Drift Angles at a Full Scale Speed of 20 Knots for the Spade Rudder at Design Draft

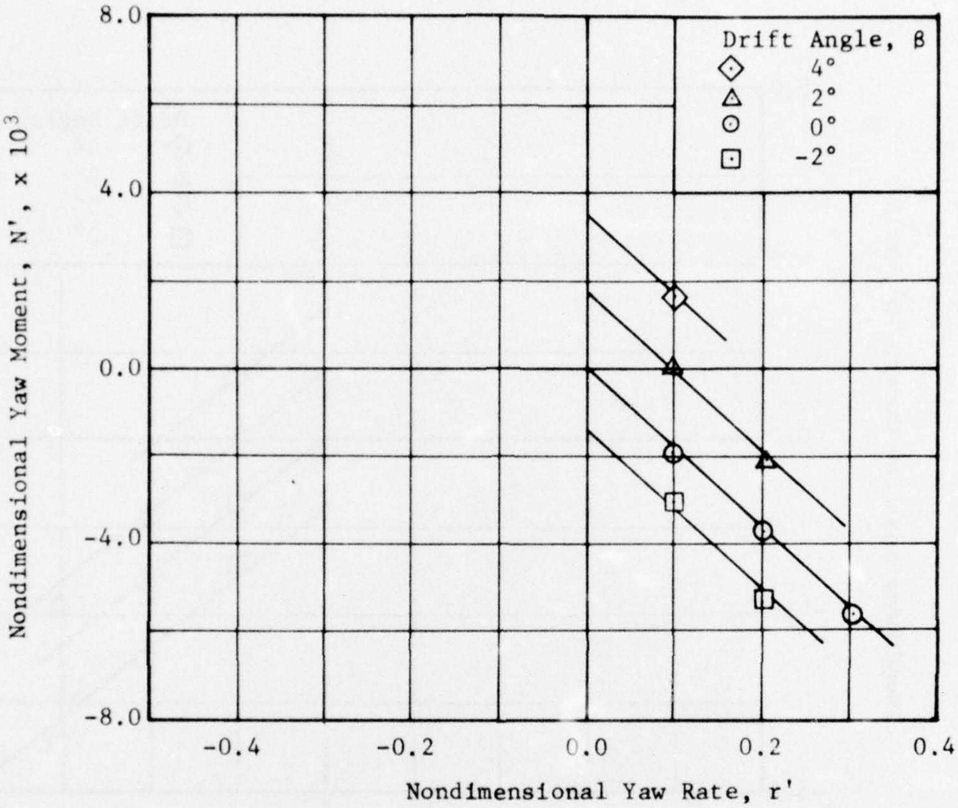

Figure 166 - Variation of Nondimensional Yaw Moment with Nondimensional Yaw Rate for a Series of Drift Angles at a Full Scale Speed of 25 Knots for the Spade Rudder at Deep Draft

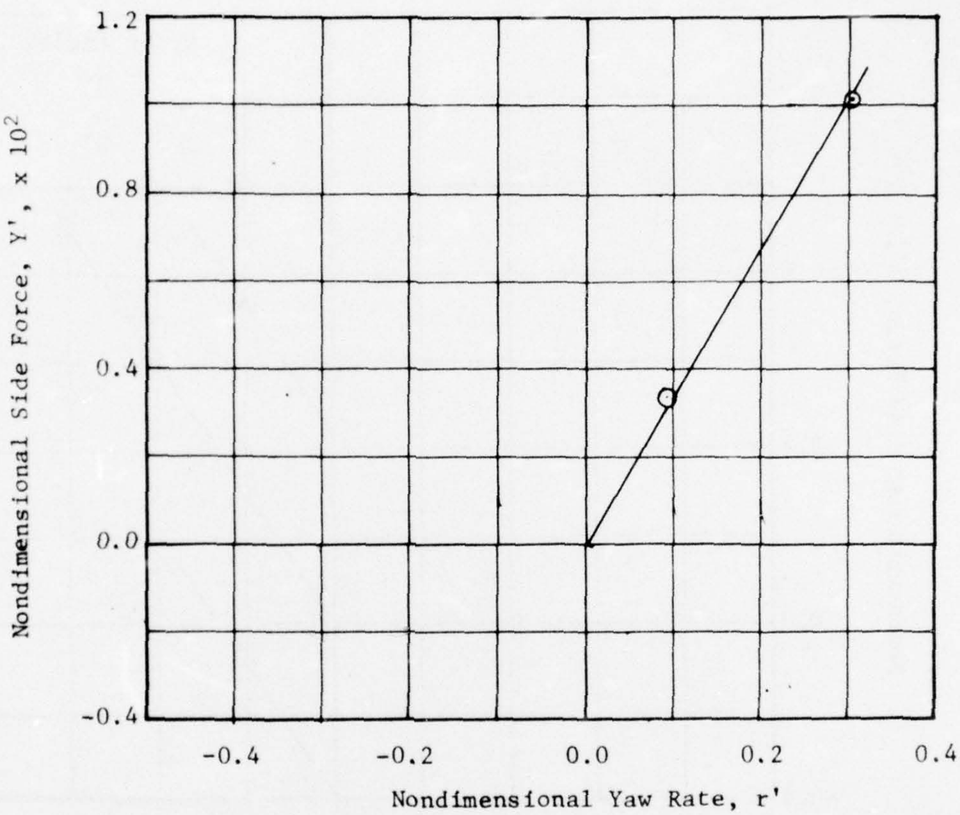

Figure 167 - Variation of Nondimensional Side Force with Nondimensional Yaw Rate for a Drift Angle of 0 Degrees at a Full Scale Speed of 10 Knots for the Spade Rudder at Deep Draft

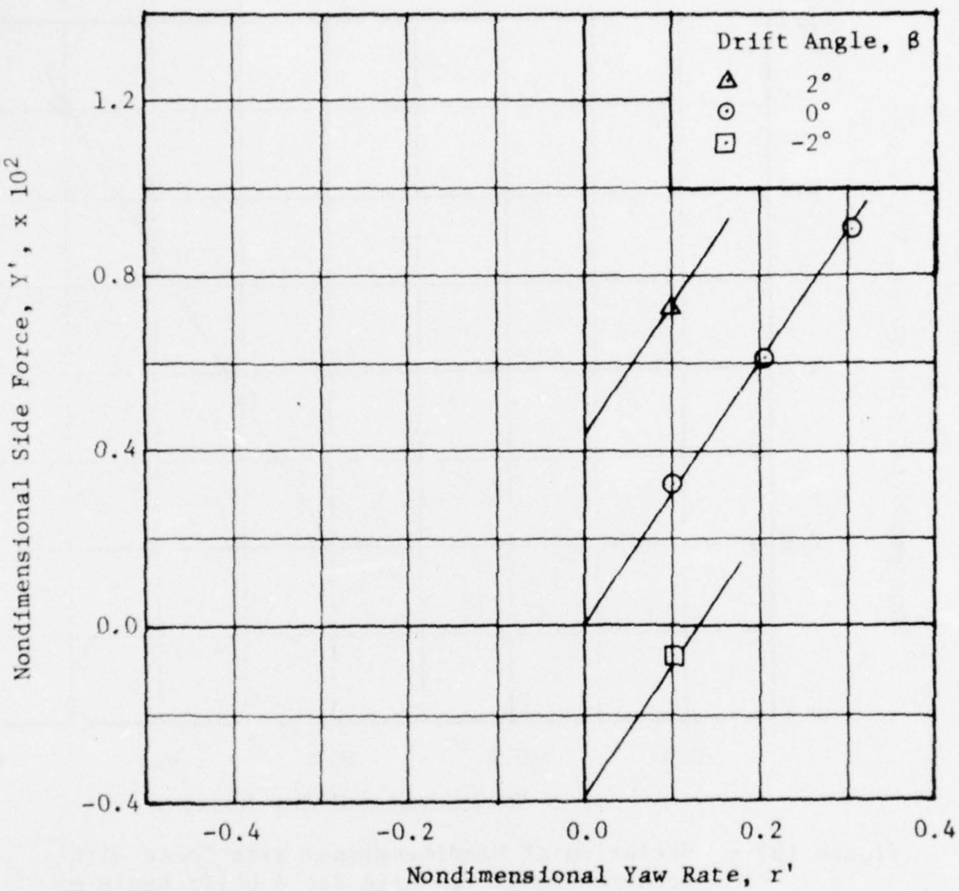

Figure 168 - Variation of Nondimensional Side Force with Nondimensional Yaw Rate for a Series of Drift Angles at a Full Scale Speed of 15 Knots for the Spade Rudder at Deep Draft

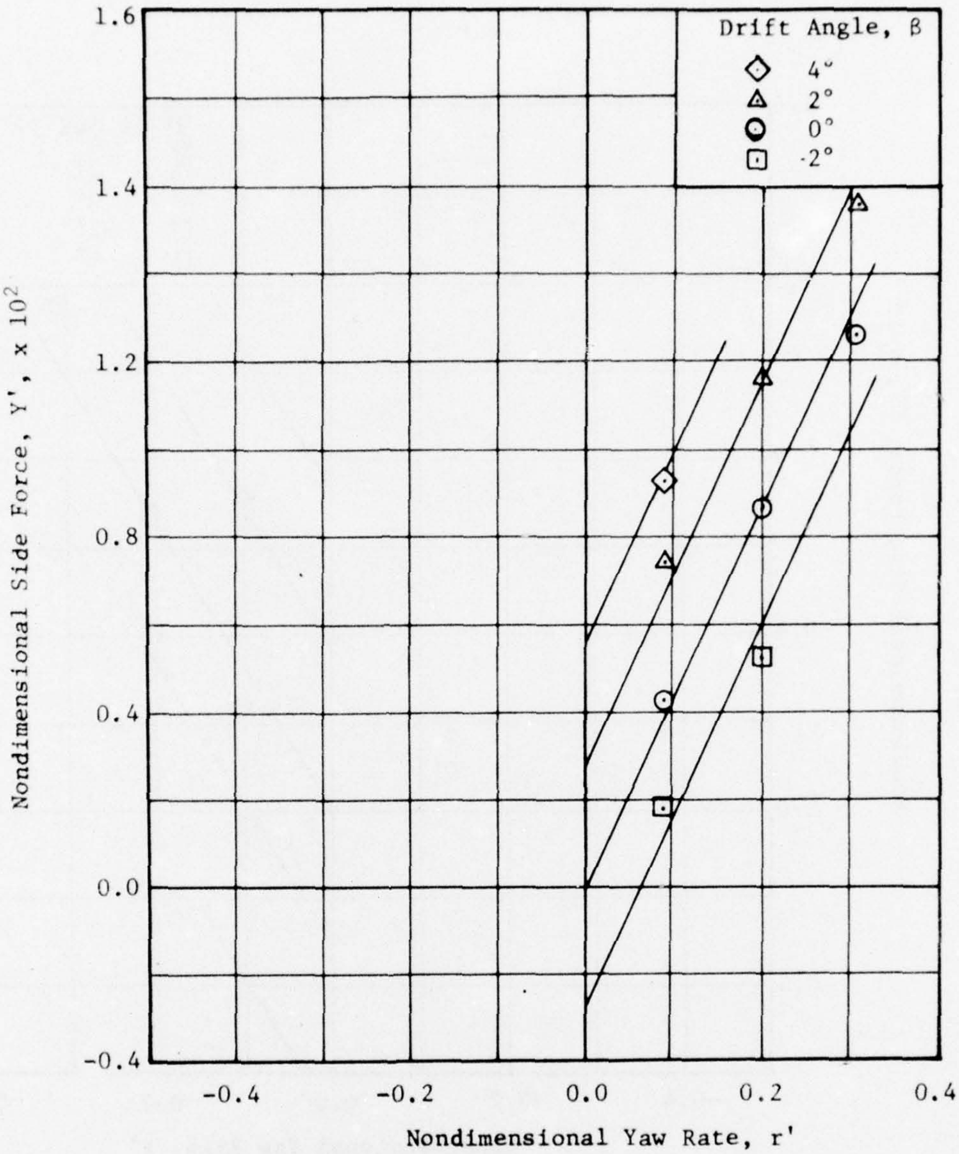

Figure 169 - Variation of Nondimensional Side Force with Nondimensional Yaw Rate for a Series of Drift Angles at a Full Scale Speed of 20 Knots for the Spade Rudder at Deep Draft

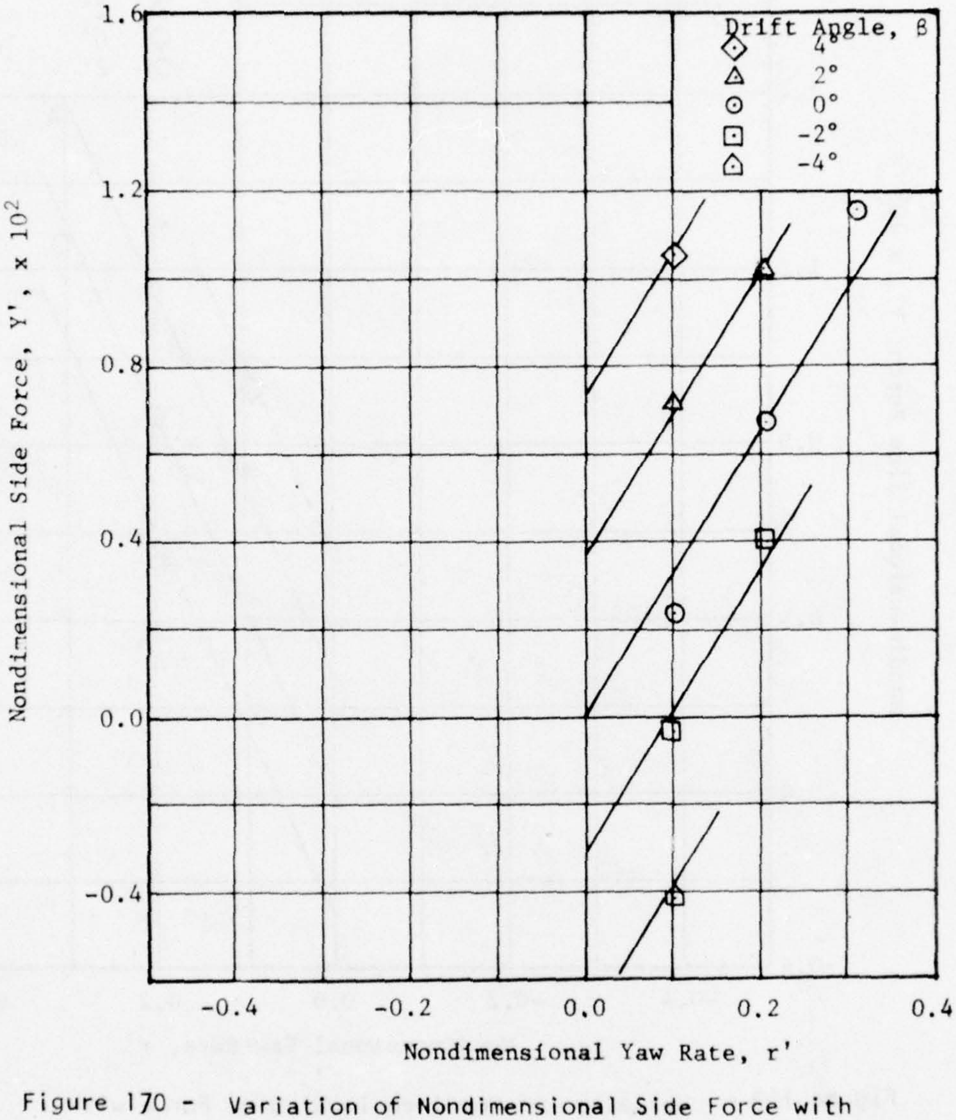

Figure 170 - Variation of Nondimensional Side Force with Nondimensional Yaw Rate for a Series of Drift Angles at a Full Scale Speed of 25 Knots for the Spade Rudder at Design Draft

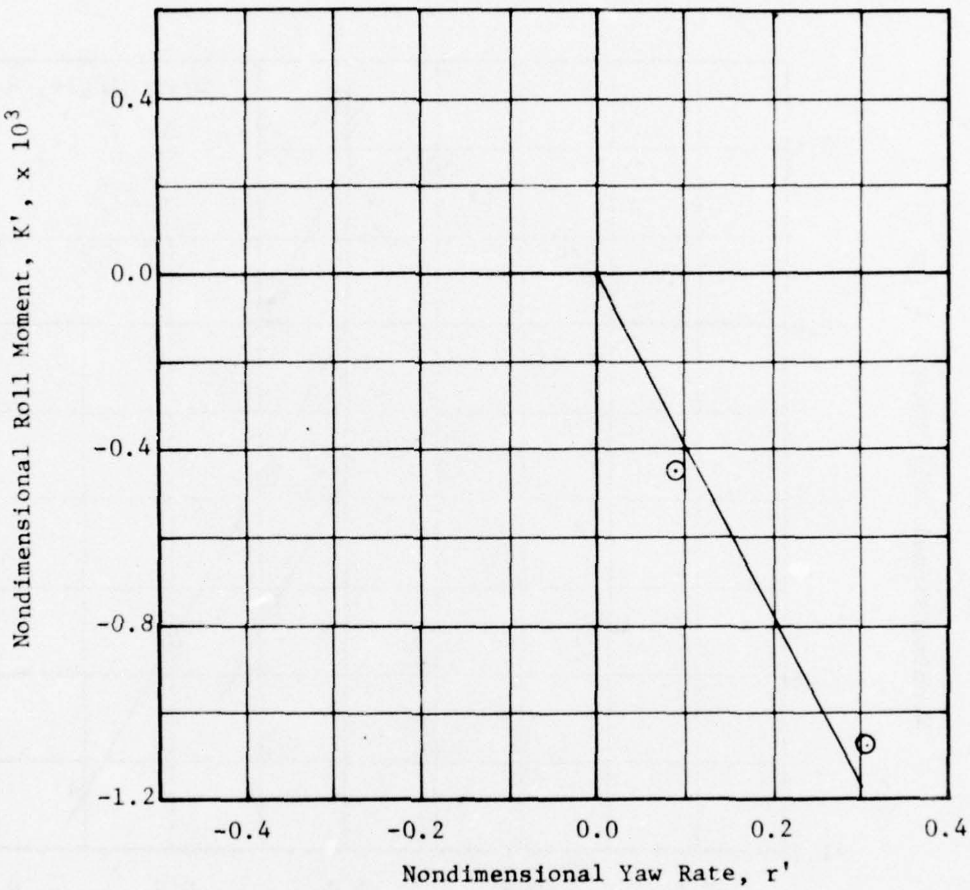

Figure 171 - Variation of Nondimensional Roll Moment with Nondimensional Yaw Rate for a Drift Angle of 0 Degrees at a Full Scale Speed of 10 Knots for the Spade Rudder at Deep Draft

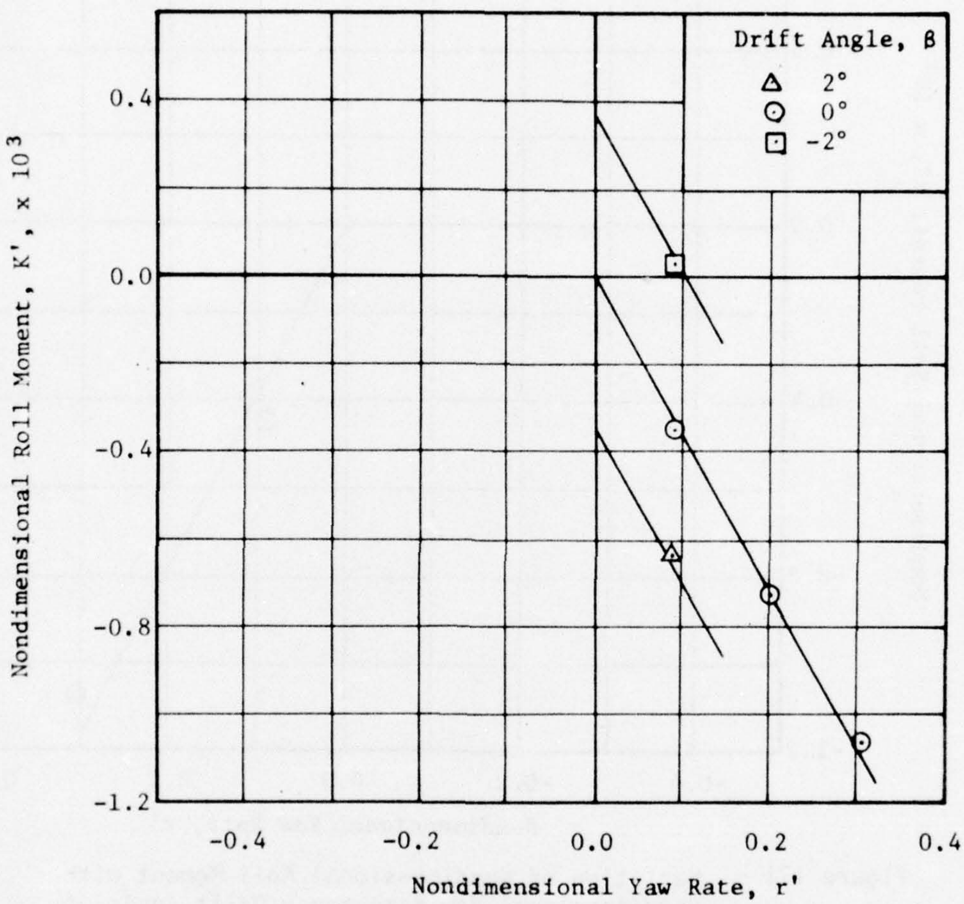

Figure 172 - Variation of Nondimensional Roll Moment with Nondimensional Yaw Rate for a Series of Drift Angles at a Full Scale Speed of 15 Knots for the Spade Rudder at Deep Draft

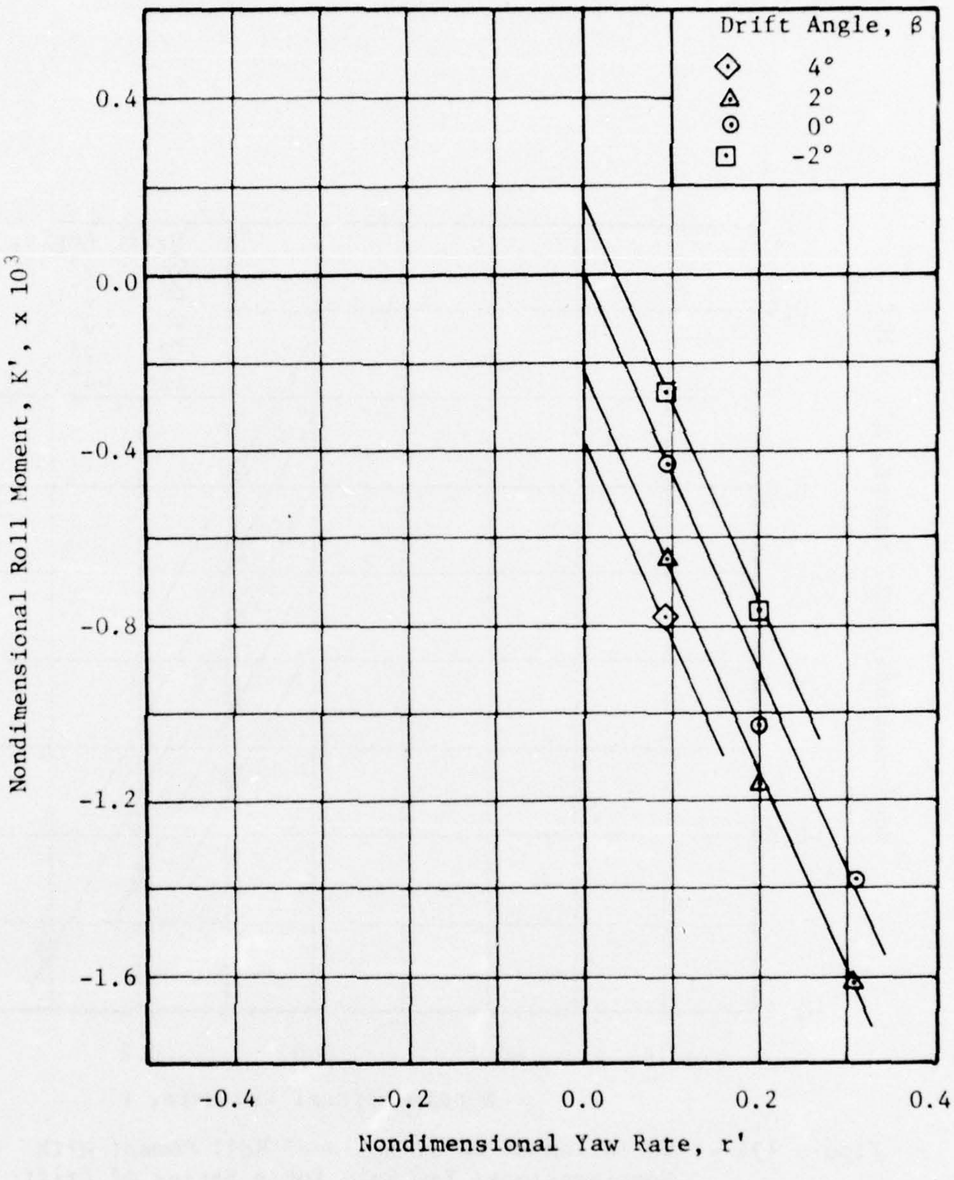

Figure 173 - Variation of Nondimensional Roll Moment with Nondimensional Yaw Rate for a Series of Drift Angles at a Full Scale Speed of 20 Knots for the Spade Rudder at Deep Draft

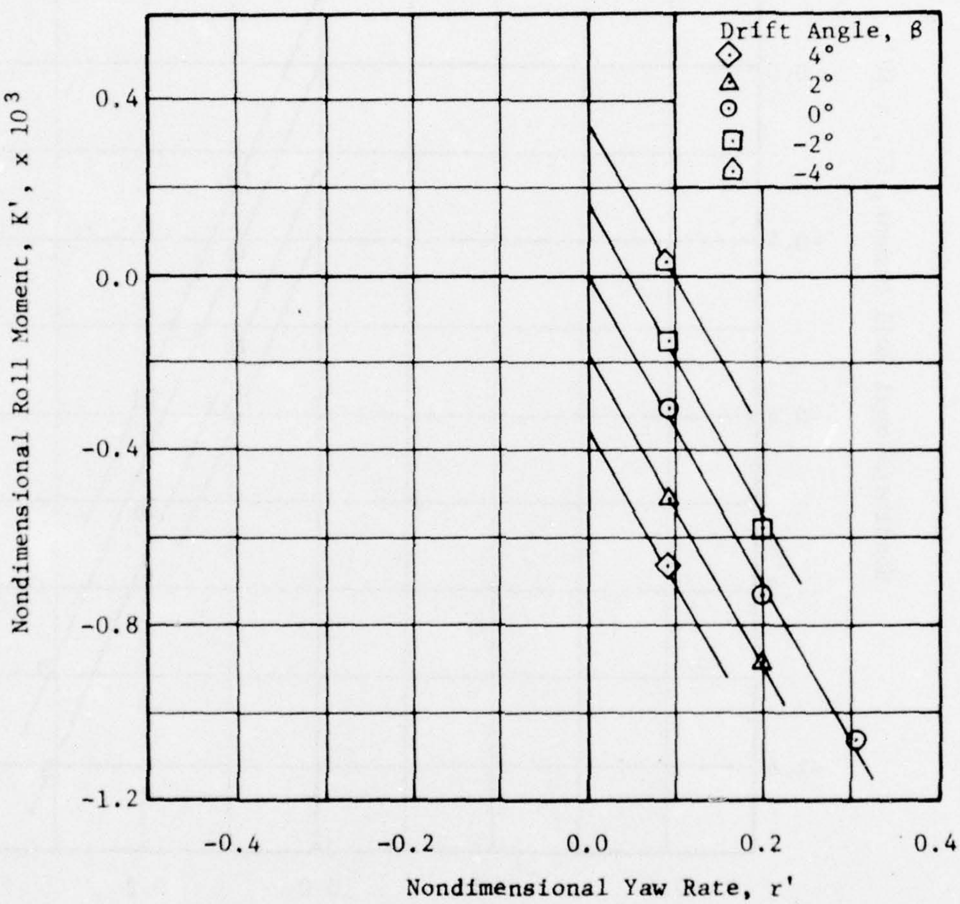

Figure 174 - Variation of Nondimensional Roll Moment with Nondimensional Yaw Rate for a Series of Drift Angles at a Full Scale Speed of 25 Knots for the Spade Rudder at Deep Draft

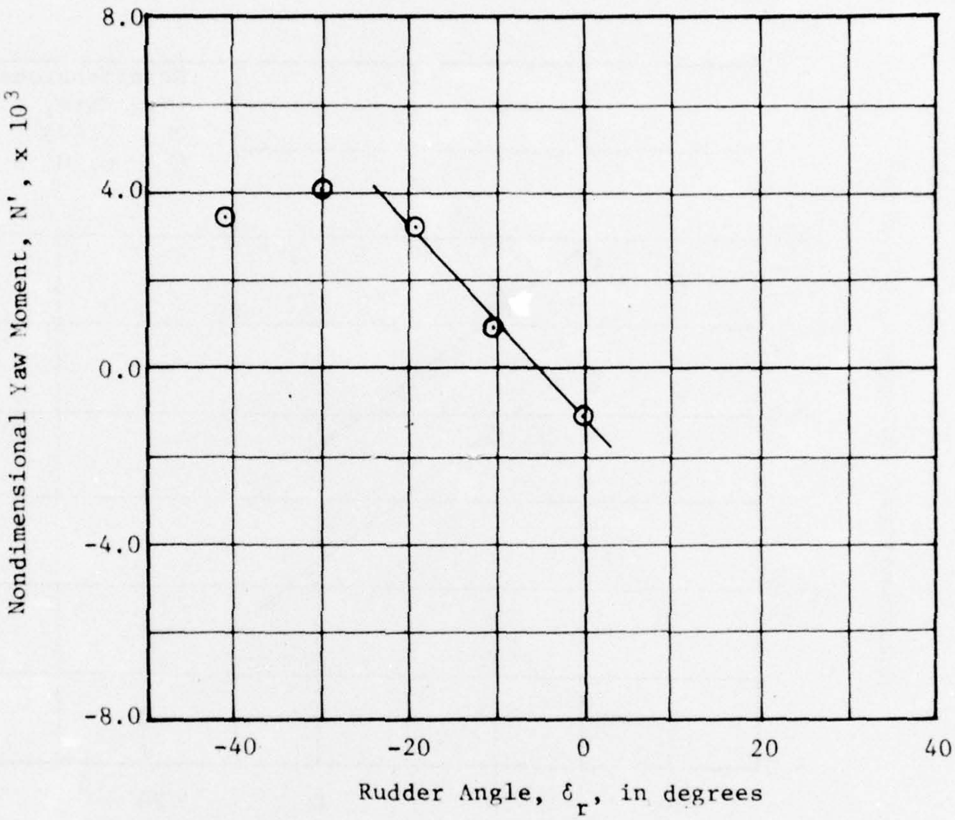

Figure 175 - Variation of Nondimensional Yaw Moment with Rudder Angle for a Nondimensional Yaw Rate of 0.093 at a Full Scale Speed of 10 Knots for the Spade Rudder at Deep Draft

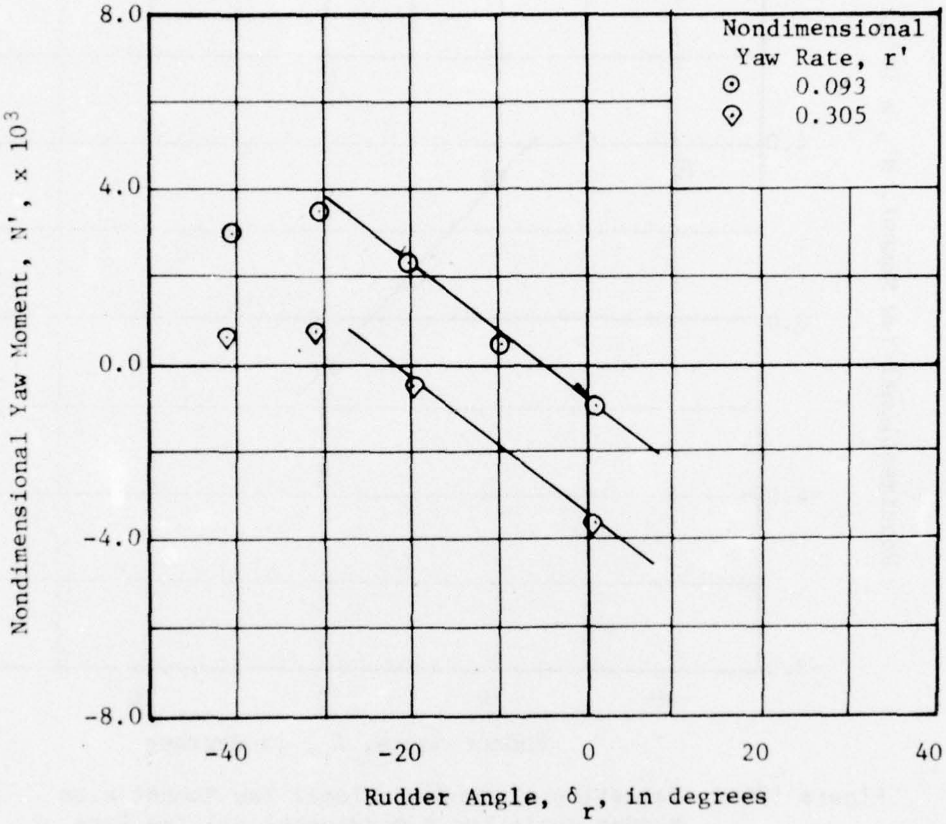

Figure 176 - Variation of Nondimensional Yaw Moment with Rudder Angle for Two Nondimensional Yaw Rates at a Full Scale Speed of 15 Knots for the Spade Rudder at Deep Draft

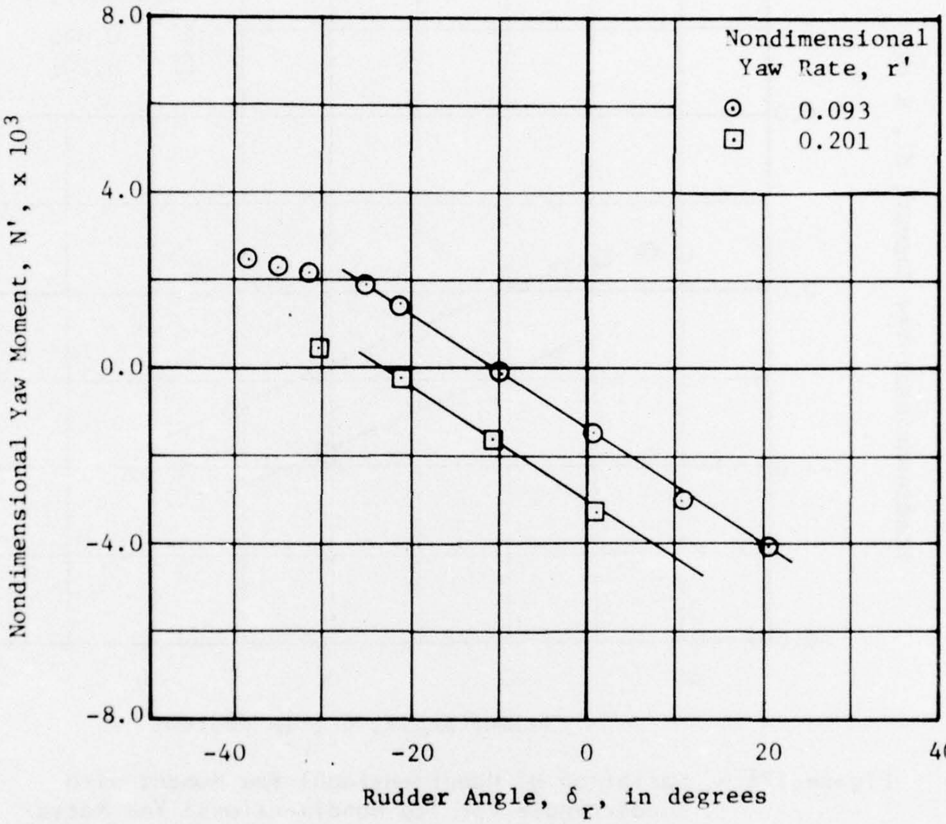

Figure 177 - Variation of Nondimensional Yaw Moment with Rudder Angle for Two Nondimensional Yaw Rates at a Full Scale Speed of 20 Knots for the Spade Rudder at Deep Draft

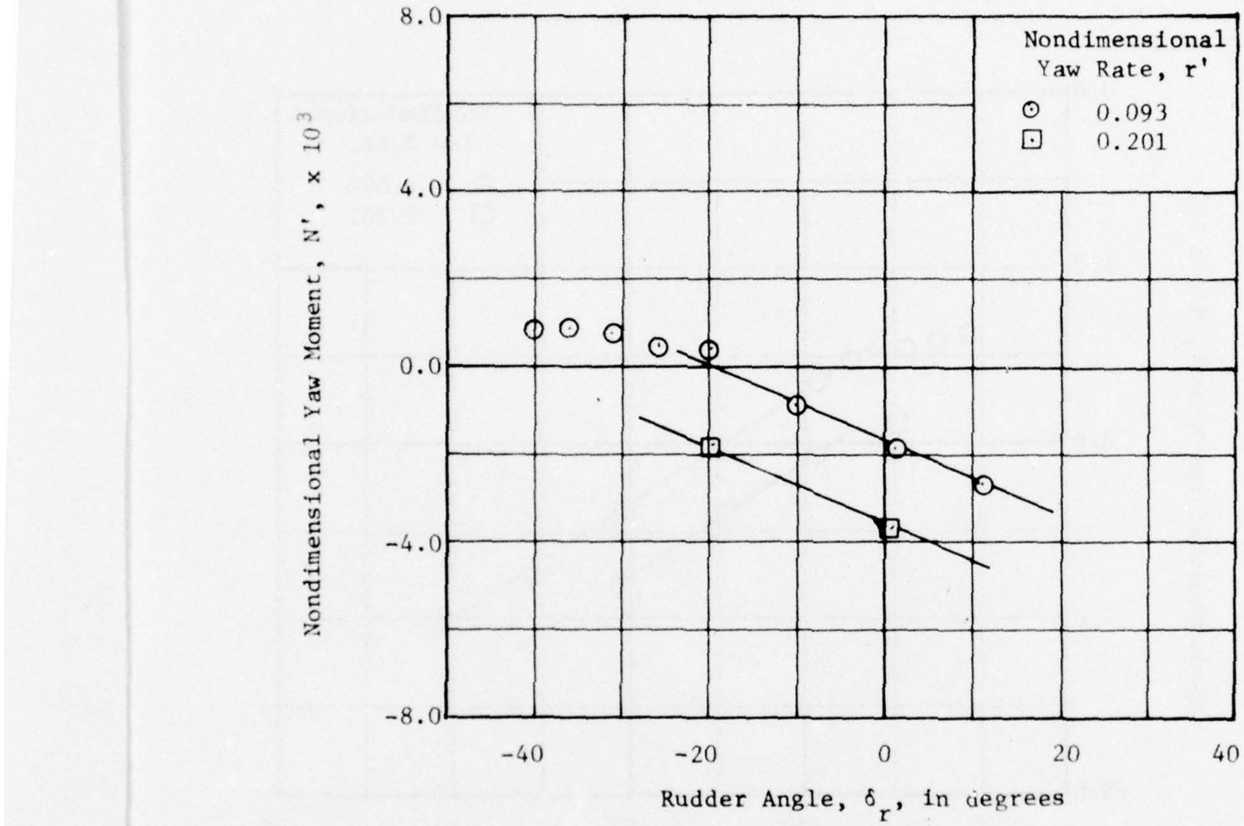

Figure 178 - Variation of Nondimensional Yaw Moment with Rudder Angle for Two Nondimensional Yaw Rates at a Full Scale Speed of 25 Knots for the Spade Rudder at Deep Draft

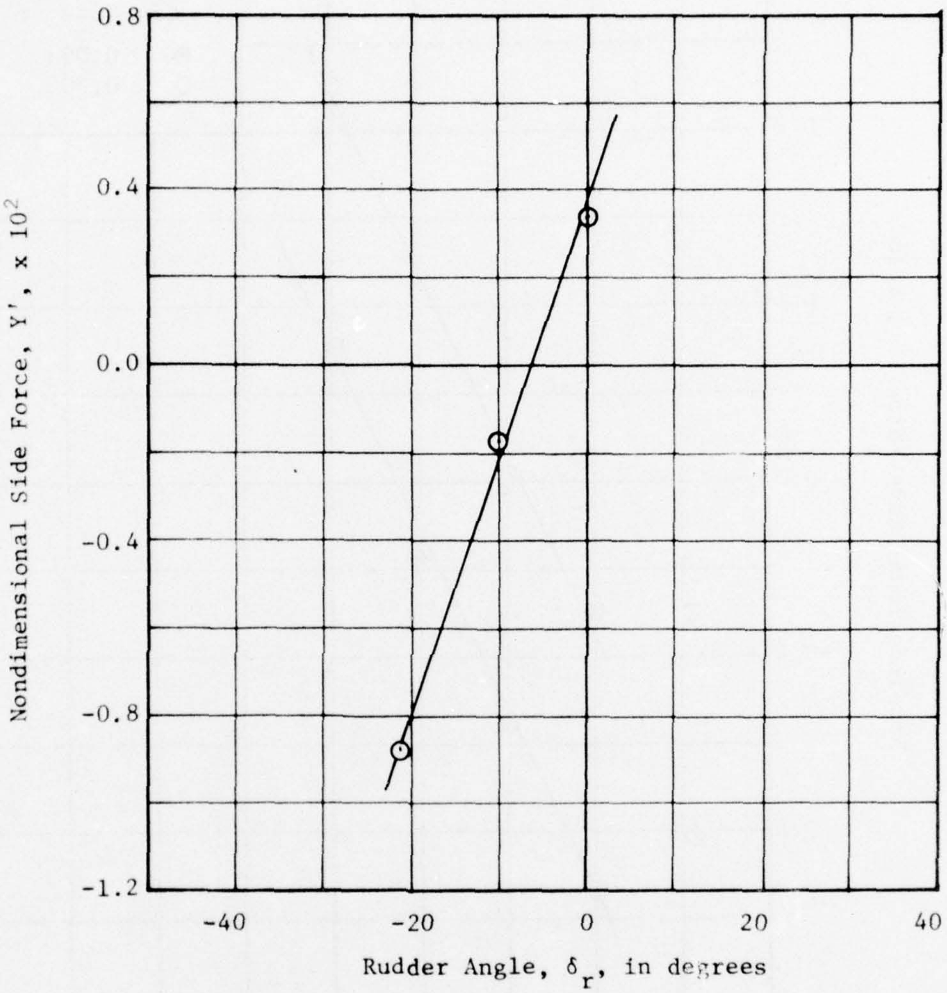

Figure 179 - Variation of Nondimensional Side Force with Rudder Angle for a Nondimensional Yaw Rate of 0.093 at a Full Scale Speed of 10 Knots for the Spade Rudder at Deep Draft

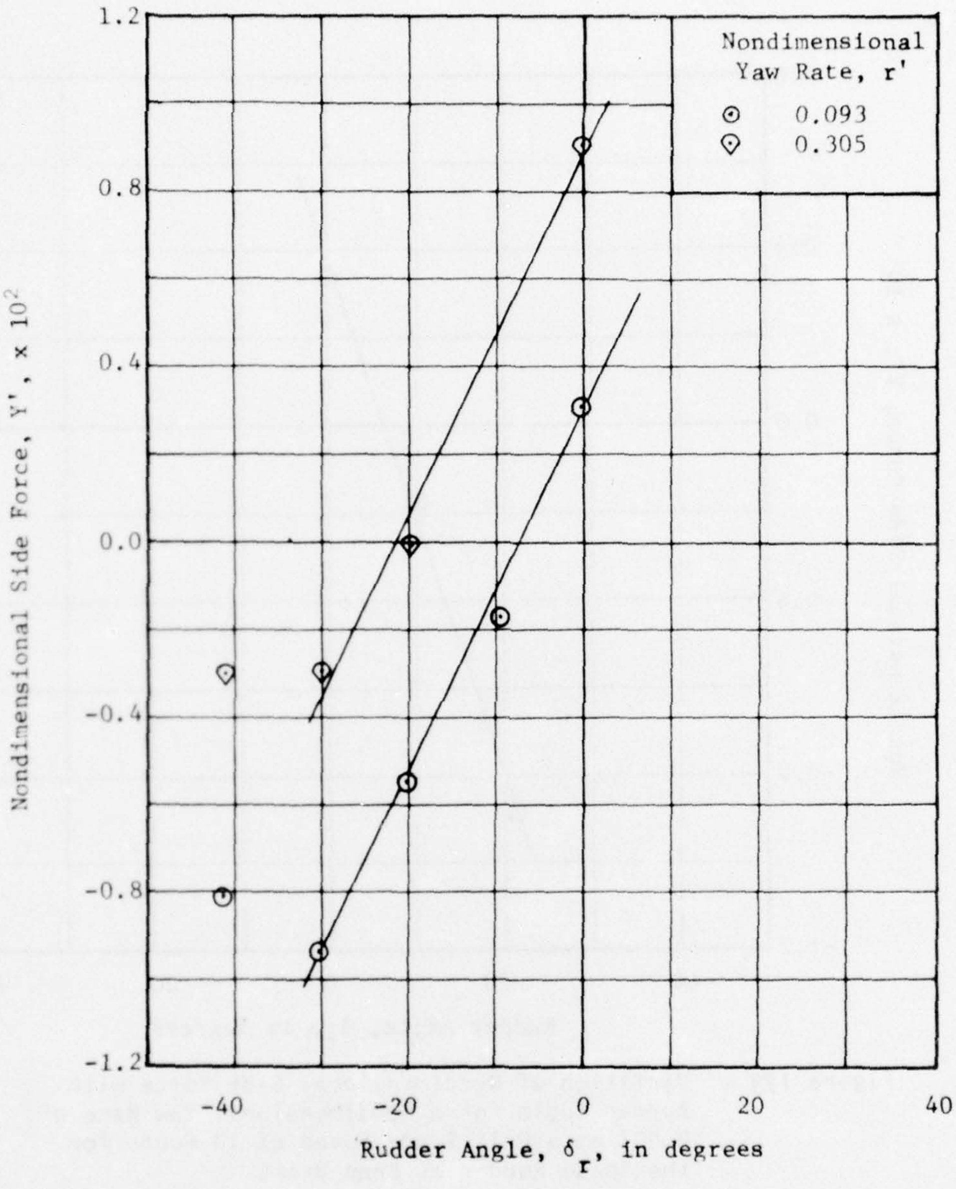

Figure 180 - Variation of Nondimensional Side Force with Rudder Angle for Two Nondimensional Yaw Rates at a Full Scale Speed of 15 Knots for the Spade Rudder at Deep Draft

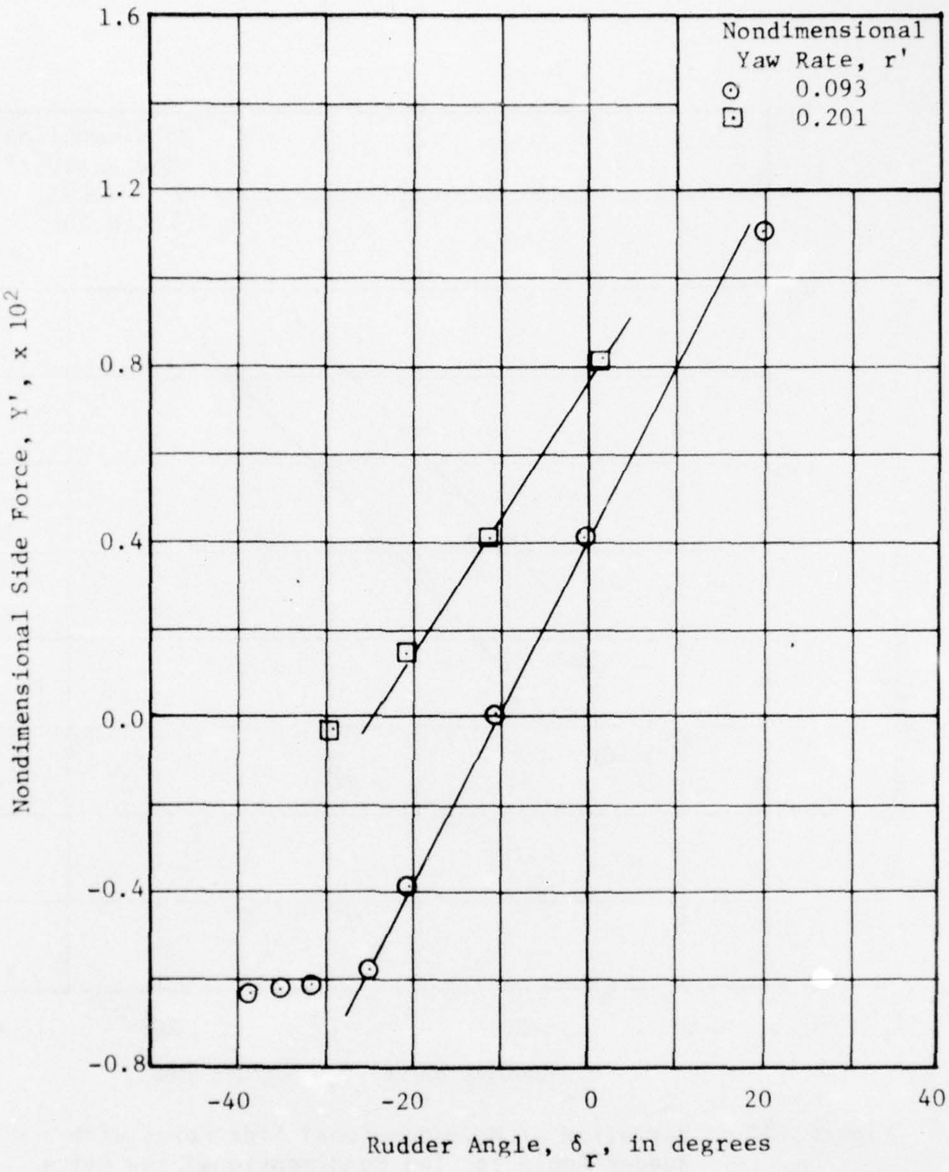

Figure 181 - Variation of Nondimensional Side Force with Rudder Angle for Two Nondimensional Yaw Rates at a Full Scale Speed of 20 Knots for the Spade Rudder at Deep Draft

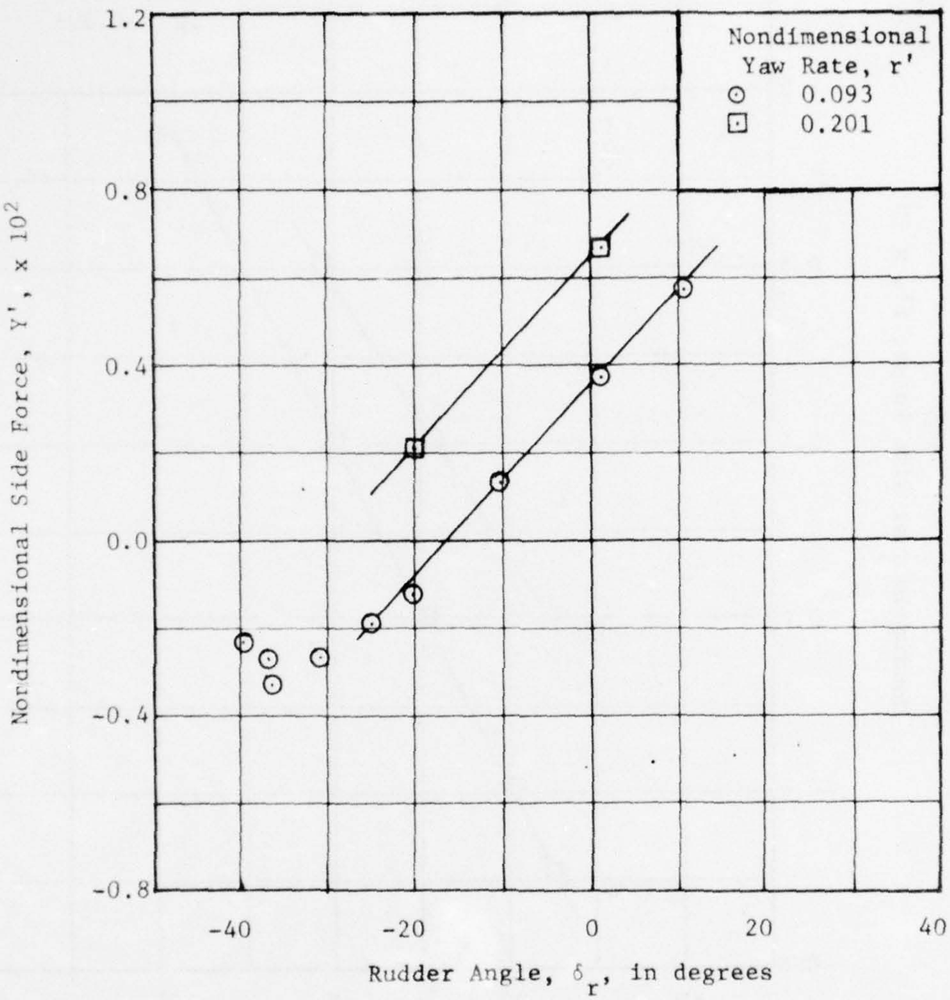

Figure 182 - Variation of Nondimensional Side Force with Rudder Angle for Two Nondimensional Yaw Rates at a Full Scale Speed of 25 Knots for the Spade Rudder at Deep Draft

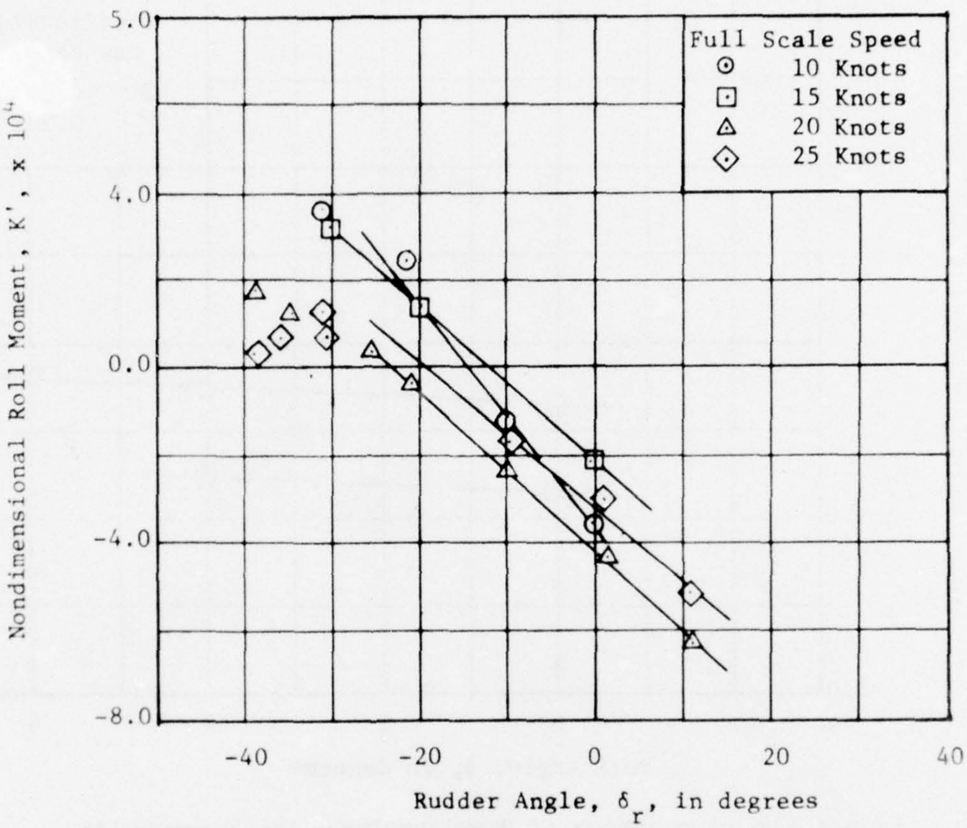

Figure 183 - Variation of Nondimensional Roll Moment with Rudder Angle for a Series of Full Scale Speeds at a Nondimensional Yaw Rate of 0.093 for the Spade Rudder at Deep Draft

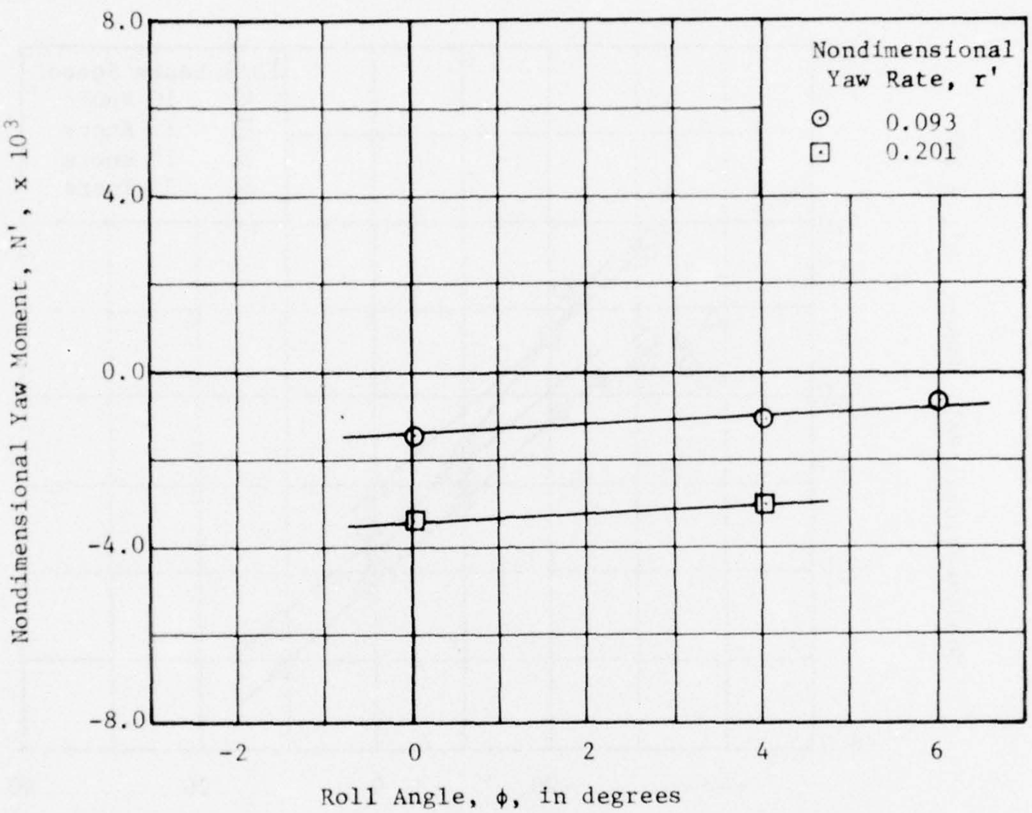

Figure 184 - Variation of Nondimensional Yaw Moment with Roll Moment for Two Nondimensional Yaw Rates at a Full Scale Speed of 20 Knots for the Spade Rudder at Deep Draft

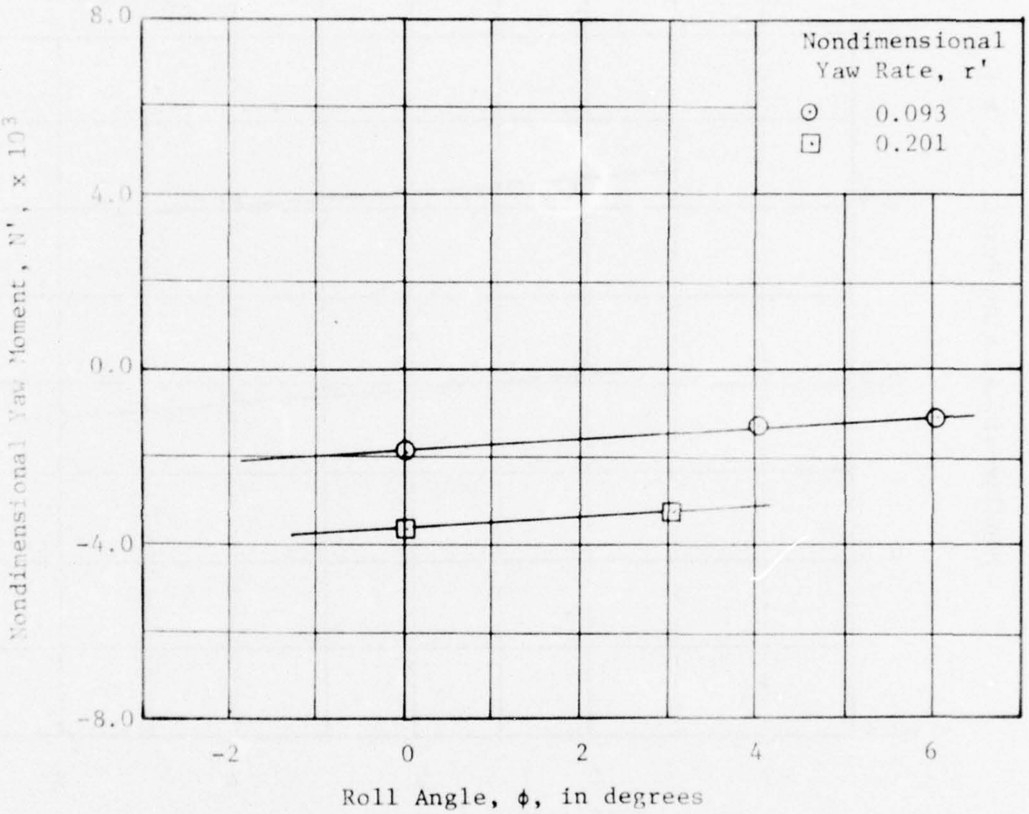

Figure 185 - Variation of Nondimensional Yaw Moment with Roll Angle for Two Nondimensional Yaw Rates at a Full Scale Speed of 25 Knots for the Spade Rudder at Deep Draft

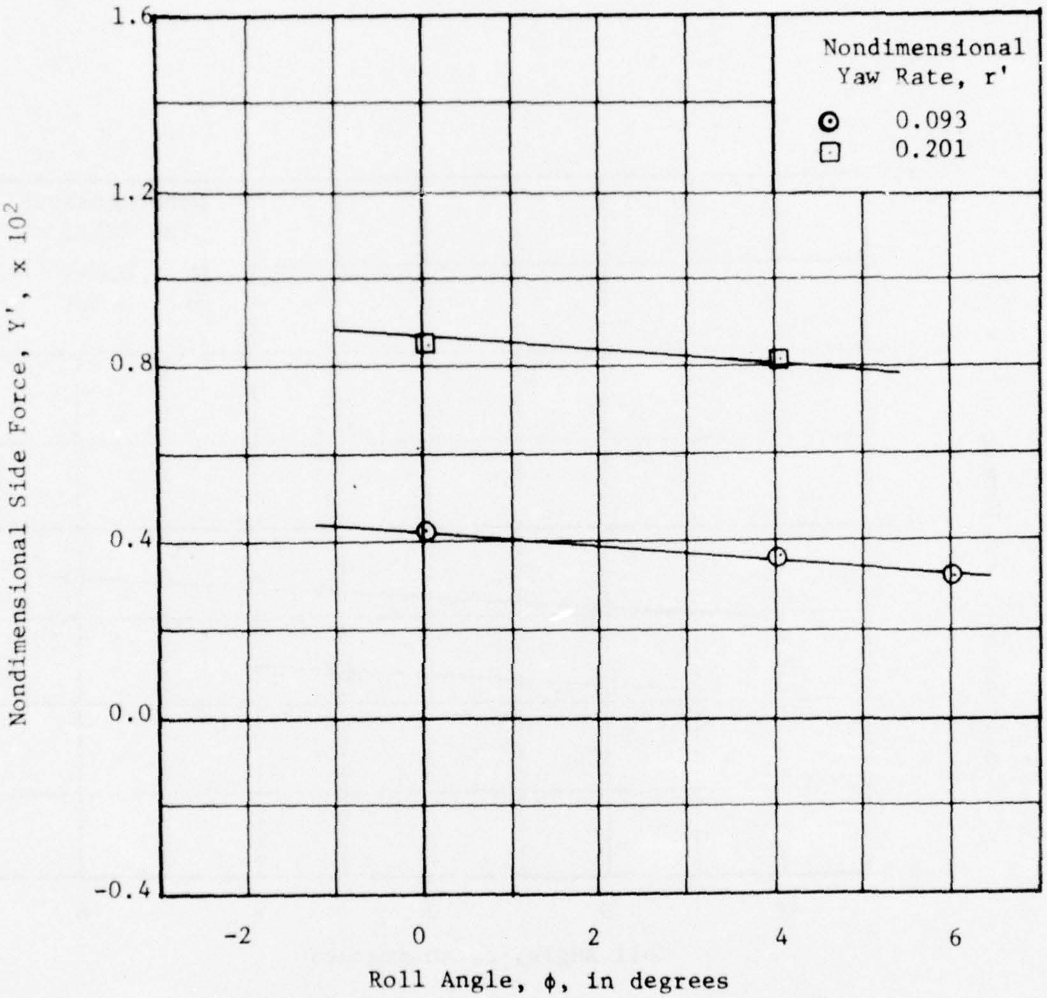

Figure 186 - Variation of Nondimensional Side Force with Roll Angle for Two Nondimensional Yaw Rates at a Full Scale Speed of 20 Knots for the Spade Rudder at Deep Draft

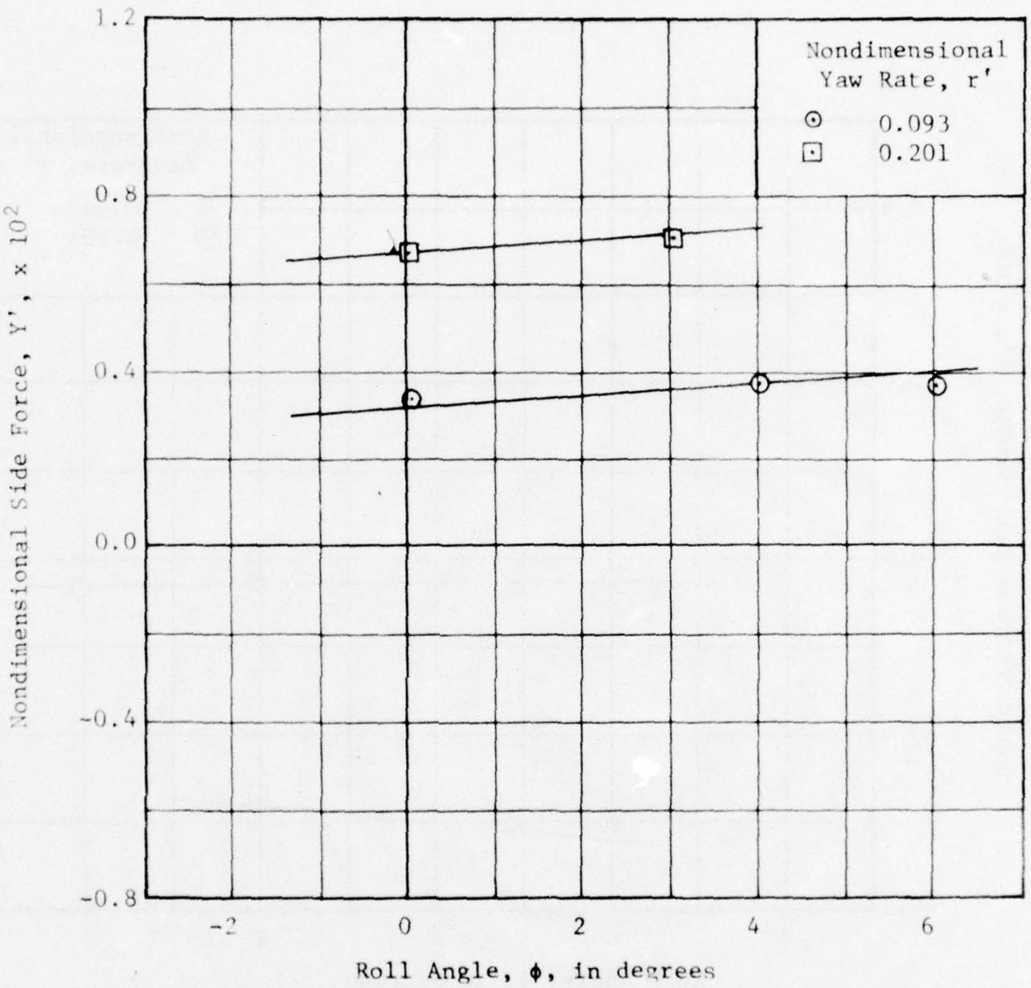

Figure 187 - Variation of Nondimensional Side Force with Roll Angle for Two Nondimensional Yaw Rates at a Full Scale Speed of 25 Knots for the Spade Rudder at Deep Draft

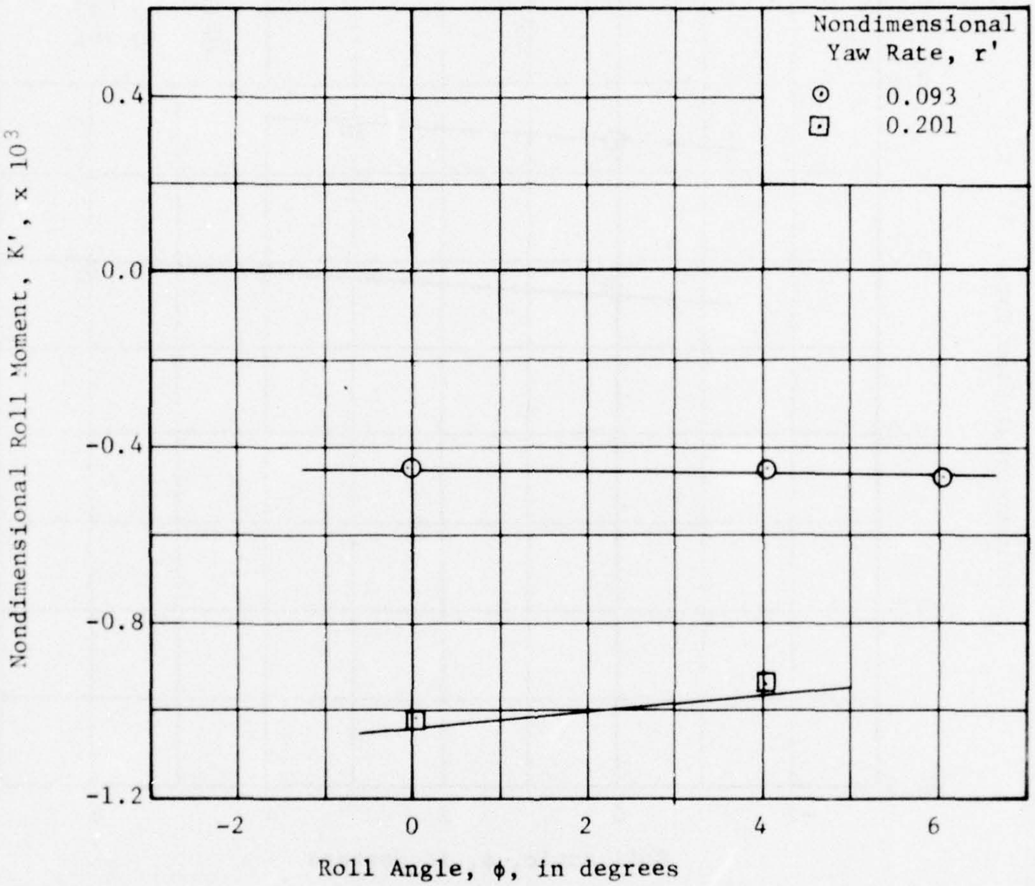

Figure 188 - Variation of Nondimensional Roll Moment with Roll Angle for Two Nondimensional Yaw Rates at a Full Scale Speed of 20 Knots for the Spade Rudder at Deep Draft

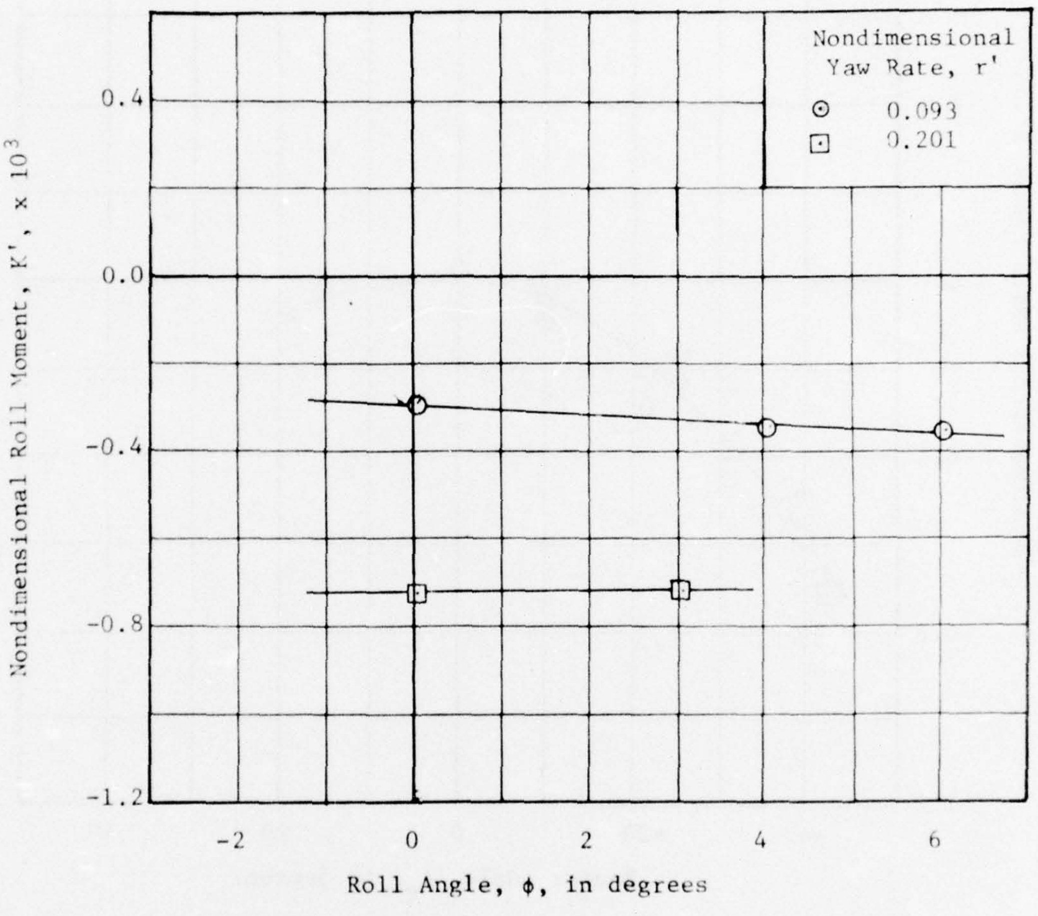

Figure 189 - Variation of Nondimensional Roll Moment with Roll Angle for Two Nondimensional Yaw Rates at a Full Scale Speed of 25 Knots for the Spade Rudder at Deep Draft

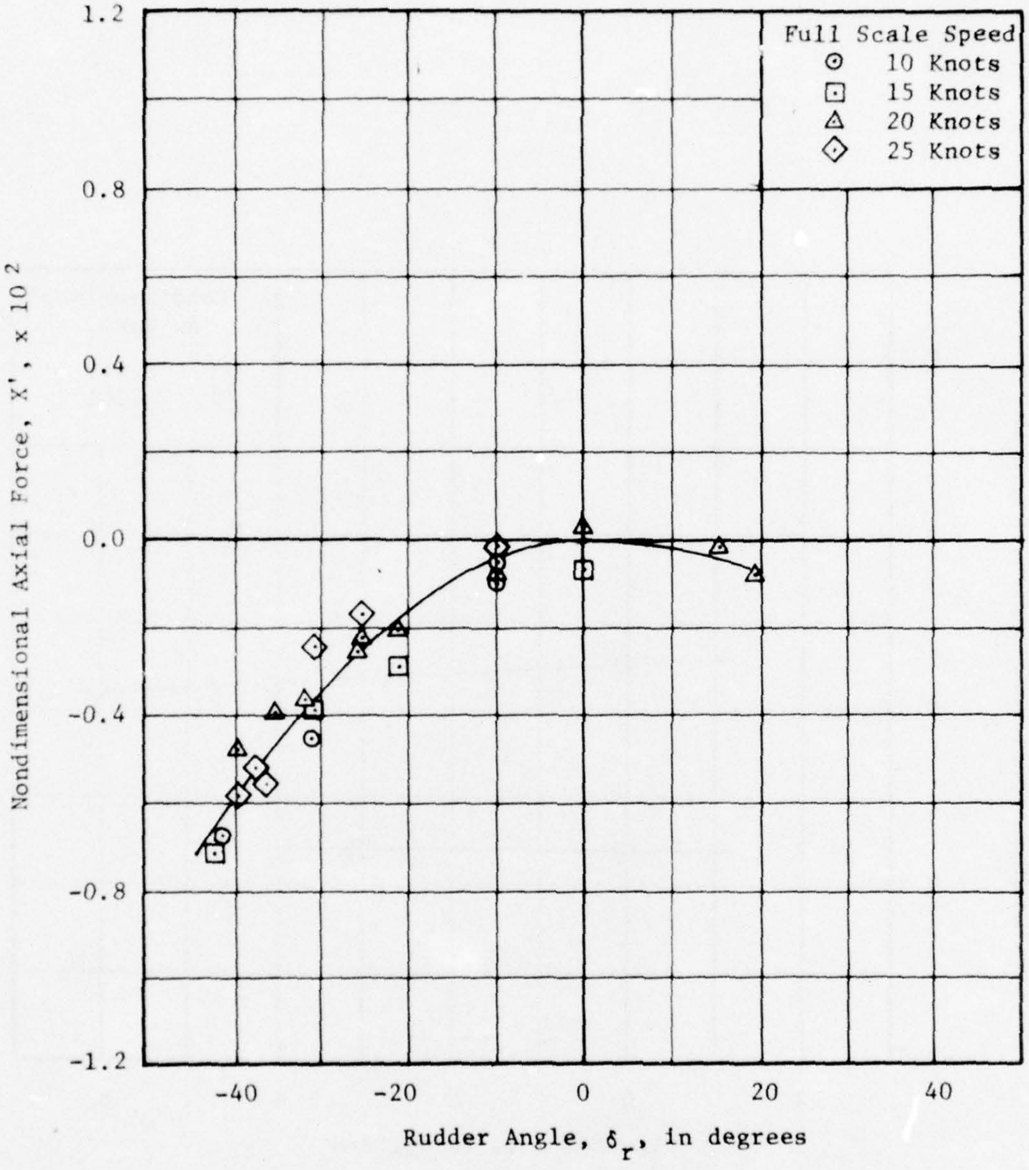

Figure 190 - Variation of Nondimensional Axial Force with Rudder Angle for a Series of Full Scale Speeds at a Nondimensional Yaw Rate of 0.093 for the Spade Rudder at Deep Draft

Appendix E

(Figures 191 to 208)
Nondimensional Data Curves for
the Fixed Forward Turning Foil

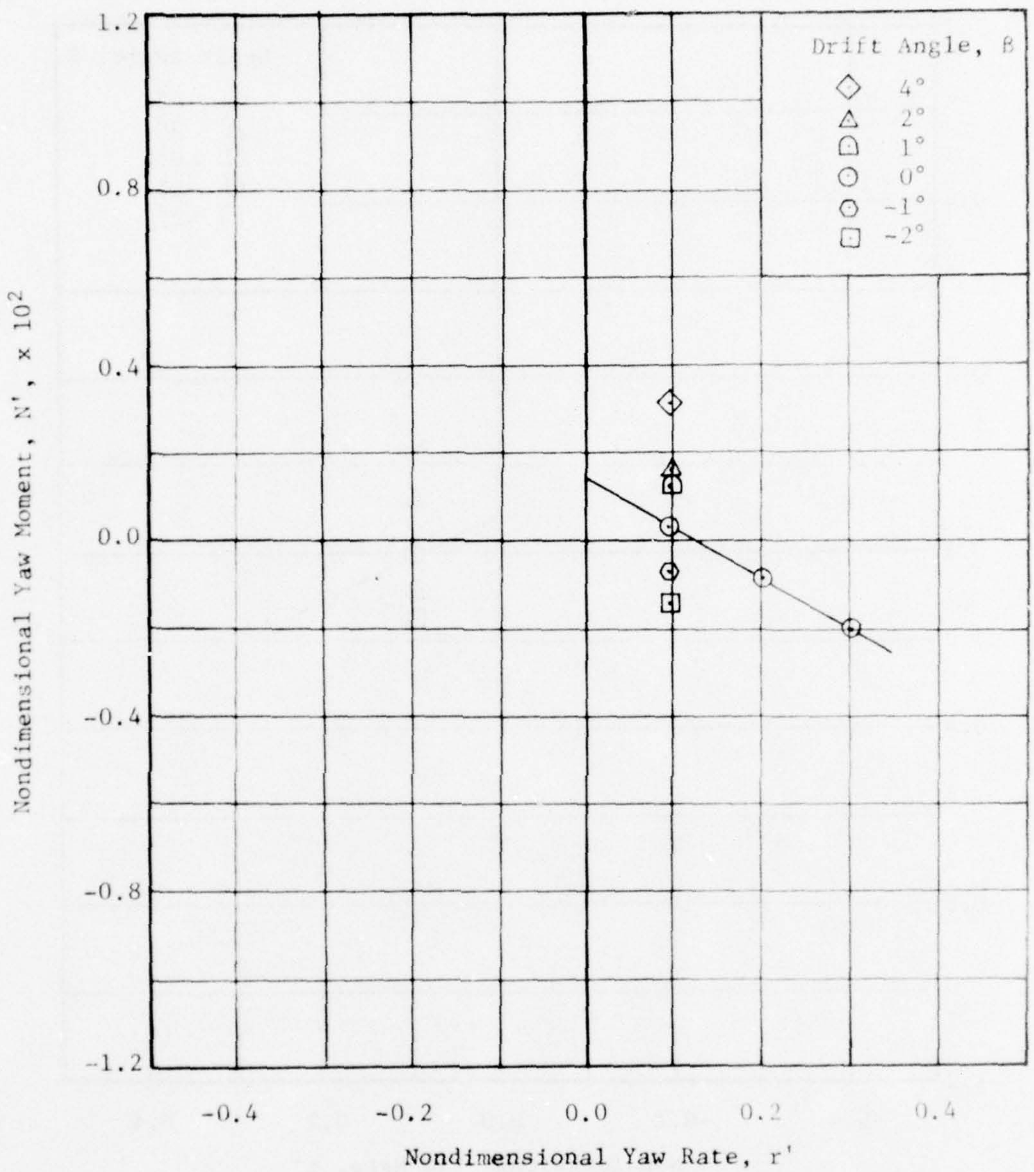

Figure 191 - Variation of Nondimensional Yaw Moment with Nondimensional Yaw Rates for a Series of Drift Angles at a Full Scale Speed of 5 Knots for the Fixed Forward Turning Foil

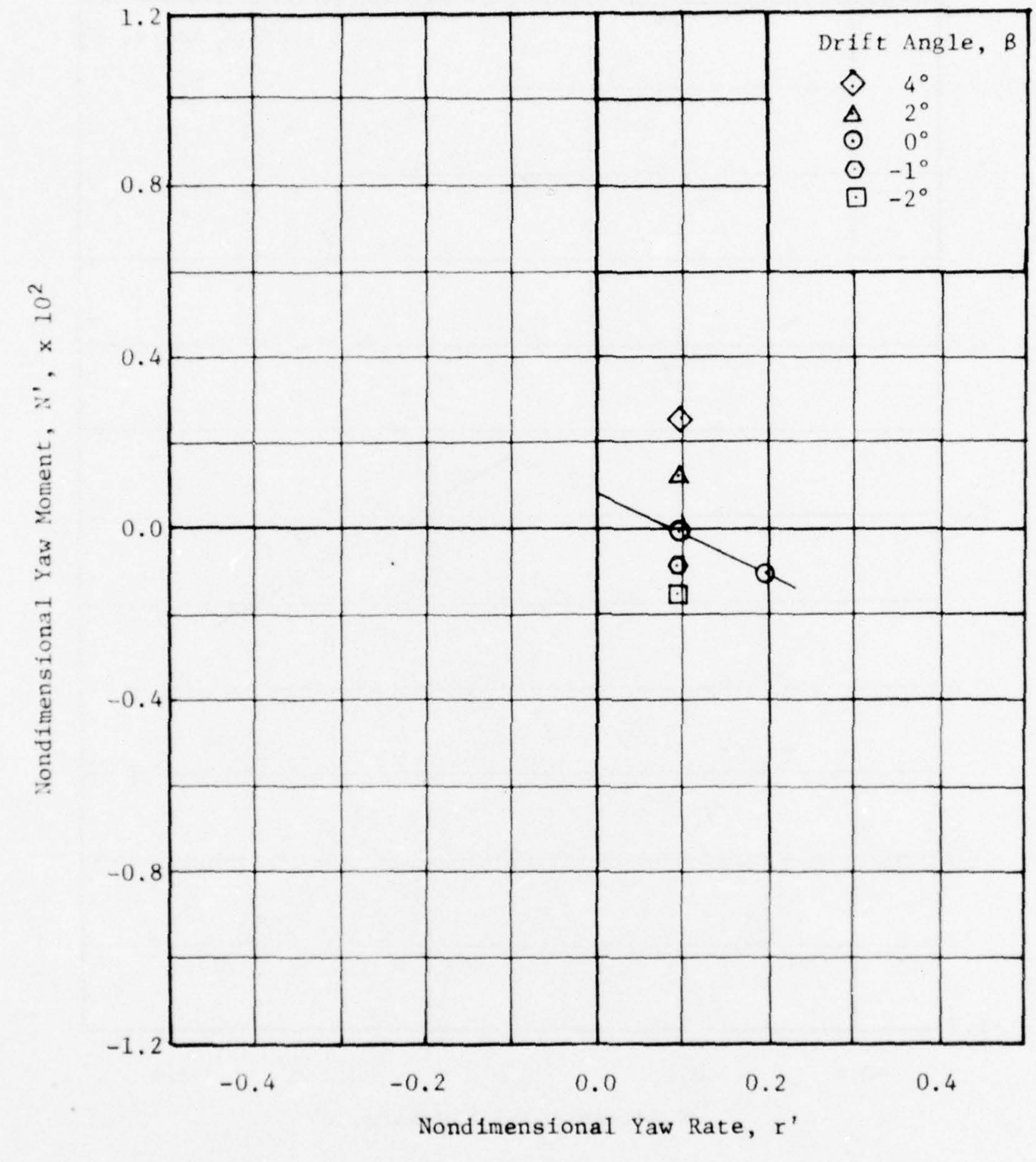

Figure 192 - Variation of Nondimensional Yaw Moment with Nondimensional Yaw Rate for a Series of Drift Angles at a Full Scale Speed of 10 Knots for the Fixed Forward Turning Foil

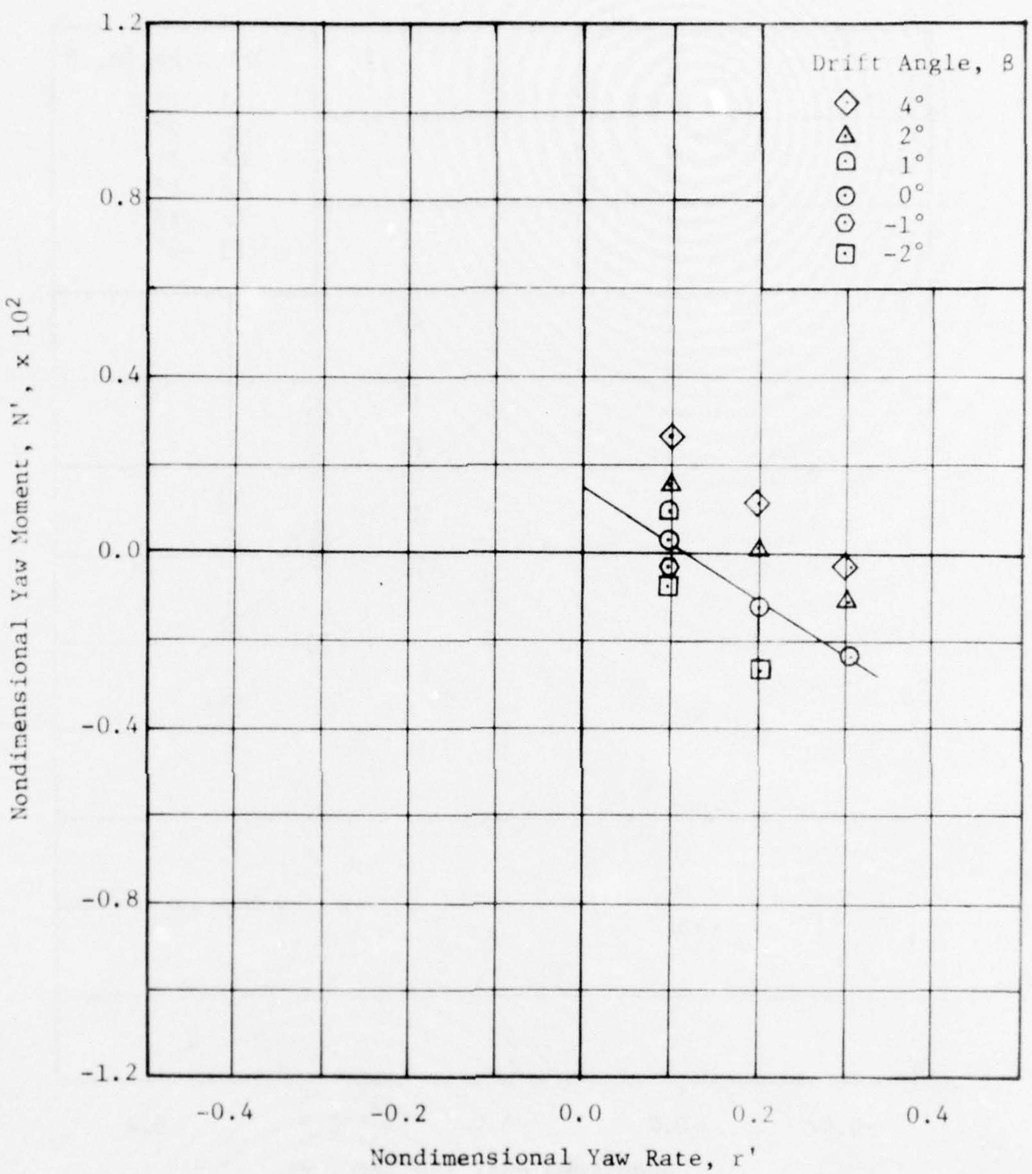

Figure 193 - Variation of Nondimensional Yaw Moment with Nondimensional Yaw Rate for a Series of Drift Angles at a Full Scale Speed of 15 Knots for the Fixed Forward Turning Foil

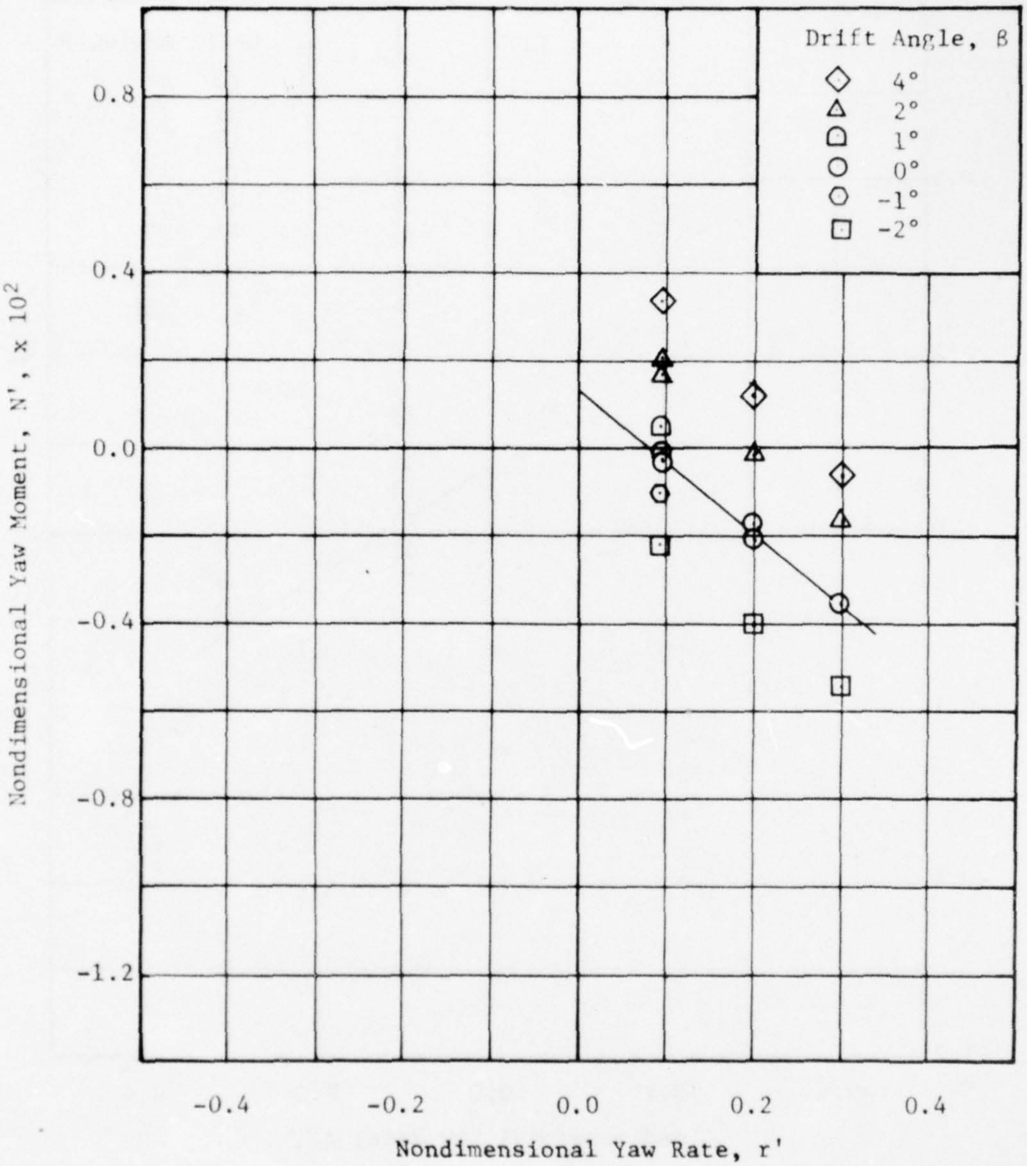

Figure 194 - Variation of Nondimensional Yaw Moment with Nondimensional Yaw Rate for a Series of Drift Angles at a Full Scale Speed of 20 Knots for the Fixed Forward Turning Foil

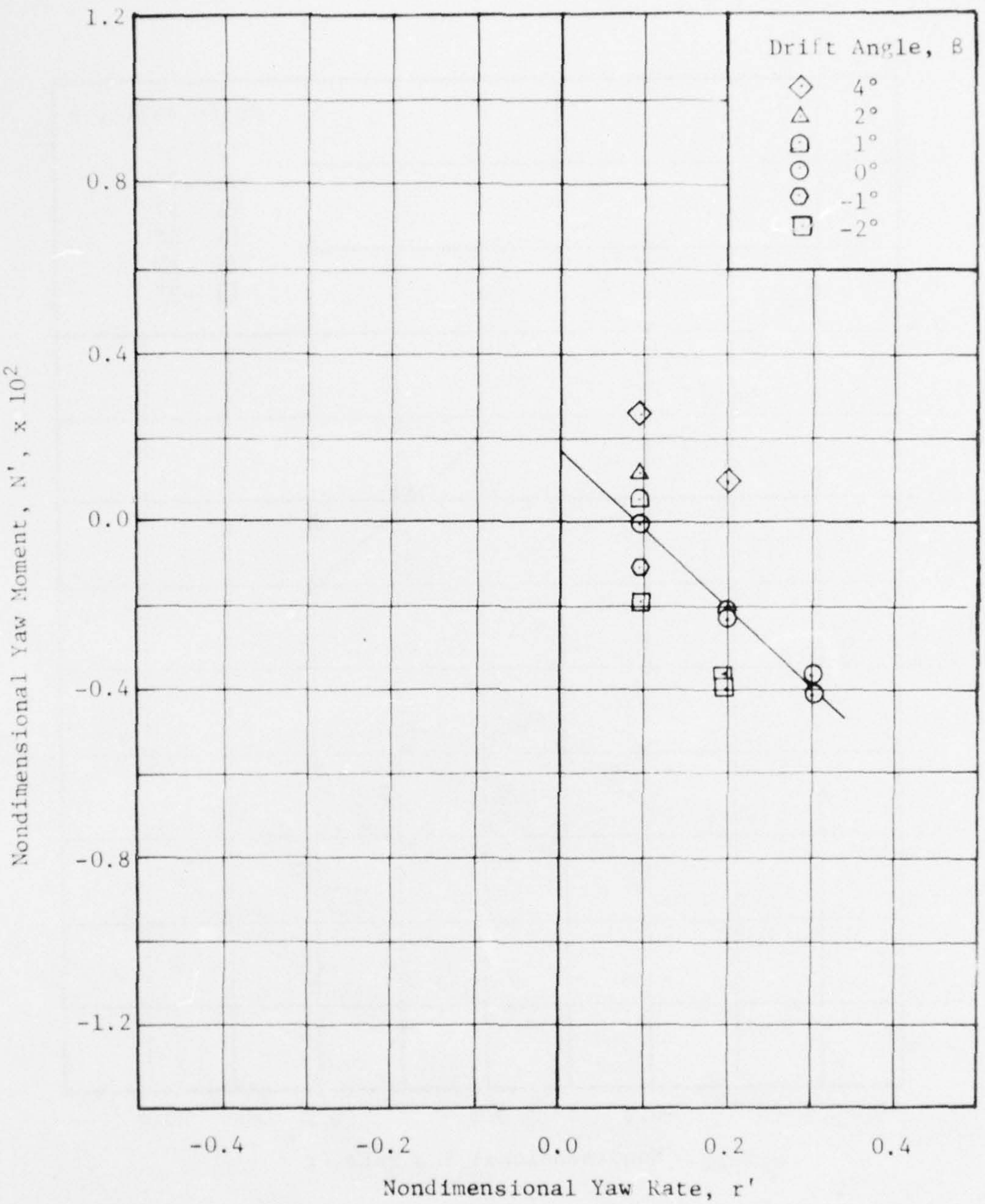

Figure 195 - Variation of Nondimensional Yaw Moment with Nondimensional Yaw Rate for a Series of Drift Angles at a Full Scale Speed of 25 Knots for the Fixed Forward Turning Foil

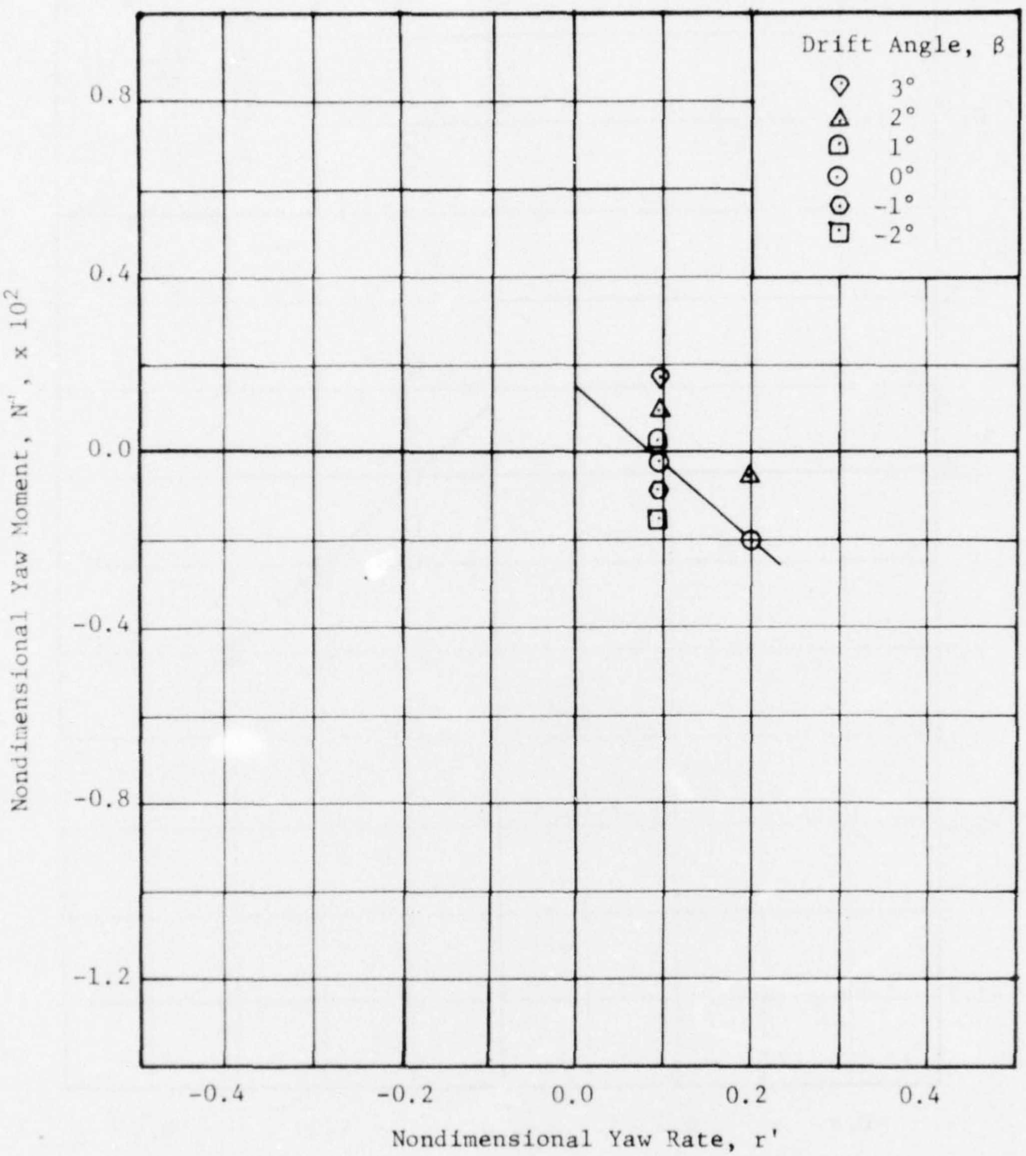

Figure 196 - Variation of Nondimensional Yaw Moment with Nondimensional Yaw **Rate** for a Series of Drift Angles at a Full Scale Speed of 28 Knots for the Fixed Forward Turning Foil

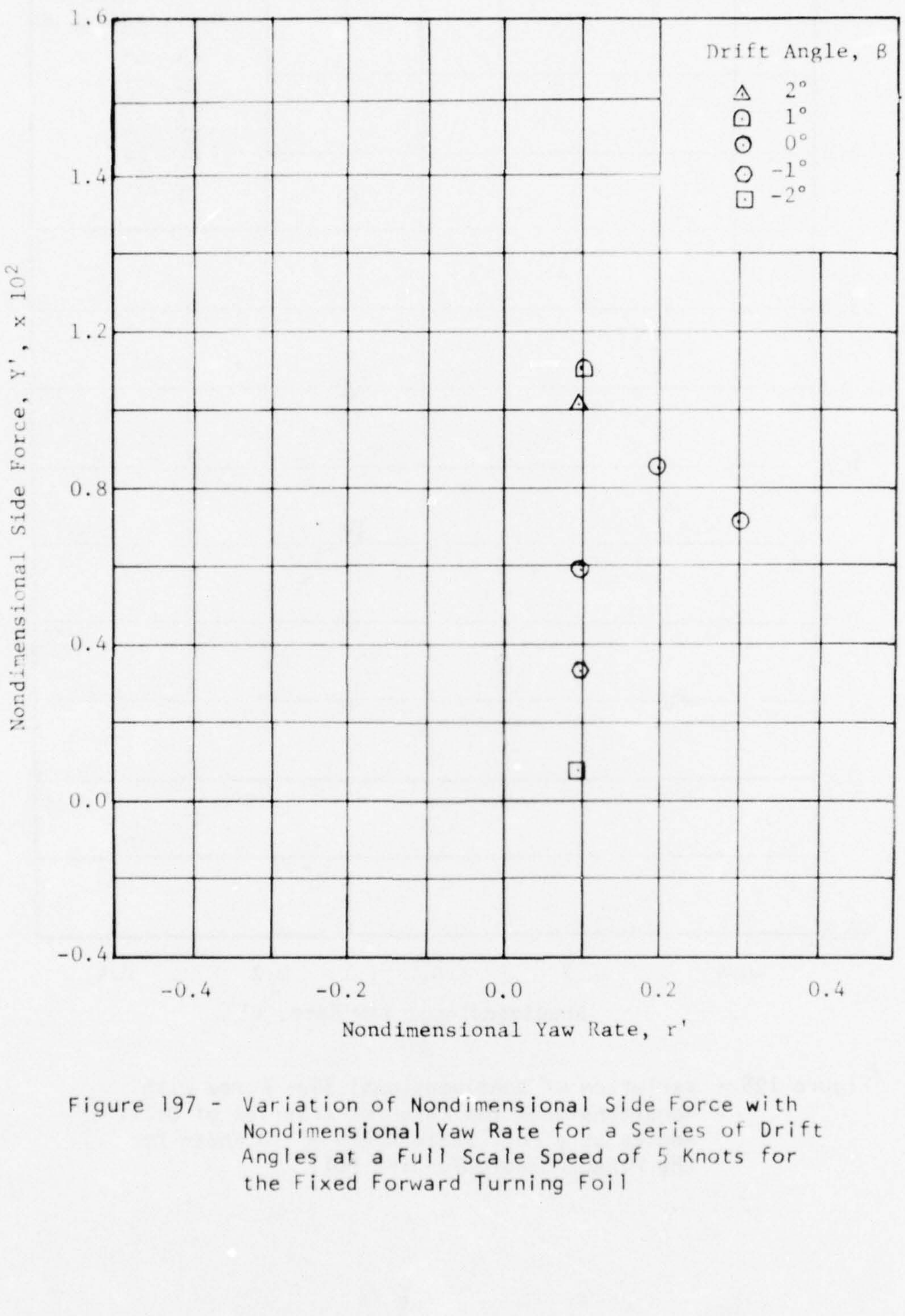

Figure 197 - Variation of Nondimensional Side Force with Nondimensional Yaw Rate for a Series of Drift Angles at a Full Scale Speed of 5 Knots for the Fixed Forward Turning Foil

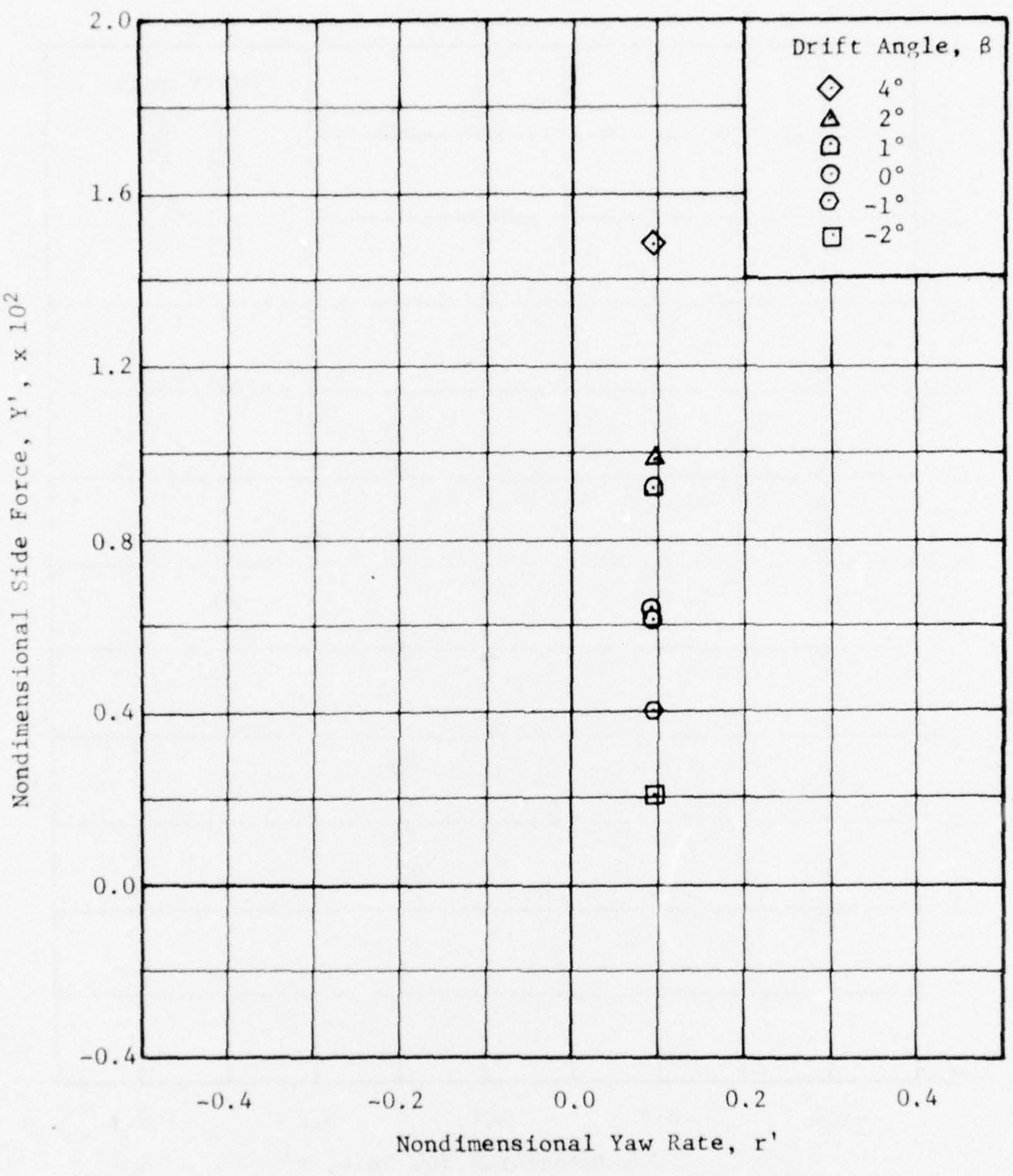

Figure 198 - Variation of Nondimensional Side Force with Nondimensional Yaw Rate for a Series of Drift Angles at a Full Scale Speed of 10 Knots for the Fixed Forward Turning Foil

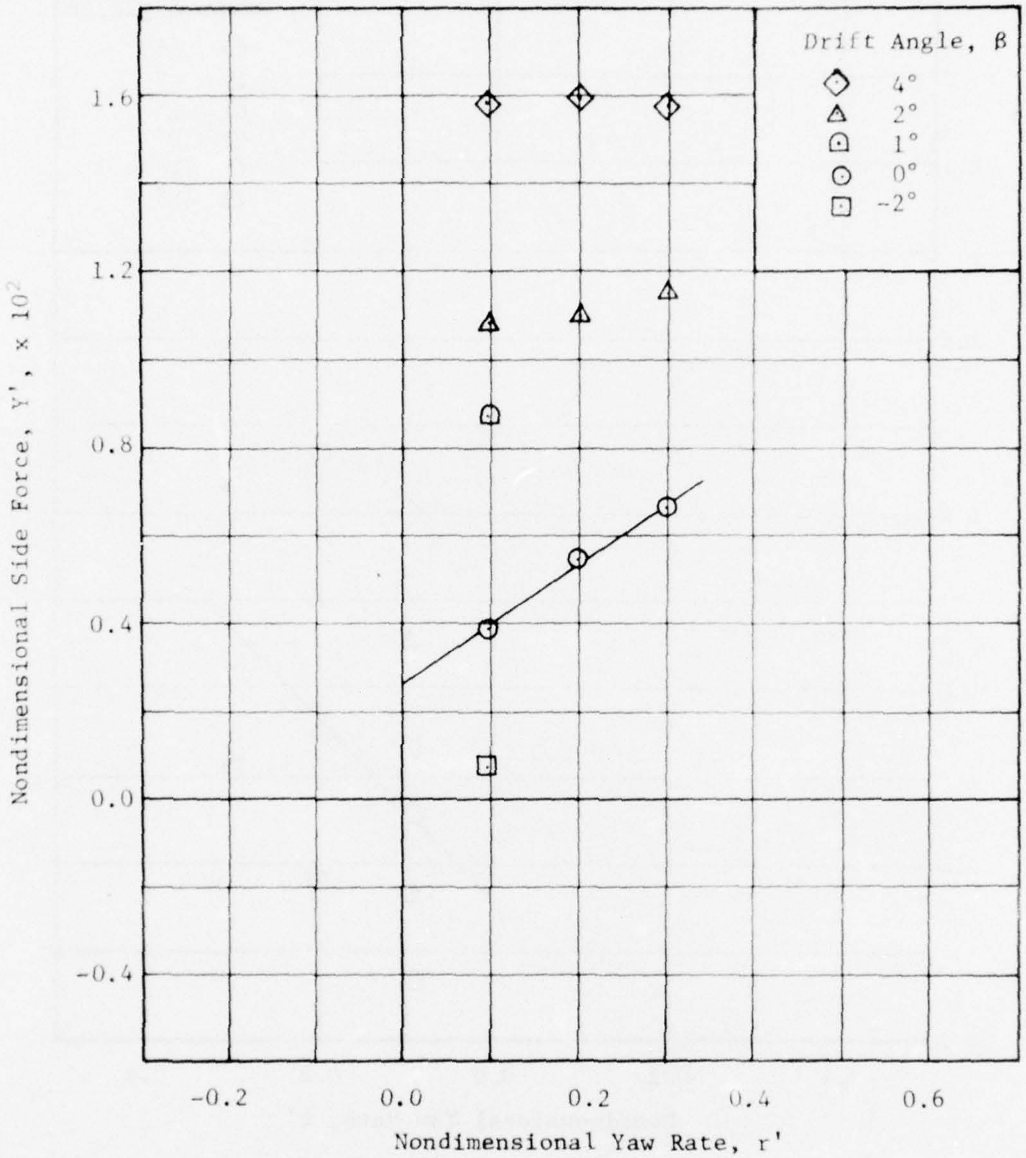

Figure 199 - Variation of Nondimensional Side Force with Nondimensional Yaw Rate for a Series of Drift Angles at a Full Scale Speed of 15 Knots for the Fixed Forward Turning Foil

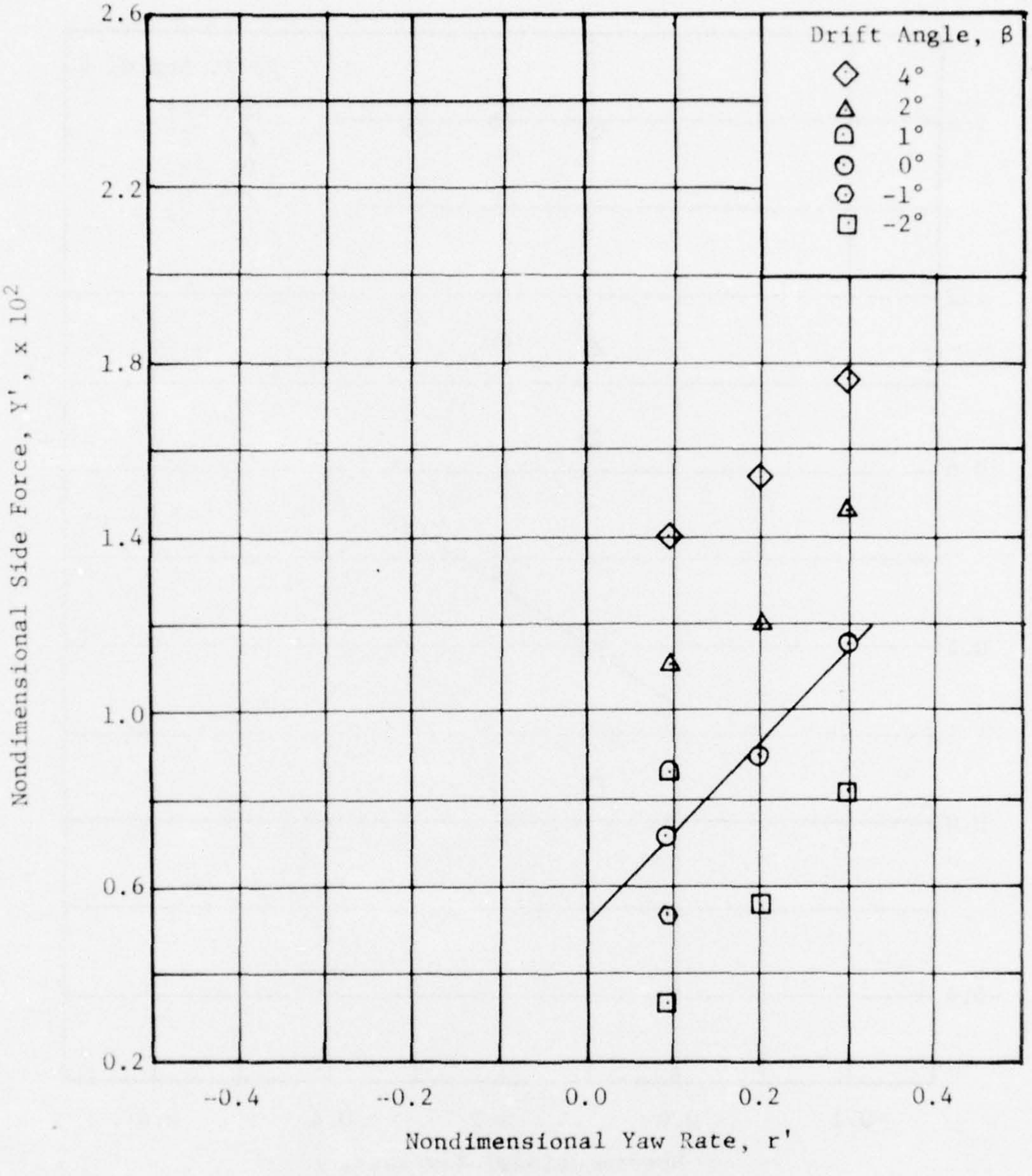

Figure 200 - Variation of Nondimensional Side Force with Nondimensional Yaw Rate for a Series of Drift Angles at a Full Scale Speed of 20 Knots for the Fixed Forward Turning Foil

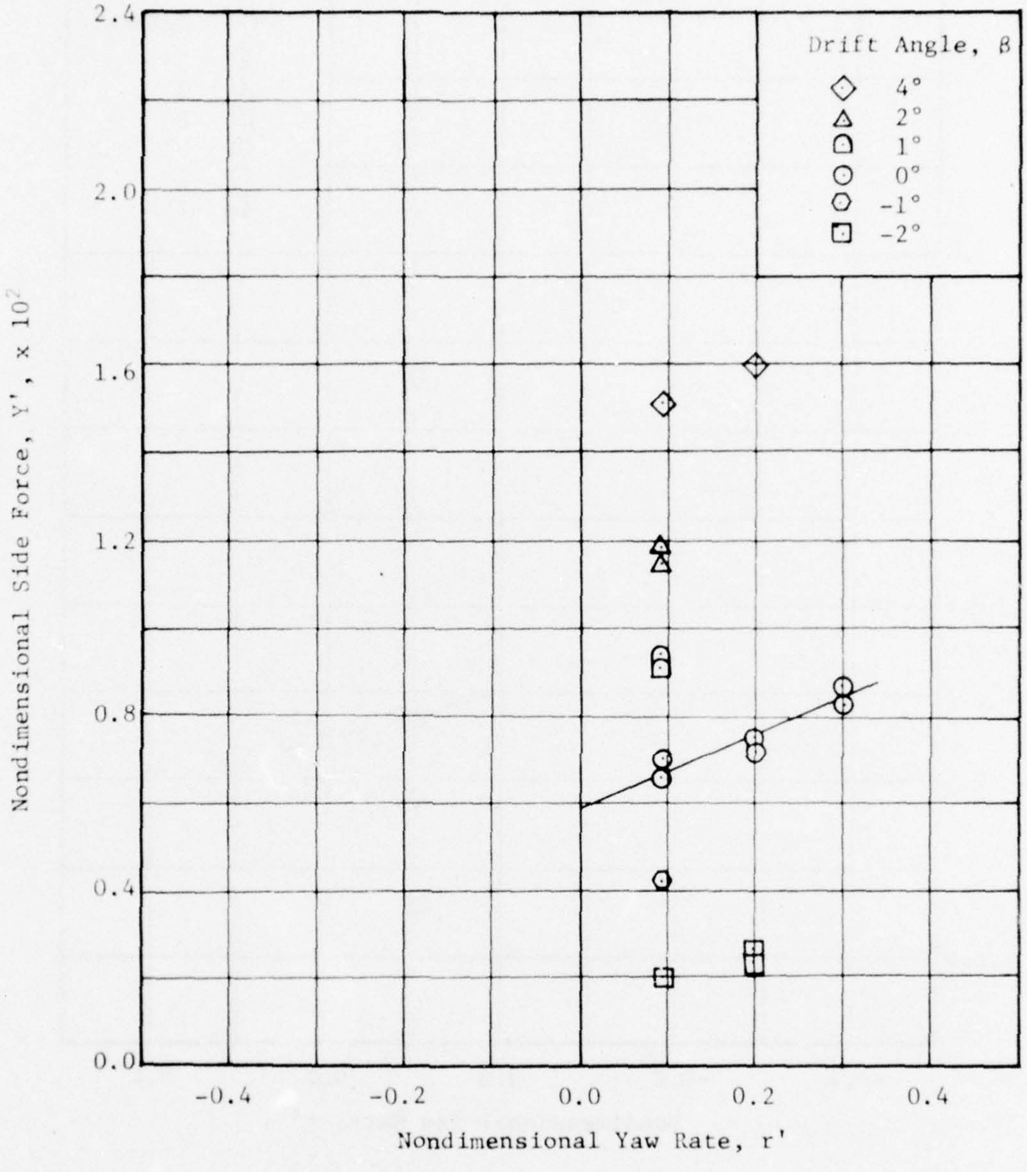

Figure 201 - Variation of Nondimensional Side Force with Nondimensional Yaw Rate for a Series of Drift Angles at a Full Scale Speed of 25 Knots for the Fixed Forward Turning Foil

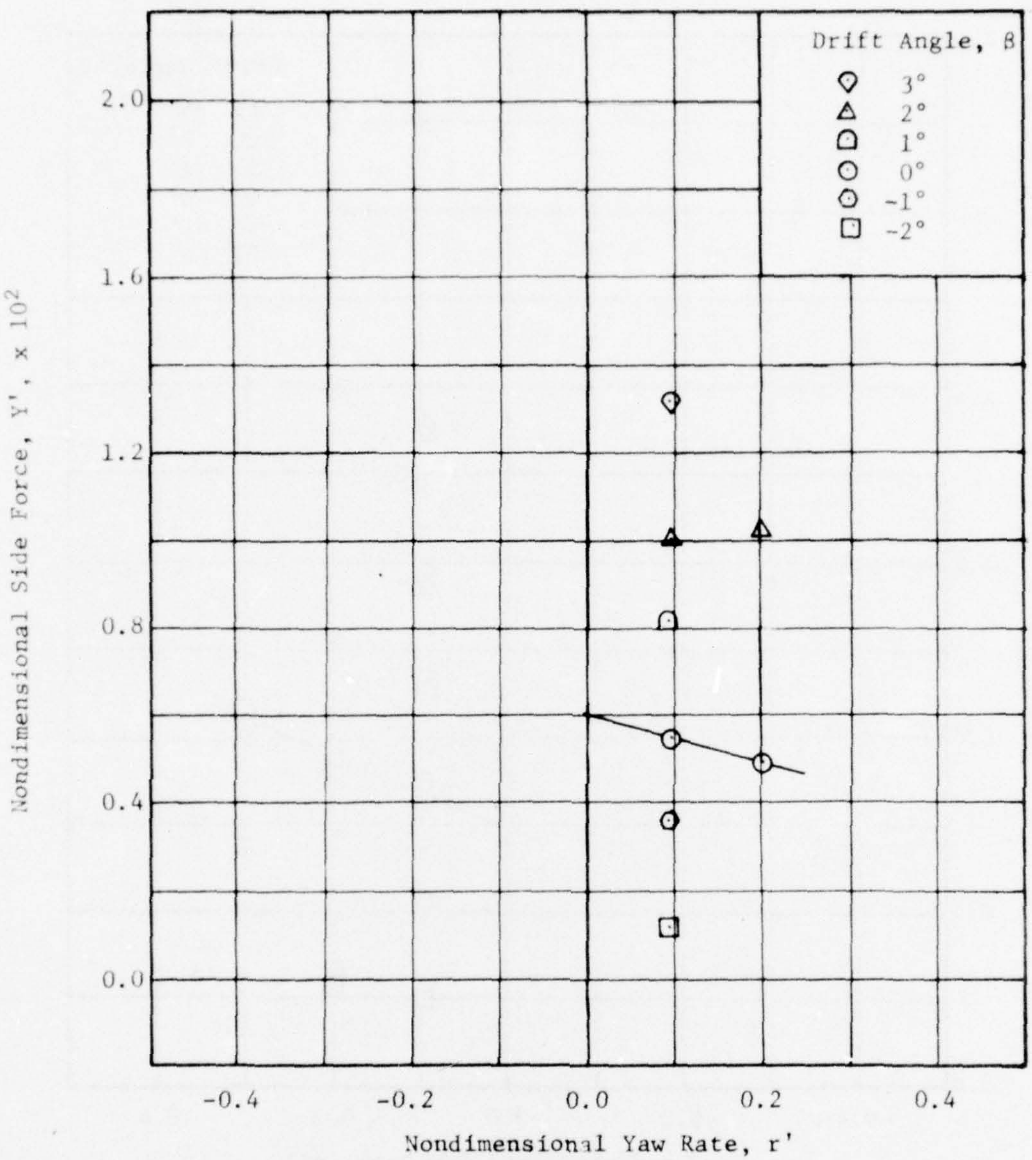

Figure 202 - Variation of Nondimensional Side Force with Nondimensional Yaw Rate for a Series of Drift Angles at a Full Scale Speed of 28 Knots for the Fixed Forward Turning Foil

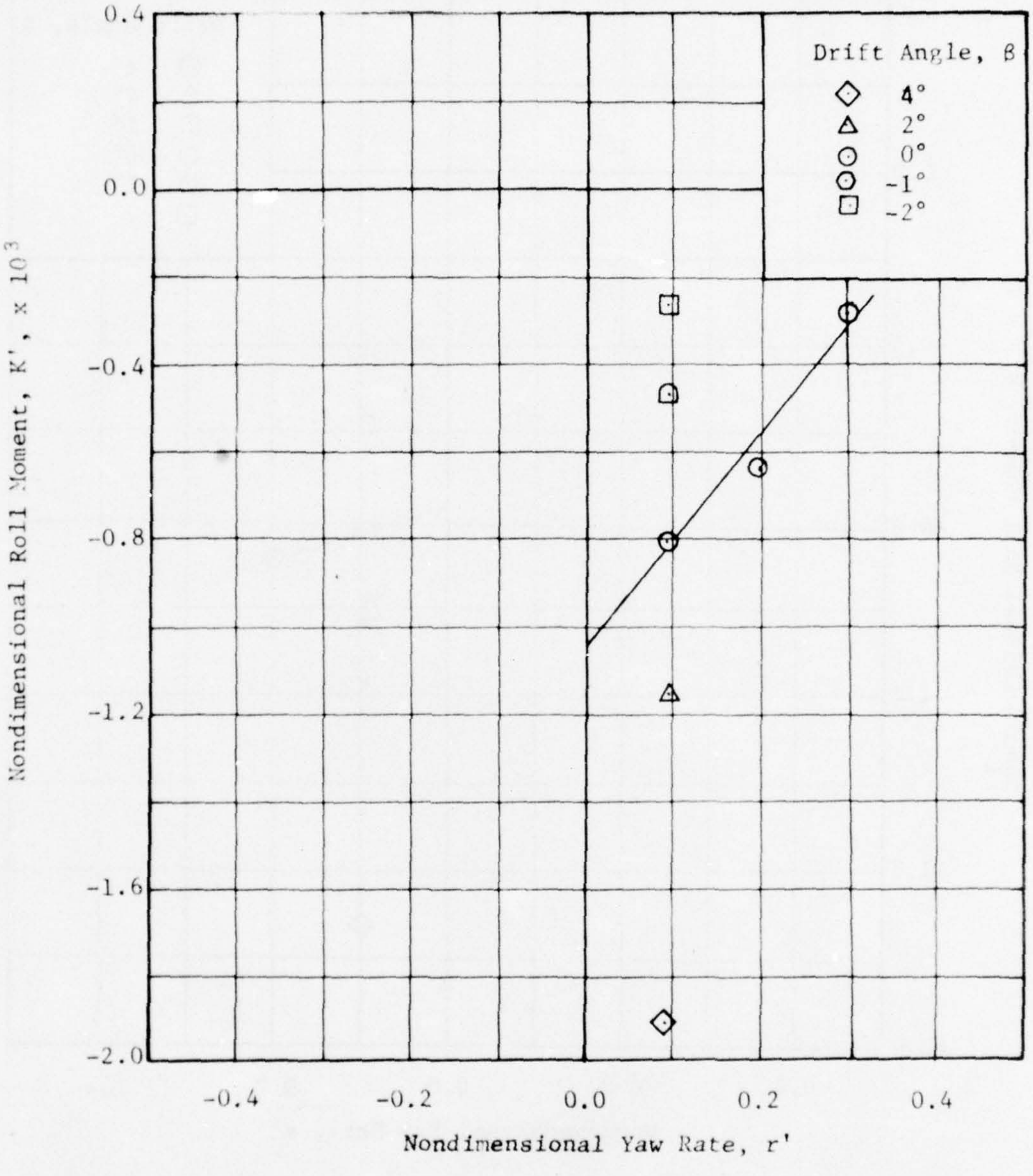

Figure 203 - Variation of Nondimensional Roll Moment with Nondimensional Yaw Rate for a Series of Drift Angles at a Full Scale Speed of 5 Knots for the Fixed Forward Turning Foil

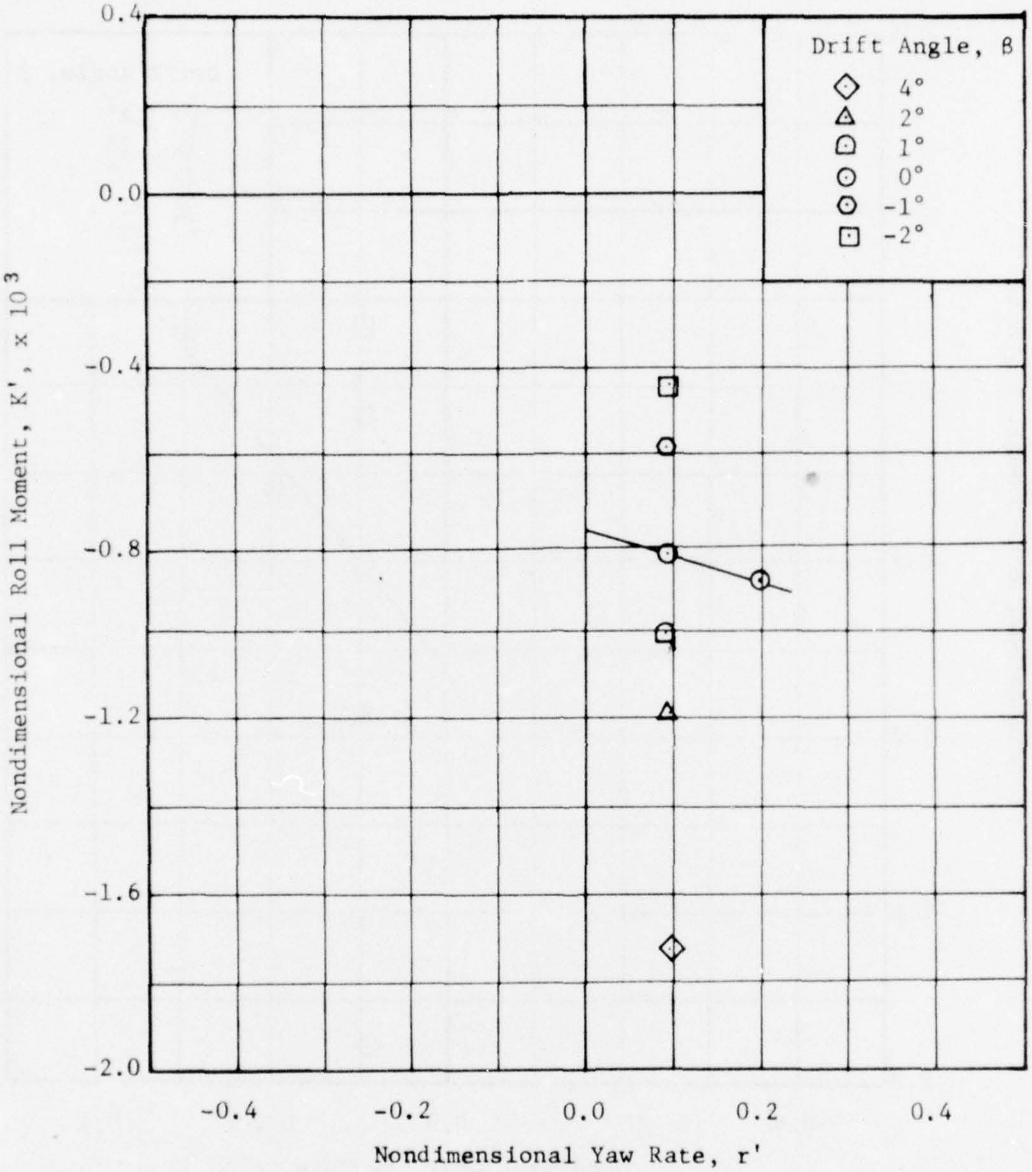

Figure 204 - Variation of Nondimensional Roll Moment with Nondimensional Yaw Rate for a Series of Drift Angles at a Full Scale Speed of 10 Knots for the Fixed Forward Turning Foil

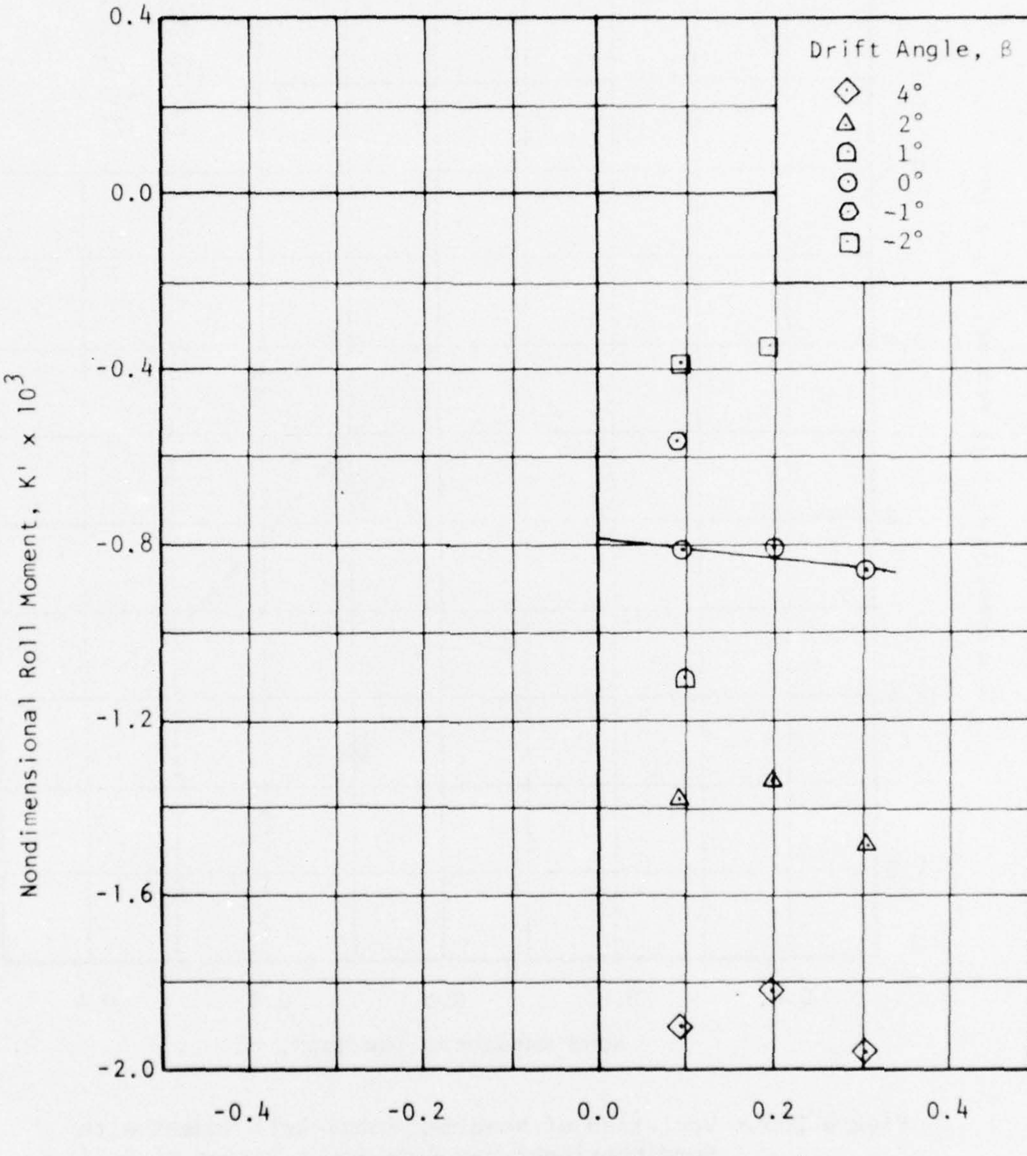

Figure 205 - Variation of Nondimensional Roll Moment with Nondimensional Yaw Rate for a Series of Drift Angles at a Full Scale Speed of 15 Knots for the Full Forward Turning Foil

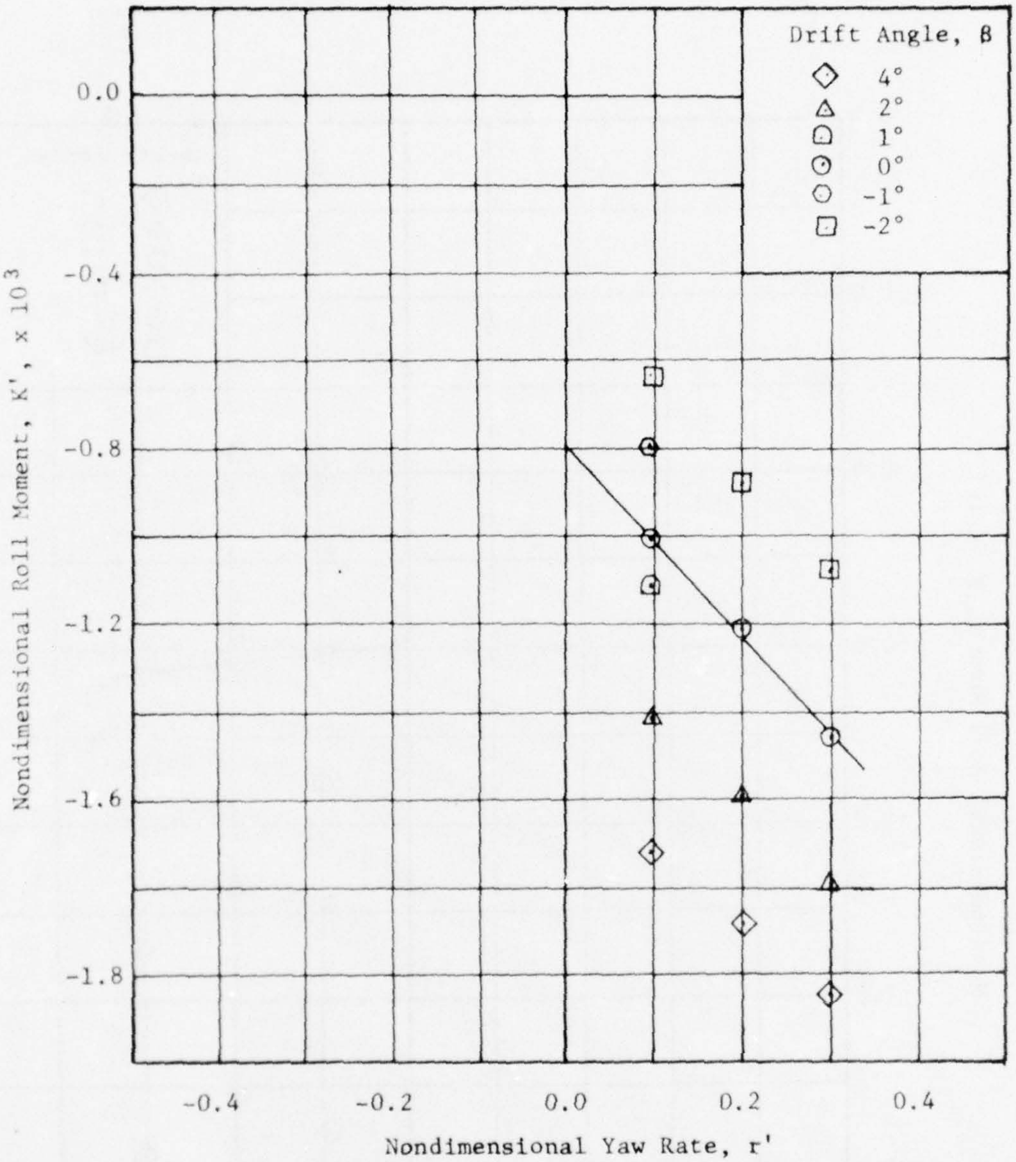

Figure 206 - Variation of Nondimensional Roll Moment with Nondimensional Yaw Rate for a Series of Drift Angles at a Full Scale Speed of 20 Knots for the Fixed Forward Turning Foil

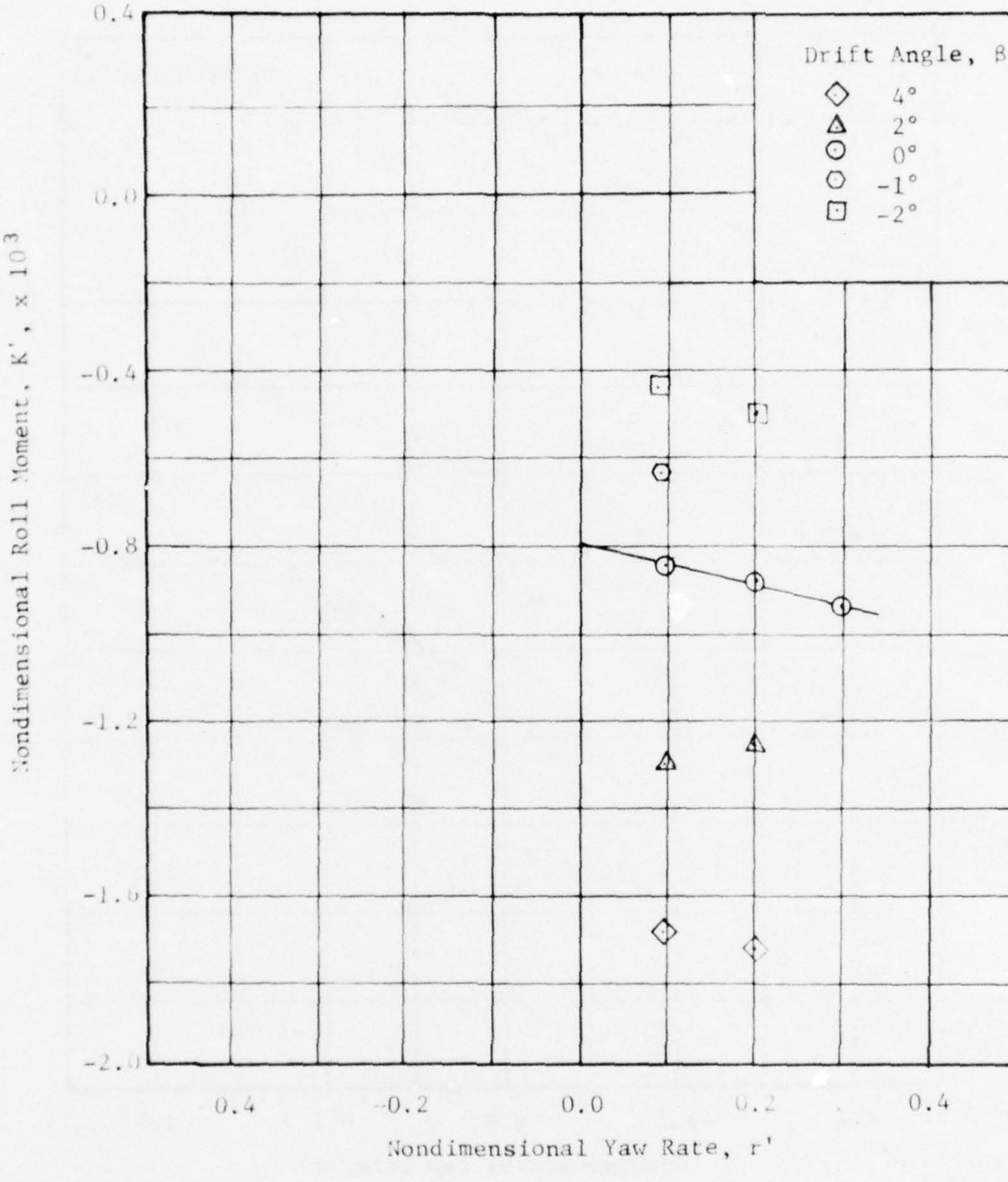

Figure 207 - Variation of Nondimensional Roll Moment with Nondimensional Yaw Rate for a Series of Drift Angles at a Full Scale Speed of 25 Knots for the Fixed Forward Turning Foil

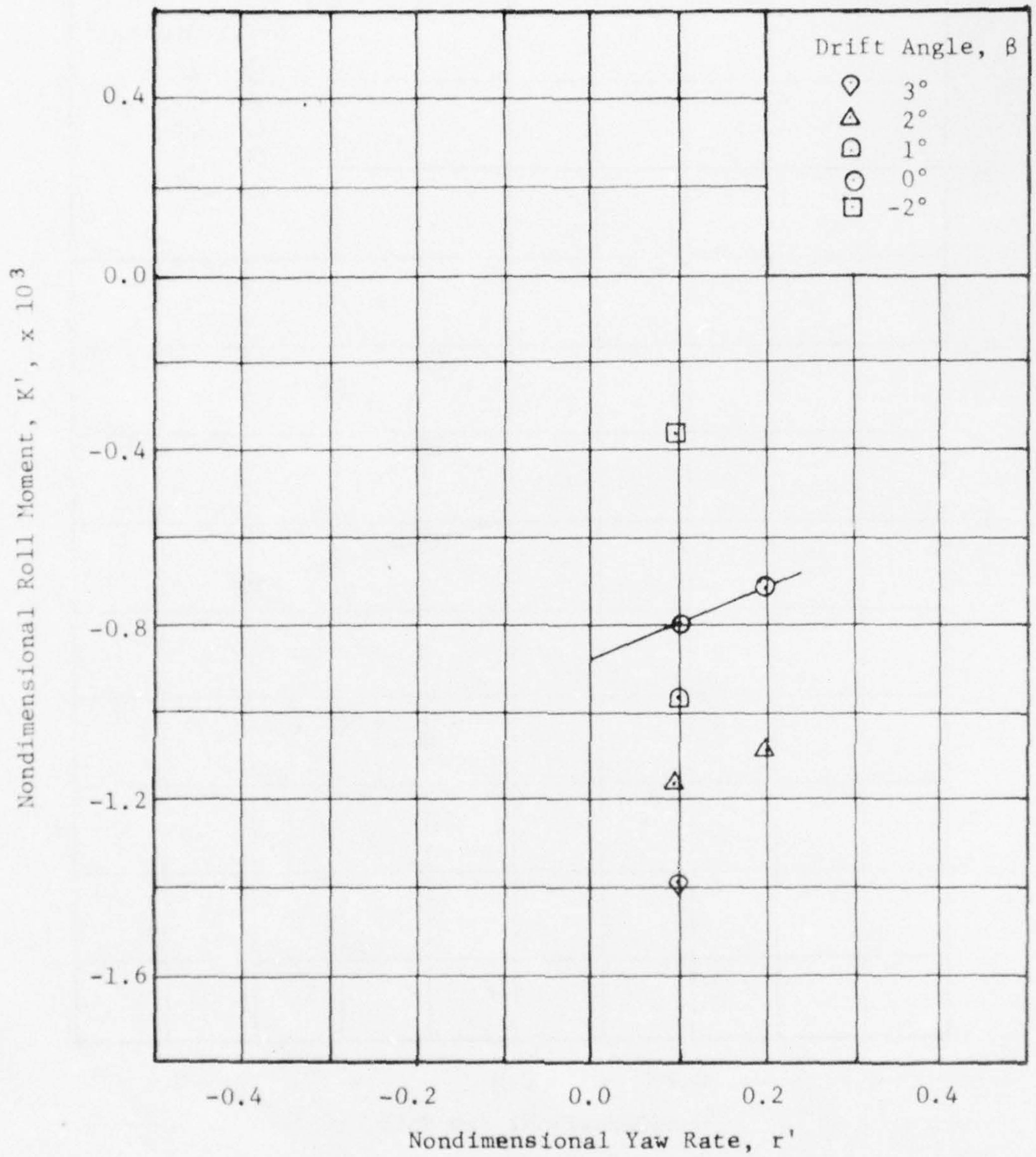

Figure 208 - Variation of Nondimensional Roll Moment with Nondimensional Yaw Rate for a Series of Drift Angles at a Full Scale Speed of 28 Knots for the Fixed Forward Turning Foil

Appendix F

(Figures 209 to 226)
Nondimensional Data Curves for
the Half-Sized Fixed Forward
Turning Foil

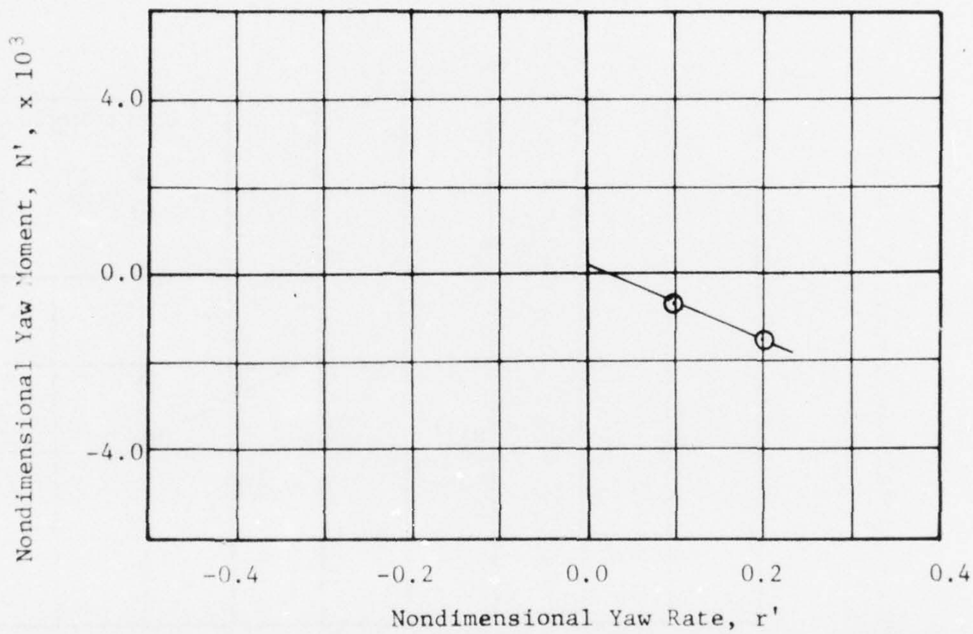

Figure 209 - Variation of Nondimensional Yaw Moment with Nondimensional Yaw Rate for a Drift Angle of 0 Degrees at a Full Scale Speed of 5 Knots for the Half-Size Fixed Forward Turning Foil

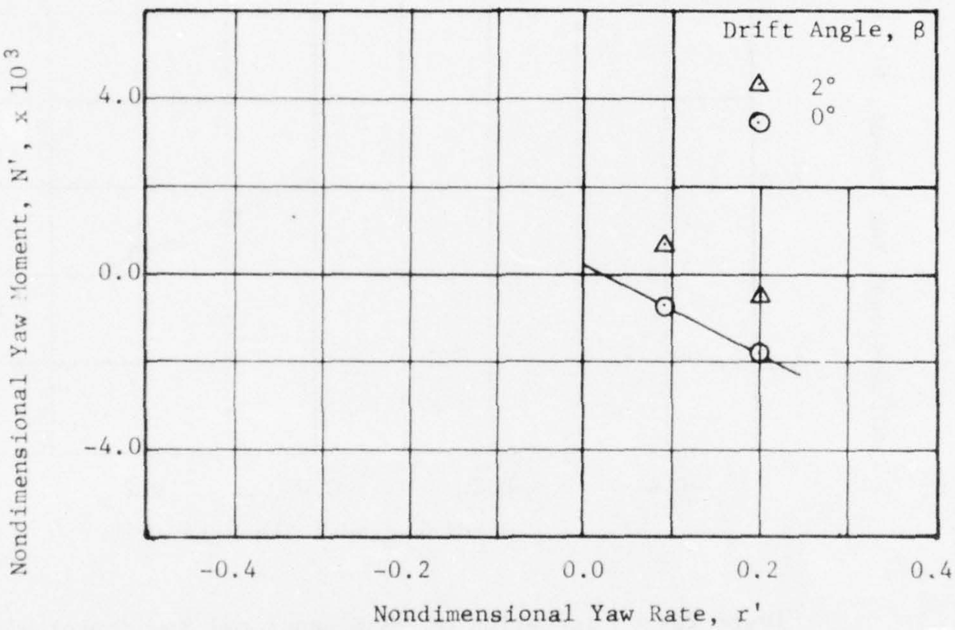

Figure 210 - Variation of Nondimensional Yaw Moment with Nondimensional Yaw Rate for Two Drift Angles at a Full Scale Speed of 10 Knots for the Half-Size Fixed Forward Turning Foil

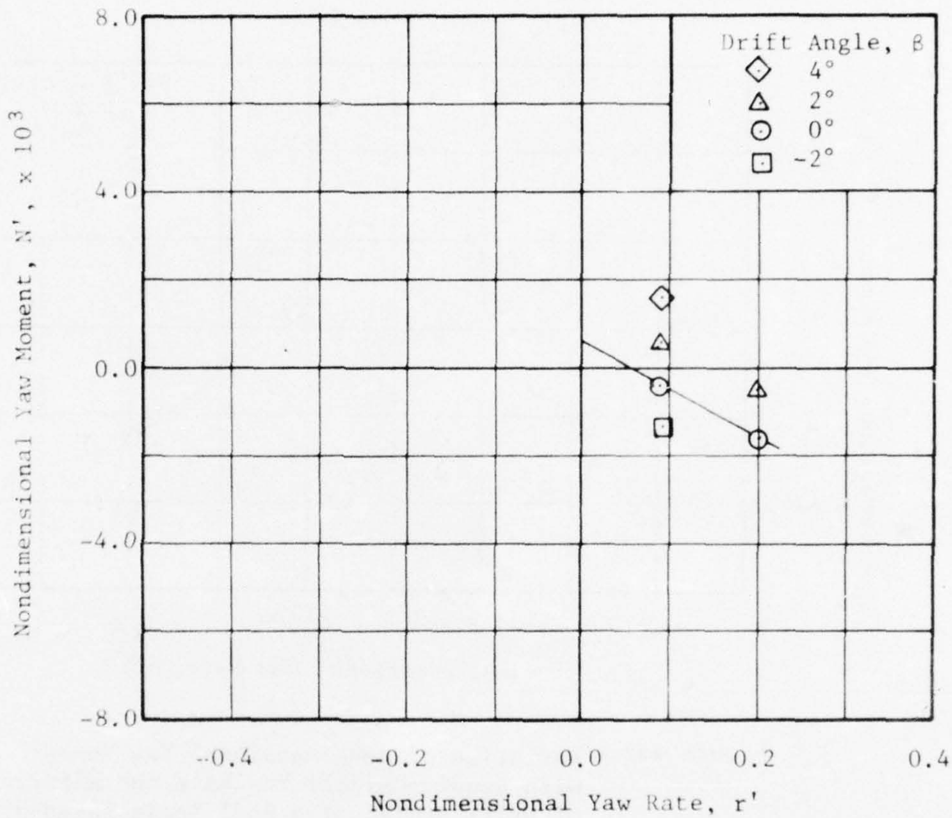

Figure 211 - Variation of Nondimensional Yaw Moment with Nondimensional Yaw Rate for a Series of Drift Angles at a Full Scale Speed of 15 Knots for the Half-Size **Fixed** Forward Turning Foil

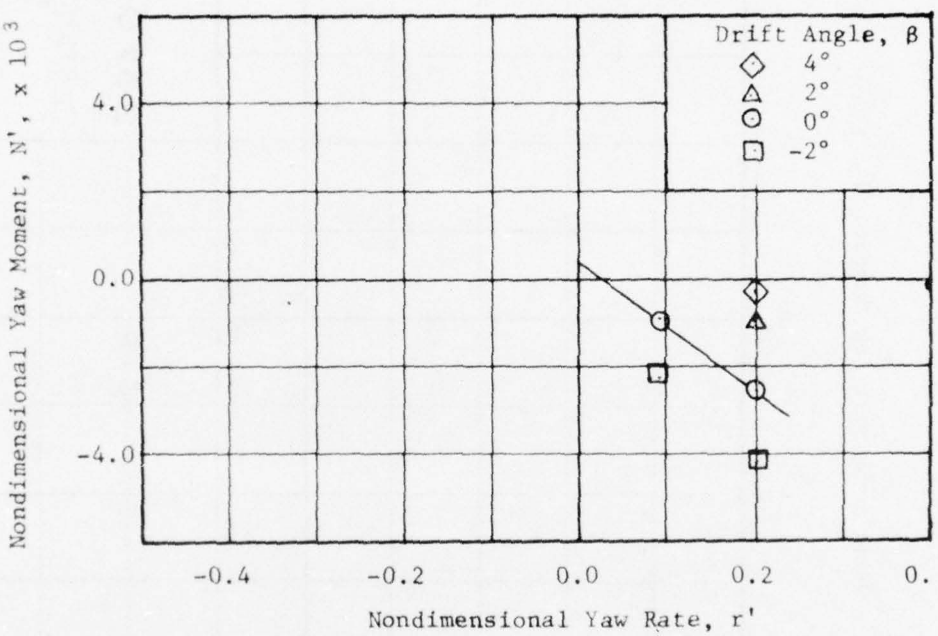

Figure 212 - Variation of Nondimensional Yaw Moment with Nondimensional Yaw Rate for a Series of Drift Angles at a Full Scale Speed of 20 Knots for the Half-Size Fixed Forward Turning Foil

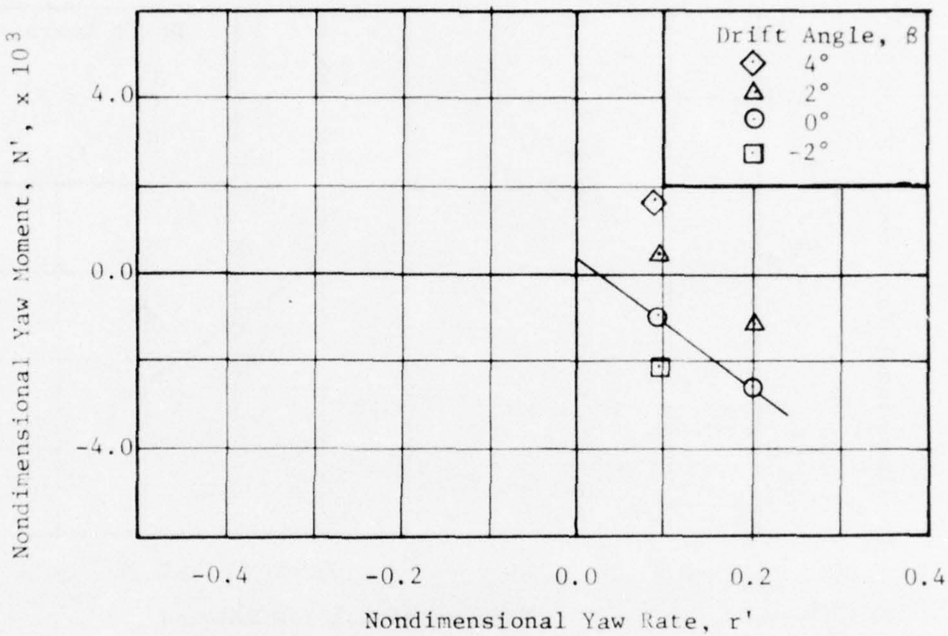

Figure 213 - Variation of Nondimensional Yaw Moment with Nondimensional Yaw Rate for a Series of Drift Angles at a Full Scale Speed of 25 Knots for the Half-Size Fixed Forward Turning Foil

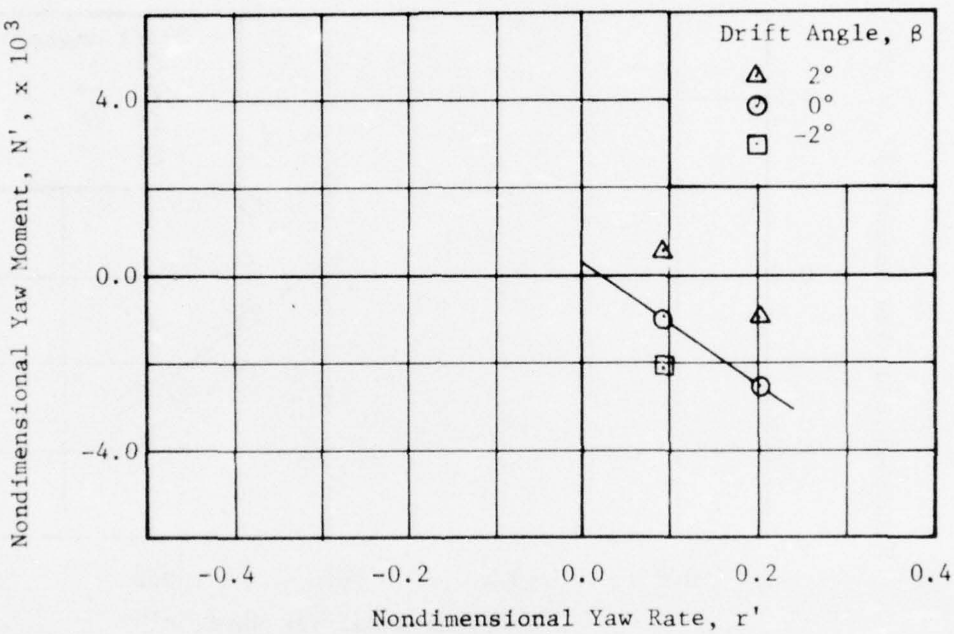

Figure 214 - Variation of Nondimensional Yaw Moment with Nondimensional Yaw Rate for a Series of Drift Angles at a Full Scale Speed of 28 Knots for the Half-Size Fixed Forward Turning Foil

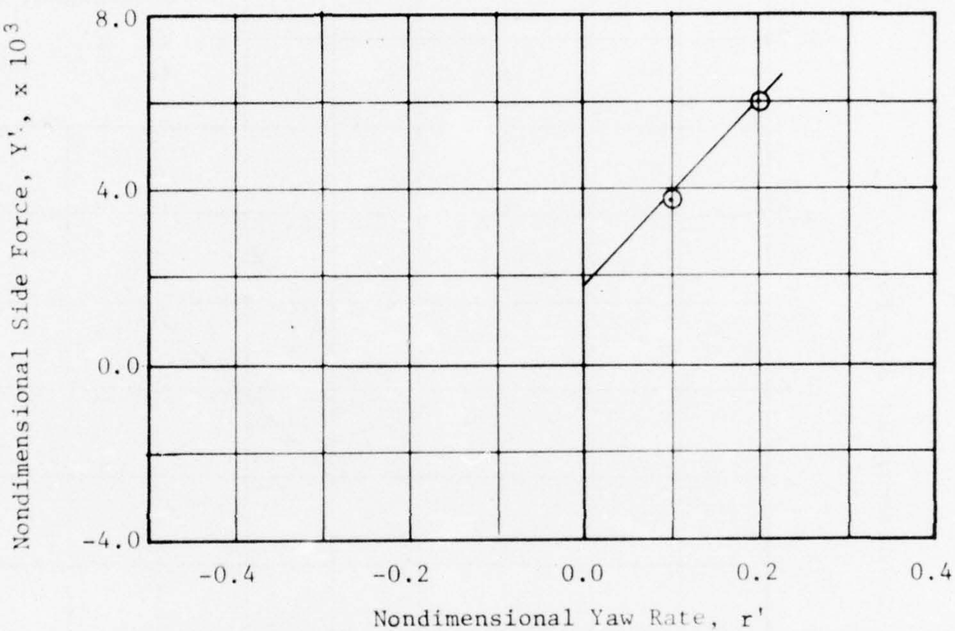

Figure 215 - Variation of Nondimensional Side Force with Nondimensional Yaw Rate for a Drift Angle of 0 Degrees at a Full Scale Speed of 5 Knots for the Half-Size Fixed Forward Turning Foil

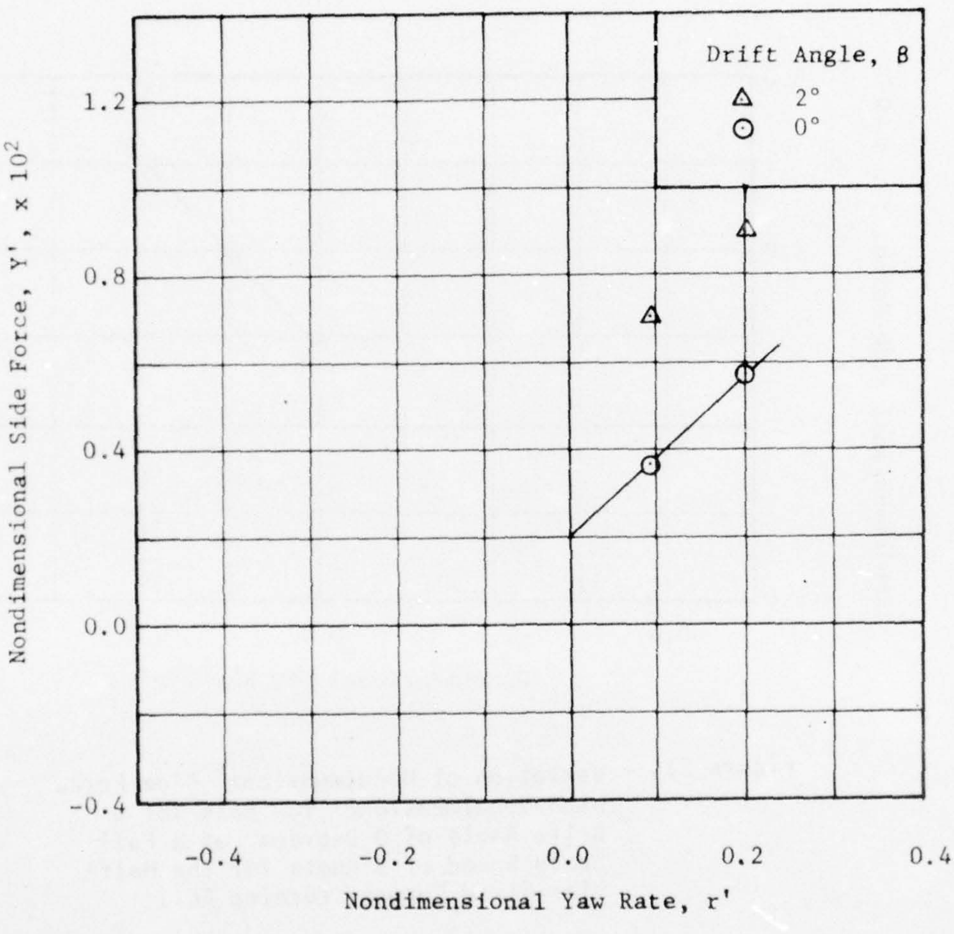

Figure 216 - Variation of Nondimensional Side Force with Nondimensional Yaw Rate for Two Drift Angles at a Full Scale Speed of 10 Knots for the Half-Size Fixed Forward Turning Foil

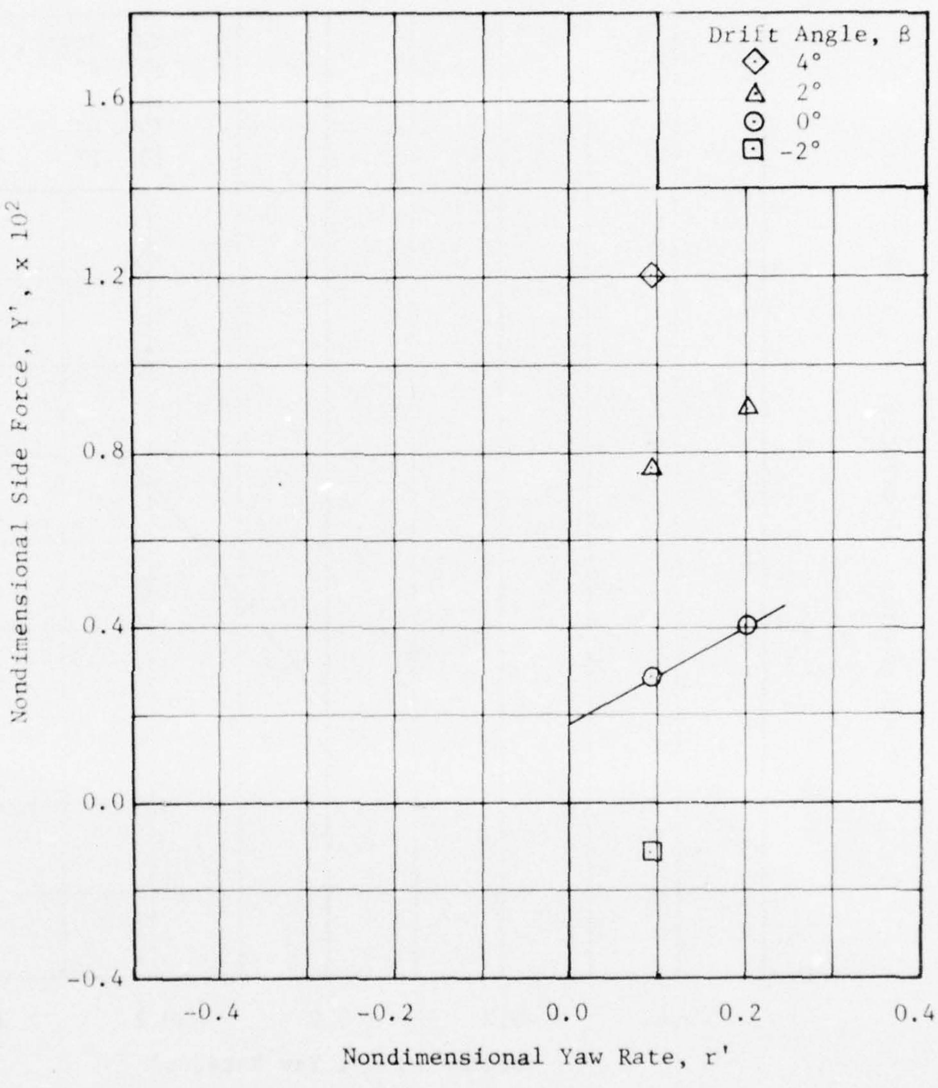

Figure 217 - Variation of Nondimensional Yaw Rate with Nondimensional Yaw Rate for a Series of Drift Angles at a Full Scale Speed of 15 Knots for the Half-Size Forward Turning Foil

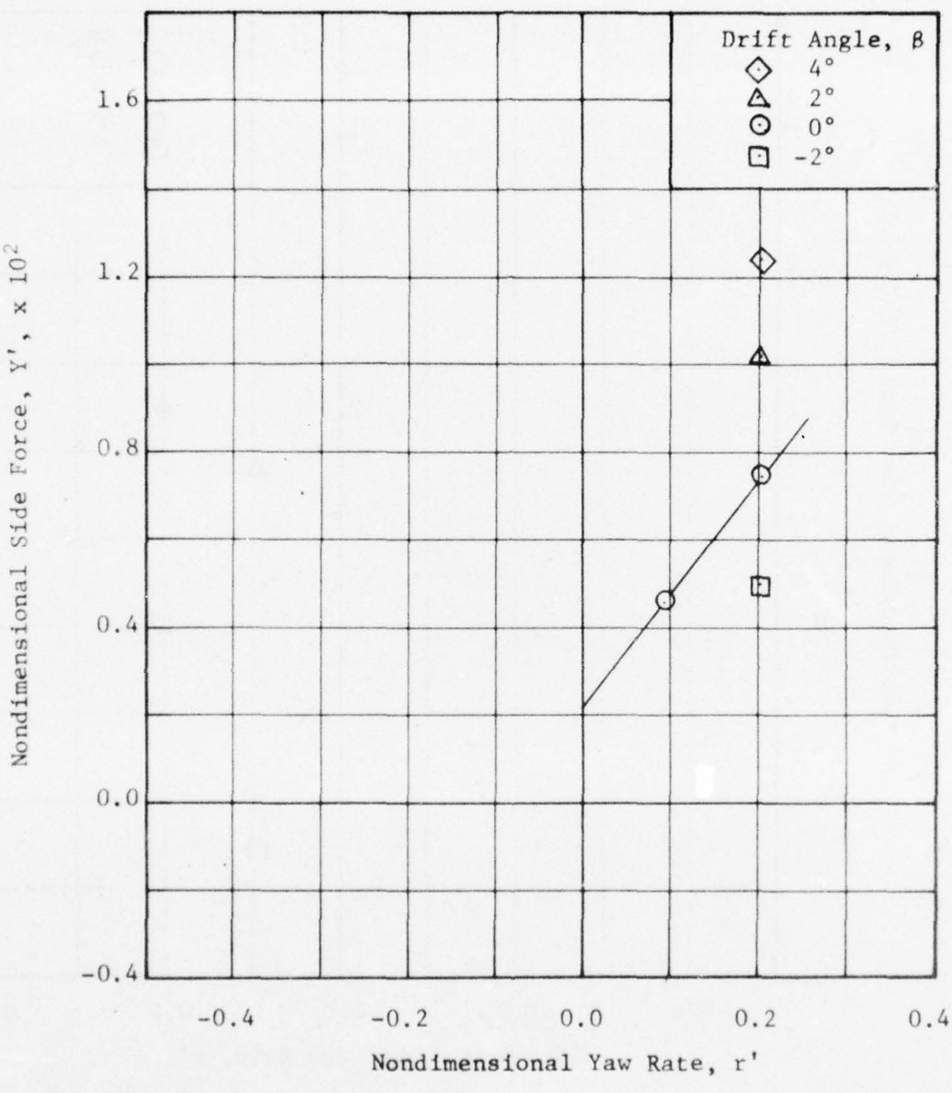

Figure 218 - Variation of Nondimensional Side Force with Nondimensional Yaw Rate for a Series of Drift Angles at a Full Scale Speed of 20 Knots for the Half-Size Fixed Forward Turning Foil

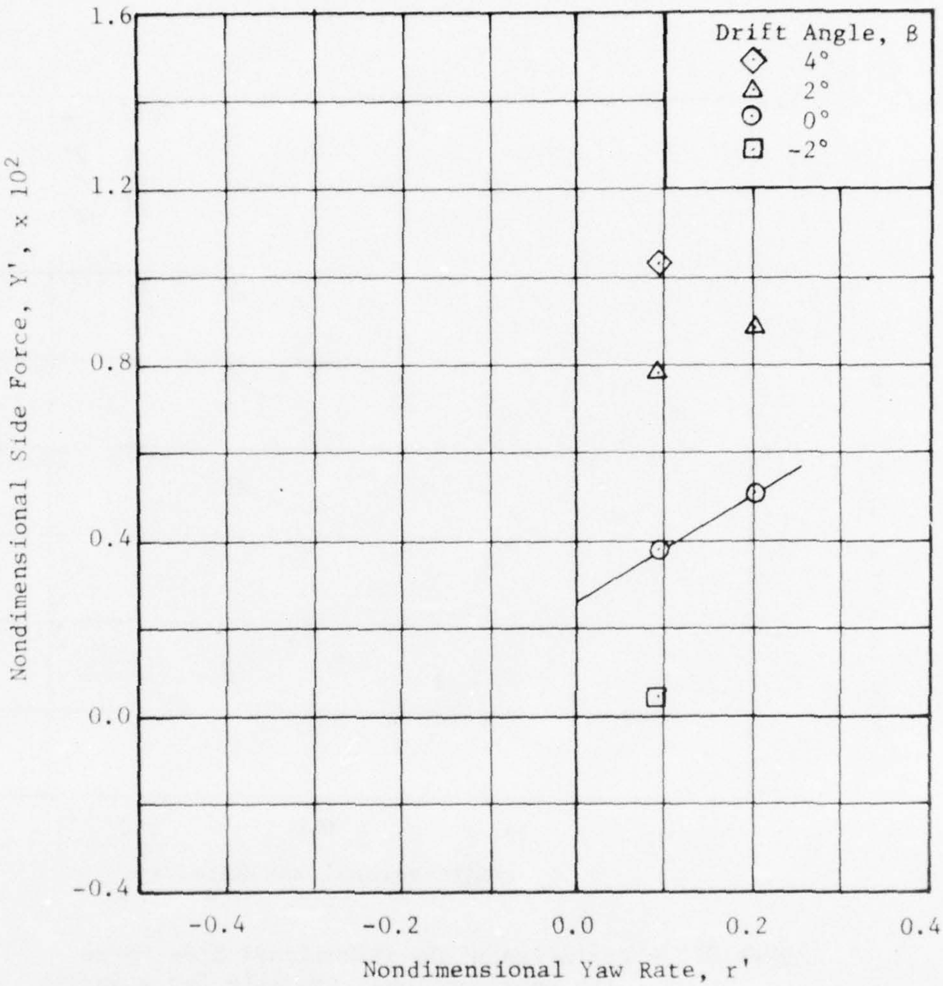

Figure 219 - Variation of Nondimensional Side Force with Nondimensional Yaw Rate for a Series of Drift Angles at a Full Scale Speed of 25 Knots for the Half-Size Fixed Forward Turning Foil

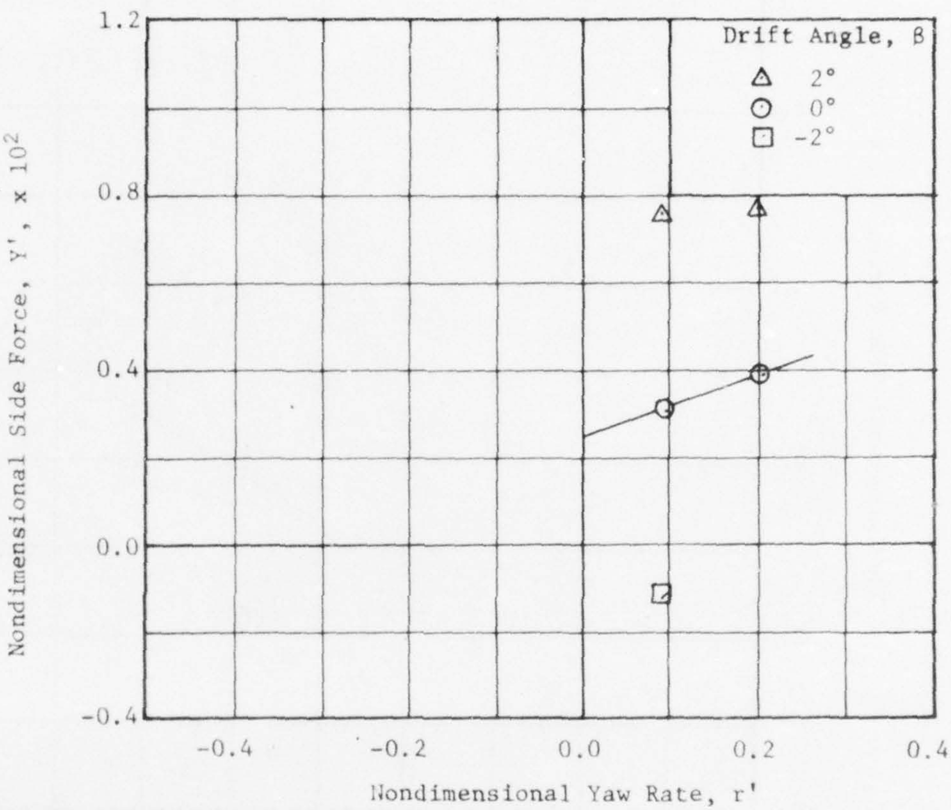

Figure 220 - Variation of Nondimensional Side Force with Nondimensional Yaw Rate for a Series of Drift Angles at a Full Scale Speed of 28 Knots for the Half-Size Fixed Forward Turning Foil

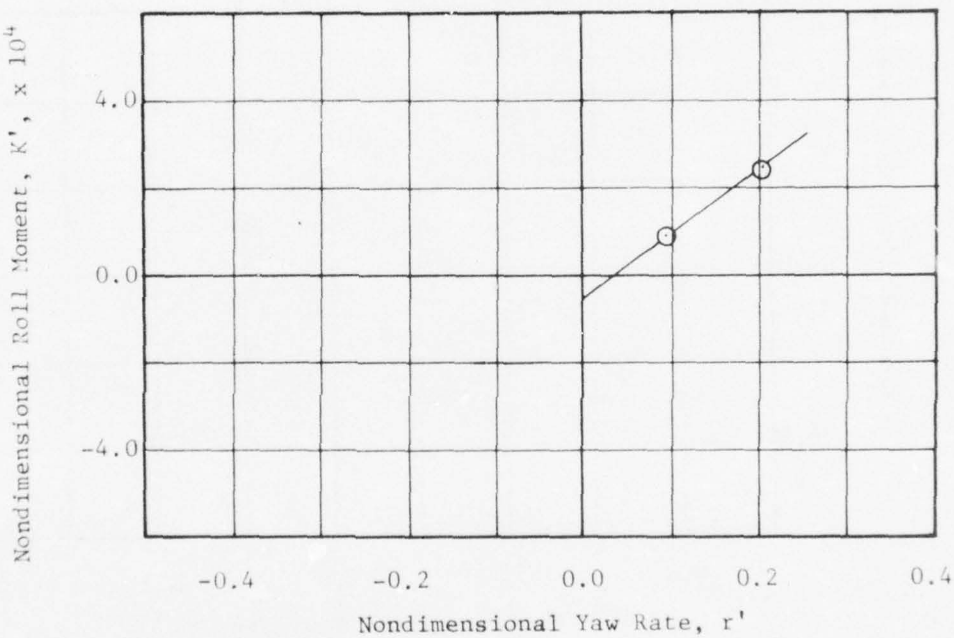

Figure 221 - Variation of Nondimensional Roll Moment with Nondimensional Yaw Rate for a Drift Angle of 0 Degrees at a Full Scale Speed of 5 Knots for the Half-Size Fixed Forward Turning Foil

AD-A034 593 DAVID W TAYLOR NAVAL SHIP RESEARCH AND DEVELOPMENT CE--ETC F/G 13/10
ROTATING ARM EXPERIMENTS FOR SWATH 6A MANEUVERING PREDICTIONS. (U)
JUL 76 J A FEIN, R T WATERS
UNCLASSIFIED SPD-698-01 NL

4 OF 4
AD
A034593

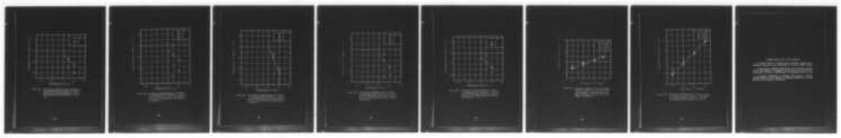

END
DATE
FILMED
2-77

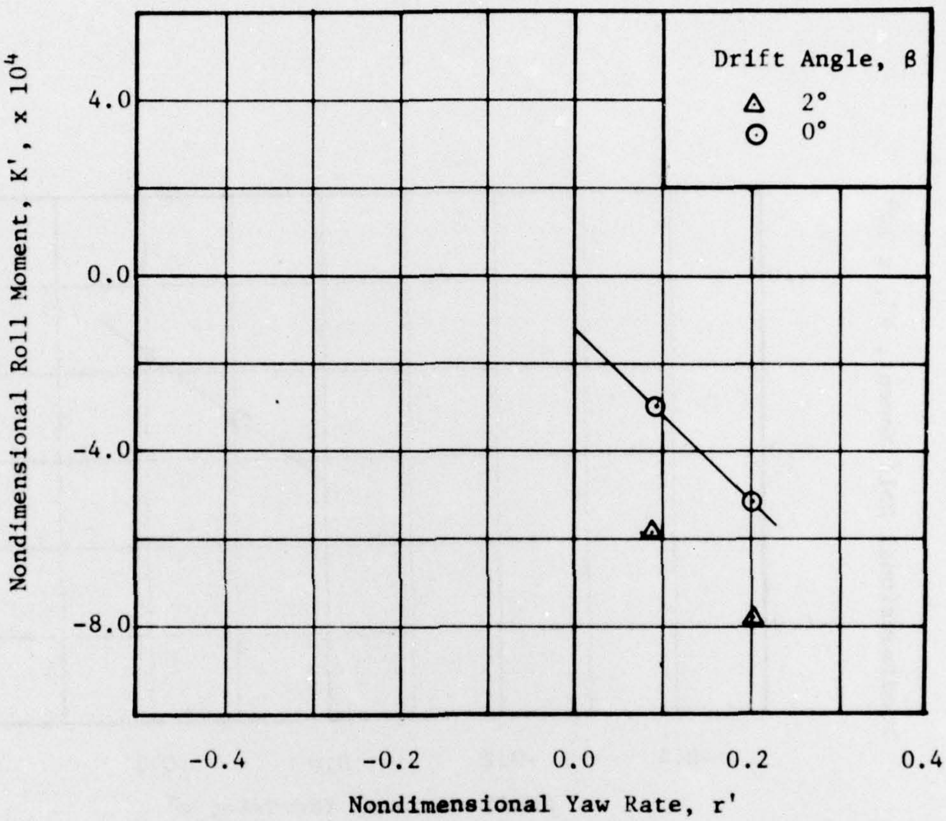

Figure 222 - Variation of Nondimensional Roll Moment with Nondimensional Yaw Rate for Two Drift Angles at a Full Scale Speed of 10 Knots for the Half-Size Fixed Forward Turning Foil

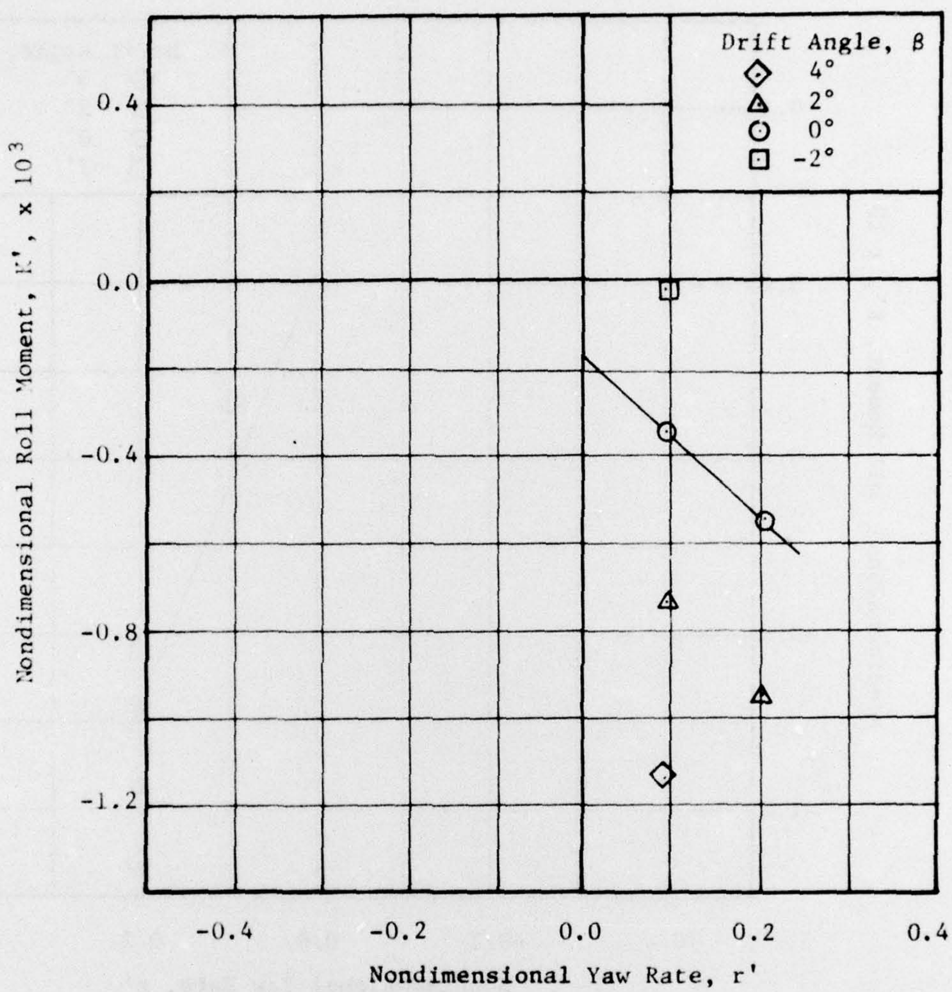

Figure 223 - Variation of Nondimensional Roll Moment with Nondimensional Yaw Rate for a Series of Drift Angles at a Full Scale Speed of 15 Knots for the Half-Size Fixed Forward Turning Foil

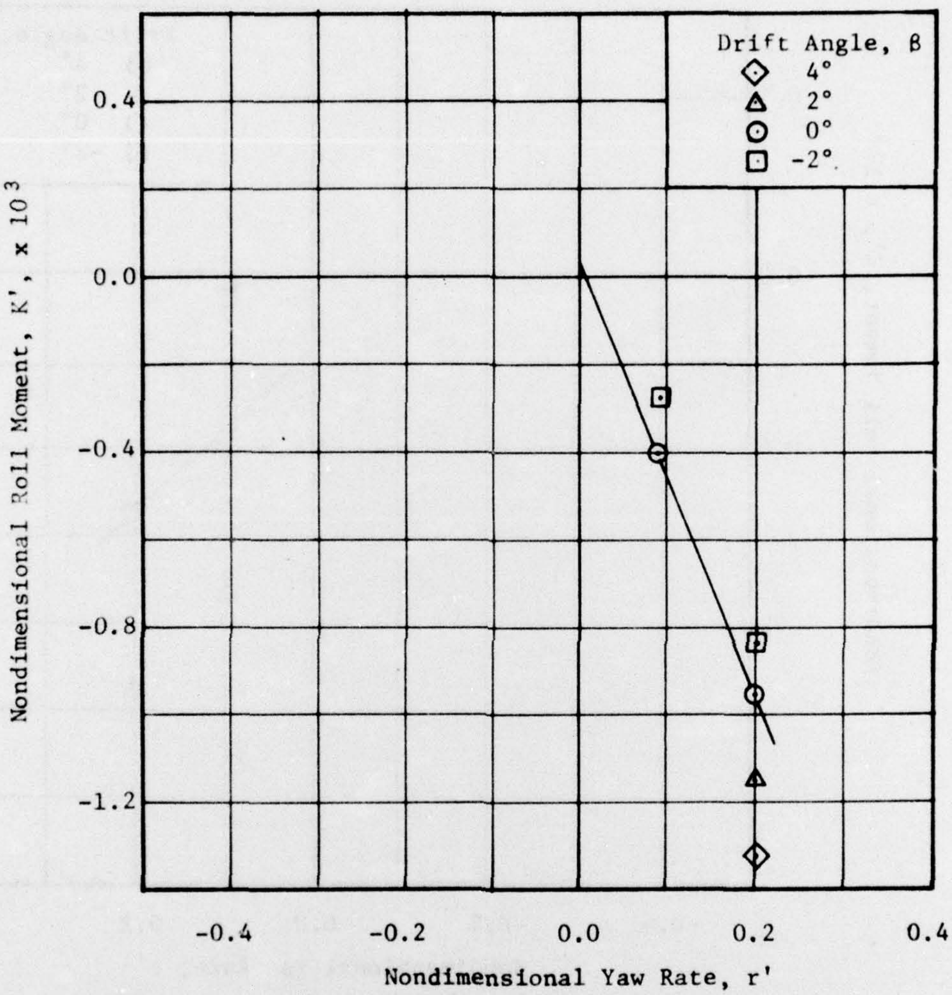

Figure 224 - Variation of Nondimensional Roll Moment with Nondimensional Yaw Rate for a Series of Drift Angles at a Full Scale Speed of 20 Knots for the Half-Size Fixed Forward Turning Foil

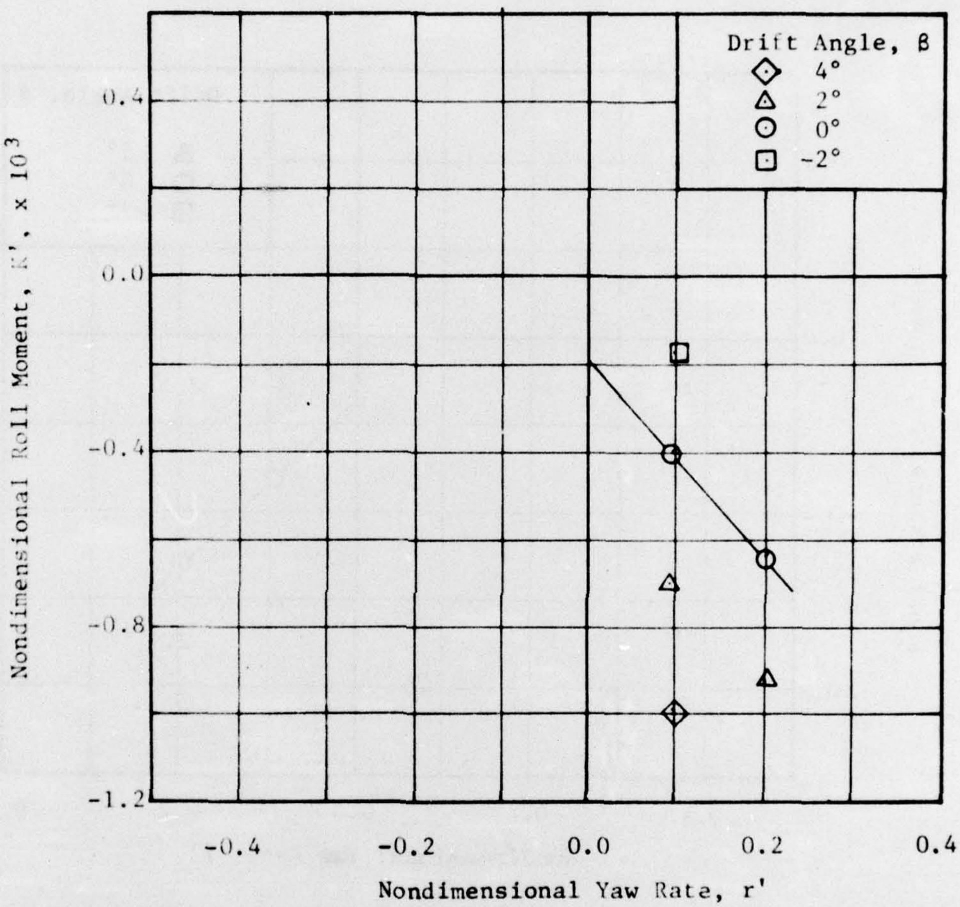

Figure 225 - Variation of Nondimensional Roll Moment with Nondimensional Yaw Rate for a Series of Drift Angles at a Full Scale Speed of 25 Knots for the Half-Size Fixed Forward Turning Foil

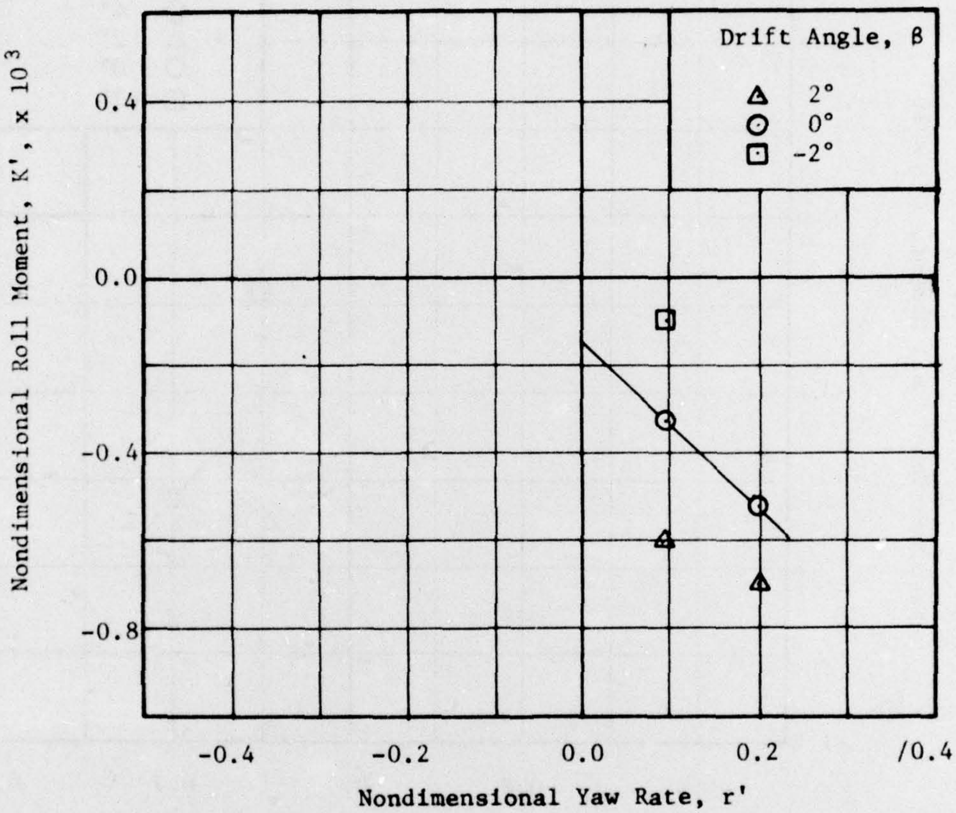

Figure 226 - Variation of Nondimensional Roll Moment with Nondimensional Yaw Rate for a Series of Drift Angles at a Full Scale Speed of 28 Knots for the Half-Size Fixed Forward Turning Foil

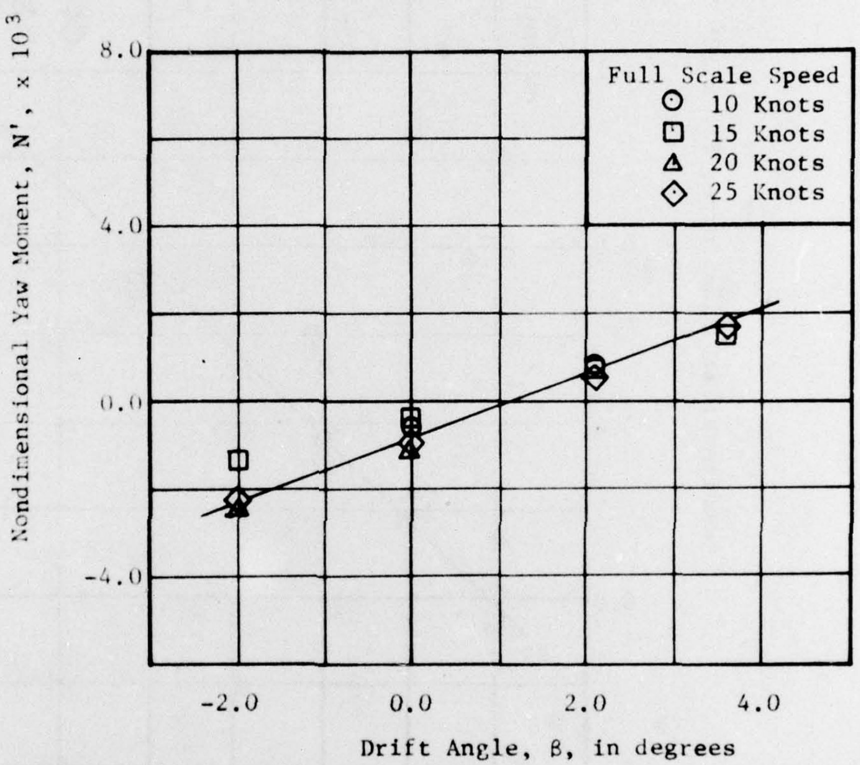

Figure 227 - Variation of Nondimensional Yaw Moment with Drift Angle for a Series of Full Scale Speeds at a Nondimensional Yaw Rate of 0.093 for the Half-Size Fixed Forward Turning Foil

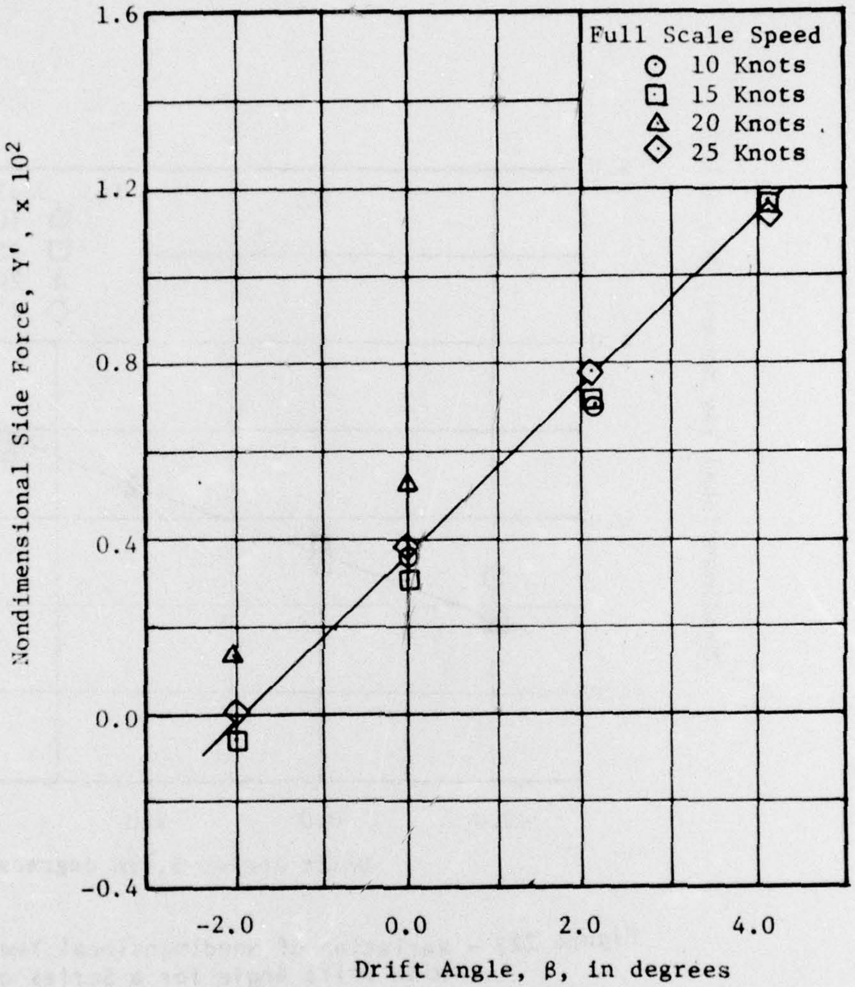

Figure 228 - Variation of Nondimensional Side Force with Drift Angle for a Series of Full Scale Speeds at a Nondimensional Yaw Rate of 0.093 for the Half-Size Fixed Forward Turning Foil

DTNSRDC ISSUES THREE TYPES OF REPORTS

(1) DTNSRDC REPORTS, A FORMAL SERIES PUBLISHING INFORMATION OF PERMANENT TECHNICAL VALUE, DESIGNATED BY A SERIAL REPORT NUMBER

(2) DEPARTMENTAL REPORTS, A SEMIFORMAL SERIES, RECORDING INFORMATION OF A PRELIMINARY OR TEMPORARY NATURE, OR OF LIMITED INTEREST OR SIGNIFICANCE, CARRYING A DEPARTMENTAL ALPHANUMERIC IDENTIFICATION

(3) TECHNICAL MEMORANDA, AN INFORMAL SERIES, USUALLY INTERNAL WORKING PAPERS OR DIRECT REPORTS TO SPONSORS, NUMBERED AS TM SERIES REPORTS; NOT FOR GENERAL DISTRIBUTION.